AB INITIO STUDIES OF EQUATIONS OF STATE AND CHEMICAL REACTIONS OF REACTIVE STRUCTURAL MATERIALS

A Dissertation
Presented to
The Academic Faculty

by

Roussislava Zaharieva

In Partial Fulfillment
of the Requirements for the Degree
Doctor of Philosophy in the
School of Aerospace Engineering

Georgia Institute of Technology
December 2011

AB INITIO STUDIES OF EQUATIONS OF STATE AND CHEMICAL REACTIONS OF REACTIVE STRUCTURAL MATERIALS

Approved by

Dr. Sathya Hanagud, Advisor
School of Aerospace Engineering
Georgia Institute of Technology

Dr. David McDowell
School of Mechanical Engineering
Georgia Institute of Technology

Dr. George Kardomateas
School of Aerospace Engineering
Georgia Institute of Technology

Dr. Tianci Jiang
General Electric Corporation

Dr. Julian Rimoli
School of Aerospace Engineering
Georgia Institute of Technology

Date Approved: August 26, 2011

To my Mother, Father, Grandmother, Grandfather, and Sister,
for her desire to change the course of time,
for his mind of an explorer,
for her free spirit,
for his unwavering will,
for her genuine love and comfort.

ACKNOWLEDGEMENTS

I would like to thank Professors Sathya Hanagud, Vigor Yang and Jeff Jagoda for guiding me, supporting me and believing in me until the full completion of my dissertation work. First, I wish to thank my advisor, Prof. Hanagud. I have grown up intellectually because of the wisdom, which he shared through our numerous and enriching discussions, both academic and philosophical. I have become a stronger person because he taught me perseverance and allowed me to appreciate the value of my own accomplishments. I would also like to express sincere appreciation to Prof. Yang for his strong inspiration and encouragement. Without his support, this work could not have been accomplished. I am also indebted to Prof. Jagoda for his numerous acts of assistance while facilitating the progress of my work towards a successful end. I am extremely grateful for my entire experience as a doctoral student and the insight I gained on the road to the final.

In addition I am thankful to my committee members, Prof. George Kardomateas, Prof. David McDowell, Dr. Julian Rimoli, and Dr. Tianci Jiang, for their time in serving on my thesis committee and providing valuable suggestions to improve the thesis. I would also like to recognize individuals, who have given me guidance throughout my Ph.D. work. My sincerest thanks are extended to Prof. Naresh Thadhani, for training me in the synthesis of nickel-aluminum nano-powder samples in the High-strain-rate Laboratory, and to Dr. Vinod

Sharma, for his advice in planning and reviewing my work. I would like to express appreciation to Prof. Adri van Duin for providing me with the opportunity to learn the art of ReaxFF while visiting his group in Penn State, which allowed me to view my research problem from a wider perspective.

I would also like to acknowledge my wonderful colleagues and friends whose presence made my Ph.D. experience cheerful and balanced. Among them, I am extending special thanks to Samer and Sofia, whose friendship and faith in me gave me the strongest power to continue looking forward, for my true self, in all aspects of my life.

TABLE OF CONTENTS

Page

DEDICATION iii

ACKNOWLEDGEMENTS iv

LIST OF TABLES ix

LIST OF FIGURES x

SUMMARY xiv

CHAPTER

1 INTRODUCTION 1

1.1 Energetic Structural Materials 2

1.2 Chemisorptions of Metals and Carbon Monoxide 4

2 BACKGROUND 7

2.1 Reactive Materials 7

2.2 Macroscopic Equations of State and Constitutive Relationships 11

2.2.1 Concepts 12

2.2.2 Theoretical Foundations and Methodology 13

2.3 Chemical Reactions of Reactive Materials 15

2.3.1 Continuum Scale Chemical Reaction Model and Computer simulation 16

2.3.2 Mesoscale Reaction Model 26

2.4 Research Issues and Thesis Outline 26

2.4.1 Research Issues 26

2.4.2 Ab Initio Techniques and Two Condensed Matter Reactants 30

2.4.3 Thesis Outline: Selected Research Tasks 33

3 ADSORPTION OF CO ON STRAINED AND HEATED TUNGSTEN 34

3.1 Background on Adsorption of CO on W 35

3.2 Research Issues Concerning Ab Initio Studies of Adsorption, Desorption and Disassociation of CO on W 39

3.3 Selected Research Program for this Research 40

3.4 Binding Energy Calculations with Uniform Compressive Strain 40

3.5 Effects of Temperature on the Binding Energy 48

4 CONSTITUTIVE RELATIONSHIPS OF DUAL FUNCTIONAL ENERGETIC STRUCTURAL MATERIALS 51

4.1 Introduction 51

4.2 Powder Mixture of Nickel and Aluminum 58

4.3 EOS of the fcc Aluminum and fcc Nickel 60

4.4 EOS of a Mixture 67

4.5 EOS of a Porous Mixture 69

4.6 Super cell approach to the EOS of a Mixture 72

4.7 Summary of the Chapter 74

4.8 Acknowledgement 74

5 AB INITIO CALCULATIONS OF CHEMICAL REACTIONS OF NICKEL AND ALUMINUM 75

5.1 Background 75

5.2 Ab Initio Techniques for Chemical Reactions 76

5.3 Sustained Reactions 77

6 EFFICIENT HYDROGEN STORAGE IN TITANIUM 85

6.1 Background 85

6.2 Problem Setting 86

6.3 Selection of Cutoff Energy and Number of K-Points 88

6.4 Binding Energy Calculations 92

7 SYNTHESIS AND DTA TESTS 96

7.1 Introduction 96

7.2 Characterizations of Thermally Induced Chemical Reactions and Porosity 99

7.2.1 Characterization using SEM 99

7.2.2 Density Measurements 101

7.2.3 DTA Tests 102

8 CONCLUSIONS AND RECOMMENDATIONS 106

APPENDIX A: A Brief Introduction to the Density Functional Theory 108

APPENDIX B: Crystalline Structure and Sections 120

APPENDIX C: Program inputs 125

APPENDIX D: Input to PHONON 159

REFERENCES 185

VITA 189

LIST OF TABLES

Page

Table 2.1: Properties of Al and Ni 21

Table 3.1: Variation of free energy (eV) and binding energy (eV) of the W(111)+CO system 43

Table 6.1: Variation of Total energy for Ti 1x1 with varying Cutoff energy & K-points 88

Table 6.2: Variation of Total energy for H_2 with varying Cutoff energy & K-points 90

Table 6.3: Variation of Binding energy with strain, of Ti+H_2 93

LIST OF FIGURES

Page

Figure 2.1: Equation of State of Al 14

Figure 2.2: Equation of State of Ni 15

Figure 2.3: Transition states for the reaction of the Iron Oxide and Al 23

Figure 2.4: Plots of Gibbs free energy as a function of temperature for reactants, products and transition states 23

Figure 2.5: Numerical results for 1-D shock induced chemical reactions 25

Figure 2.6: Numerical results for shock induced chemical reactions 25

Figure 2.7: Ni and Al at 100 ^{o} C and 650 ^{o} C, respectively 30

Figure 2.8: CO and W: “On-Top” adsorption 31

Figure 3.1: Convergence of binding energy as a function of cutoff energy 42

Figure 3.2: Effect of uniform compression on the binding energy 43

Figure 3.3: W (111) before relaxation, perspective view 44

Figure 3.4: W (111) before relaxation, without perspective view 45

Figure 3.5: W (111) before relaxation, top view 45

Figure 3.6: W (111) after relaxation: (a) with perspective view; (b) and (c) without perspective view 46

Figure 3.7: W (111) + CO before geometry optimization with perspective view 46

Figure 3.8: W (111) + CO before geometry optimization without perspective view 47

Figure 3.9: W (111) + CO after geometry optimization 48

Figure 3.10: The binding energy for the W(111)+CO system under temperature 49

Figure 3.11: Binding energy variation for ~4 fs 50

Figure 4.1: Ab initio procedure to construct EOS 52

Figure 4.2: Ab initio technique 53

Figure 4.3: Density Functional Theory 54

Figure 4.4: Kohn Sham Theory 55

Figure 4.5: Kohn Sham Theory – Approximations (1) 56

Figure 4.6: Kohn Sham Theory – Approximations (2) 57

Figure 4.7: Kohn Sham Theory – Approximations (3) 58

Figure 4.8: (a) The cold curve of Al, (b) the lattice thermal energy of Al vs. temperature at selected lattice parameters 65

Figure 4.9: (a) The cold curve of Ni, (b) the lattice thermal energy of Ni vs. temperature at selected lattice parameters 65

Figure 4.10: The thermodynamically complete equation of state of fcc Al (left) and Ni (right) 66

Figure 4.11: Comparisons of EOS by ab initio isotherm EOS at 300K and shock Hugoniot of Al and Ni 66

Figure 4.12: The procedure for the EOS of mixture by using (a) homobaric mixture Theory, (b) uniformly blended mixture theory 67

Figure 4.13: The equation of state of stoichiometric mixture 3Al+Ni, by (a) homobaric mixture theory, (b) uniformly blended mixture theory 69

Figure 4.14: Comparison of the 300K isotherm EOS of mixture by using homobaric and uniform mixture theories 69

Figure 4.15: The thermodynamically complete EOS of a 3Al+Ni mixture of 15% (volume) porosity 71

Figure 4.16: The isotherm EOS of a 3Al+Ni mixture of 15% (volume) porosity

at 10-3, 300, and 1000 K 72

Figure 4.17: A Super Cell of the mixture 73

Figure 4.18: Comparison of EOS 73

Figure 5.1: Gas molecule CO and Tungsten (111) layers 78

Figure 5.2: Aluminum molecules on-top of seven (111) Nickel layers 79

Figure 5.3: Phase diagram of Nickel and Aluminum 80

Figure 5.4: Initial configurations of Nickel and Aluminum layers 81

Figure 5.5: (111) layers of Nickel and Aluminum 82

Figure 5.6: JMol plots of Ni-Al (111) layers with increasing temperature 83

Figure 5.7: Formation of NiAl 83

Figure 6.1: Top view and side view of Ti 1x1 (neighbour cells shown for orientation) 87

Figure 6.2: Top views of Ti 2x2 and 4x4 HCP cells used in the calculations 87

Figure 6.3: Side views of 2x2 and 4x4 cells used in the calculations 88

Figure 6.4: Variation of Total energy with Cutoff Energy for Ti 1x1; kp = irreducible number of K-points, energy in eV 89

Figure 6.5: Variation of Total energy with K-points for Ti 1x1; ec = cutoff energy, energy in eV 90

Figure 6.6: Variation of Total energy with Cutoff energy for H_2; kp = irreducible number of K-points, energy in eV 91

Figure 6.7: Variation of Total energy of H_2 with Cutoff energy and K-points mesh; ec = cutoff energy, energy in eV 91

Figure 6.8: Positioning of Ti + H_2 92

Figure 6.9: Possible binding sites 93

Figure 6.10: Variation of Binding energy with strain, for two supercells of Ti+H_2: gap (Ti-H) = 0.8 Å and 1.2 Å 94

Figure 7.1: Species and mixture 97

Figure 7.2: Pressed Ni+Al powders 97

Figure 7.3: Mold used for pressing samples 98

Figure 7.4: MTS 810 (left); Hydraulic press (right) 98

Figure 7.5: SEM of starting species: Nano Al, x20K (left); Micro Al, x1K (right) 100

Figure 7.6: SEM of starting species: Nano Ni, x20K (left); Micro Ni, x1K (right) 100

Figure 7.7: SEM of starting species: CNT, x20K (left); Carbon Fibers, x1K (right) 100

Figure 7.8: SEM of (a) pressed nano-powder sample of Ni/Al/CNT/Epoxy, x50k; and (b) pressed micro-powder sample of Ni/Al/Fiber/Epoxy, x200 101

Figure 7.9: Comparison of the %TMD of pressed samples. Pressure vs. density of micro and nano Ni+Al + %vol Teflon, Carbon fiber and Epoxy 102

Figure 7.10: DTA of pressed micro-powder samples 103

Figure 7.11: DTA of pressed nano-powder samples 103

Figure 7.12: DTA of a pressed nano-powder sample with Carbon fiber and Teflon 104

Figure 7.13: DTA of all pressed samples 104

Figure 7.14: DTA of starting powders 105

SUMMARY

The motivations for the research issues addressed in this thesis are based on the needs of the aerospace structural analysis and the design community. The specific focus is related to the characterization and shock induced chemical reactions of multi-functional structural-energetic materials that are also known as the reactive structural materials and their reaction capabilities.

Usually motivation for selection of aerospace structural materials is to realize required strength characteristics and favorable strength to weight ratios. The term strength implies resistance to loads experienced during the service life of the structure, including resistance to fatigue loads, corrosion and other extreme conditions. Thus, basically the structural materials are single function materials that resist loads experienced during the service life of the structure. However, it is desirable to select materials that are capable of offering more than one basic function of strength. Very often, the second function is the capability to provide functions of sensing and actuation. In this thesis, the second function is different. The second function is the energetic characteristics. Thus, the choice of dual functions of the material are the structural characteristics and energetic characteristics. These materials are also known by other names such as the reactive material structures or dual functional structural energetic materials. Specifically the selected reactive materials include mixtures of selected metals and metal oxides that are also known as thermite mixtures, reacting intermetallic combinations

and oxidizing materials. There are several techniques that are available to synthesize these structural energetic materials or reactive material structures and new synthesis techniques constitute an open research area.

The focus of this thesis, however, is the characterization of chemical reactions of reactive material structures that involve two or more solids (or condensed matter). The subject of studies of the shock or thermally induced chemical reactions of the two solids comprising these reactive materials, from first principles, is a relatively new field of study. The published literature on ab initio techniques or quantum mechanics based approaches consists of the ab initio or ab initio-molecular dynamics studies in related fields that contain a solid and a gas. One such study in the literature involves a gas and a solid. This is an investigation of the adsorption of gasses such as carbon monoxide (CO) on Tungsten. The motivation for these studies is to synthesize alternate or synthetic fuel technology by Fischer-Tropsch process.

In this thesis these studies are first to establish the procedure for solid-solid reaction and then to extend that to consider the effects of mechanical strain and temperature on the binding energy and chemisorptions of CO on tungsten. Then in this thesis, similar studies are also conducted on the effect of mechanical strain and temperature on the binding energies of Titanium and hydrogen. The motivations are again to understand the method and extend the method to such solid-solid reactions. A second motivation is to seek strained conditions that favor hydrogen storage and strain conditions that release hydrogen easily when needed.

Following the establishment of ab initio and ab initio studies of chemical reactions between a solid and a gas, the next step of research is to study thermally induced chemical reaction between two solids (Ni+Al).

Thus, specific new studies of the thesis are as follows:

1. Ab initio Studies of Binding energies associated with chemisorption of (a) CO on W surfaces (111, and 100) at elevated temperatures and strains and (b) adsorption of hydrogen in titanium base.
2. Equations of state of mixtures of reactive material structures from ab initio methods.
3. Ab initio studies of the reaction initiation, transition states and reaction products of intermetallic mixtures of (Ni+Al) at elevated temperatures and strains.
4. Press-cure synthesis of Nano-nickel and nano-aluminum based reactive material structures and DTA tests to study experimentally initiation of chemical reactions, due to thermal energy input.

CHAPTER 1

INTRODUCTION

The motivations for the research issues addressed in this thesis are based on the research needs of the aerospace structural analysis and the design community. The specific focus is to the characterization of multi-functional structural-energetic materials or reactive structural materials and their shock induced or thermally induced reaction capabilities. Because the subject of studies of the shock or thermally induced chemical reactions of the two solids that comprise these reactive materials, from first principles (or quantum molecular dynamics approaches), is a relatively new field of study it is necessary to identify parallel fields of the ab initio or ab initio-molecular dynamics studies. Several such studies in the literature involve gases and solids. One such study investigates the adsorption, desorption and disassociation of gasses such as carbon monoxide (CO) on Tungsten. The motivation for these studies is to synthesize alternate or synthetic fuel by Fischer-Tropsch process. Thus first steps to establish solid-solid reactions are to repeat these studies and use the procedure to construct ab initio-molecular dynamics procedure for solid-solid shock induced chemical reactions. Also, this published study of CO adsorption on W does not contain results on the effect of strain; it is a new contribution to include this effect. A second field of gas and a solid is that of H_2 and Titanium for hydrogen storage in fuel cells. Thus, it is necessary to repeat these studies and extend them to consider the effects of mechanical strain and temperature on the binding energies of Titanium and hydrogen.

Following the establishment of ab initio and ab initio studies of chemical reactions between a solid and a gas, the next step is to formulate ab initio-molecular dynamics procedure for thermally induced chemical reactions between two solids (Ni+Al). The next section contains the explanation of the concept of structural energetic materials and the need to study the initiation and sustained reactions in these materials.

1.1 Energetic Structural Materials

Usually the choice of aerospace structural materials depends on their strength characteristics and their strength to weight ratios. The term strength implies resistance to expected loads during the service life of the structure including resistance to fatigue loads, corrosion and extreme loading conditions. Thus, basically the structural materials have a single function of resisting loads experienced during the service life of the structure. However, it is desirable to provide materials that are capable of offering more than one basic function of strength. Very often, the second function is the capability to provide functions of a sensor and control actuator. In this thesis, the second function does not include sensing or control actuation. The second function is to include energetic characteristics. Thus, the dual functions of the material are the structural characteristics and energetic characteristics. These materials are also known by other names such as the reactive material structures or dual functional structural energetic materials. Specifically the selected reactive structural materials include mixtures of selected metals and metal oxides that are also known as thermite mixtures; reacting intermetallic combinations and oxidizing materials. Techniques to synthesize these

structural energetic materials or reactive material structures, with desired strength and energetic characteristics, are an open research area.

First motivations to study reactive material mixtures are traceable to synthesis of materials with unique microstructures by the use of shock-induced synthesis [1.1-1.4]. Reactions in such a process of synthesis are exothermic. The release of extensive amount of heat and formation of gasses in some cases is the traceable to an exploration of such combination of materials as alternate energetic materials [1.5-1.14] in comparison to conventional energetic materials (or colloquially known as explosives). The combination of thermite mixtures and intermetallic mixtures also leads to energetic materials that are less sensitive to impact and thermal loads.

In summary, the reactive material structures have dual functions. These dual functions are useful in many applications. Some of the applications are as casings for warheads and solid rocket motors. When reactive structural materials become warhead casings material, the reactive material-structure has to (a) protect the traditional; explosives or energetic materials housed inside the casing and fuses enclosed in the casing while the casing itself is capable of withstanding impact loads resulting from the target impact. These impact loads result when the warhead impacts selected targets, at high striking velocities. In many cases the warhead penetrates through the target. In these operations the strength-function of the dual functional material is important and no chemical reaction of the reactive material structure is expected

to initiate. Following the impact and penetration, the reactive material-structure is expected to react and add to the energy released by the enclosed conventional energetic material. Thus, during the first stage of impact and penetration there are two failure criteria, One is the strength-based failure criterion and the second is the failure criterion of no chemical reaction during the phase of impact and penetration through selected targets at selected striking velocities. Thus, it is necessary to understand the chemical reactions in a reactive material-structure. The discussion in the next chapter entitled "Background" addresses these chemical reactions.

1.2 Chemisorptions of Metals and Carbon Monoxide

The study of chemical reactions of reactive material structures involves chemical reaction of two condensed matter reactants due to thermal loads or shock loads. There are theoretical models at the continuum scale level [2.16] and mesoscale level [2.14] to study these chemical reactions. However the goals of this thesis are to study these by using ab initio molecular dynamics. Most of the ab initio studies of chemical reactions relate to catalysis and sensor designs. These ab initio studies, however, consider adsorption, chemisorption and catalytic reactions between one condensed matter (metal) and gasses such as CO and hydrogen or oxygen. Thus, most of the published works that use ab initio (quantum mechanics and density functional theory) molecular dynamics do not consider reactions between two condensed matters such as nickel and aluminum, with and without strains, defects and elevated temperatures resulting from shock loads. First, it is necessary to formulate

procedures to study shock or thermally induced chemical reactions in mixtures of solids by the use of ab initio (quantum mechanics and density functional theory) molecular dynamics techniques. The approach in this thesis is to first repeat the studies of adsorption, desorption and disassociation of solid-gas reactions. For example, published literature on W (tungsten) and CO [1.15-1.21] or Ti and hydrogen are cases of interest. Then use the validation procedures to investigate solid-solid reactions of inter metallic mixtures, such as nickel and aluminum.

Even in the ab initio-molecular dynamics studies of W+CO and Ti+H_2, the effects of mechanical strain on the chemical reaction is a new area of research. Goals are to explore the effects of strain and temperature on the adsorption, desorption and possible disassociation in W+CO and Ti+H_2 chemical reactions by the use of ab initio molecular dynamics before proceeding to the formulation of procedures for Ni+Al chemical reactions.

The specific W+CO chemical reaction has applications to the Fisher-Tropsch process [1.22-1.24]. The process derives its name after the inventors Fisher and Tropsch (1920s) to produce synthetic fuel in petroleum-poor but coal rich countries such as Germany and South Africa, using coal. Today, the process is of significant amount of interest existing in its improvement to produce alternative fuels including bio-fuels. In principle, the Fischer-Tropsch reaction is as follows.

$$(2n+1)H_2 + n(CO) = C_n H_{2n+2} + n(H_2 O) \qquad (1.1)$$

In this equation “n” is a positive integer. Catalysts disassociates CO in to C and O and favor a reaction that results in n >1 in the equation (1.1). The number n=1 results in methane that is not desired. Iron and Cobalt are the original choice of catalysts. Currently, the use of tungsten (W) is of interest because of its potential as an efficient catalyst (Chen et. al.). Chen et. al. [1.20] report a study of the binding energy of adsorption, without considering the effects of strain or the effects of elevated temperature of W. The motivation of selection of the process is to reproduce the results of Chen et. al. and extend the results to include the effects of different types of strains. The next step is the study of the effects of elevated temperature and defects to explore possible disassociation. The formulated procedures and techniques then become foundation for the studies of condensed matter-reactants of reactive material-structures, with or without strain and elevated temperature resulting from shock impacts or laser induced heat.

Another solid-gas reaction of interest is Ti+H_2. Besides forming a foundation for the study of Ni +Al shock or thermally induced chemical reaction, the subject of the binding energy of hydrogen on Ti with strains is of a significant amount of interest in explaining the hydrogen storage capabilities for fuel cell applications. The area that is explained in the thesis is to determine a strain state with high binding energy for hydrogen input and storage. Then explore the change of strain condition that reduces the binding energy for easy release of hydrogen for combustion in fuel cells.

CHAPTER 2

BACKGROUND

In this chapter the concept of structural energetic material or reactive structural material is described. Then, the previous work on continuum scale modeling and continuum scale models for shock induced chemical reactions are described. Then, research issues and the thesis outline are presented.

2.1 Reactive Materials

The different reactive materials that form the foundations for the reactive material-structures or structural-energetic material form three types of reactive material mixtures, without techniques for synthesis and/or binding techniques. These are as follows [2.1].

- Metal/metal oxide mixtures (thermites);
- Metal/metal mixtures (intermetallics); and
- Combustible metals (metal to metal oxide reaction).

To discuss the possible design of mixtures for specific use, some of the characteristics of a few selected thermite mixtures, intermetallic mixtures and combustible oxidizing metals are as follows [2.1]. Then, the next step is to select a mixture to meet specified goals or requirements. The following table (Hanagud 2008 [2.2]) presents the mixture density and combustion energy densities of selected reactive materials. There is an exhaustive list of possible reactive materials

[2.1]. This list contains a few combinations for purposes of illustration.

I. THERMITE MIXTURES:

Reactive Materials	**Mixture Density g/cc**	**Reaction Temperature Degrees Kelvin**	**Heat of Reaction Calories/gram**
1.3Mg + B2O3	1.785	6,389/3,873	2,134
2Al + Ni2O3	4.045	5,031/3,187	1,292
2Y +Ni2O3	4.636	7,614/3,955	1,120
2Al + Fe2O3	4.175	4,382/3,135	945
4Al + 3MnO2	4.014	4,829/2,918	1,159
Al + KclO4	2.5		3000

II. INTERMETALLIC MIXTURES

Reactive Materials	**Mixture Density g/cc**	**Reaction Temperature Degrees Kelvin**	**Heat of Reaction Calories/gram**
2B + Ti	3.603	3,043	1,320
Mo + 2Si	4.582	3,498	207
2B + Hf	8.232	3,945/3,653	742
Al + Ni	5.165	2,362/1,910	330
Hf + C	9.084	4,441/4,222	315
Al + Ta	9.952	1,011	57

2C + Th	8.169	3,073	247
2B + Ta	10.36	2,666	

III. COMBUSTIBLE OXIDIZING METALS

Metal/Metal Oxide	**Metal Density g/cc**	**Reaction Temperature Degrees Kelvin**	**Heat of Reaction Calories/gram**
Hf / HfO2	11.4	2,495	1,491
Ta/Ta2O5	16.6	3,390	1,390
Al / Al2O3	2.7	933	7,422
Mg / MgO	1.5	923	6,241
Mn /Mn3O4	7.3	1,519	2,012
Mo / MoO3	9.1	2,896	1,856
Nb /Nb2O5	8.57	2,750	2,443
Ti /TiO2	4.5	1,693	4,714
Y /Y2O3	4.47	1,799	2,819
W /WO2	19.3	3,695	767

Reactive material mixtures of metal and metal oxide or thermite mixtures yield very high enthalpic energy, following a chemical reaction. However, the density of the thermite mixture is very low in comparison to a standard structural material such as steel (7.8

grams/cc). On the other hand, intermetallic mixtures do have high densities. For example, the intermetallic mixture of hafnium and carbon has a density of approximately 9 g/cc. The resulting densities are comparable to that of steel. However the released enthalpic energy, following a sustained chemical reaction, of these intermetallics is very low. The combustible or oxidizing metals yield very high enthalpic energy following a sustained chemical reaction. However, a reaction initiation needs high temperatures. Thus, the designs of reactive material structures, of density similar to that of structural steel with a released high enthalpic energy following a chemical reaction, need hybrid mixtures of different types of reactive materials. One combination of such a material that has been suggested (Hanagud 2008) is a mixture of Hf + 2B (33%) with Al (20%) and Tantalum (47%). Such a hybrid mixture has a density of 11grams per cubic centimeter and has the potential to release 2,344 calories per gram if the material is designed to initiate the much needed chemical reaction of the combustible metal Al reaction following the intermetallic reactions. It is possible to synthesize these energetic structural materials as monolithic materials or as sandwich structures that has not been tried before. The structural strength depends on the synthesis procedures. This is still an open research area.

Before these materials are incorporated in to practical designs, it is necessary to develop techniques to synthesize these dual functional materials and characterize these materials. The characterization includes the determination of the constitutive relations to analyze for stresses and analyze the chemical reaction process to study the reaction behavior. The

characterization also includes the determination of failure criteria. As discussed before, in dual functional materials, there are two branches of the failure criteria. This is due to the conflicting requirements that the structure must provide the needed strength during phases of operation when strength is necessary and the material must be capable of reacting during phases of operation when a chemical reaction and a release of the heat content are important. We do not want a chemical reaction when only strength is desired. For example, if the reactive structural material is used as a casing for the warhead, it is necessary that the casing withstands the shock loads that result from the impact and penetration of the target. However it is also important that these casings release energy, with a chemical reaction, when the warhead functions as a weapon.

2.2 Macroscopic Equations of State and Constitutive Relationships

The next step is to characterize the materials. The goals are to determine the macroscopic equations of state and complete constitutive equations of reactive materials and reactive material composites, theoretically, without the expensive gas gun or flyer plate tests. This step is necessary because tests for different ratios of mixture components are expensive. Limited number of tests, however, is necessary to validate the theoretically determined equations of state. The current state of the art or technology, on the basis of published research [2.2-2.10] is sufficient to determine the equation of state of crystalline metals. There is also reported literature on the characterization of binary alloys [2.11]. Recently, Jiang and Hanagud also discuss techniques to study the equation of state of ternary alloys [2.12].

However, the study of equation of state of reactive mixtures by ab initio methods is still an open research area [2.7, 2.8, 2.13].

2.2.1 Concepts

It is necessary to determine the constitutive relations for the reactive materials and reactive material composites under conditions of finite deformations. Usual methods of determining such constitutive relations are through gas gun or flyer plate impact tests. Very often the tests are primarily to determine the equation of state [p = P (ρ)].The equation of state is a part of the constitutive equation. The complete constitutive equations describe the relationship between all the stress components and the strain components. The reactive materials of interest consist of mixtures and composites and it is necessary to obtain the equations of state, as a function of the ratio of the mixture constituents (or the percentage of each constituent and the voids). This requires a large number of tests for each selected hybrid reactive material or the reactive material composite. This results in a significant number of tests, a significant amount of time and is expensive. Thus, the goals are to determine the constitutive equations, including the equations of state from theoretical calculations, without conducting tests and validate the theoretical calculation by conducting limited number of tests. This is a part of the research of this thesis work as it is not addressed in previous research work in the literature.

2.2.2 Theoretical Foundations and Methodology

Theoretically, Helmholtz free energy determines the constitutive equations, for small deformations. For finite deformations a similar procedure it is necessary to consider appropriate changes to include finite deformation strains and the principle of objectivity to account for the superimposed rigid body rotations. In addition to the principle of objectivity, it becomes necessary to impose crystalline symmetry conditions or the anisotropic effects. The next question concerns the determination of the Helmholtz free energy from theoretical methods. This is possible only by going beyond the continuum mechanics formulation into quantum mechanics where a solid is considered to be a collection of heavy particles or nuclei (positively charged) and very light particles or electrons (negatively charged). For N nuclei, there is ZN number of electrons for an atom. This is known as the many-body-problem. Because of the very light particles, it is necessary to consider the problem as a quantum many-body-problem and the problem formulation is by the Schrödinger's equation. The electron density and distribution change due to their initial positions and the mechanical strain. The current state of the technology is to use the approximation of density functional theory to obtain the ground state energy for various densities or strained configurations. Then, the energy due to lattice phonon (thermal) contribution by density function perturbation theory or quantum molecular dynamics and electron thermal contribution are additions to the ground state energy. This yields energy as a function of the temperature and density. Then, procedures to bridge from quantum many-body-problem to the continuum are based on the thermodynamic principles. For example, if we are interested only in the part of

the constitutive equations that concern the equation of the following equations the procedure is as follows:

$$e(v,T) = e_c(v) + e_l(v,T) + e_e(v,T) \tag{2.1a}$$

$$S = \int_0^T \frac{\partial e}{\partial T}\frac{dt}{T}; \qquad f = e - TS; \qquad P = \frac{\partial f}{\partial v} \tag{2.1b}$$

The published literature, to date, considers crystalline metals or alloys. As stated before, the determination of the mixture constitutive equation is a new area and forms a part of this thesis. The following results illustrate [2.2] the accuracy of the methods of determining the equations of state of crystalline metals.

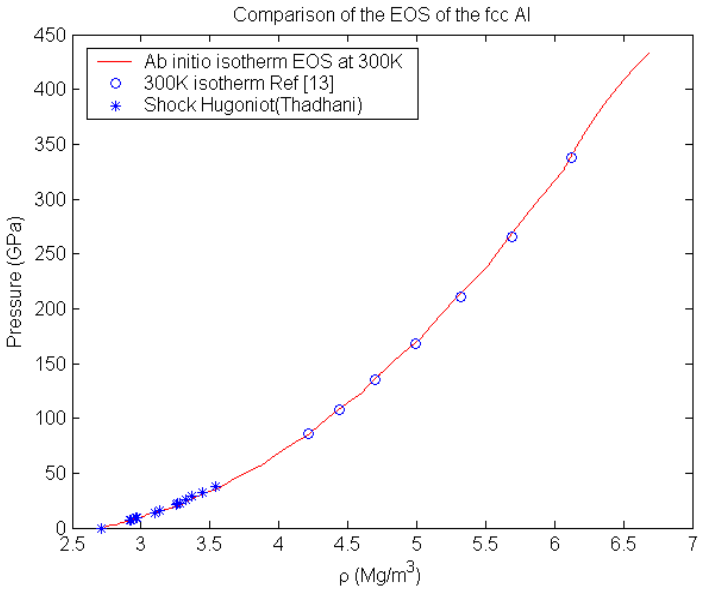

Figure 2.1: Equation of State of Al

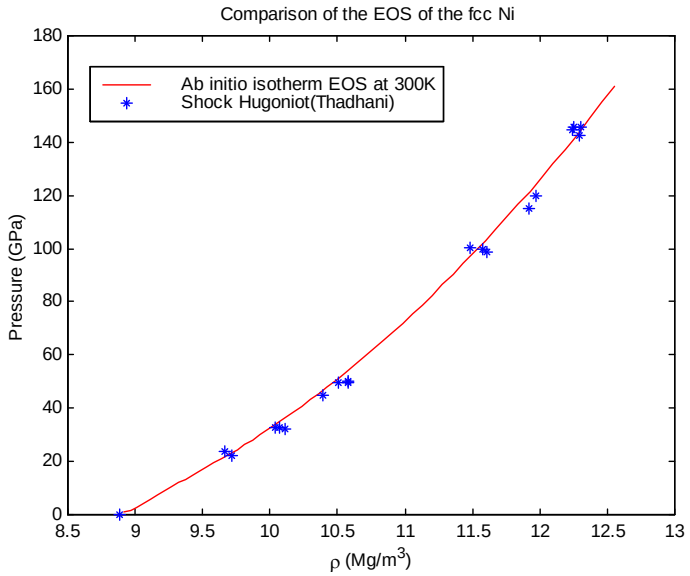

Figure 2.2: Equation of State of Ni

2.3 Chemical Reactions of Reactive Materials

The goal many researchers in the field of reactive material structures is to develop a fundamental understanding of shock induced chemical reactions of reactive materials, The second area concerns models to couple the reactions and detonation waves of organic energetic materials to the inorganic energetic material systems. This section discusses models for shock induced or assisted chemical reactions of reactive materials, in a continuum or meso- scale.

As stated before, the initiation and sustained chemical reactions in reactive materials material systems, in macro scales, are due to researchers [1.1-1.6] Graham, Thadhani, Bosolough,

Horie, Nesterenko, Eakins and others. Most of the published works discuss the issues of mechanical deformations, fracture of reactants, mixing of reactants, plastic flow and pore collapse, in the frame of equilibrium thermodynamics. Bosolough, through his experiments reports that the rate of increase of temperature was too high to be explained only by mechanisms such as mixing, diffusion and plastic flow. To accommodate some of the observations, a chemical reaction model is proposed by Vindhya Narayanan, Lu and Hanagud. In this model, a shock-induced chemical reaction model is proposed in the frame works of non-equilibrium thermodynamics and mixture theories, in a continuum or macro scale. This work displayed reactions, product formation and rise of temperature due to the exothermic reactions during one-dimensional numerical integration of the impact problem and appropriate equations. Also, procedures to identify the transition state and the needed activation energy to reach the transition state, from enthalpic energy considerations, are discussed in this work. In mesoscale, Do and Benson discuss a model, but with infinite diffusion rate. This is modified with a finite diffusion rate model by Reding and Hanagud [2.15].

2.3.1 Continuum Scale Chemical Reaction Model and Computer Simulation

In this section, the continuum scale Chemical reaction model of Narayanan, Lu and Hanagud [2.16] is briefly summarized here. In traditional hydrocodes mixture theory is not used. A mixture theory is used to describe various species of the porous binary energetic material. According to this mixture theory, all components occupy the same physical infinitesimal

space. Each species carries a partial stress while the pores carry no stress. Each species has a different velocity. In order to describe the mixture, conservation and constitutive equations are required as given below.

2.3.1.1 Conservation Equations

1. Mass Balance Equation:

$$\frac{\mathrm{d}\,\bar{\rho}}{\mathrm{d}\,t} + \bar{\rho}\frac{\partial\,\bar{v}}{\partial\,x} = 0 \tag{2.2}$$

2. Concentration Balance Equation:

$$\bar{\rho}\frac{d\,{}^{s}c}{dt} + \frac{\partial\,{}^{s}g}{\partial x} = \Theta\,{}^{s}M^{s}\varsigma \tag{2.3}$$

This equation is obtained from the mass balance equation and is used in conjunction with equation (2.2) to describe the concentration of each species of the mixture.

***3. Linear Momentum Balance Equation*:**

$$\bar{\rho}\frac{d\,\bar{v}}{dt} + \sum_{s}\frac{\partial({}^{s}v^{s}g)}{\partial x} = \frac{\partial\bar{\sigma}_{xx}}{\partial x} \tag{2.4}$$

4. Energy Balance Equation:

$$\bar{\rho}\frac{d\bar{e}}{dt} = -\frac{\partial\bar{\bar{q}}}{\partial x} + \bar{\sigma}_{xx}\bar{V}_{xx} + \sum_{s}\Theta\,{}^{s}M^{s}\varsigma^{s}\mu \tag{2.5}$$

$$\frac{\mathrm{d}}{\mathrm{dt}} = \frac{\partial}{\partial \mathrm{t}} + \bar{\mathrm{v}}_{\mathrm{k}}\frac{\partial}{\partial \mathrm{x}_{\mathrm{k}}}\ , \qquad \bar{\bar{q}} = \sum_{s}\left[{}^{s}q + {}^{s}e\,{}^{s}g - {}^{s}\sigma_{xx}\,{}^{s}\hat{v}\right] \tag{2.6}$$

2.3.2.2. Constitutive Relations

The porosity of the mixture α is defined as the ratio of the specific volume of the mixture to the specific volume of the solid. Then, $\bar{P} = \alpha \bar{P}_s\left(\bar{v}/\alpha, \bar{T}\right)$, where, $\bar{P}_s$ is the average pressure.

Porosity and Pore Collapse flux: The evolution equation for the porosity is related to rate of change of pressure in the mixture. $\bar{J}^{\alpha}$ is the non-equilibrium flux related to porosity. The pore collapse flux is taken to be a function of temperature, pressure and deviatoric stress as shown in equation (2.7).

$$\bar{\tau}_{\alpha}\dot{\bar{J}}^{\alpha} = -\bar{J}^{\alpha} + k_{\alpha p}\frac{\partial \bar{P}}{\partial x} + k_{\alpha T}\frac{\partial \bar{T}}{\partial x} + k_{\alpha\sigma}\frac{\partial \bar{\sigma}^{d}}{\partial x} \tag{2.7}$$

$k_{\alpha p}$, $k_{\alpha T}$ and $k_{\alpha\sigma}$ are material constants for pore collapse and $\bar{\tau}_{\alpha}$ is the relaxation time associated with the pore collapse. The relaxation time constant incorporates the fact that processes such as pore collapse do not take place at the shock front but occur only after a time lag.

Evolution of Heat Flux: The heat flux is described in the framework of extended irreversible thermodynamics. A relaxation time is introduced to modify the Fourier heat conduction equation to account for the time delay behind the shock front.

$$\bar{\tau}_{q}\dot{\bar{\bar{q}}} = -\bar{\bar{q}} - \bar{k}_{q}\frac{\partial \bar{T}}{\partial x} \quad \text{where } \bar{k}_{q} = \sum_{s}{}^{s}k_{q} \tag{2.8}$$

$\bar{k}_q$ the heat conduction coefficient and $\bar{\tau}_q$ i the relaxation time are associated with the transport of heat flux.

Chemical Reaction: Chemical reaction is initiated by a trigger for when the mixture energy is increased. This amount of energy that is needed to initiate the reaction is called activation energy. The rate at which a chemical reaction proceeds is measured by the quantity Θ, which is called the chemical reaction rate. The most well known and much used Arrhenius model is modified to account for the time delay behind the shock front.

$$\bar{\tau}_\Theta \dot{\Theta} + \Theta = {}^{+}A \exp\left(-\frac{{}^{+}E}{R\bar{T}}\right) \prod_{s+} \left[{}^{s+}\chi\right]^{s+\varsigma} \tag{2.9}$$

where $\bar{\tau}_\Theta$ is described to account for the relaxation time for the chemical reaction, R denoted the universal gas constant, T is introduced as the symbol for the temperature, A is known as the pre-exponential factor, + refers to the reactant group and ${}^{s+}\chi$ is introduced as the concentration of reactant species *s* in moles per liter.

It is assumed that the stress tensor in the mixture is a sum of the hydrostatic and deviatoric components. The deviatoric components were further divided into equilibrium and non-equilibrium components. The material is considered to be elastic-ideally plastic to describe the stress deviator.

2.3.2.3. Problem of Ni+3Al

A mixture of Ni-Al is now analyzed. The reaction equation is assumed to follow the equation: $Ni + 3Al \rightarrow NiAl_3$. This is true for temperatures less than 600° C.

For a numerical simulation, the problem of one-dimensional strain is studied. The initial velocity of all species of the mixture is assumed to be zero and the density of the mixture is obtained from the mixture theory. The Birch-Murnaghan EOS is used to describe the EOS of the individual species of the mixture.

$$P_i(\nu_i, \theta_i) = \frac{\beta_{\theta_0}}{n}\left[\left(\frac{\nu_i}{\nu_{i_0}}\right)^{-n} - 1\right] + C_{\nu_i}\left(\frac{\Gamma_0}{\nu_0}\right)_i \left(T_i - T_{i_0}\right) \tag{2.10}$$

here $C_\nu = T\left(\frac{\partial s}{\partial \nu}\right)_T$ is the constant volume specific heat, $\Gamma = \nu\left(\frac{\partial P}{\partial e}\right)_\nu$ is the Grüneissen parameter and

$\beta_T = -\nu\left(\frac{\partial P}{\partial \nu}\right)_\theta = \beta_{T_0}\left(\frac{\nu}{\nu_0}\right)^{-n}$ in which β_{T_0} and n= $\beta_{T_0}^{'}$ are constants specific to each species.

Table 2.1: Properties of Al and Ni

Property	**Al (s)**	**Ni (s)**
ρ_0 (kg/m^3)	2700	8909
β_{T_0} (GPa)	7.64	18.85
n	3.56	4.10
Γ	2.35	2.00
C_v (kJ/kg K)	0.931	0.512

The material properties for $NiAl_3$ were obtained from those of the reactants by using the mixture theory.

The activation energy is defined as the energy required by the reactants to reach an intermediate stage in the reaction process called the activated complex, where there are both reactant and product like features. According to Zewail [2.42], this intermediate stage or transition structure consisted of any and all stages that had potential energies significantly different from the reactants and products. The transition state, one that defined the reaction rate, would then be the saddle point in the reaction path - the state that had the highest energy. At the continuum level, the transition state is identified from energy considerations. The Gibbs free energy of each of the possible transition states as well as the reactants and

products were plotted [2.16] (Fig. 2.3). The state, which had energy greater than both the reactants and products but the lowest among all the identified and possible transition states, was selected as the most probable transition state. The following were identified as possible transition states: Ni_3Al(s or l) + Al(s); Ni(l) + 3Al(s); Ni(l) + 3Al(l) ; NiAl(s) + 2Al(s); NiAl(s) + 2Al(l); NiAl(l) + 2Al(s).

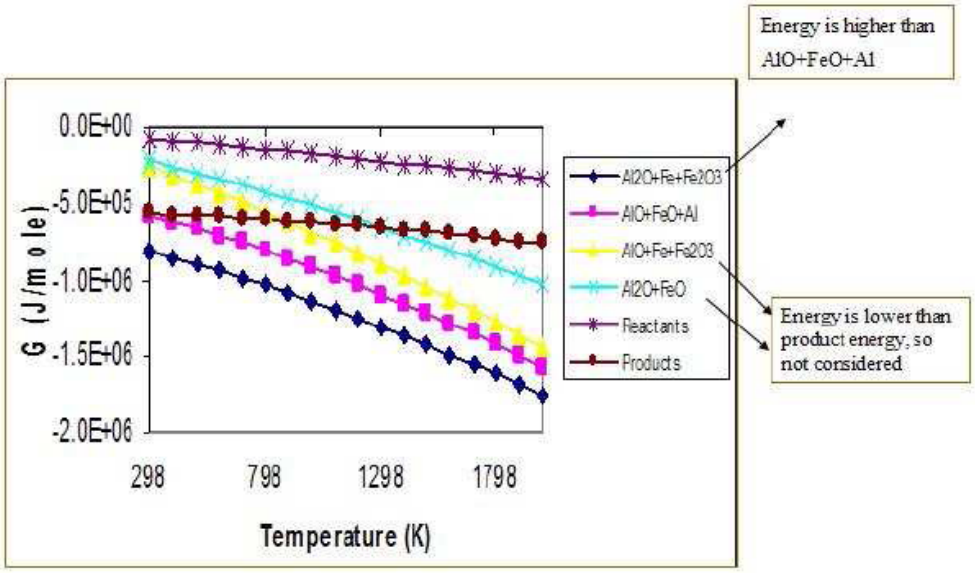

Figure 2.3: Transition states for the reaction of Iron Oxide and Al

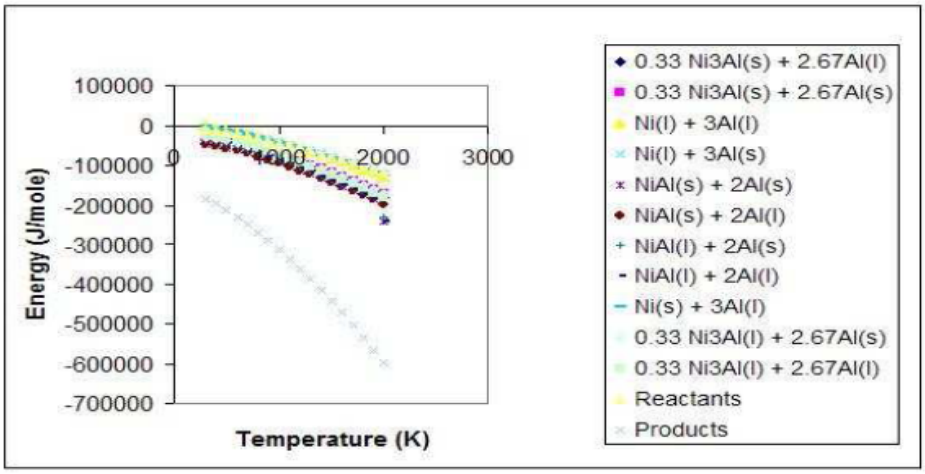

Figure 2.4: Plots of Gibbs free energy as a function of temperature for reactants, products and transition states

The transition state Ni(l) + 3Al(l) is the only one which had energy greater than both the reactants and products in the temperature range 298K to 2000K and is thus, chosen as the transition state for the reaction between Ni and Al. These results suggested a very high reaction initiation temperature and thus should be verified experimentally or by quantum mechanics many-body problem results.

A one-dimensional strain problem is used to study shock-induced chemical reactions in Ni and Al in a 50-50% ratio by volume mixture. The specimen was of length of 4mm and is subjected to a pressure boundary condition. The initial velocity of all particles was considered to be 0. The transition state had been obtained to be Ni(l) + Al(l), as shown in the previous section. An initial porosity of 1.5 is considered for the numerical simulation. The material is considered to be ideally plastic.

The figure below represented the plot that was obtained for a comparison study of two cases 1) a pressure of 7GPa and 2) 12GPa. This plot shows that the pressure and temperature increase for a higher pressure of 12GPa as compared to the case of 7GPa. Consequently due to the increased pressure and temperature, chemical reaction initiated and there was greater chemical reaction for the latter case than the former. This is observed from the concentration of the product. This figure also depicted the three waves – the elastic wave, non-linear shock wave and the delayed chemical reaction zone, thus showing the time delay in chemical reaction initiation.

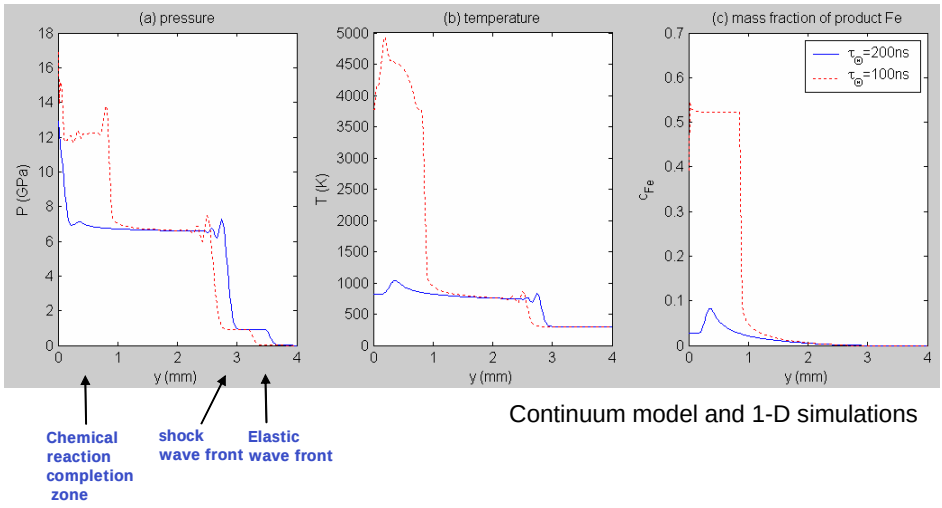

Figure 2.5: Numerical results for 1-D shock induced chemical reactions

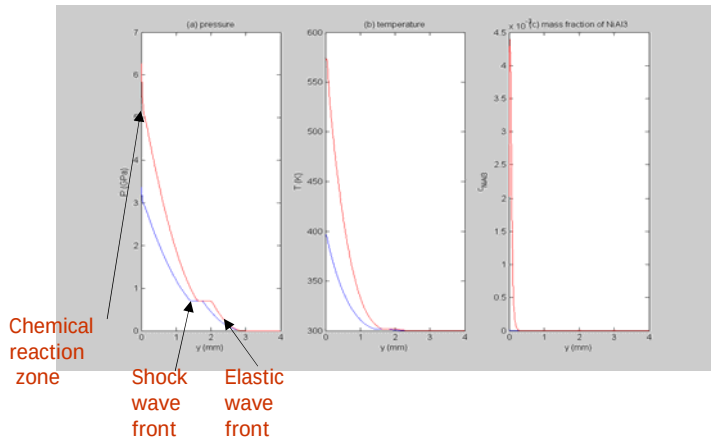

Figure 2.6: Numerical results for shock induced chemical reactions

2.3.2 Mesoscale Reaction Model

Reding and Hanagud developed a mesoscale reaction model. In this model, discrete clusters (also called as particles) are modeled. Each cluster of nickel or aluminum is modeled as a continuum. The large deformation impact dynamics of such a mesoscale system was first studied using the RAVEN Code. Results of the analysis provided a post shock conditions at the interfaces of the reactants. This information was used to incorporate a finite-time diffusion model to study the movement of the products of the reaction past the reactants to initiate new reactions. The model was not incorporated into a unified computer code to study reactions, similar to that presented in the previous section.

2.4. Research Issues and Thesis Outline

2.4.1 Research Issues

As discussed before, the initiation and sustained chemical reactions in reactive materials or reactive material structures, in macro scale, are addressed by Graham, Thadhani, Bosolough, Nesterenko, Horie, Eakins and others. Most addressed the issues of mechanical deformations, fracture of reactants, mixing of reactants, plastic flow and pore collapse, in the frame of equilibrium thermodynamics. Bosolough, through his experiments, observed that the rate of increase of temperature was too high to be explained by mechanisms such as mixing, diffusion, pore collapse and plastic flow. To accommodate Bosolough's comments and other related observations in experiments models by Thadhani and Horie, a chemical reaction model, with non-equilibrium thermodynamics and mixture theory was proposed by

Narayanan, Lu and Hanagud. In this model, a shock-induced chemical reaction model was in the frame works of non-equilibrium thermodynamics and mixture theories were still in a continuum or macro scale. This work displayed reactions, product formation and rise of temperature due to the exothermic reactions. The effectiveness of the model is illustrated by formulating a computer simulation of a one-dimensional numerical integration of the partial differential equations associated with a impact problem. This wok also, developed procedures to identify the transition state and the needed activation energy to reach the transition state, from enthalpic energy considerations. In mesoscale, Do and Benson discussed a model, but with infinite diffusion rate. This was modified with a finite diffusion rate model by Reding and Hanagud [2.15].

In these preceding works, the focus was on different processes that brought the reactants in close proximity with each other. Investigators were not focusing on the fact that actual chemical reactions were due to exchange of electrons and formed a process that followed the fact that the reactants were close to each other within a distance of few Angstroms, for the reactions to initiate.

The initiation of the reactions and the sustained chemical reactions also depended on the fact that the post shock processes were capable of taking the reactants to the transition state. Depending on the phases of the products, the sustained reactions proceeded unless it is affected by other processes such a need for the reactants to move past the products, to form

new contact zones. Also, it is to be noted that the transition state obtained by Narayanan, Lu and Hanagud assumed that the transition states form only through a thermal energy input, static conditions and in the framework of equilibrium thermodynamics. Other shock induced or assisted effects such as the strains (and associated stresses), strain rates, different velocities of the reactants, effects of any defects are ignored.

In reality, the reactions may initiate at different temperatures if these effects are included. It is for this reason, it is necessary to study these fundamental processes by the use of ab initio techniques and ab initio-molecular dynamics (or quantum molecular dynamics) to determine the transition state and the following reactions, In an ab initio molecular dynamics the calculation of intermolecular forces are at each time step of molecular dynamics, from approximate solution to the Schrodinger's equations by the use of density functional theory, on the basis of the new positions of the ions. In many other molecular dynamics approaches, such as the ReaxFF code, this is not done at each time step. The ab initio- molecular dynamics results can again be bridged to meso- and continuum scales by using the principle of thermodynamics. The ab initio-approach is the new work in this thesis. Ab initio studies are to explain paths to the transition state and the reaction initiation and the reaction path.

The example of the reaction of Ni + Al is in this thesis. The ab initio molecular dynamics yield possible bonds at each step and the associated energies. As a first step, systematically, different combinations of thermal input and mechanical strain effects form the inputs,

without completely simulating all other shock-induced effects. Then, at each step it is possible to calculate the amount of energy absorbed by the reactants indicating an endothermic reaction until transition state products Ni+Al is observed. Then, the reaction becomes exothermic with the formation of products. Different combination of thermal input and mechanical strain input is to simulate some of the post shock effects or the effect (or the explosive reaction of organic energetic materials if they are used to initiate the reactions of reactive materials or reactive material structures. To set up the initial configuration for ab initio molecular dynamics the optimized electronic structure of the reactant combinations, their surface orientations and constitutive equations are necessary under strain and initial temperature conditions.

In addition to the constitutive equations and results from ab-initio molecular dynamics, other characteristics such as, the effect of strain rate, defect size and concentration on local heating, diffusion, mixing and the on-set of failure are necessary to simulate the shock-induced chemical reactions in a continuum scale with computer codes such as the codes commercially known as the "hydro-codes". Prior to the direct formulation of computer simulations (integration of appropriate conservation and constitutive equations) the analysis of results is at a mesoscale, then formulated to bridge to the continuum scale for use in hydrocodes, because some effects such as the mixing of reactants are easy to simulate in a mesoscale.

2.4.2 Ab initio Techniques and Two Condensed Matter Reactants

As discussed in the chapter1, the study of chemical reactions of reactive material structures involves at least two condensed matter reactants that are subjected to shock loads, with elevated temperatures. Most of the ab initio studies of chemical reactions, in the field of chemistry and engineering, are usually concerned with catalysis and sensor designs. These ab initio studies usually consider adsorption, chemisorption and catalytic reactions between one condensed matter (metal) and gasses such as CO. Thus, most of the published works do not consider reactions between two condensed matters such as nickel and aluminum, with strains, defects and elevated temperatures resulting from processes such as impact and the resulting shock loads. The specific class of ab initio problems that is related to the chemical reactions of intermetallics is as follows:

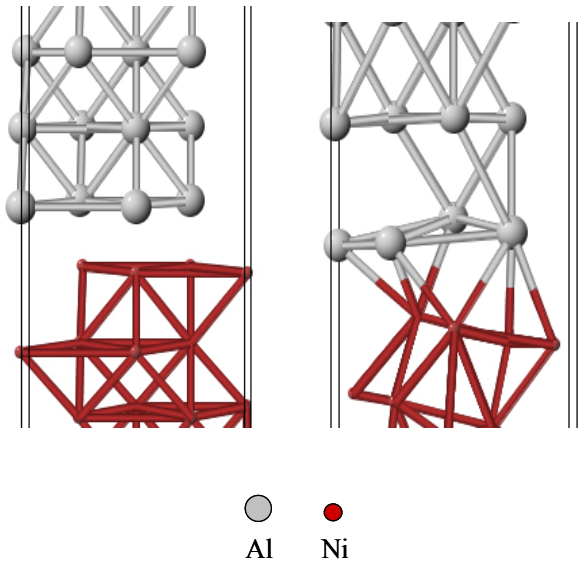

Figure 2.7: Ni and Al at 100 ^{o} C and 650 ^{o} C, respectively

However, the current ab initio research in the field of chemistry and engineering study problems such as the following class of problems.

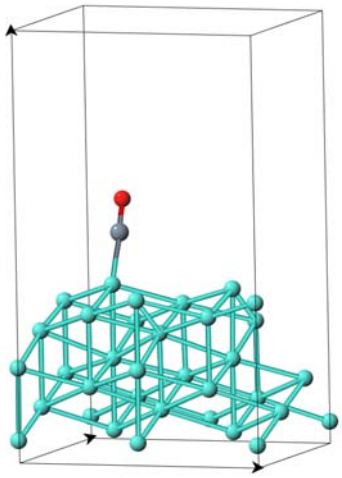

Figure 2.8: CO and W: “On-Top” adsorption

The problem studied is that of the adsorption and possible disassociation of CO on tungsten surfaces. Specifically, this type of processes is of interest in improving the Fisher-Tropsch process for production of alternative fuels to petroleum. The process is named after the inventors Fisher and Tropsch who practically produced (1920s) synthetic fuel for use in trucks in Germany, a petroleum-poor country. Today, the process is being studied extensively to improve the efficiency and cost of the process and produce alternative fuels to compete with the petroleum-based fuels. In principle the reaction is as follows.

$(2n+1)H_2 + n(CO) = C_n H_{2n+2} + n(H_2O)$

In this equation “n” is a positive integer. Catalysts are selected first to disassociate CO in to

C and O and secondly to favor a reaction that results n >1. The number n=1 results in methane that is not desired. Iron and Cobalt are the original choice of catalysts. Currently, the use of tungsten (W) is being explored as an efficient catalyst.

The studies on the adsorption and chemisorption of CO on W started as research in experimental studies during late 1950s. Some of the early papers are by Ehrlich (The J. Chemical Physics, 34, 39, 1961); Madey et. al. (The J. Chemical Physics, 42, 4 19650 and discussions in the volumes of advances in catalysis, systematic ab initio studies, with the evaluation of binding energies are due to Chen, Scholl and Johnson (J. Phys. Chem. B 2006) and Scheijen, Niemantsverdriet and Curulla-Ferre, J. Phys. Chem. C 2008). In these theoretical studies, both alpha and beta state of CO are considered but at their ground states (zero degrees Kelvin). Their studies do not consider the effects of strain as discussed in some of the recent publications with metals other than tungsten. All the papers do not consider elevated temperature effects.

The interaction of tungsten with hot gasses such as CO, HCl, O and H_2O are also important in studying the erosion of tungsten nozzles, due to interaction with the combustion products of solid propellants in solid rocket motors. Of course the nozzle is also subjected to strains in addition to elevated temperatures.

Now, returning to the works of Chen, Scholl and Johnson, Chen et. al. have reported a study

of binding energy of adsorption, without considering the effects of strain of W or the effects of elevated and temperature of tungsten. They also have not discussed the convergence of the DFT calculations as a function of the cutoff energy and k-points. The goals of this thesis work are to reproduce the results of Chen et. al., check for convergence and extend the results to include the effects of different types of strains, elevated temperature and defects. The techniques are then modified to study reactions of condensed matter-reactants of reactive material-structures.

2.4.3 Thesis Outline: Selected Research Tasks

1. **1.** Ab initio Studies of Binding energies associated with chemisorption of (a) CO on W surfaces (111, and 100) at elevated temperatures and strains and (b) adsorption of hydrogen in titanium base. Then conduct similar studies concerning Ti+H and extend the results to improve the hydrogen storage of fuel cells by use of strain.
2. **2.** Equations of state of mixtures of reactive material structures from ab initio methods.
3. **3.** Ab initio studies of the reaction initiation, transition states and reaction products of intermetallic mixtures of (Ni+Al) at elevated temperatures and strains.
4. **4.** Press-cure synthesis of nano-nickel and nano-aluminum based reactive material structures and DTA tests to study experimentally initiation of chemical reactions, due to thermal energy input, to validate the ab initio results.

CHAPTER 3

ADSORPTION OF CO ON STRAINED AND HEATED TUNGSTEN

The details of the research studies, in this chapter, result from two specific objectives. The first objective is to understand ab initio chemical reaction studies by comparing the results with published literature. The subject of the chemisorptions and disassociation of CO (carbon monoxide) on W (tungsten) are of significant interest in improving the synthetic fuel (energy) production techniques. The previous density functional theory-based work on the adsorption of W+CO does not describe convergence studies due to the selection of a cutoff energy and selection of k-points. Thus, the first step is to conduct these convergence studies. Then, the second objective is to explore the effects of mechanics and thermo mechanics on chemisorptions. Results of the research work during the past decade [3.1-3.6] indicate that the effect of certain types of mechanical strain alters the adsorption process. Thus, the specific goals of the second objective are to explore the effects of strain on the binding energy, resulting from the adsorption process. This subject of research has a new name of "chemo-mechanics". Results of the second objective has also significant amount of benefit in another branch of energy related research concerning fuel-cells. In this area the subject of hydrogen storage in metals such as titanium is important. Depending on the type of strain, both storage and release of hydrogen are affected. The objective is to study changes in the binding energy due to strain and select strain as a control in efficient adsorption and release of hydrogen for combustion.

3.1 Background on Adsorption of CO on W

The chemical reaction of CO with hydrogen is of interest in producing synthetic fuels. The chemical reaction of interest involves the following types of chemical reactions [3.7-3.15].

$$(2n+1)\ H_2 + n\ (CO) = C_n + H_{(2n=2)} + n(H_2O)$$

The resulting hydrocarbons are alkanes. All hydrocarbons other than n=1 are of interest in producing synthetic fuels. The chemical mechanisms require conversion of CO to C-O bonds via possible initial formation of surface bound metal carbonyls. Thus, catalysts, such as cobalt, iron and ruthenium are necessary to complete the required chemical reaction through disassociation of CO, at temperatures varying between 150 to 300 degrees Celsius. Other catalyst, such as Nickel usually favors an undesirable product, such as methane (n=1). During the past few years other catalysts, including tungsten, are subjects of investigation.

The original process is the result of studies by Franz Fischer and Hans Tropsch [1.22] during 1920s. Historically, the process benefits coal-rich geographical areas. For example, Germany is the beneficiary of the process in producing fuel for trucks in 1930s. Other beneficiaries include South Africa. More recent exploration of the process is by U.S. Air force. Thus, the subject of adsorption of CO on W, with mechanical strain, is of significant amount of interest to improve the Fischer-Tropsch process, in search for alternate sources of energy.

There are many reported studies on the subject of the adsorption of CO on W since the 1960s. More specifically, CO adsorption on transition metal surfaces has been subject of significant interest from the point of view of understanding catalysis. Of special interest in studies related to W and CO is because of the opinion of many researchers that W is the borderline of disassociative adsorption as we move from left to right of the periodic table, of transition metals. There are significant amount of discussion concerning the disassociation and non disassociation of CO on W as a function of it's α or different β states. Kim, Boo and Lee discuss this subject in 2009. Their discussions point in the direction of disassociative adsorption. In their paper, which is experimental in nature, they also display binding energies as a function of the temperature.

The objectives this research is to focus on the mechanisms of adsorption of CO on W through density functional theory-based ab initio studies of the binding energy. (The basic concepts of the Density Functional Theory and some related applications are discussed in Appendix A)The publications in this area are relatively few. In a publication of 1999, Ryu et. al. present a study that uses molecular orbital theory, by using three layers. For a bcc metal three layers represent the minimum number of layers for W (111) surface studies. In 2006, Chen, Scholl and Johnson [1.20] present a density functional theory-based study of adsorption and disassociation of CO on W (111). In their studies, they calculate binding energies, vibrational frequencies and diffusion/disassociation pathways of CO on W. Specifically, they consider both clean and carbon – preadsorbed W (111) surfaces. They use Vienna ab initio simulation

(VASP) package to perform the density functional theory-based calculations. They use revised Perdue-Burke-Ernzerhof (rPBE) exchange-correlation functional. Reasons for selecting rPBE, instead of PW91 are because of published results concerning prediction of binding energies that are compatible with experimental observations [3.22]. For electron-ion interactions, they use projector augmented wave (PAW) pseudopotentials. They also use a smearing technique, with a smearing width of 0.1 electron volts to minimize the errors in Hellmann-Feynman forces, due to electron free energy. The sampling of Brillouin zone is with 13 irreducible k-points (5x5x1) of Monkherst-Pack scheme [3.23]. They also consider 6 to 11 layers of W-slab. Their calculations suggest that a consideration of 6 layers yield sufficient accuracy. However they do not perform convergence studies with varying cutoff energies but they select 400 eV arbitrarily.

Calculations of binding energies (E_b) by Chen et. al. [1.20] use the following definition.

$$E_b = E_a + E_{slab} - E_{a/slab} \tag{3.1}$$

In this equation, E_a is the energy of the isolated molecule of CO. The term E_{slab} is energy of the W (111) slab and the term $E_{a/slab}$ is the energy of the slab with adsorbed CO. With this definition, a positive value of E_b corresponds to a stable adsorption. All calculations are at the ground state or zero degrees Kelvin. In addition to the calculation of the binding energy,

Chen, Scholl and Johnson also calculate vibrational frequencies by diagonalizing the Hessian matrix of selected atoms. The calculation of Hessian matrix also uses the VASP techniques. Their calculation of diffusion and disassociation pathways is by the use of nudged elastic band method.

Following the work of Chen, Scholl and Johnson, Scheijen, Niemantsverdriet and Curulla-Ferre [2.19] report a DFT-based study of the adsorption, Desorption and disassociation of CO on W (100) surface. Calculations in this thesis follow the procedures of Chen, Scholl and Johnson for binding energies and vibrational frequencies. In the paper they also refer to an earlier theoretical work on adsorption of CO on W (100) by Lee et. al., which uses extended molecular orbital by Huckel. The DFT-based theory for the adsorption of CO on W is still restricted to two papers.

In 2009, Kim, Boo and Lee report on experimental studies of the adsorption behavior of CO on W at elevated temperatures by using synchrotron radiation. Both the technique and observations at elevated temperatures pose new questions than answers, suggesting that additional ab initio studies are necessary to understand the mechanisms of adsorption, desorption and disassociation of CO on W.

3.2 Research Issues Concerning Ab Initio studies of Adsorption, Desorption and Disassociation of CO on W

In density functional theory-based ab initio studies of adsorption desorption and disassociation of CO on W, the current publications consider binding energies at zero degrees Kelvin. The publications consider only adsorption of CO on unstrained W (111) and W (1OO), their ground state binding energies and the vibrational frequencies. To understand the subject and answer many unanswered questions some additional work is necessary in the following areas.

(1) First item is to check results of Chen et. al. for convergence on the basis of different selection of cutoff energy.

(2) Research results of the past ten years clearly indicate that metals with strain have the potential to change the chemical reactivity. Thus, it is of significant amount of interest to study (a) changes in the binding energy, vibrational frequency and possible disassociation of CO on W with different amount and types of strain on W (111), W (100) and W (110). VASP package is useful in these studies. Studies with zero strain provide a check of the new work with the results presented by Chen et. al. Also, it is necessary to examine the effect of fixing several layers of W on the projected results.

(3) To answer some of the questions concerning the effect of elevated temperature on adsorption, desorption and disassociation of CO on W, it is necessary to address the issues through the use of ab initio-molecular dynamics (or quantum molecular dynamics (QMD) studies.

(4) The third item is to combine different combination of 3-dimensional strain and elevated temperature on the adsorption, desorption and disassociation of CO on different W surfaces.

3.3 Selected Research Program for this Research

Because a detailed program is extensive, specific studies of the research discussed in this chapter are restricted to the following tasks.

(1) Check for convergence on the basis of selection of cutoff energies and selection of k-points.

(2) Validate the procedure by comparing the studies at a value of zero strain with the results of Chen et. al. by using the VASP package.

(3) Study the effects of uniform compression and extension on the binding energy of CO on W (111) at zero degrees Kelvin.

(4) Study the effects of elevated temperature on the binding energy of CO on W (111), by using ab initio molecular dynamics techniques.

3.4 Binding Energy Calculations with Uniform Compressive Strain

Chen et. al. in 2006 report on the results from density functional theory calculations using the VASP package at 0° K for the α binding site of CO on W(111) surface, modeled by a 7-layered W slab and one CO molecule. They use a primitive unit cell (1x1 rhomboidal cell)

for the 111 cross-section of W, i.e. one W atom per layer. In all our calculations (except for one) we use a 2x√3 rectangular unit cell, called "2x2" for convenience. There are four W atoms per layer, so the CO coverage is ¼. We also use for comparison a 1x√3 rectangular unit cell, called "1x2" for convenience. There are two W atoms per layer, and the CO coverage is ½. In all calculations the lower 3 layers are fixed. We also examine a 2x2 cell with an additional geometric constraint, namely the angles of the upper 4 layers are fixed, which prevents shearing deformation to alter the BCC system.

Before presenting the results, a first study is to examine the effect of the cutoff energy. The paper of Chen et. al. does not describe such calculation. The following plot summarizes all calculations with varying cutoff energies.

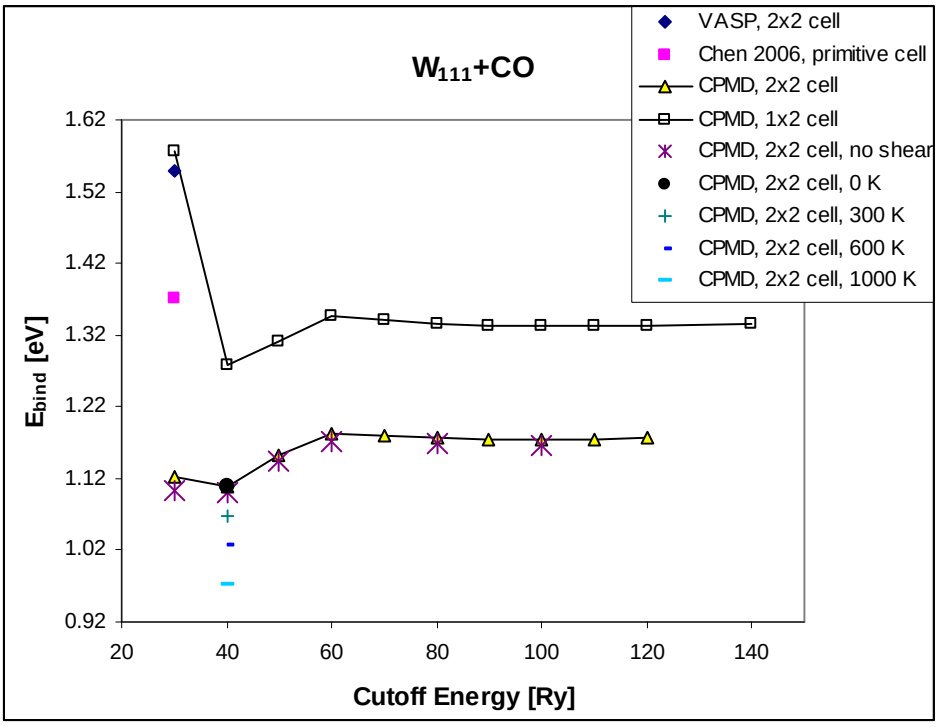

Figure 3.1: Convergence of binding energy as a function of cutoff energy

The following are the observations from this cutoff energy studies. In the paper by Chen, Scholl and Johnson, the cutoff energy is 400 eV (or approximately 29.4 Ry). The figure clearly indicates that this is not in the range of convergence. It is necessary that the cutoff energy is at least 80 Ry or higher. This corresponds to at least 800ev. Thus the calculations are done with at least 60 Ry or 800 eV. Similarly the cell size of 2x2 is necessary. Further, in some of the calculations it is necessary that the BCC structure is maintained with angular constraints. These are "no shear" condition in the figure. The binding energy calculations, at zero degrees Kelvin, are in Table 3.1 for different magnitudes of compressive strain.

Table 3.1: Variation of free energy (eV) and binding energy (eV) of the W(111)+CO system

Strain	E_W	E_{CO}	E_{W+CO}	E_{bind}
0.90	-323.131344	-14.790398	-339.849869	1.928127
0.95	-331.307796	-14.790540	-347.837424	1.739088
0.970	-332.091033	-14.790562	-348.509058	1.627463
0.975	-332.111390	-14.790560	-348.511606	1.609656
0.99	-331.794706	-14.790643	-348.147241	1.561892
0.995	-331.562528	-14.790583	-347.905370	1.552259
1.00	-331.257072	-14.790658	-347.595933	1.548203

It is also necessary to calculate the binding energy of W, accurately at least to the sixth decimal place because of the large differences in the energies of W and CO. A plot of the change of binding energy with uniform compressive strain is in the following figure. In all these calculations, the CO is in the α - state as shown in the JMol plots (Figs. 3.3-3.9).

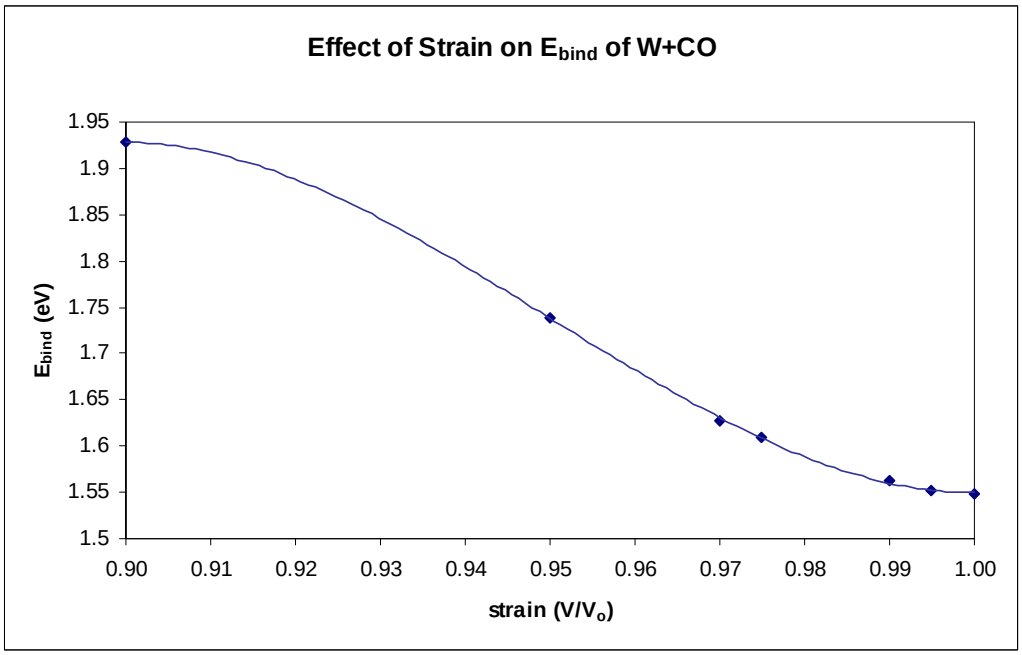

Figure 3.2: Effect of uniform compression on the binding energy

The relaxations of W and W+CO are also visualized through JMol plots as shown below.

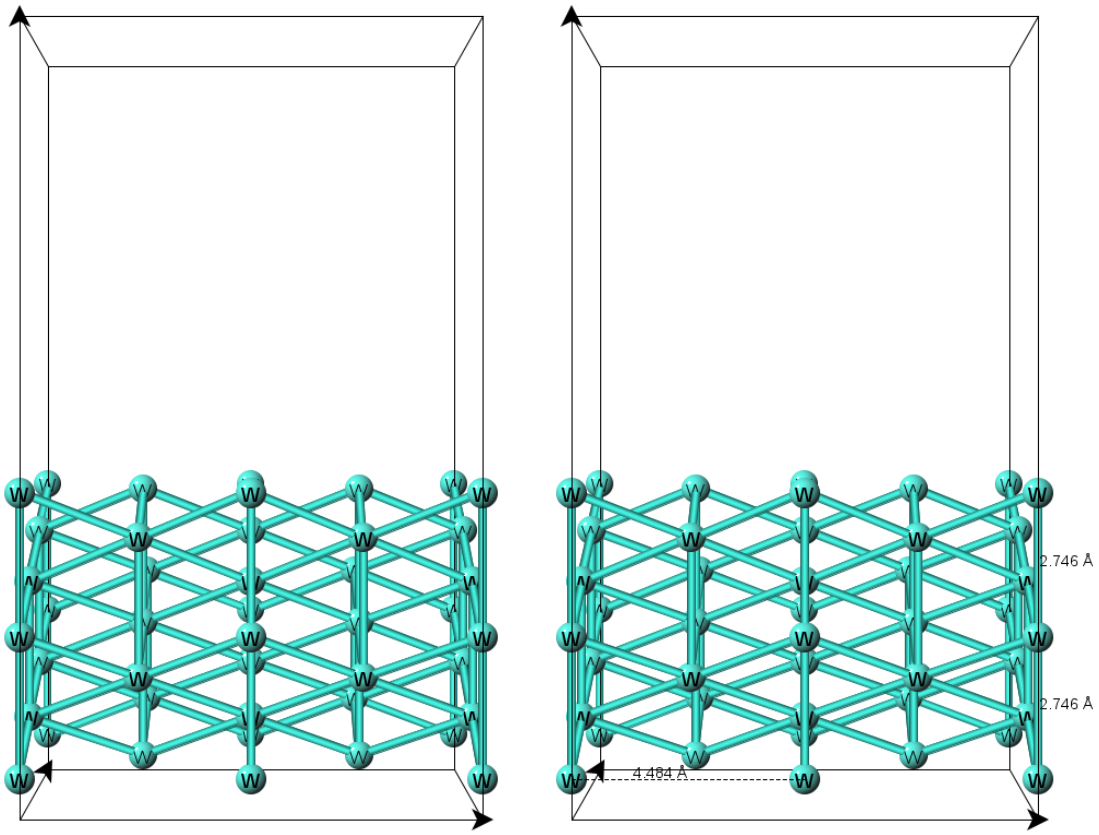

Figure 3.3: W (111) before relaxation, perspective view

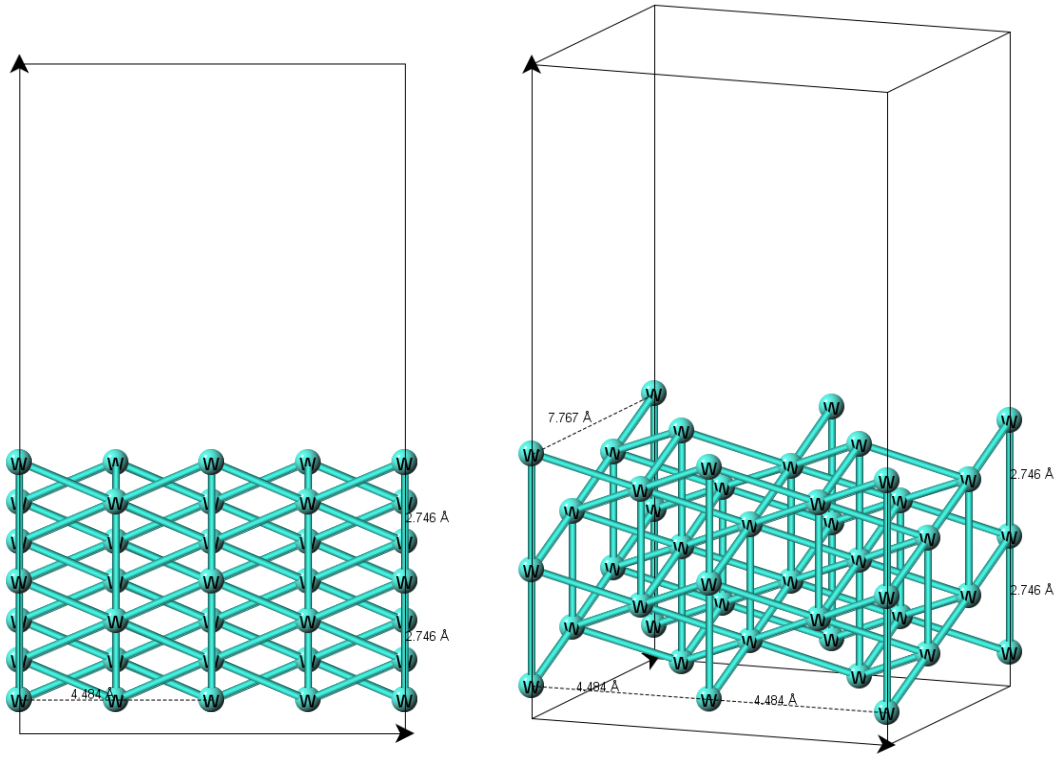

Figure 3.4: W (111) before relaxation, without perspective view

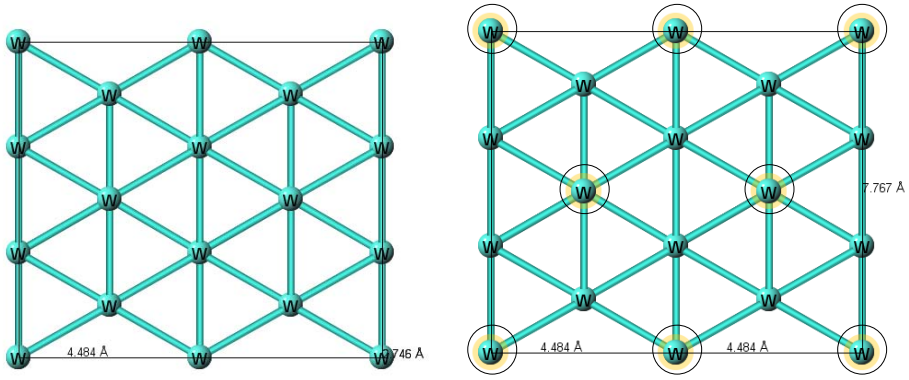

Figure 3.5: W (111) before relaxation, top view

Note: The highlighted/circled atoms are the ones from the uppermost W layer, i.e. the free (111) surface.

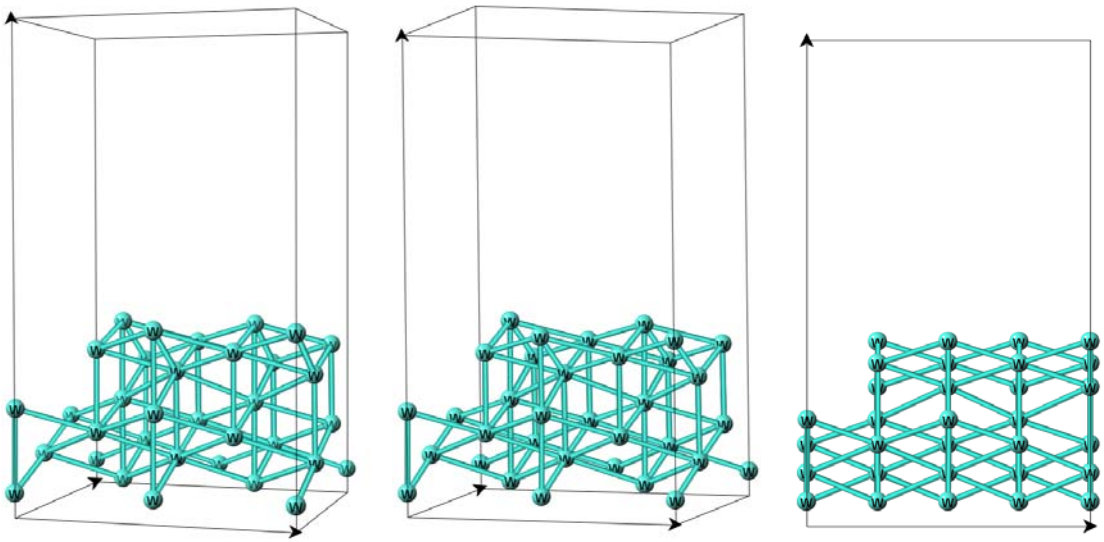

(a) (b) (c)

Figure 3.6: W (111) after relaxation: (a) with perspective view;
(b) and (c) without perspective view

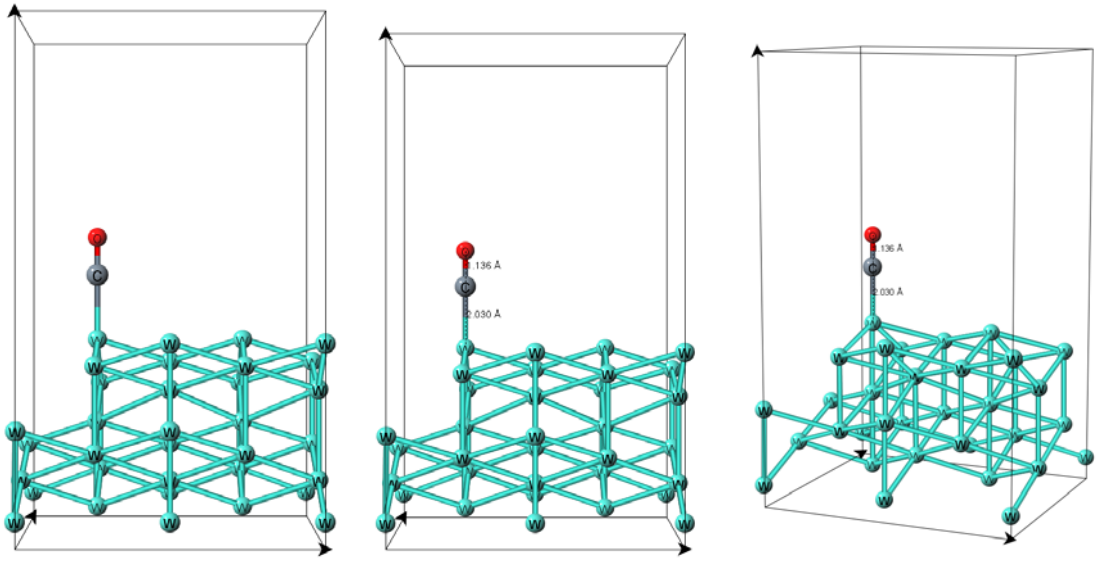

Figure 3.7: W (111) + CO before geometry optimization with perspective view

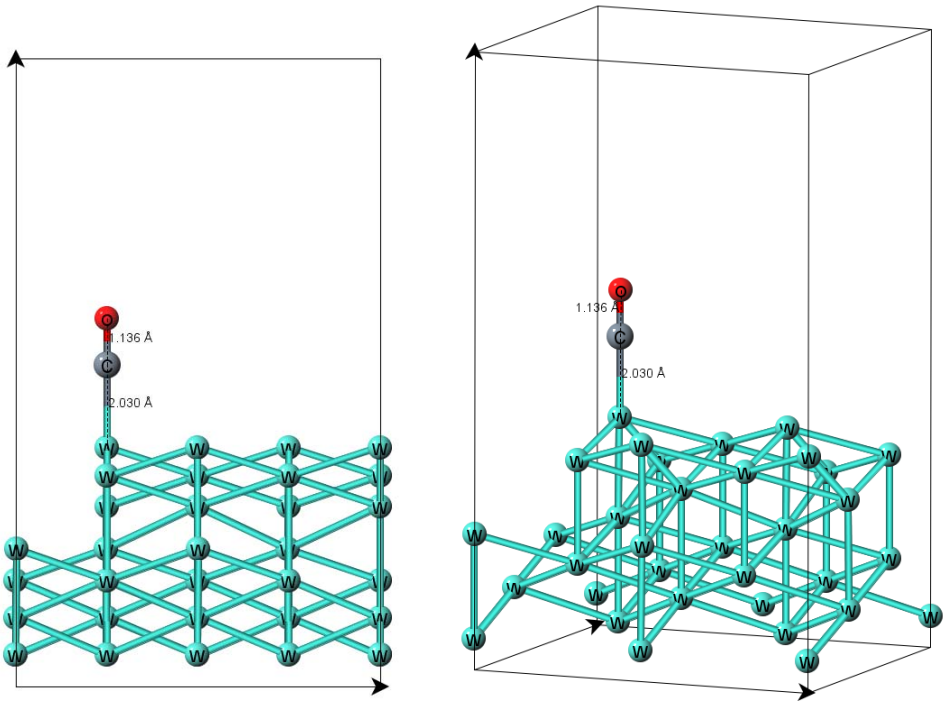

Figure 3.8: W (111) + CO before geometry optimization without perspective view

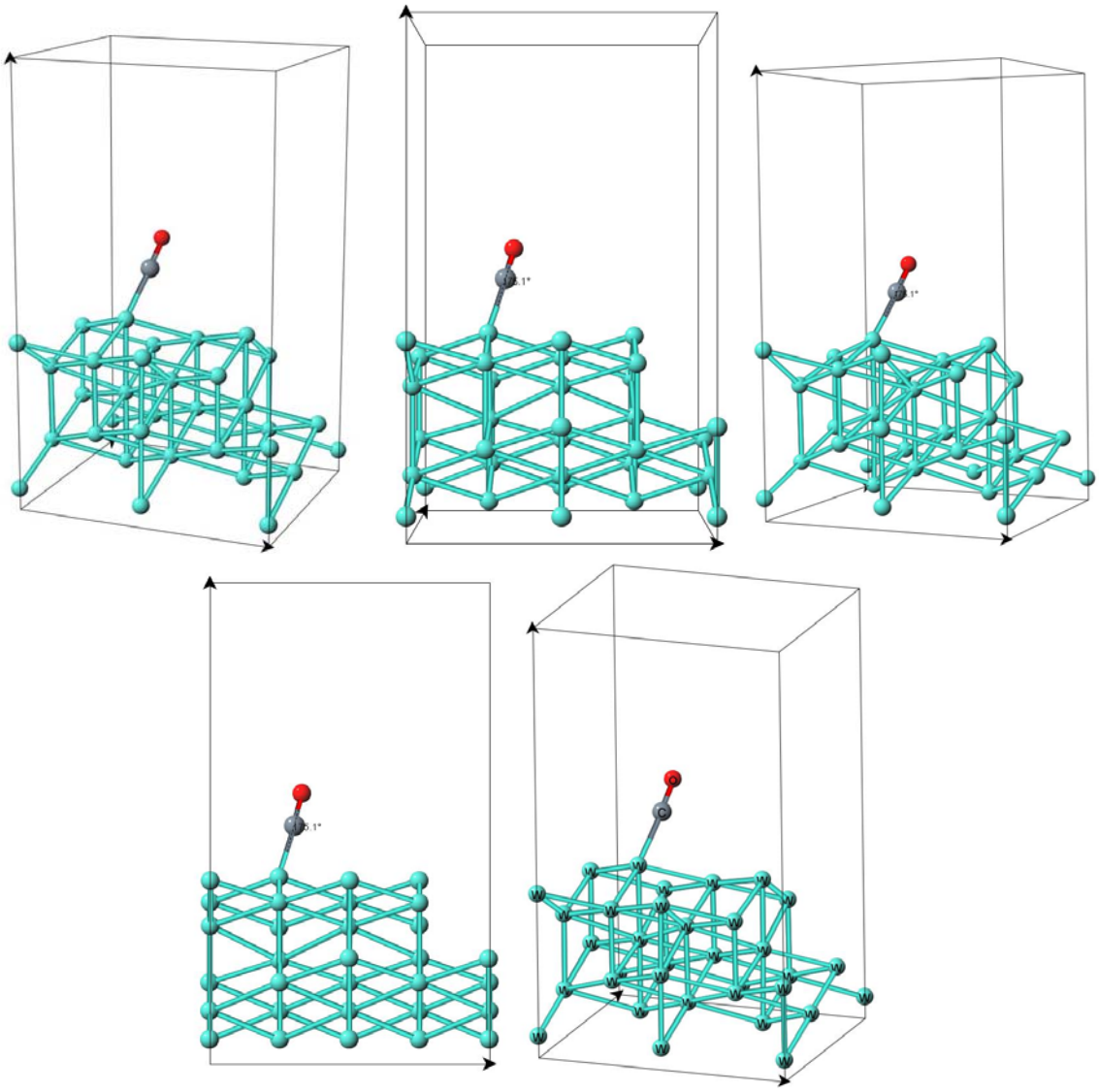

Figure 3.9: W (111) + CO after geometry optimization

3.5 Effect of Temperature on the Binding Energy

The effect of temperature on the binding energy of the W(111)+CO system was examined by performing quantum molecular dynamics simulations. This was accomplished by using Car-

Parinello Molecular dynamics procedure where the mass of the electrons were artificially increased to improve the computational efficiency without significantly altering the ion motion and the temperature (CPMD). The molecular dynamics calculations proceeded for certain duration of time. The wave function convergence was controlled by optimizing the wave function at each time step. The plots below show the first 80 steps (~10 fs) of the simulations, and in greater detail – the first 30 steps (~4 fs). The increase in temperature has a diminishing effect on the binding energy. There is certain variation of E_b as the simulation proceeds (see next plot), which is exhibited more strongly at higher temperatures. This is to be examined in detail, as this could be due to desorption or disassociation of CO. However, the first 10 steps data are as follows:

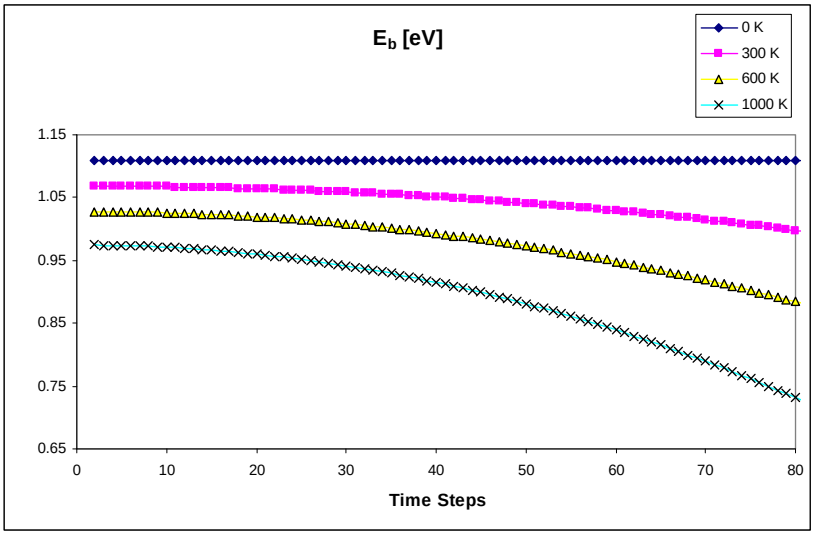

Figure 3.10: The binding energy for the W(111)+CO system under temperature

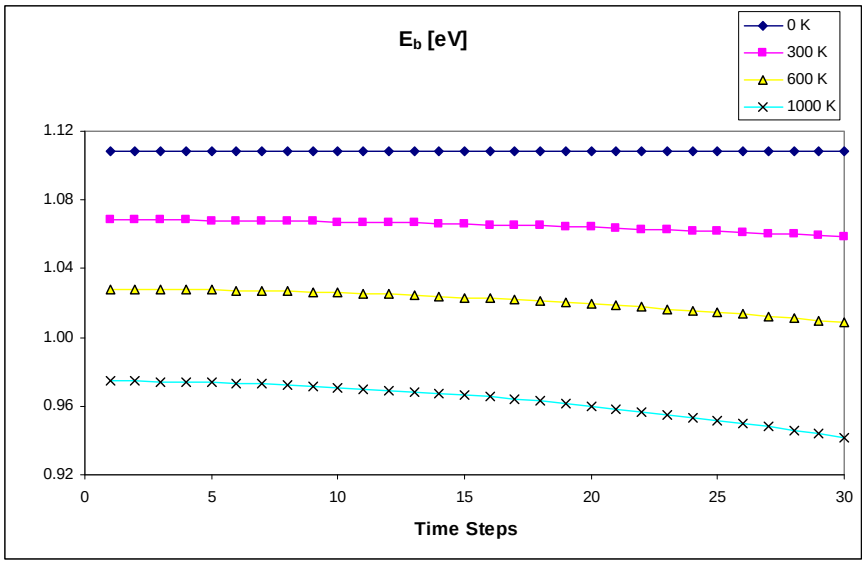

Figure 3.11: Binding energy variation for ~4 fs

CHAPTER 4

CONSTITUTIVE RELATIONSHIPS OF DUAL FUNCTIONAL ENERGETIC STRUCTURAL MATERIALS

4.1 Introduction

In this chapter, a specific dual functional material is considered, to study the equation of state of mixture. The dual functional structural energetic material considered is a mixture or a composite of nickel, aluminum and binders. This is not an alloy or a compound. In pursuit of formulating the constitutive relationships for such materials, a first step is the determination of the thermodynamically complete equation of state $P=P(\rho,T)$ for the selected intermetallic mixture of nickel and aluminum, with or without the binder and reinforcements, for pressures up to 300GPa and temperatures up to 1000K. The calculations for the equation of state (EOS) are in the framework of the density functional theory (DFT), using generalized gradient approximations and ultra soft pseudopotentials as shown in Fig. 4.1 to 4.7. The phonon modes are calculated by using the density functional perturbation theory (DFPT). First, the EOS for each species is obtained based by using density functional theory and DFPT. Because first principles are not used for mixtures, continuum mixture theories are utilized first to obtain the EOS for the mixture by using DFT and DFPT based approach for individual components. Then, a super cell approach, similar to the virtual crystal approximation, and first principle methods are used to compute the equation of state and the results are compared with the mixture theory results. Two mixture theories are proposed,

which correspond to the two limiting cases. The nature of the real mixture is intermediate to those of the two idealized mixtures and hence can be modeled as a weighted combination of the two cases. The derived EOS for nickel and aluminum mixture is compared with the results from tests on mixtures.

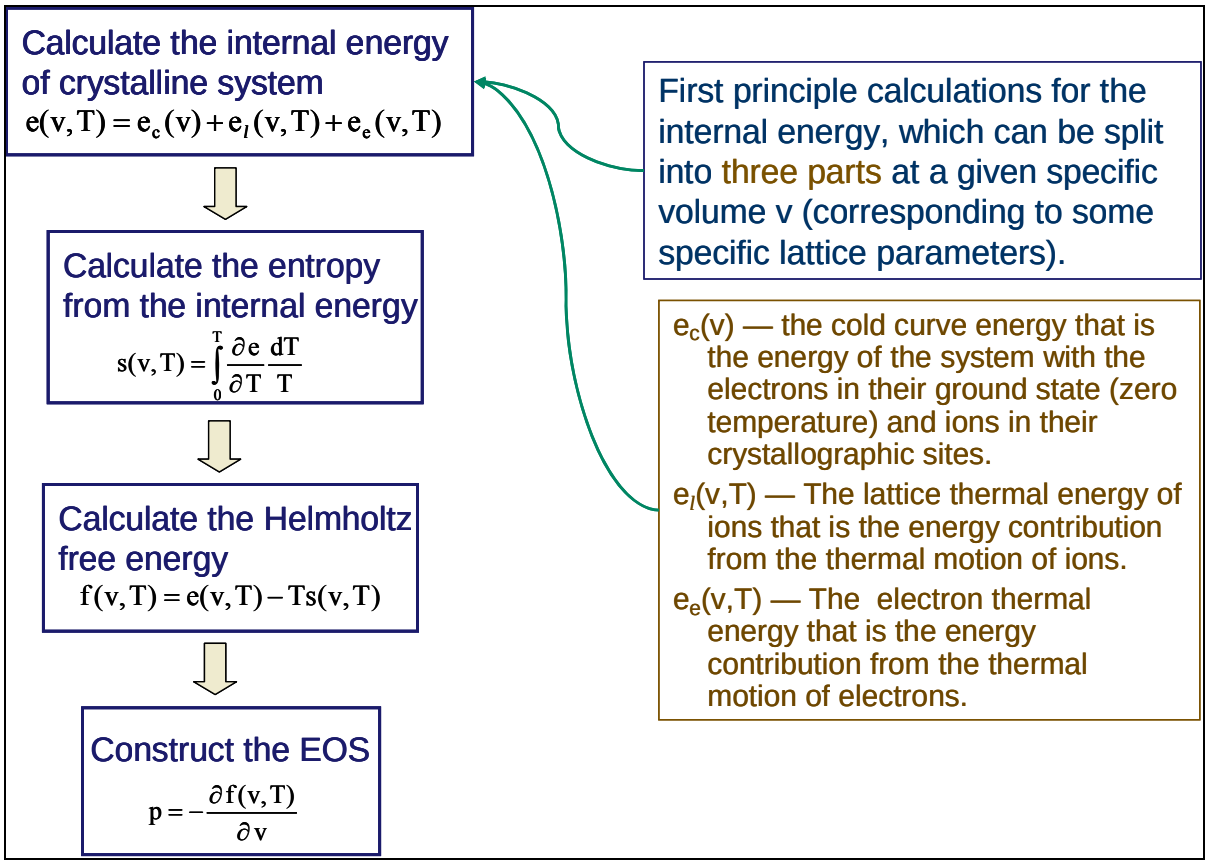

Figure 4.1: Ab initio procedure to construct EOS

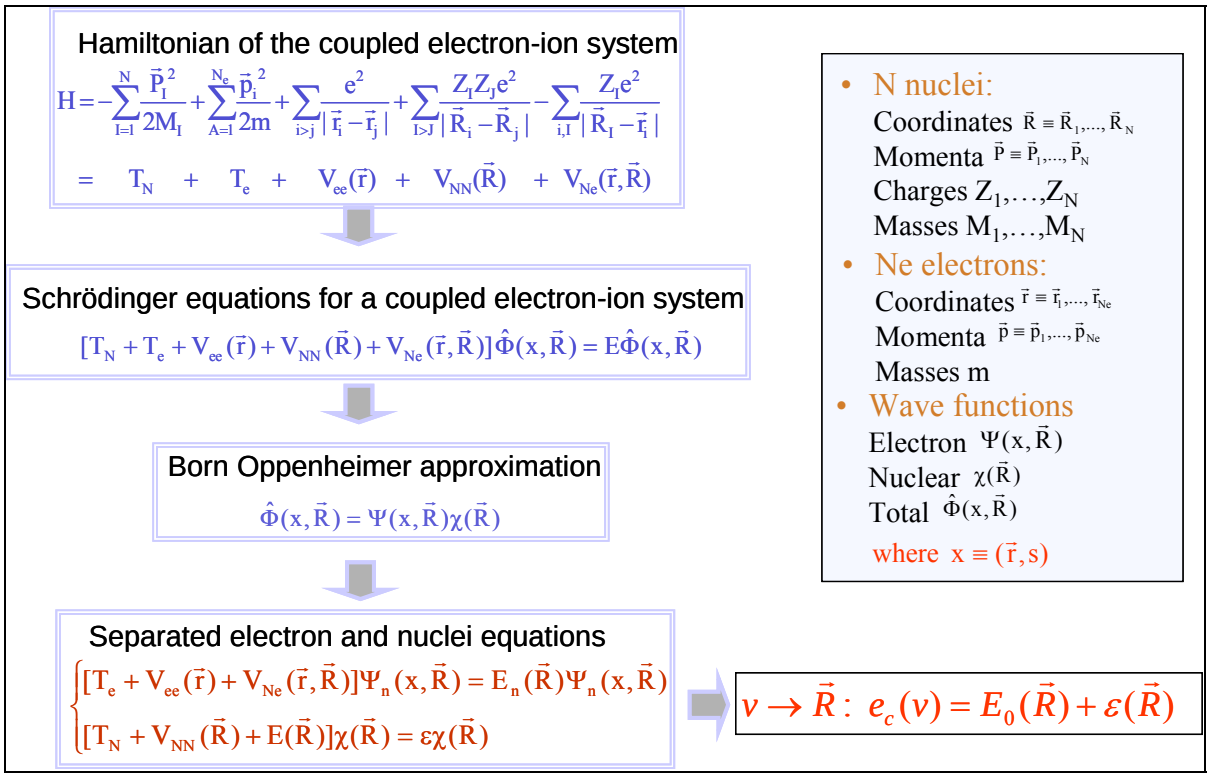

Figure 4.2: Ab initio technique

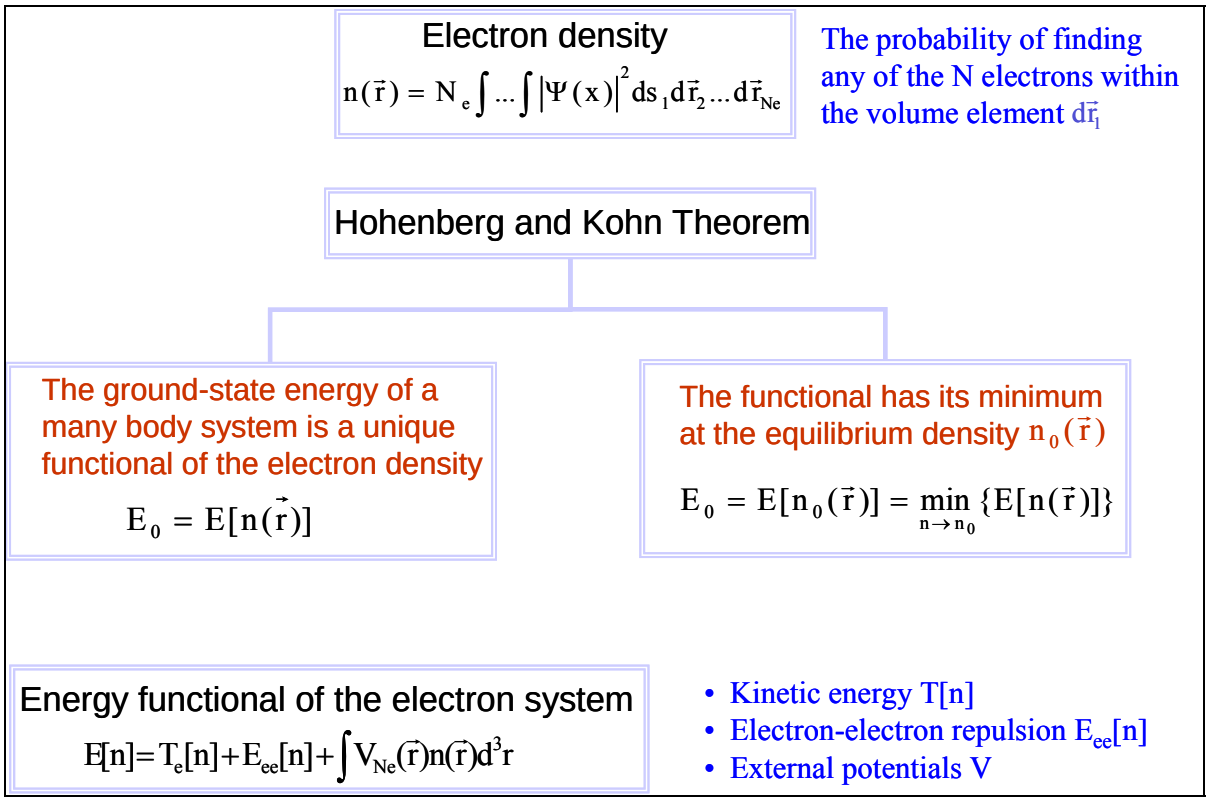

Figure 4.3: Density Functional Theory

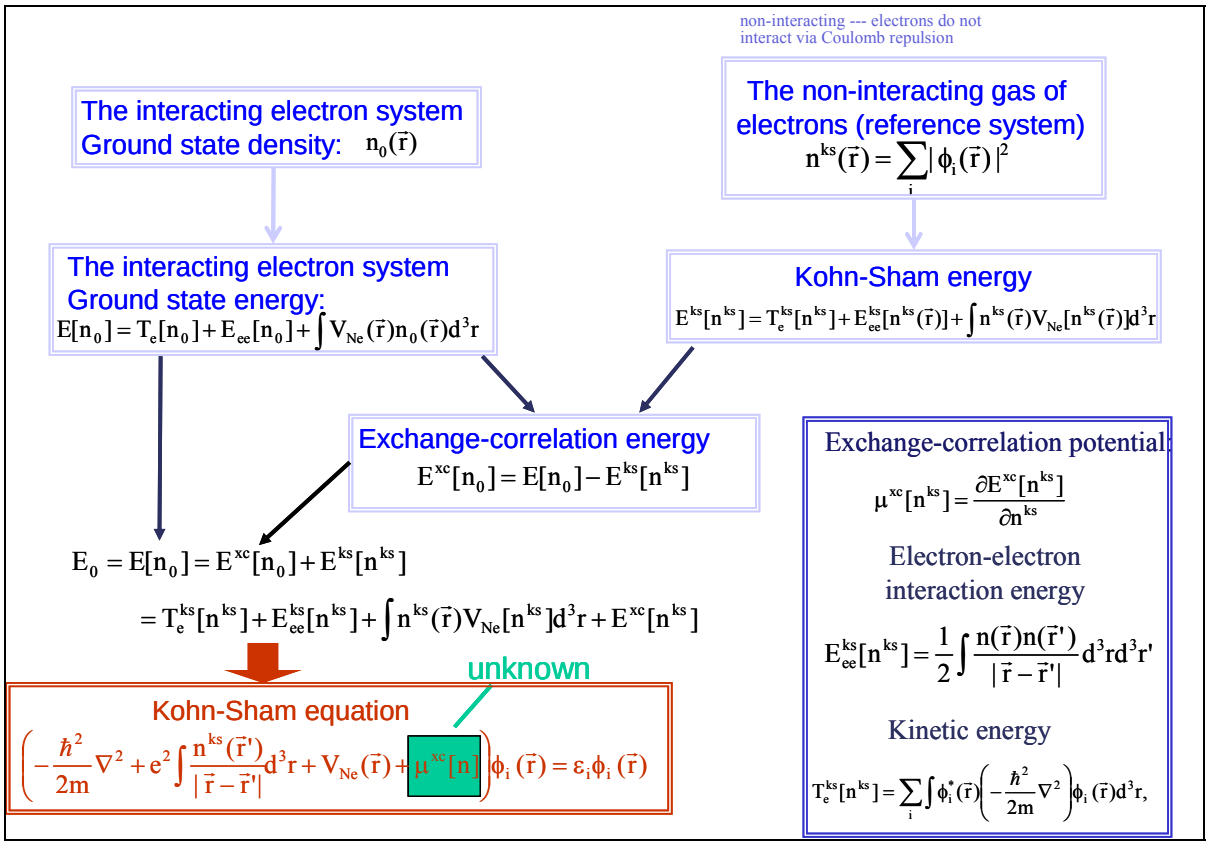

Figure 4.4: Kohn Sham Theory

- Approximation of the exchange-correlation energy $E^{xc}[n]$
  - *Local density approximation*: $E^{xc}[n]$ is approximated by the *exchange-correlation energy $\varepsilon^{xc}[n]$ of a homogeneous electron gas with the local density n*

$$E^{xc}[n(\vec{r})] = \int n(\vec{r})\varepsilon^{xc}[n(\vec{r})]d^3r$$

  - *Local spin density approximation*: including the spin effect

$$E^{xc}[n(\vec{r},\uparrow), n(\vec{r},\downarrow)] = \int n(\vec{r})\varepsilon^{xc}[n(\vec{r},\uparrow), n(\vec{r},\downarrow)]d^3r$$

  - *Generalized gradient approximation*: including the effects of gradient of density

$$E^{xc}[n(\vec{r},\uparrow), n(\vec{r},\downarrow)] = \int f[n(\vec{r},\uparrow), n(\vec{r},\downarrow), \nabla n(\vec{r},\uparrow), \nabla n(\vec{r},\downarrow)]d^3r$$

$$\mu^{xc}[n] = \frac{\partial E^{xc}[n]}{\partial n} - \nabla \cdot \frac{\partial E^{xc}[n]}{\partial(\nabla n)}$$

Current strategy is to adjust f such that it satisfies all known properties of the exchange-correlation hole and energy of different variants: *Perdew-Wang (PW), Becke-Perdew (BP), Lee-Yang-Parr(LYP), Perdew-Burke-Ernzernhof (PBE)*

Figure 4.5: Kohn Sham Theory – Approximations (1)

$$\left(-\frac{\hbar^2}{2m}\nabla^2 + e^2\int\frac{n^{ks}(\vec{r}')}{|\vec{r}-\vec{r}'|}d^3r + V_{Ne}(\vec{r}) + \mu^{xc}[n]\right)\phi_i(\vec{r}) = \varepsilon_i\phi_i(\vec{r})$$

- Basis functions for Kohn-Sham orbitals $\phi_i(r)$ for the non-interacting electron system
  - *Slater type or Gaussian type orbitals*
  - *Plane waves* (PW): Plane waves are not localized. Large numbers of plane waves are needed to reproduce atomic cores → pseudopotential
  - Linearized *augmented plane waves* (LAPW): Add atomic-like states to the plane-wave basis --- Expand the valence part of molecular orbitals in plane waves, the core part in compact atomic basis function
  - Projector augmented waves (PAW): The wave function is a superposition of different terms: a plane wave part, the so-called pseudowavefunction, and expansions into atomic and pseudo atomic orbitals at each atom.

Figure 4.6: Kohn Sham Theory – Approximations (2)

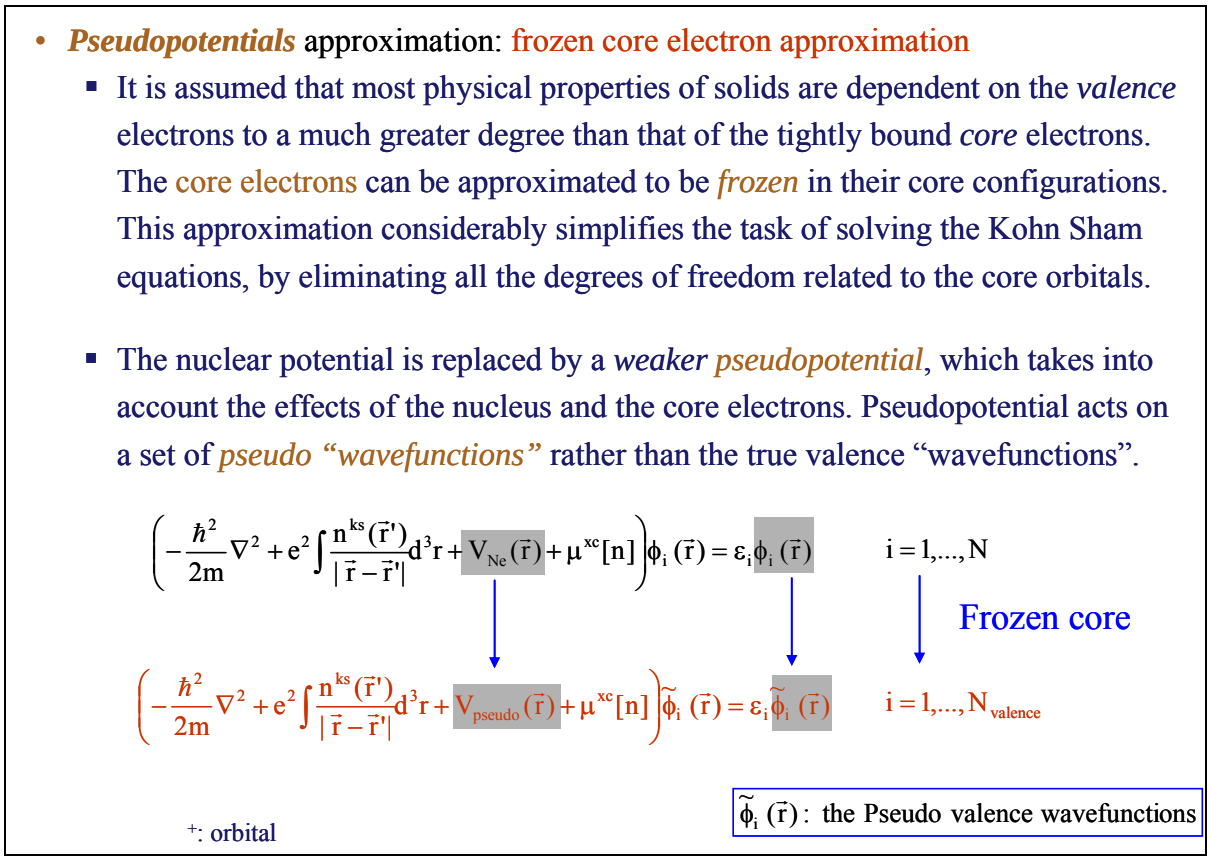

Figure 4.7: Kohn Sham Theory – Approximations (3)

4.2 Powder Mixture of Nickel and Aluminum

A thermodynamically complete EOS is the dependence of pressure on the specific volume and temperature. The EOS is one part of the complete constitutive relations applicable to the shock analysis of solids. The other part of the constitutive equation consists of the relationships between stress deviators and deformation, assuming isotropy. Traditionally, methods of obtaining EOS of solids are by using experimental measurements. The complete EOS requires a large number of tests and measurements at different state points.

Determination of EOS of mixtures increases the complexity by adding another variable of the ratio of mixture components. However, the extreme difficulty of the temperature measurement in shocked systems unavoidably results in the presentation of incomplete EOS. Thus, at the design stage of new materials, the experimental determination of EOS involves a tremendous effort at high cost. Therefore, using quantum mechanics (DFT)-based calculations to obtain EOS of new materials seems very appealing. The most important point is that these procedures have the potential to provide the thermodynamically complete EOS, $P=P(\rho,T)$, by the use of DFPT or quantum molecular dynamics procedures.

There is a significant amount of literature on the use of the first principles to calculate EOS of solids, crystalline metals and semi conductor materials. The focus in this chapter is the mixture of two metals or the composite of two metals and a polymer binder. In general, the mixture is a disordered material. However, methods of determining EOS of disordered intermetallic mixtures are do not exist. There are a significant number of publications to determine the electronic structures of binary interstitial and substitutional alloys. The usual assumption is that the alloys assume a minimum energy states. Our problem is different. We are studying mixtures of intermetallic structural energetic materials. These are at a higher energy state and assume minimum energy states only after chemical reactions that release energy and form products like Ni_3Al. Thus, for the energetic intermetallic mixture, such as, the Al-Ni mixture, the procedure to obtain the EOS of the mixture by using quantum mechanical calculations is as follows. First, the EOS is obtained for each individual component from first-principle calculations. The selected ab initio methods use the pseudo potential-plane-wave methods. More specifically, the procedure uses the generalized gradient

approximations and the ultrasoft pseudopotentials. The prediction of the EOS is in two parts: the static-lattice EOS and thermal effects. The range of the pressure and the temperature of consideration are up to 300 GPa and 1000K. As known, the melting temperatures of aluminum and nickel at the ambient pressures are about 933 K and 1728 K, respectively. Also theoretical predictions indicate that aluminum was theoretically predicted to undergo the pressure-induced crystallographic phase sequence from fcc→hcp→bcc, at predicted phase transition pressures; 205±20GPa and 565±60 GPa. In this work, the range of pressure and temperatures precludes possible polymorphic phase transitions.

Then, the EOS of the mixture is first obtained by two different methods. First, the EOS is approximated using appropriate mixture theories, namely homobaric mixture theory and uniformly blended mixture theory. Then, a super cell ab initio method is formulated. This method followed, in principle, similar to the virtual crystal approximation of Bellaiche and Vanderbilt. The details are given in the following sections. In all calculation of mixture theories different amounts of porosity are also considered.

4.3 EOS of the fcc Aluminum and the fcc Nickel

Determination of EOS of Al and Ni is not a new work. It is presented here for the purpose of continuity in the discussion of EOS of the mixture of Ni+Al. Ab initio calculations yield the internal energy of the crystalline system as the electron ground state energy. Density functional perturbation theory calculations yield the thermal excitation effects as a function of the specific volume (or density) and temperature. Specifically, the internal energy $e(v,T)$ is split into the cold curve $e_c(v)$ (zero-temperature frozen-ion isotherm) and the thermal

contributions from the ions $e_I(v,T)$ and electrons $e_e(v,T)$ where v and T are the specific volume and temperature of the system.

$$e(v,T) = e_c(v) + e_I(v,T) + e_e(v,T) \tag{4.1}$$

(a) ***The cold curve energy*** $\mathbf{e_c(v)}$ or the electron ground state energy, is the energy of the system with electrons in the ground state and ions in their crystallographic sites associated with some specific volume v. The quantum mechanical calculations (DFT) yields the zero-point energy of the system for a given lattice parameter (a measure of the specific volume of the system). The configuration of the lattice does not change and only the scale (or lattice parameters) varies.

For the fcc nickel and aluminum, only the lattice parameter 'a' is governing the set-up of a given specific volume. The prediction of the electron ground states is by using the density functional theory with the plane-wave pseudopotentials implementation via the density functional theory-based calculation procedures using the VASP package. The choice of the local density approximation and the generalized gradient approximation are to model the exchange and correlation according to the characteristics of system. The effects of core electrons are frozen by the use of pseudopotentials, while the plane wave expansion or a projector augmented wave basis set expands the outer electrons. A finite number of basis states, which is an approximation, corresponds to an energy cutoff in the expansion. Appropriate convergence studies determine both the energy cutoff values and the number of

K-points that are necessary for specified energy convergence criteria. The total energy convergence criteria is set to 10^{-5} eV.

The fcc Al crystal is in Space groups Fm3m and Pm3m, with a=b=c(=4.04Å equilibrium), α=β=γ=90°, while Ni is in Space group Fm3m with a=b=c(=3.52Å equilibrium), α=β=γ=90°. The cold curves for Al and Ni are shown in Figs. 4.8 and 4.9. In this study, the projector augmented-wave basis is used.

(b) ***The electron thermal energies*** $\mathbf{e_e(v,T)}$ are due to perturbations of the electron occupation numbers from their ground states. The calculation of the electron thermal contribution is from the electron band structure that populates the calculated states according to the Fermi-Dirac statistics. In the assumptions of the pseudopotential approach, the band structure refers to the outer electrons only and the core electrons are assumed to be fixed at all temperatures. The energy levels are by direct estimation of $e_e(v,T)$ or by the use of a numerical distribution function g(E). Given the density of levels g(E), the chemical potential μ is a function of temperature T by constraining the total number of valence electrons N.

$$\int_{-\infty}^{\infty} f(E)g(E)dE = N \quad \text{and} \quad f(E) = \frac{1}{e^{(E-\mu)/kT}+1} \tag{4.2}$$

In this equation, f(E) is the probability of occupation of a fermions state of energy E. This relation is not readily invertible to find the variation of μ with *T*. The determination of the quantity μ is by an iterative inversion algorithm. At *T*=0, μ is equal to E_F, Fermi energy. As T→ ∞, μ→0. Since the values of μ must lie between 0 and E_F , the relation is solved by

bisection. Following the determination of μ(T), the expectation value of the electronic energy is by the following equation.

$$\langle E \rangle = \int_{-\infty}^{\infty} Ef(E)g(E)dE \tag{4.3}$$

Thermal contributions due to electrons are usually small for many solids in the shock regime associated with particle velocities up to 1500 m/s.

(c) ***The lattice thermal energies*** $\mathbf{e_l(v,T)}$ is the contribution of thermal excitation of ions. The calculations are from the phonon modes of the lattice. Phonons represent the internal motions of a lattice about its center of mass by perturbations of the ion positions from their ground states. The phonon modes are from the eigenvalue problem of the structure defined by a given set of lattice parameters with the squared phonon frequencies representing the eigenvalues of the dynamic matrix. Ab initio elements of the dynamic matrix D_{ij} are from calculation of forces on the j^{th} atom when the i^{th} atom is perturbed from equilibrium by a finite displacement u_i.

$$D_{ij} = \frac{\partial^2 \Phi}{\partial \vec{u}_i \partial \vec{u}_j} \approx \frac{\partial \Phi(\vec{u}_i)}{\partial \vec{u}_j} \frac{1}{\left|\vec{u}_i\right|} \tag{4.4}$$

The symbol for the ground-state energy is Φ. This approach of calculating the restoring forces directly avoids the need to assume explicit forms of inter-atomic potentials. The solution of the phonon eigen-problem is for each set of wave vectors, for a given set of lattice parameters to obtain g(ω), the density of phonon states. The variation of lattice thermal energy $E_l(T)$ with temperature at a given density is then found by populating the phonon

modes according to the Boltzmann statistics. This approach is for each set of lattice parameters (for each specific volume). $e_l(v,T)$ is then found from $E_l(T)$ by normalizing to three modes per atom and using a suitable interpolation scheme.

$$E_l(T) = \sum_i g(\omega_i)\hbar\omega_i\left(\frac{1}{e^{\hbar\omega_i/kT}-1}+\frac{1}{2}\right) \tag{4.5}$$

In this work, the calculation of the dynamic matrix D_{ij} is from perturbation of the chosen ions from the equilibrium positions in the VASP package. The phonon modes calculation is accomplished by the use of the PHONON software. In the PHONON, the lattice thermal energy $e_l(v,T)$ and the associated free energy $f_l(v,T)$ are direct outputs. However, we also compare these direct outputs with the calculations by using the Boltzmann statistics in equation (4.5) and some thermodynamic relations. They agree very well with each other. The lattice thermal energy for Al and Ni at various specific volumes is shown in Fig. 4.8 and Fig. 4.9.

(d) ***Thermodynamically Complete EOS***: Following the determination of the total internal energy of the system, the associated free energy f(v,T) is as follows.

$$f(v,T) = e_c(v) + f_l(v,T) \tag{4.6}$$

The calculation of the thermodynamically complete EOS is from the following equation,

$$P(v,T) = \frac{\partial f(v,T)}{\partial v} \tag{4.7}$$

For the calculations, we use discrete lattice parameters a, i.e. discrete specific volume v. Then, we calculate the free energy at discrete v and T values. The accuracy of the

differentiation in equation (4.7) depends on the intervals of discrete v and T. Higher order polynomials interpolate the values between these intervals. Discrete "a", for the fcc Al, vary the values from 3.0 to 4.0 Å at intervals of 0.1 Å. Additional calculations are necessary at the points close to the equilibrium lattice parameter 4.04 Å. They are 3.92, 3.94, 3.96, 3.98, 4.04, and 4.045 Å. Similarly, discrete "a", for the fcc Ni, vary from 2.7 to 3.5 at intervals of 0.1 Å. Small interval 0.01 Å is necessary for values between 3.4 Å and 3.52 Å, which is near the equilibrium lattice parameter. Following this procedure, we determine the thermodynamically complete EOS for Al and Ni. They are in Fig. 4.10. The ab initio 300K isotherm EOS for Al and Ni agree with the experimental shock Hugoniot data. The comparisons are in Fig. 4.11 (a) and (b), respectively.

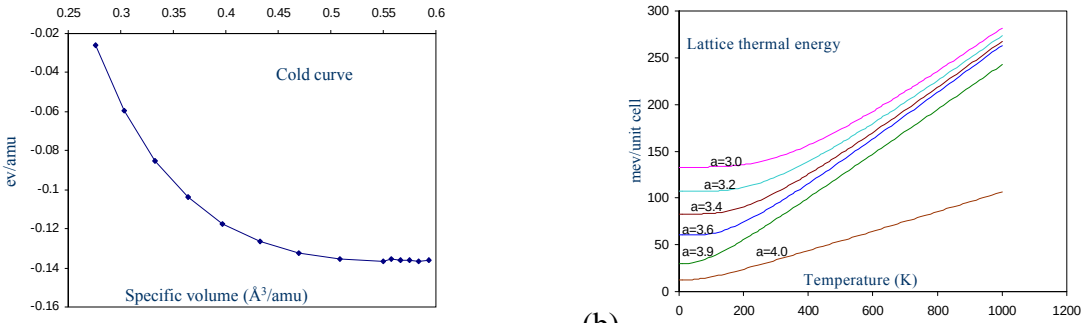

(a) (b)

Figure 4.8: (a) The cold curve of Al, (b) the lattice thermal energy of Al vs. temperature at selected lattice parameters

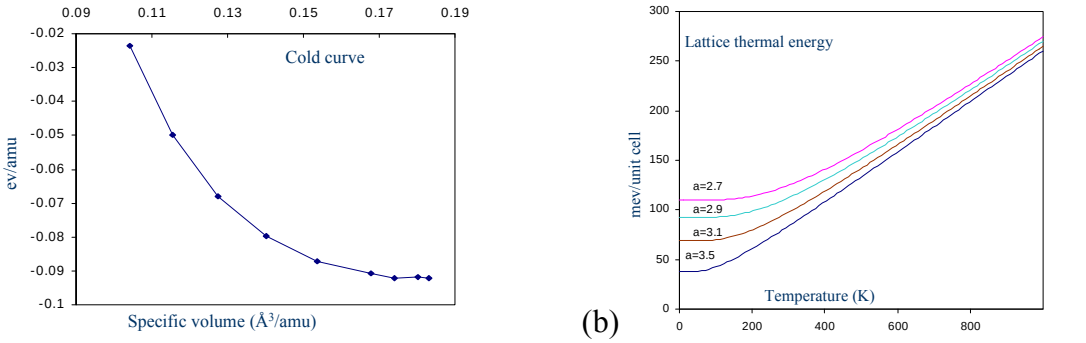

(a) (b)

Figure 4.9: (a) The cold curve of Ni, (b) The lattice thermal energy of Ni vs. temperature at selected lattice parameters

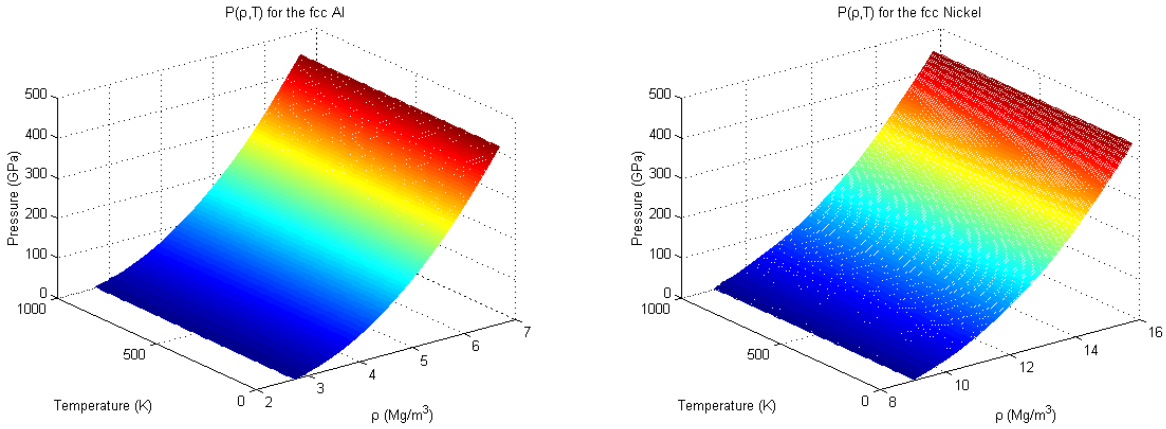

Figure 4.10: The thermodynamically complete equation of state of fcc Al (left) and Ni (right)

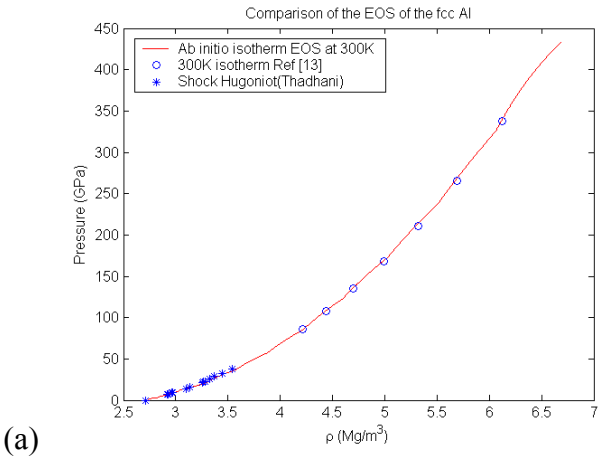

(a)

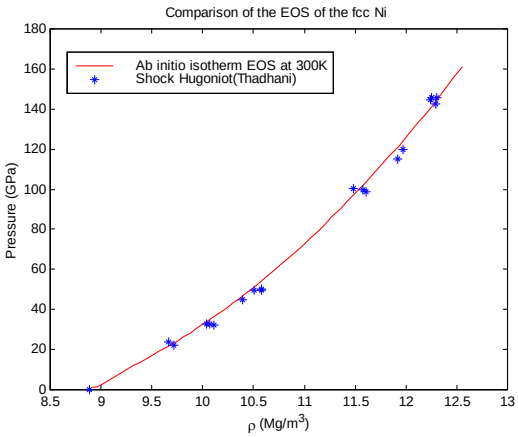

(b)

Figure 4.11: Comparisons of EOS by ab initio isotherm EOS at 300K and shock Hugoniot. (a) Al, experimental data from Thadhani (low pressures) and (high pressures, with assumed ρ_0=2.67kg/m^3); (b) Ni, experimental data from Thadhani

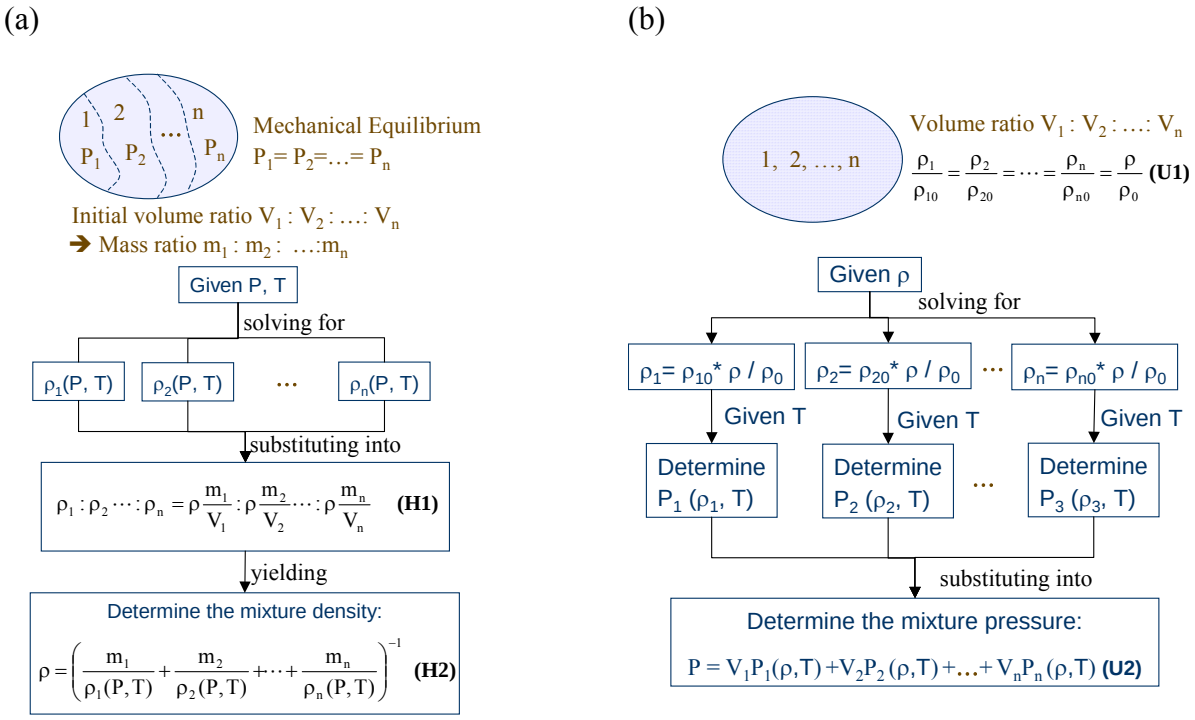

Figure 4.12: The procedure for the EOS of mixture by using (a) homobaric mixture theory, (b) blended mixture theory

4.4 EOS of a Mixture

First, the EOS of mixture is calculated by using a mixture theory that uses a weighted combination of two limiting cases, one of which is equivalent to a series combination of the components (homobaric mixture theory) and the other is equivalent to a parallel combination of the components (uniformly blended mixture theory). These calculations are for purposes of EOS using super cells. Thus, this approach uses ab initio EOS of individual components of the mixture with an empirical mixture theory. In the first case, the interface between components is in mechanical equilibrium, by assumption, and every component occupies its own fractions of volume and mass. The relations in equations (H1), as shown in Fig. 4.12 (a), hold. While in the parallel case, different components deform at the same strain. It indicates

the relations in equations (U1) as in Fig. 4.12 (b). The procedures for constructing the EOS of mixture by these two mixture theories are in Figs. 4.12 (a) and 4.12 (b), respectively. For the homobaric mixture theory, given P and T, every component of mixture experiences the same P and T. We obtain the density of every individual component $\rho_i(P,T)$ (i=1, 2, …, n) from its known EOS. Then we substitute $\rho_i(P,T)$ into equation (H2) (as shown in Fig. 4.12 (a)), by solving equations (H1), to obtain the EOS of mixture. For the uniformly blended mixture theory, given the density of the mixture ρ, we solve for the corresponding density of every component ρ_i (i=1, 2, …, n) from equations (U1). From the EOS of component, we determine the component pressure $P_i=P_i(\rho_i,T)$ (i=1, 2, …, n). The determination of the mixture pressure P is by the summation of component pressure weighted by its component volume fractions as in equation (U2) in Fig. 4.12 (b). By using this procedure, we the EOS for a stoichiometric mixture: Ni + 3Al (mass ratio 58%**:**42%), based on these two mixture theories. The results are in Fig. 4.13 (a) and (b). This equation of state is for an "ideal material". In practice, it is not possible to obtain mixtures without any void content. The 300K isotherms EOS of mixture, obtained by using the two mixture theories, are in Fig. 4.14. As expected, the EOS from homobaric mixture theory is 'softer' than that from uniformly blended mixture theory. In reality, the nature of the mixture is intermediate to that of the two idealized mixtures and hence is modeled as a weighted combination of the two cases.

(a) (b)

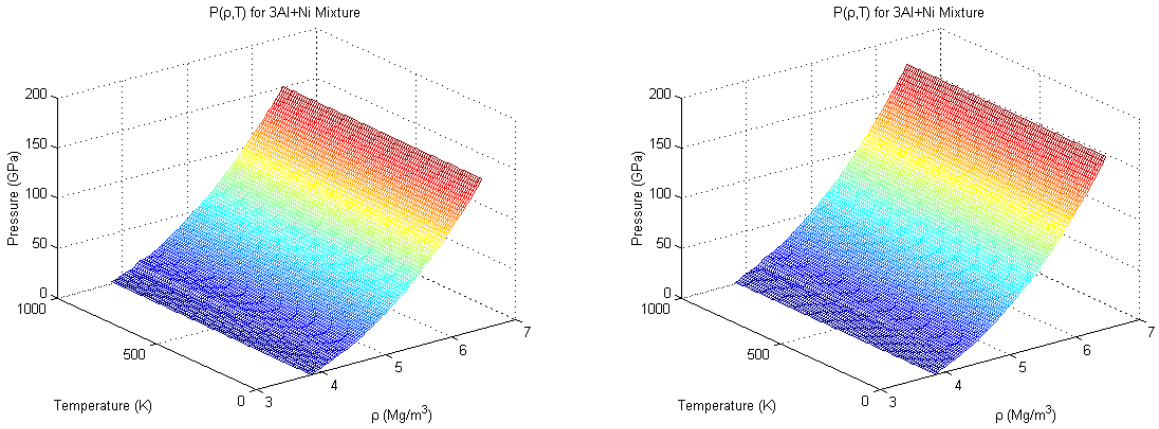

Figure 4.13: The equation of state of stoichiometric mixture 3Al+Ni, by (a) homobaric mixture theory, (b) uniformly blended mixture theory

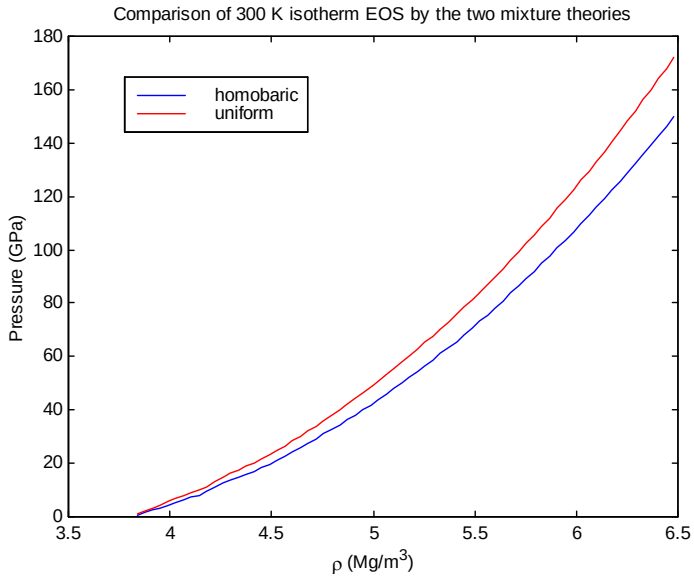

Figure 4.14: Comparison of the 300K isotherm EOS of mixture by using homobaric and uniform mixture theories

4.5 EOS of a Porous Mixture

As discussed before, the currently available experimental or processing techniques do not permit the synthesis of intermetallic mixtures with full density without any voids. There is

always some accompanying porosity. Usually, the materials synthesized in the laboratory leads to intermetallic Ni and Al mixtures that have densities in the range of 75% - 88% of the material with no voids. Some researchers think of that the existence of porosity and its collapse is necessary to provide the enough energy to overcome the energy barriers for chemical reactions to release the stored energy in the energetic mixture. Therefore, the EOS of porous mixture is very important for the applications of these energetic materials. To construct the EOS of a porous mixture, we introduce the porosity (or air) as the third component consisting of the mixture. We use van der Waals EOS for air, which is suitable at relatively high pressures (for a gas).

$$\left(P + \bar{a}\rho^2\right)\left(\frac{1}{\rho} - b\right) = RT \tag{4.8}$$

In this equation, the constant ' $\bar{a}$ ' accounts for the repulsion between molecules and increases the forces between them. The constant 'b' accounts for the volume physically occupied by molecules and decreases the effective open volume. The calculation of the numerical values of $\bar{a}$ and b are as follows.

$$\bar{a} = \frac{27R^2T_{critical}^2}{64P_{critical}} \qquad b = \frac{RT_{critical}}{8P_{critical}} \tag{4.9}$$

For air, at 1 atm and 0 °C, the density of air is 1.29 kg/m^3. The critical temperature $T_{critical}$ and pressure $P_{critical}$ of air, corresponding to the critical point for phase changes from liquid and gas, are $T_{critical}$=132.5 °K and $P_{critical}$=3.77 MPa. As discussed, the homobaric mixture is

softer than the uniformly blended mixture. Especially, when introducing air as the third component, which has very little stiffness compared to the other two solid components, the mixture is very soft at low pressures, which is indicated by the observation that the pore collapse occurs at very low pressures. Therefore, the homobaric assumption is more appropriate to model the porous mixture at low pressures. For a 3Al+Ni mixture of 15% porosity, we use the homobaric mixture theory to approximate the EOS of the porous mixture. The thermodynamically complete EOS is in Fig. 4.15. The 0, 300 and 1000K isotherm EOS are in Fig. 4.16. The pore collapse occurs at pressures around 4MPa and the mixture becomes fully dense.

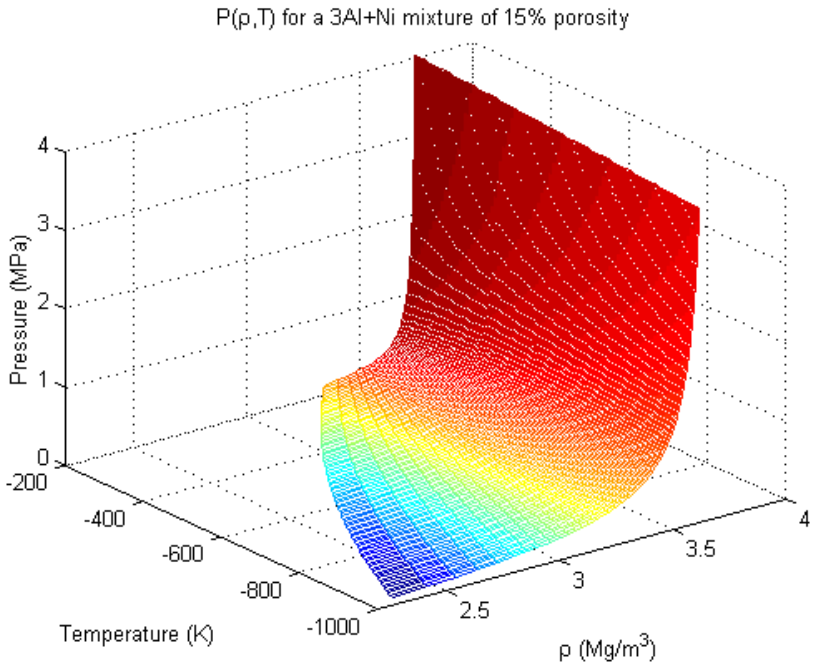

Figure 4.15: The thermodynamically complete EOS of a 3Al+Ni mixture of 15% (volume) porosity

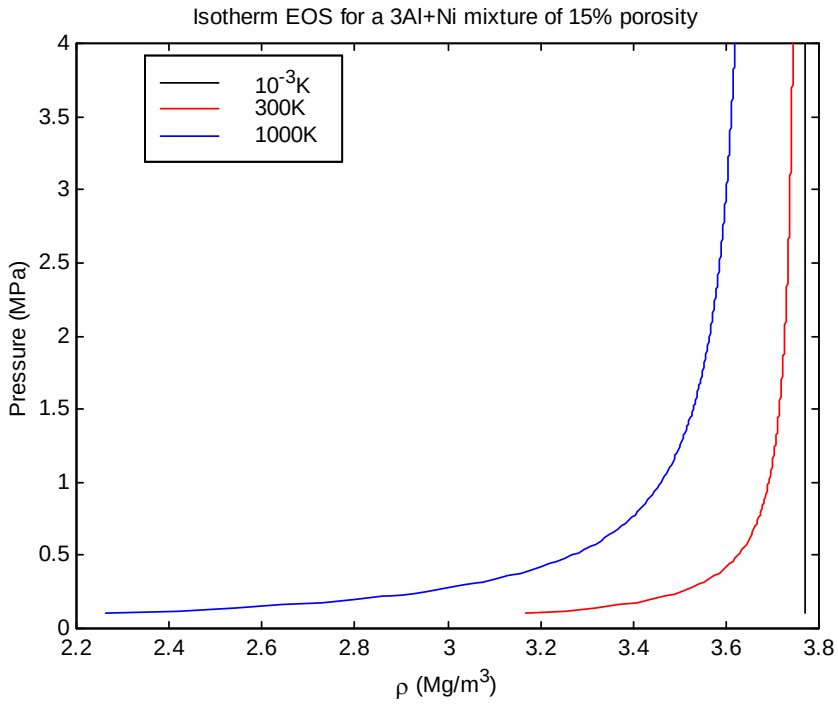

Figure 4.16: The isotherm EOS of a 3Al+Ni mixture of 15% (volume) porosity at 0, 300, and 1000 K

4.6 Super cell Approach for the EOS of a Mixture

Next, a super cell approach, similar to the virtual crystal approximation is pursued. The formulation of the super cell of Ni+Al is shown in Fig. 4.17. The super cell is formed similar to crystalline cells of Ni or Al. Some results are shown in Fig. 4.18. Additional details are described in a separate paper.

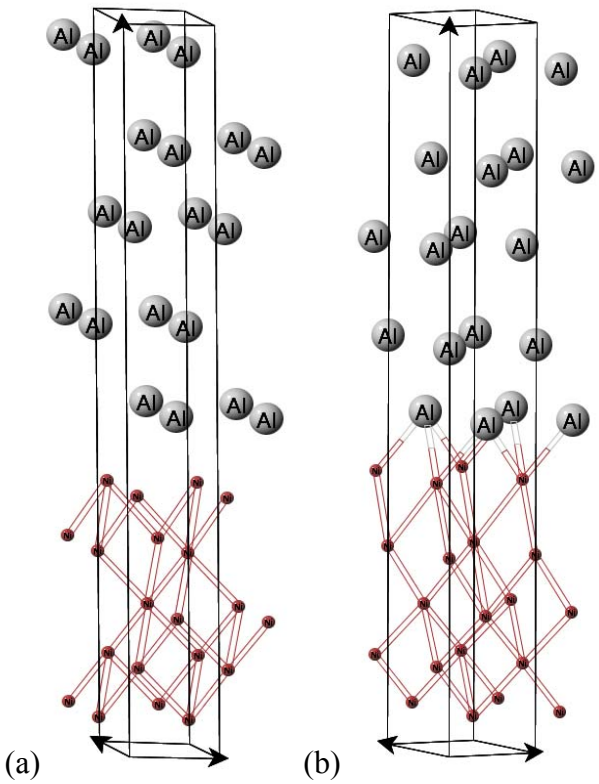

Figure 4.17: A Super Cell of the mixture

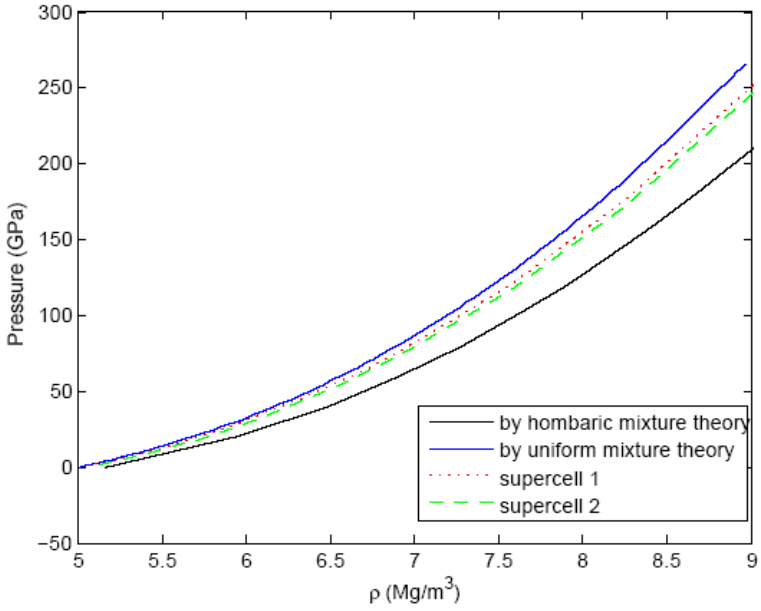

Figure 4.18: Comparison of EOS

4.7 Summary of the Chapter

In this work, we use the ab initio techniques to obtain the fully thermodynamic EOS of a porous energetic inter-metallic mixture of nickel and aluminum. First, the EOS determination for each individual component consisting of the mixture is from the thermodynamic relations and based on the DFT-based calculation of internal energy. Then, two different mixture theories as two limiting cases of reality are discussed and used to calculate the EOS of mixture. The results of EOS are compared with the experimental shock Hugoniot data and agree reasonably well. The EOS of porous mixture is also constructed by introducing air as the other constructing component. The pore collapse process is indicated in the obtained EOS. More accurate ab initio approach to the calculation of the equations of states of mixtures requires the consideration of a super-cell with porosity. Accurate mixture consideration requires that they be subjected to the same pressure but varying strains.

4.8 Acknowledgements

The author gratefully acknowledges the guidance of Dr. Xia Lu, in addition to the guidance of Dr. Hanagud. The advice of Dr. Lu was through personal guidance when Dr. Lu was at Georgia Tech and through written calculation procedures.

CHAPTER 5

AB INITIO CALCULATIONS OF CHEMICAL REACTIONS OF NICKEL AND ALUMINUM

5.1 Background

To date, the chemical reactions of intermetallic mixtures, such as nickel and aluminum are of interest to understand the shock induced or assisted chemical reactions of reactive materials. Other areas of interests are to synthesize materials with unique microstructures through the passage of shock waves through selected intermetallic mixtures. Most of the models are in the continuum scale. There are some models in the mesoscale. In the mesoscale, each reactant is again in a continuum scale. Some of the published works are by Graham, Thadhani, Bosolough, Horie, Marzianov, Eakins, Narayanan, Lu, Reding and Hanagud. Some of the reported studies focus on the mechanisms that lead to chemical reactions. These include effects such as, the pore collapse, plastic strains and mixing. Thadhani and Eakins consider microstructure of the mixture of reactive materials such as nickel and aluminum. They simulate the microstructure in numerical simulation. They study fragmentation of components of the mixture and the state of the close proximity of the reacting components, as a result of the passage of the shock wave. These calculations are primarily in two dimensions.

Lu, Narayanan and Hanagud propose a different model in a continuum scale. This model uses a continuum mixture theory. They propose the use of two different mixture theories. One is the classic mixture theory of Truesdell. The second is the simply connected boundary-based mixture theory of Lu and Hanagud for use in shock compression of

solids. In addition to the mixture theory, the model is in the frame of non-equilibrium thermodynamics. The purpose of using non-equilibrium thermodynamics is to explain the time delay of the on-set of chemical reactions after the shock wave passes through the solid. The model considers reactive material mixtures such as thermite mixtures (iron oxide and aluminum) and intermetallic mixtures. The mixture theory and the associated constitutive equations accommodate for the reactants, transition state products and the resulting final products. The initiation criterion for the chemical is by the energy associated with the pore collapse, plastic work and viscous effects. The formulation includes procedures to obtain the transition state; the activation energy needs to attain the transition state and the release of heat energy on the basis of the difference between the transition state energy and the energy of the final products of the reaction. These energies are in the model to calculate the initiation and sustained chemical reactions. A numerical simulation is by Muscle-Scheme under conditions of one dimensional strain. Examples illustrate the on-set of chemical reactions by estimating the concentration of key reaction products in the mixture. For example in the shock induced or assisted chemical reaction of iron oxide and aluminum, theory and numerical calculations track the amount of iron in the mixture to track the completed reaction.

5.2 Specific Research Issues

Thus, work to date presents different mechanisms that contribute to the activation energy and take the reactants to the transition state, for an initiation of the chemical reactions. Some of these different mechanisms include pore collapse and plastic work. Additional works include non-equilibrium thermodynamic models for time delays and inclusion of

microstructures in computations to explain mixing of reactants that bring reactant in close proximity. However, in actual chemical reactions there are exchange of electrons and formation of new bonds. Because all the previous works are in continuum scale, it is not possible to study these phenomena. Thus, it is necessary to go beyond continuum to quantum mechanics scales to seek mechanisms of reactions with exchange of electrons and formation of new bonds.

Publications in related fields lead to the studies of chemisorptions of CO on W and hydrogen on Titanium. Chapters III and VI discuss the details. In these studies, chemical reactions are between a gas and a solid (or a condensed matter). Goals of this thesis is to study shock induced or assisted chemical reactions of two solids. In particular, the two specific solids of interest in this chapter are Ni and Al.

5.3 The case of liquid Al

Suggestions of some of the previous studies are that the aluminum is in a liquid phase before the initiation of reactions. The studies in Chapter III of W and CO consider a molecule of the gas CO on top of tungsten as shown in Fig. 5.1.

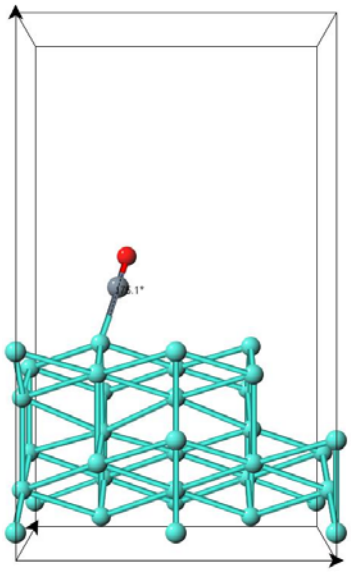

Figure 5.1: Gas molecule CO and Tungsten (111) layers

If aluminum melts at 650 degrees centigrade the nickel is still in a solid state. Thus first series of studies in this investigation considers aluminum molecules on the top of 111-layers of nickel as shown in Fig. 5.2.

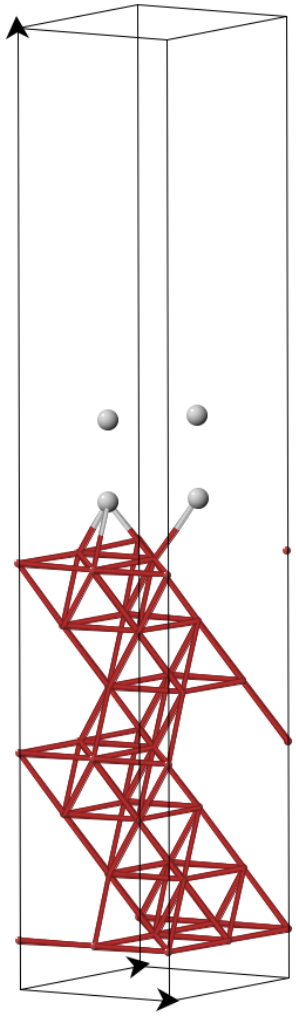

Figure 5.2: Aluminum molecules on-top of seven (111) Nickel layers

This study indicated the formation of Ni_3Al. This was checked with the phase diagram for Ni-Al as shown in Fig. 5.3. This is because of the fact that we had large number of Ni atoms and only two aluminum molecules. Furthermore, our differential thermal analysis tests indicated that the reactions of Ni and Al occurred at temperatures 550 degrees centigrade where aluminum was still a solid. Thus, the model of using only 2 aluminum molecules on the top of seven layers of nickel-111 was changed to a model where seven

layers of solid aluminum-111 was placed on the top of seven layer of nickel-111 layers as shown in Fig. 5.4.

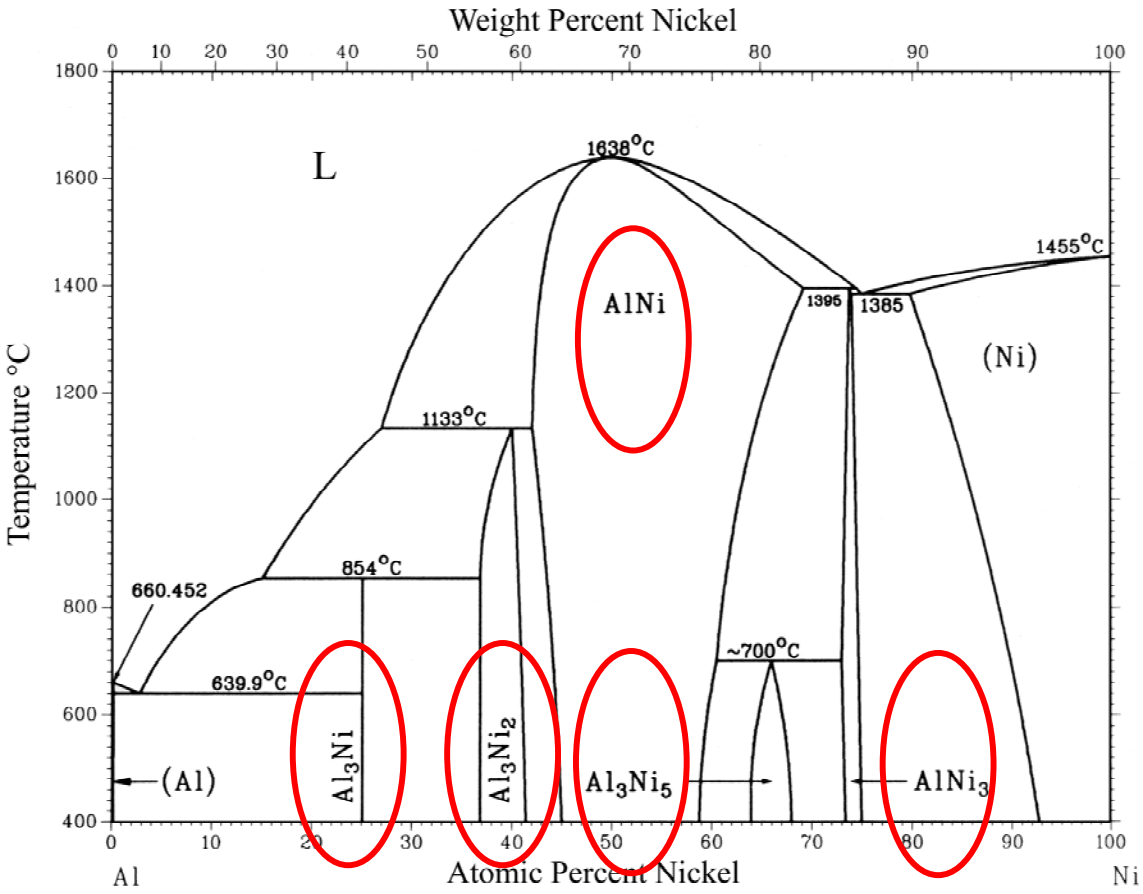

Figure 5.3: Phase diagram of Nickel and Aluminum

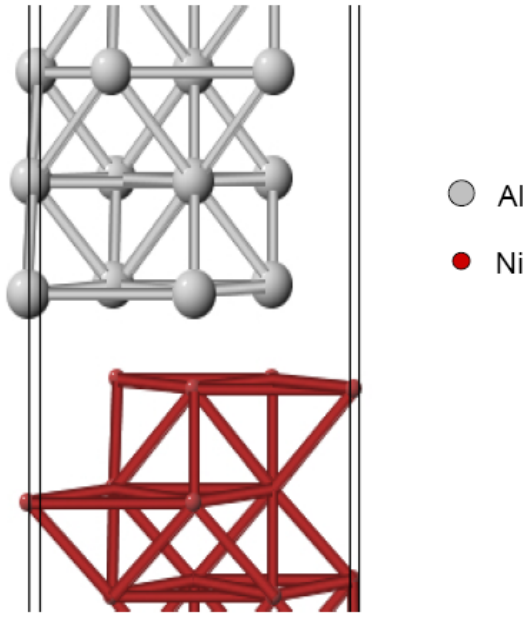

Figure 5.4: Initial configurations of Nickel and Aluminum layers

To model the formation of Ni_3Al at temperatures below 640 degrees centigrade the following model is considered. The primary goals were to model the shock-induced or shock assisted chemical reactions. In principle, it is possible to simulate a shock impact conditions at the ab initio molecular dynamics level. As a first step, goals are to study thermally induced chemical reactions of nickel and aluminum. In the next step, we consider straining of the mixture.

Following procedures, similar to that of W + CO, we use ab initio molecular dynamics or quantum molecular dynamics by the use of Car-Parinello molecular dynamics. In this procedure the force field is computed at every step by the use of density functional theory-based calculations. To improve the computational efficiency the electrons have artificially higher than their actual mass. The increased mass is selected to improve the

computational efficiency but not large enough to alter the expected ion motion and the resulting temperature conditions. The model is as shown in Fig. 5.6.

Figure 5.5: (111) layers of Nickel and Aluminum

The calculations are conducted at different constant temperatures. Evolution of the structure with configuration of an initial gap of 1.9 Angstroms separation between the nickel aluminum layers is presented in Fig. 5.6. During the molecular dynamics calculations the fcc crystalline orientations of nickel and aluminum are maintained in some calculations.

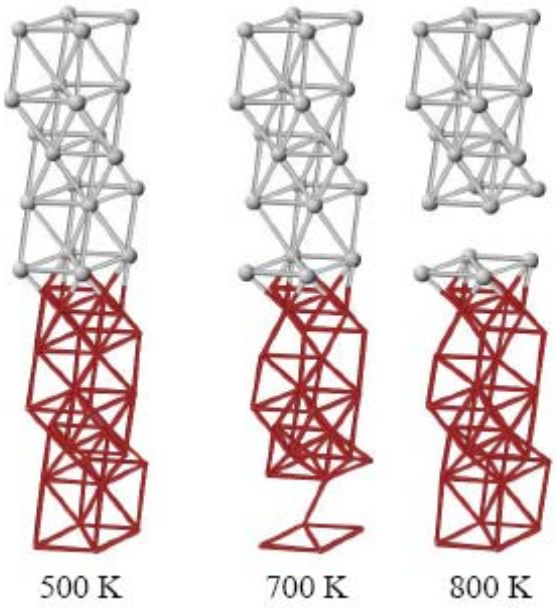

Figure 5.6: JMol plots of Ni-Al (111) layers with increasing temperature

As seen, $NiAl_3$ is formed at 500 degrees centigrade which is below the melting temperature of aluminum. To visualize $NiAl_3$, a magnified JMol plot is given in Fig. 5.7.

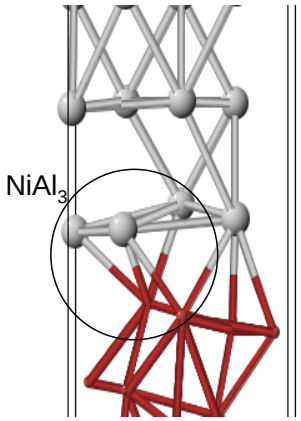

Figure 5.7: Formation of $NiAl_3$

Thus, it has been possible to show the formation of $NiAl_3$ from ab initio molecular dynamics. Now, it is possible to study the mechanism leading to the chemical reaction by

different rates of heating, different gaps, different layer sizes and shock conditions. It is also possible to consider different types of layers and more than two solids, including possible reinforcements.

CHAPTER 6

EFFICIENT HYDROGEN STORAGE IN TITANIUM

6.1 Background

Hydrogen, as a fuel is very desirable. First 1kg of hydrogen has the potential to yield the same energy as on gallon of gasoline that weighs 2.7 kilograms. In addition the production of energy in fuel cells, through reaction of hydrogen and oxygen, the resulting product is not polluting the environment. However, the problem of efficient and compact storage of hydrogen is not a solved problem. There are research efforts to store hydrogen in carbon, metal-organic frameworks (MOF) and as metal hydrides. This focus of the research described in this chapter concerns the storage of hydrogen in metals (metal hydrides) and improvement of desirable characteristics of the storage through mechanical strains.

For efficient operations, it is necessary to store large amount of hydrogen and release it quickly as needed [6.1, 6.2]. Very often, conditions that store large amounts of hydrogen in metals lead to a strong bonding of metals to hydrogen or strong binding energy. The strong binding energy between the metal and hydrogen is not favorable in a quick and efficient release of hydrogen, for purposes of energy producing reaction. There are some research efforts to explore the storage of hydrogen at molecular levels instead of in the atomic level. The discussions of research here is to explore mechanical strains to increase binding energy to store hydrogen and reverse mechanical strain to reduce biding energy when it is necessary to release hydrogen for purposes of reaction.

6.2 Problem Setting

First, the selected metal in this study is titanium because of the low density and the resulting light weight storage medium. The objective is to explore the effect of mechanical strain on the binding energy between hydrogen and titanium with compressive and tensile strains. To study these effects, the selected methods are ab initio methods, with density functional approximation that also form discussions of chapter III.

For all calculations 7 layers of titanium are considered, bottom 4 are fixed and top 3 are free. The lattice parameters are as follows.

a=2.93647940097882

c/a=1.57517351266119

Cell dimensions for 1x1 are taken as:

1*a x 1*a x 7.5*c

Cell dimensions for 2x2 are taken as:

2*a x 2*a x 7.5*c

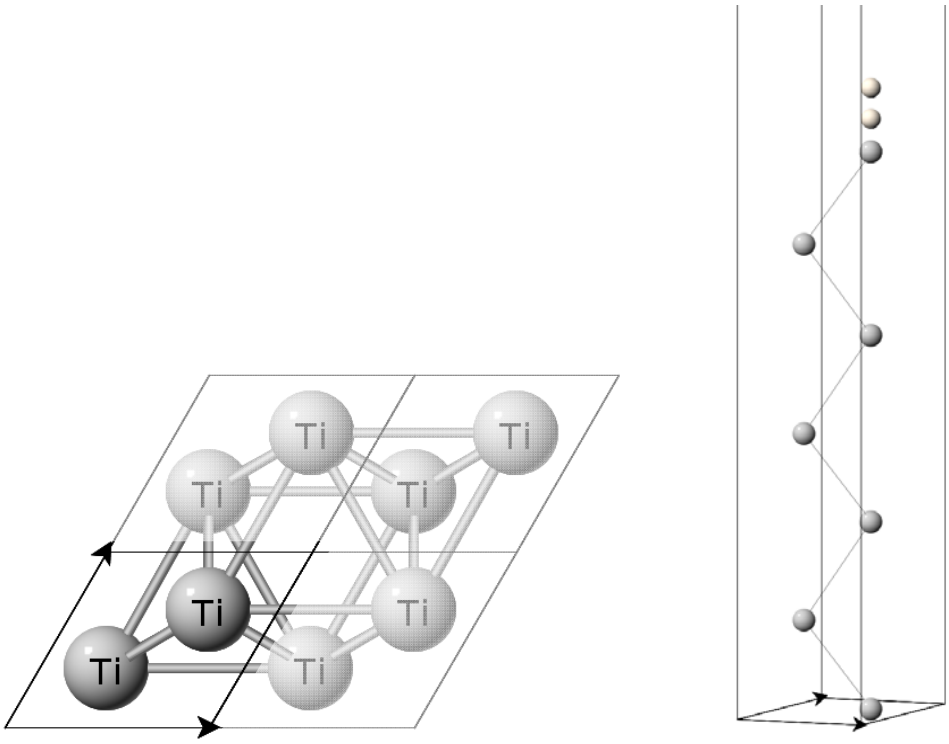

Figure 6.1: Top view and side view of Ti 1x1 (neighbour cells shown for orientation)

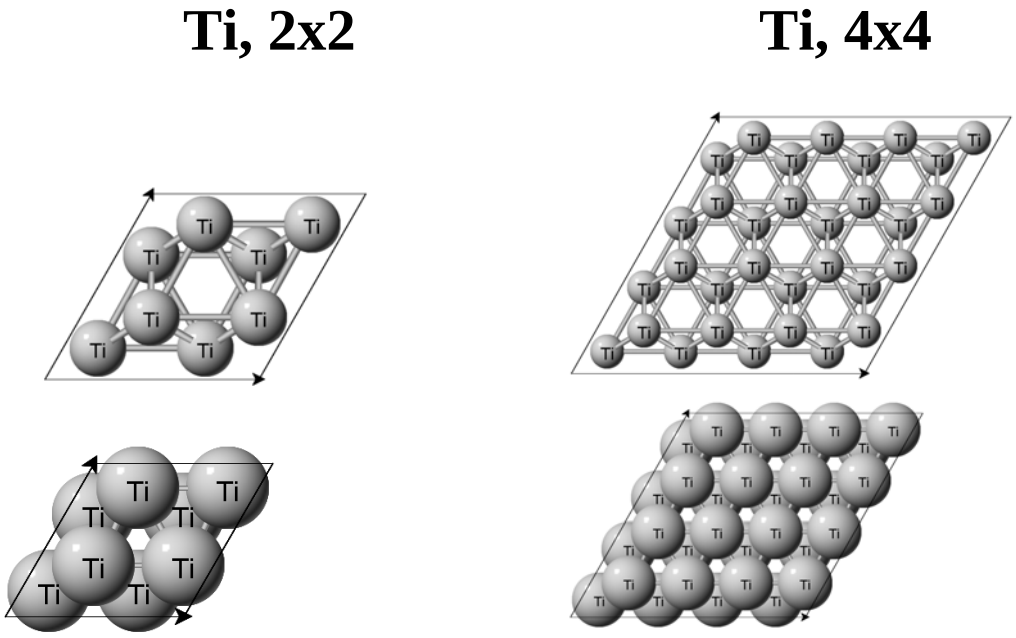

Figure 6.2: Top views of Ti 2x2 and 4x4 HCP cells used in the calculations

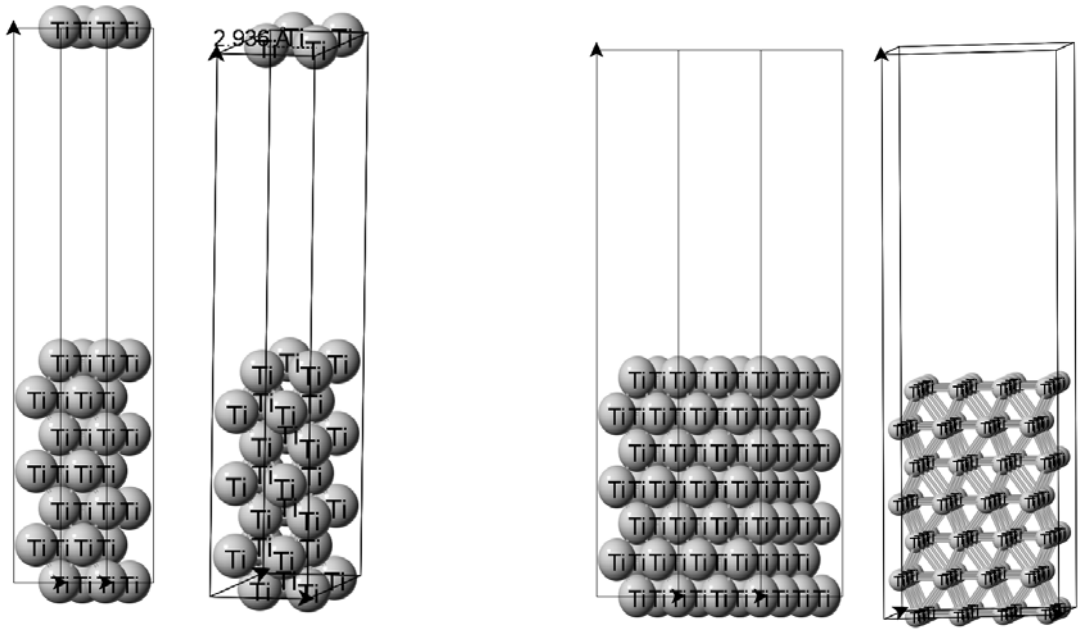

Figure 6.3: Side views of 2x2 and 4x4 cells used in the calculations

6.3 Selection of Cutoff energy and Number of K-Points

Before proceeding with the calculation of the binding energies, with and without mechanical strains, it is necessary to establish the cutoff energy (ENCUT) selection and the selection of number of K-points that result in the desired calculations. A summary of the calculations are in the following table.

Table 6.1: Variation of Total energy for Ti 1x1 with varying Cutoff energy & K-points

KPOINTS = 5x5x1 grid = 9 irreducible kpoints		KPONTS = 15x15x1 = 64	
ENCUT	TOTEN	ENCUT	TOTEN
400	-52.652551	400	-52.564689
600	-52.655339	600	-52.567440
800	-52.656919	800	-52.569197
870	-52.656402	870	-52.568656
1000	-52.655152	1000	-52.567545
1200	-52.655103	1200	-52.567325
KPOINTS = 9x9x1 = 25		KPOINTS = 19x19x1 = 100	
ENCUT	TOTEN	ENCUT	TOTEN
400	-52.541250	400	-52.564997

600	-52.544012	600	-52.567747
800	-52.545751	800	-52.569487
870	-52.545163	870	-52.568948
1000	-52.544034	1000	-52.567843
1200	-52.543837	1200	-52.567639
KPOINTS = 11x11x1 = 36			
ENCUT	TOTEN		
400	-52.580253		
600	-52.582980		
800	-52.584722		
870	-52.584157		
1000	-52.583047		
1200	-52.582853		

The plots of the results of Table 6.1 are represented in Fig. 6.4.

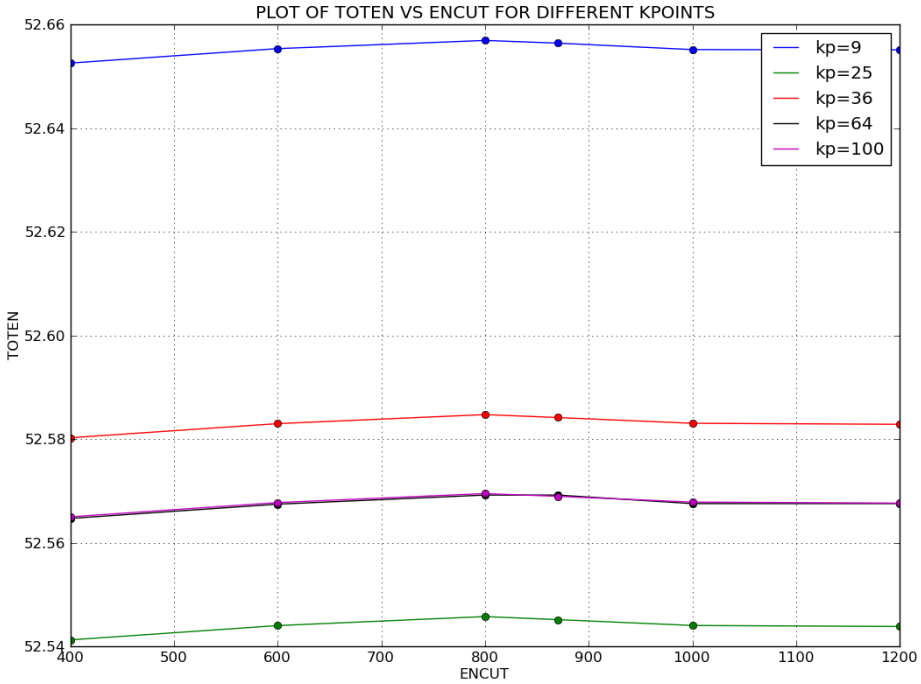

Figure 6.4: Variation of Total energy with Cutoff energy for Ti 1x1;
kp = irreducible number of K-points, energy in eV

The following figure combines the variation of total energy with both K-points and cutoff energy.

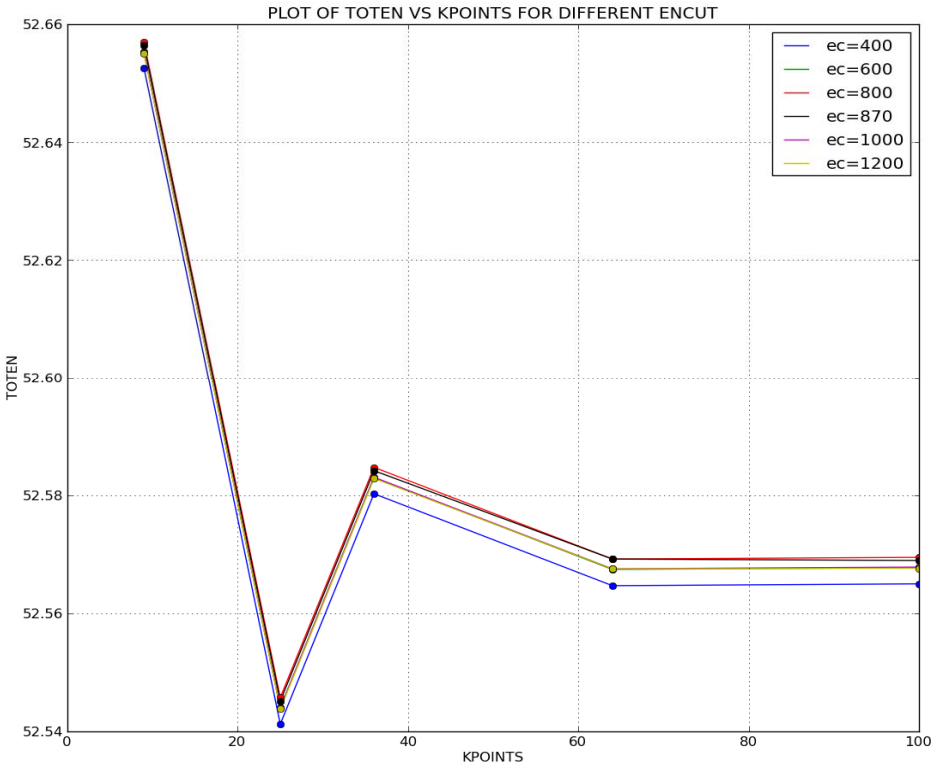

Figure 6.5: Variation of Total energy with K-points for Ti 1x1;
ec = cutoff energy, energy in eV

Thus, to obtain an accuracy with a tolerance of 0.015 eV taking ENCUT = 600 eV and KPOINTS grid = 11x11x1 is sufficient. Then, similar convergence studies for hydrogen are as follows.

Table 6.2: Variation of Total energy for H_2 with varying Cutoff energy & K-points

KPOINTS = 5x5x1 = 9		KPOINTS = 15x15x1 = 64	
ENCUT	TOTEN	ENCUT	TOTEN
400	-6.7839808	400	-6.7840224
600	-6.7980848	600	-6.7980739
800	-6.7987126	800	-6.7987040
1000	-6.7988120	1000	-6.7988031
KPOINTS = 9x9x1 = 25		KPOINTS = 19x19x1 = 100	
ENCUT	TOTEN	ENCUT	TOTEN
400	-6.7839982	400	-6.7840391
600	-6.7980749	600	-6.7980758
800	-6.7987038	800	-6.7987040
1000	-6.7988026	1000	-6.7988030

KPOINTS = 11x11x1 = 36	
ENCUT	TOTEN
400	-6.7841354
600	-6.7980760
800	-6.7987039
1000	-6.7988031

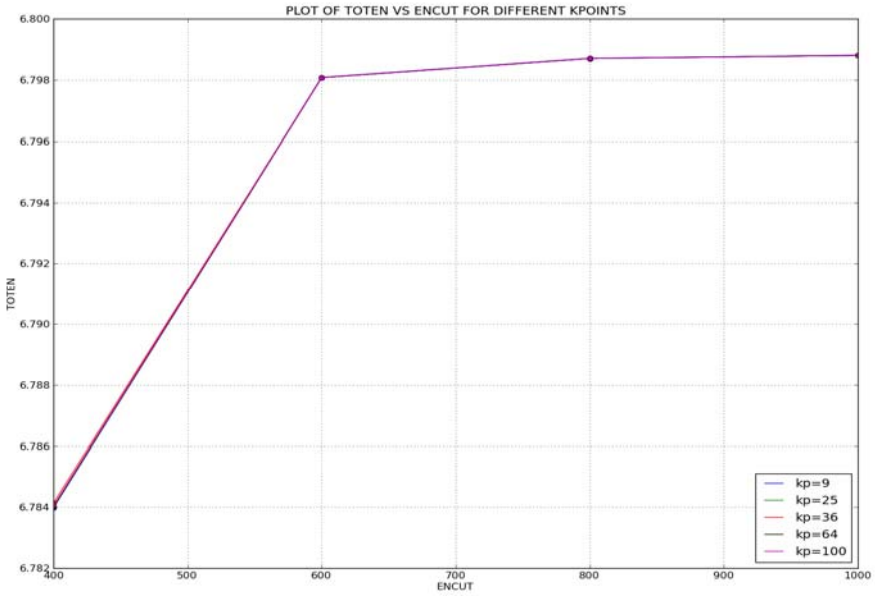

Figure 6.6: Variation of Total energy with Cutoff energy for H_2; kp = irreducible number of K-points, energy in eV

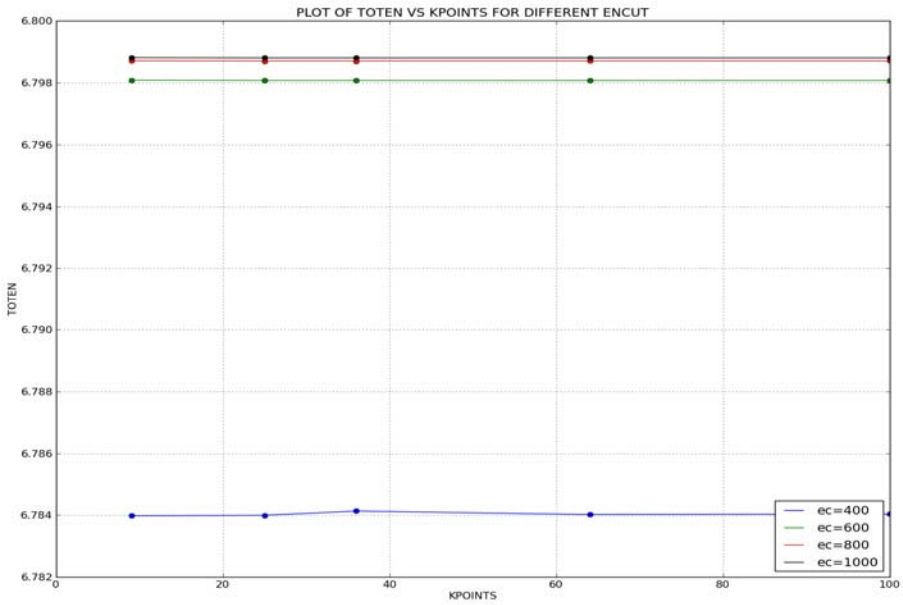

Figure 6.7: Variation of Total energy of H_2 with Cutoff energy and K-points mesh; ec = cutoff energy, energy in eV

6.4 Binding Energy Calculations

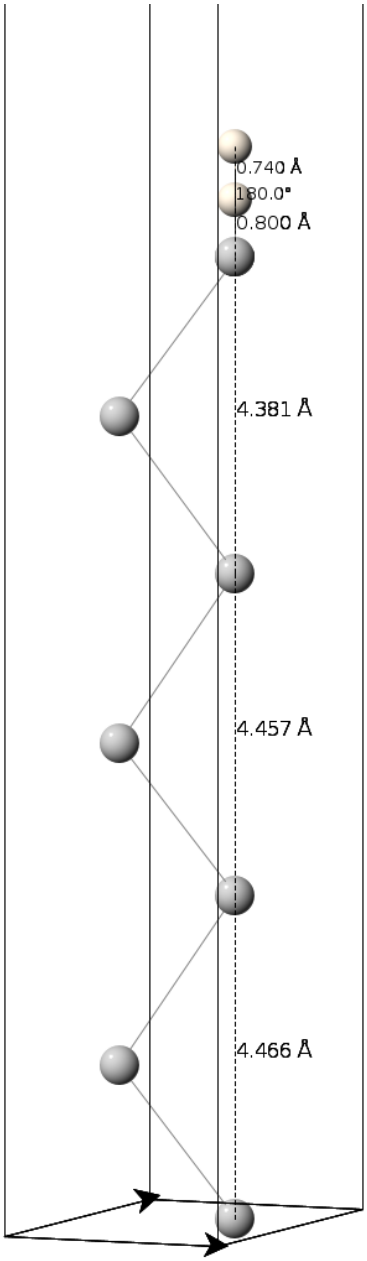

Figure 6.8: Positioning of Ti + H_2

The position of H_2 molecule is vertically in the top position. Figure 6.8 represents the starting geometry before the relaxation of Ti+H_2. The volumetric strain (v/v_0) values taken for Ti are 0.98, 0.96, 0.94, 0.92, 0.90, 0.85, 1.02, 1.04, 1.06, 1.08, 1.10, and 1.15. The possible binding sites are as shown below.

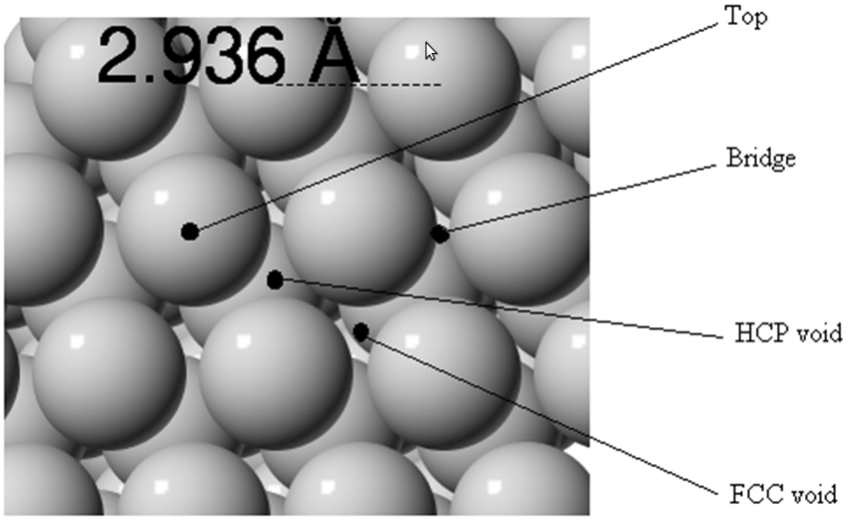

Figure 6.9: Possible binding sites

The distance between the upper most Ti layer and the lower H atom is 0.8 A and 1.2 A. Then, binding energy per molecule of Hydrogen = (TOTEN_Ti + TOTEN_H2) - TOTEN_TiH2. The variations of the binding energy with strain are in the following table.

Table 6.3: Variation of Binding energy with strain, of Ti+H_2

D=0.8				
STRAIN	TOTEN_Ti	TOTEN H2	TOTEN_TiH2	BINDING E
0.85	-51.987962	-6.7988031	-58.63197	-0.15479
0.94	-52.544944	-6.7988031	-59.18795	-0.15580
0.96	-52.582405	-6.7988031	-59.38237	0.00116
0.98	-52.594605	-6.7988031	-59.39664	0.00323

1.00	-52.582980	-6.7988031	-59.38790	0.00612
1.02	-52.550367	-6.7988031	-59.35703	0.00786
1.04	-52.498004	-6.7988031	-59.30211	0.00530
1.06	-52.427287	-6.7988031	-59.23637	0.01028
1.08	-52.340174	-6.7988031	-59.15263	0.01365
1.10	-52.238321	-6.7988031	-59.05233	0.01521
1.15	-51.926180	-6.7988031	-58.74234	0.01736
D=1.2				
STRAIN	TOTEN_Ti	TOTEN H2	TOTEN_TiH2	BINDING E
0.85	-51.987962	-6.7988031	-58.77158	-0.01519
0.90	-52.382532	-6.7988031	-59.17579	-0.00554
0.92	-52.478298	-6.7988031	-59.27354	-0.00356
0.94	-52.544944	-6.7988031	-59.34339	-0.00036
0.96	-52.582405	-6.7988031	-59.38074	-0.00047
0.98	-52.594605	-6.7988031	-59.39781	0.00440
1.00	-52.582980	-6.7988031	-59.38669	0.00491
1.02	-52.550367	-6.7988031	-59.35657	0.00740
1.04	-52.498004	-6.7988031	-59.30739	0.01058
1.06	-52.427287	-6.7988031	-59.23548	0.00939
1.08	-52.340174	-6.7988031	-59.14929	0.01031
1.10	-52.238321	-6.7988031	-59.05199	0.01486
1.15	-51.926180	-6.7988031	-58.74240	0.01741

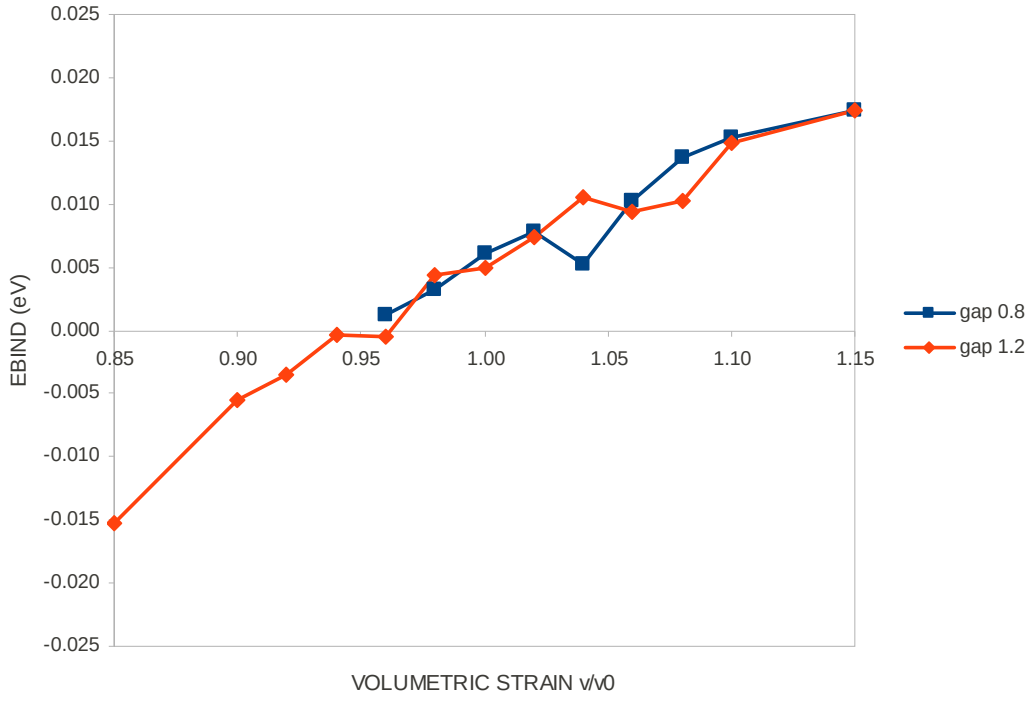

Figure 6.10: Variation of Binding energy with strain, for two supercells of Ti+H_2: gap (Ti-H) = 0.8 Å and 1.2 Å

From the preliminary calculations, the binding energy changes with strain. It is possible to increase the binding energy with compressive strain and reduce the binding energy with tensile strain.

CHAPTER 7

SYNTHESIS AND DTA TESTS

7.1 Synthesis

The synthesis method uses mixing of the powders in specified ratios, followed by partial curing of the epoxy binder and completed by static pressing of the semi-solid mixture. The maximum compressive load used was 24,000 lbs. Tests using max load of 50,000 lbs are scheduled. The fabrication procedure consists of the following steps:

1. *First disperse CNT in DMF (Dimethyl Formamide) solvent. Use sonification for an effective disperson for a duration of 12-18 hours.*
2. *Add and mix Nickel and Aluminum powders to the mixture of CNT and DMF. Then remove DMF by evaporation.*
3. *Separately mix the polymers. This consists of mixing the epoxy resin, the hardener, and the plasticizer.*
4. *Mix together the Ni-Al mixture with the polymer mixture. Use a mechanical mixer as necessary. Then evaporate the plasticizer (1/2 hour).*
5. *Partially cure the mixture at room temperature. It was found that 2-4 hour cure will produce a visco-elastic sample that can be compressed to the desired density. The pressing was accomplished in a specially designed and fabricated mold with load increments of 1000 lbs to a final load of 24,000 lbs (or 55,000 lbs) over a duration of 1 hour. The temperature of the compressed specimen was continuously monitored with a thermocouple.*

The starting powders and a ready mixture are shown in Fig. 7.1. Pressed samples are shown in Fig. 7.2. The mold used to press the cylindrical rod is shown in Fig. 7.3.

Figure 7.1: Species and mixture

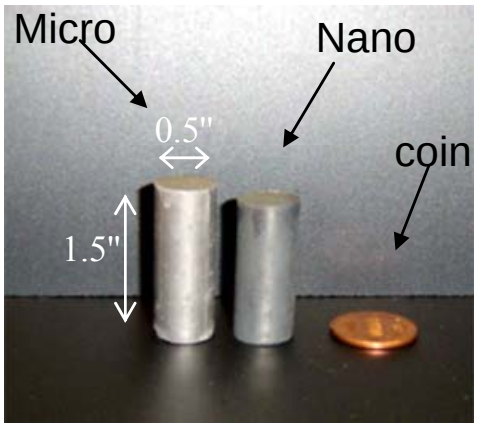

Figure 7.2: Pressed Ni+Al powders

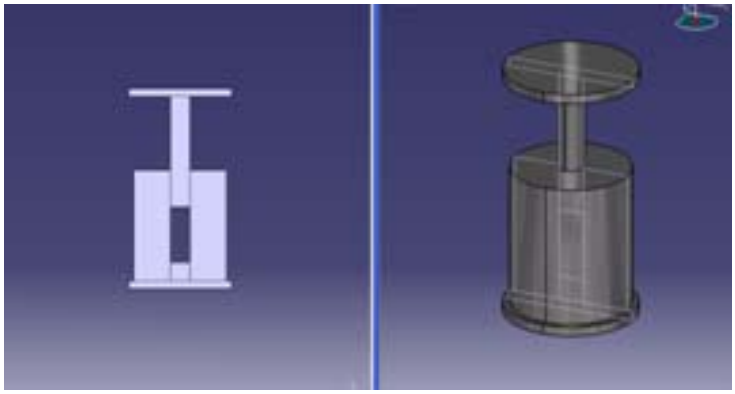

Figure 7.3: Mold used for pressing samples

The MTS 810 Loading Fixture, with a capacity of 55,000 lbs, and the Carver Hydraulic Press, with a capacity of 24,000 lbs are shown in Fig. 7.4.

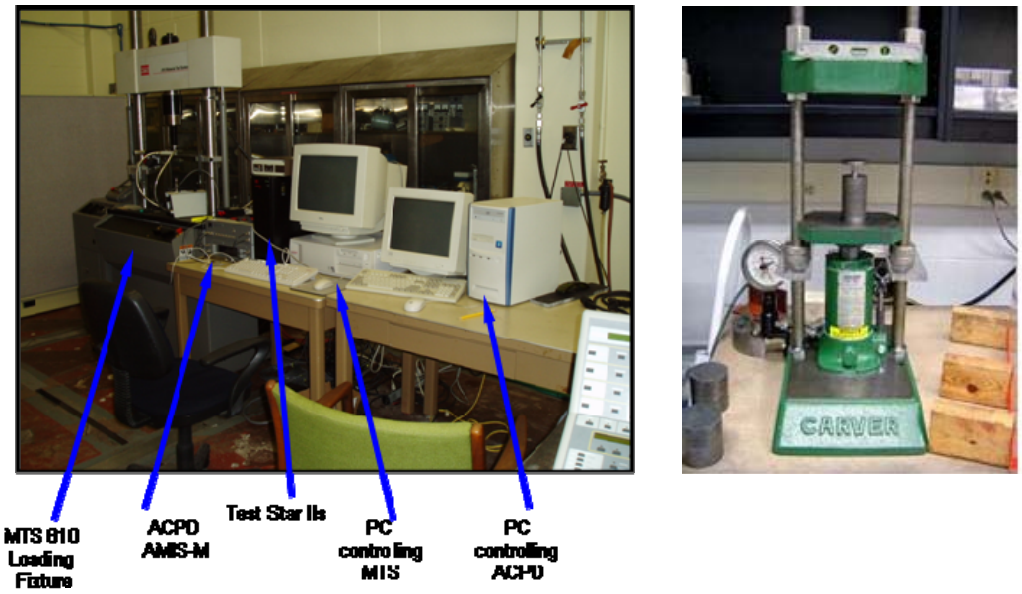

Figure 7.4: MTS 810 (left); Hydraulic press (right)

7.2 Characterization of Thermally Induced Chemical Reactions and Porosity

7.2.1 Characterization using SEM

Initial characterization of fabricated materials is performed using scanning electron microscopy (SEM) analysis, which reveals distribution of Ni and Al particles in the polymer matrices. SEM data from the staring species are shown on Figs. 7.5, 7.6 and 7.7. Nano powders are given with a magnification factor of 20,000. Micro powders are given with a magnification factor of 1,000. SEM data from the pressed samples are shown in Fig. 7.8. Two samples composed of nano NiAl+CNT+Epoxy, and of micro NiAl+carbon fibers+Teflon+Epoxy, are shown in 7.8(a) and 7.8(b), respectively. The round formations with brighter color correspond to the Ni and Al particles. The darker media surrounding the Ni and Al are the Epoxy, Teflon and Carbon reinforcements. On the images shown, one cannot distinguish between the carbon, Teflon and Epoxy, because of the charging of the non-conductive epoxy matrix. Coating the surface of the examined sample with a conductive layer will allow to obtain an image of the carbon fibers and CNT as well.

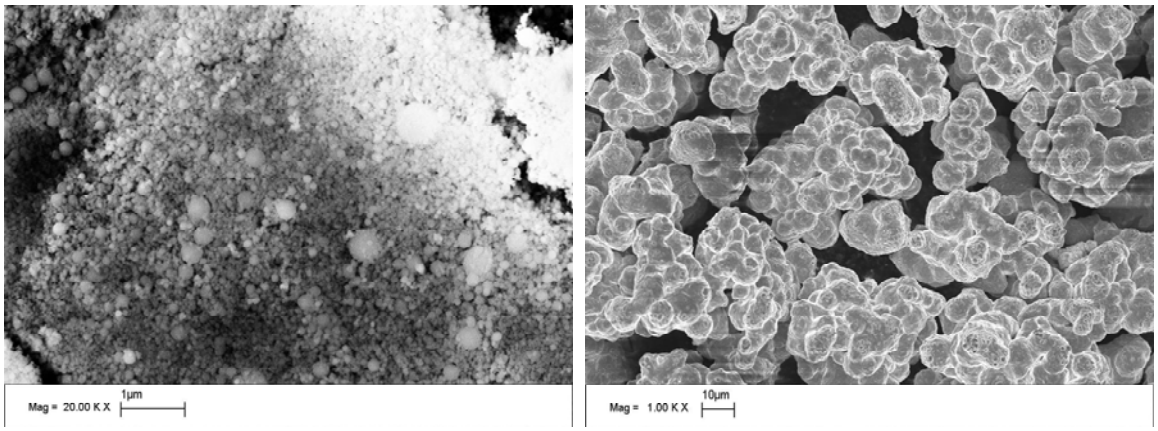

Figure 7.5: SEM of starting species: Nano Al, x20K (left); Micro Al, x1K (right)

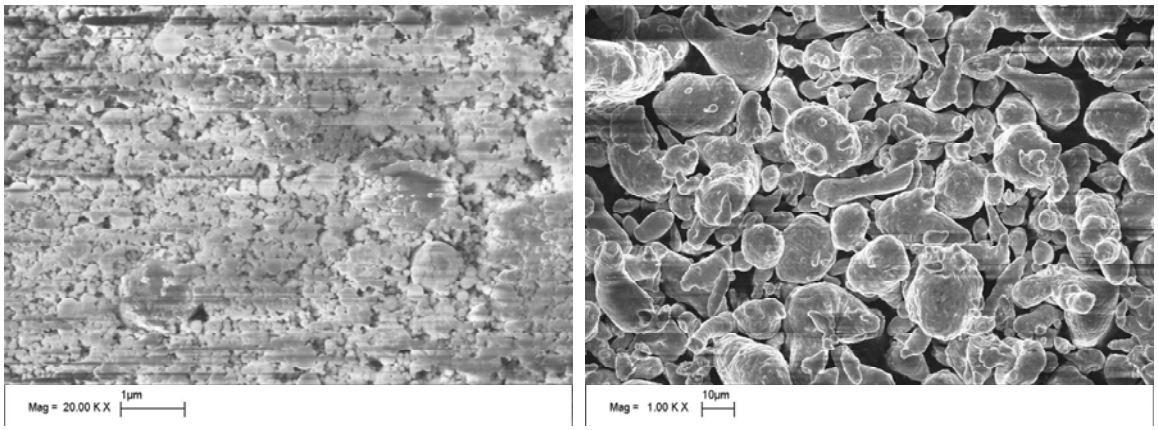

Figure 7.6: SEM of starting species: Nano Ni, x20K (left); Micro Ni, x1K (right)

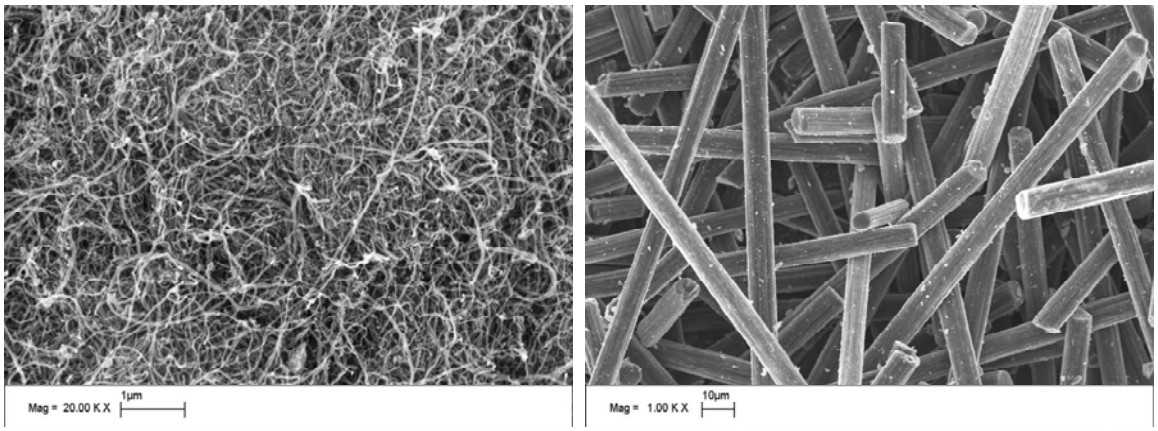

Figure 7.7: SEM of starting species: CNT, x20K (left); Carbon Fibers, x1K (right)

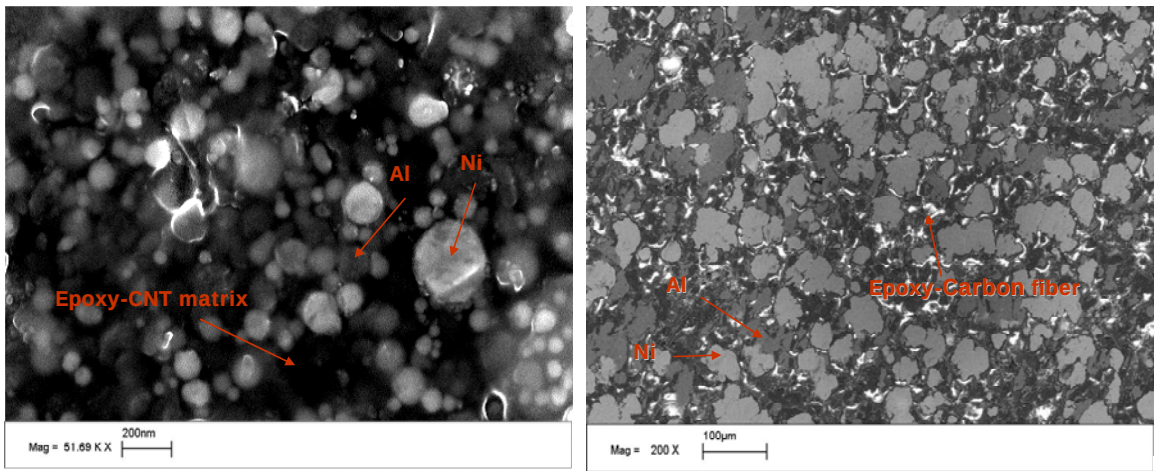

(a) (b)

Figure 7.8: SEM of (a) pressed nano-powder sample of Ni/Al/CNT/Epoxy, x50k; and (b) pressed micro-powder sample of Ni/Al/Fiber/Epoxy, x200

7.2.2 Density Measurements

Density measurements are indicators for the porosity in the pressed materials. The effect on % TMD (theoretical maximum density) of reinforcements, time for Epoxy semi-curing, and Teflon content is summarized in Fig. 7.9. Non-reinforced specimens made of Ni/Al/Teflon are represented by the blue curve. Reinforced Ni/Al specimens are shown by the purple curve. One can conclude that the reinforced specimens are compressed to a higher % TMD at the same applied pressure.

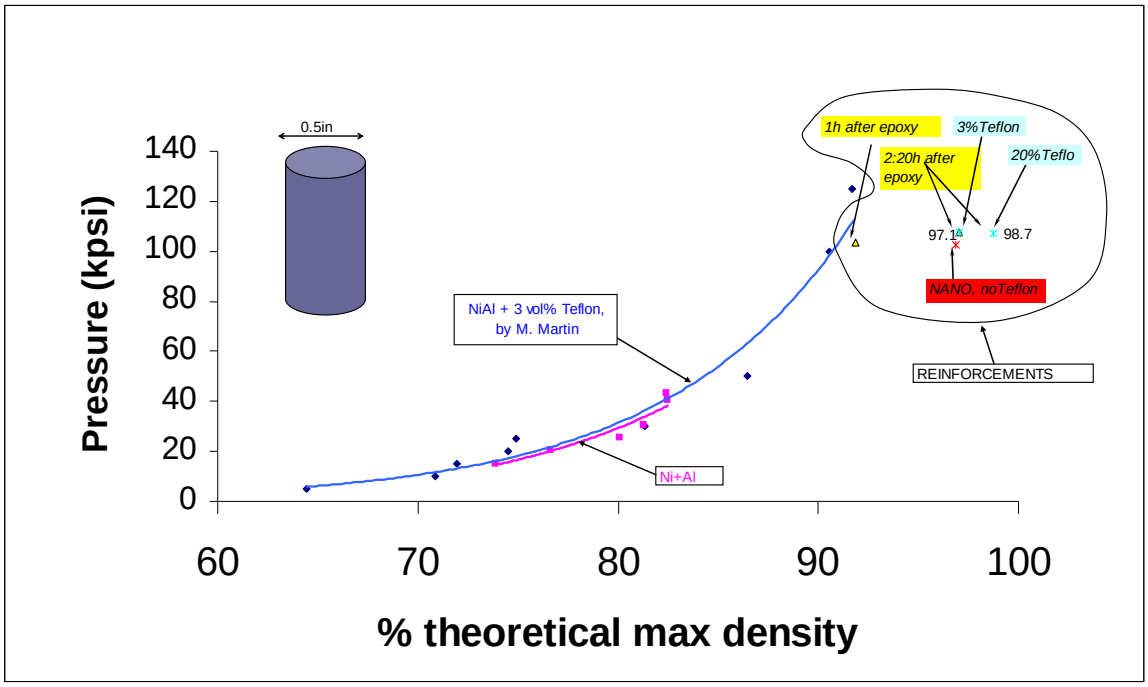

Figure 7.9: Comparison of the %TMD of pressed samples. Pressure vs. density of micro and nano Ni+Al + %vol Teflon, Carbon fiber and Epoxy

7.2.3 DTA Tests

DTA analysis was performed on the pressed samples as well as on the starting powders. Information for the composition of the various samples can be used to make conclusions for the character of reactions demonstrated by the DTA tests. Micro and nano pressed samples are shown on Figs. 7.10 and 7.11, respectively. It is obvious that a chemical reaction in the micro specimens occurs at 650 ºC, while in the nano specimens it is at 600 ºC. One can conclude that a specimen composed of nano powders will react at a slightly lower temperature. As a reference, DTA of pure Al powder (Fig. 7.14) indicates an endothermic process at 660 ºC, which corresponds to the melting temperature of Aluminum.

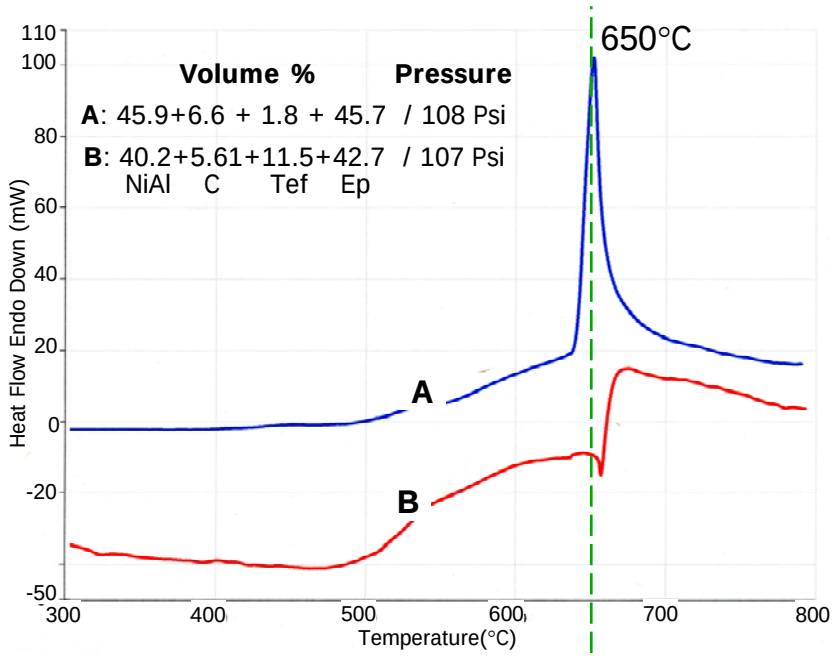

Figure 7.10: DTA of pressed micro-powder samples

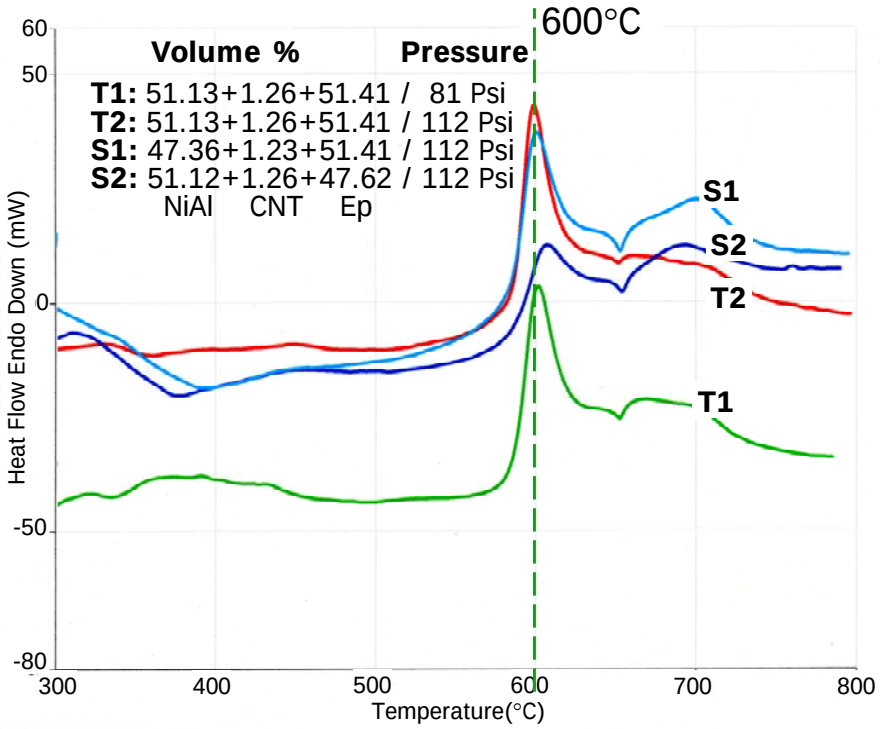

Figure 7.11: DTA of pressed nano-powder samples

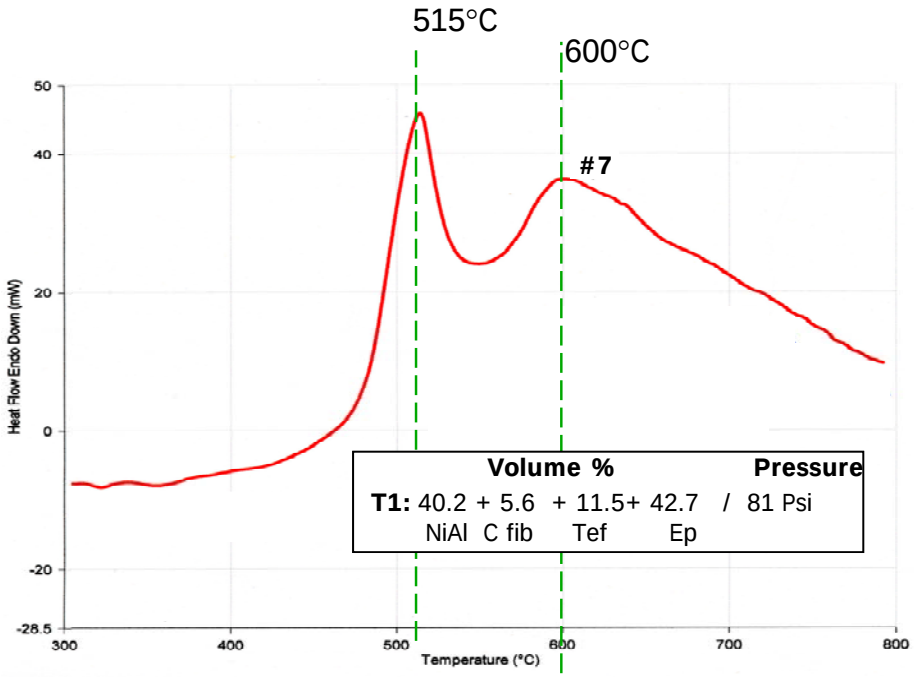

Figure 7.12: DTA of a pressed nano-powder sample with Carbon fiber and Teflon

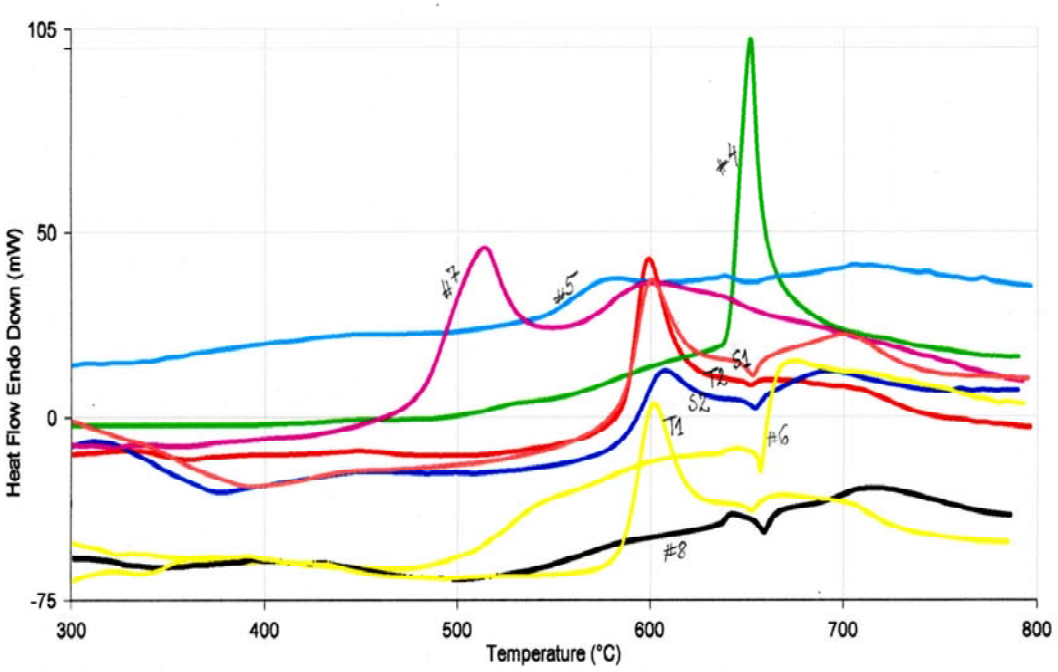

Figure 7.13: DTA of all pressed samples

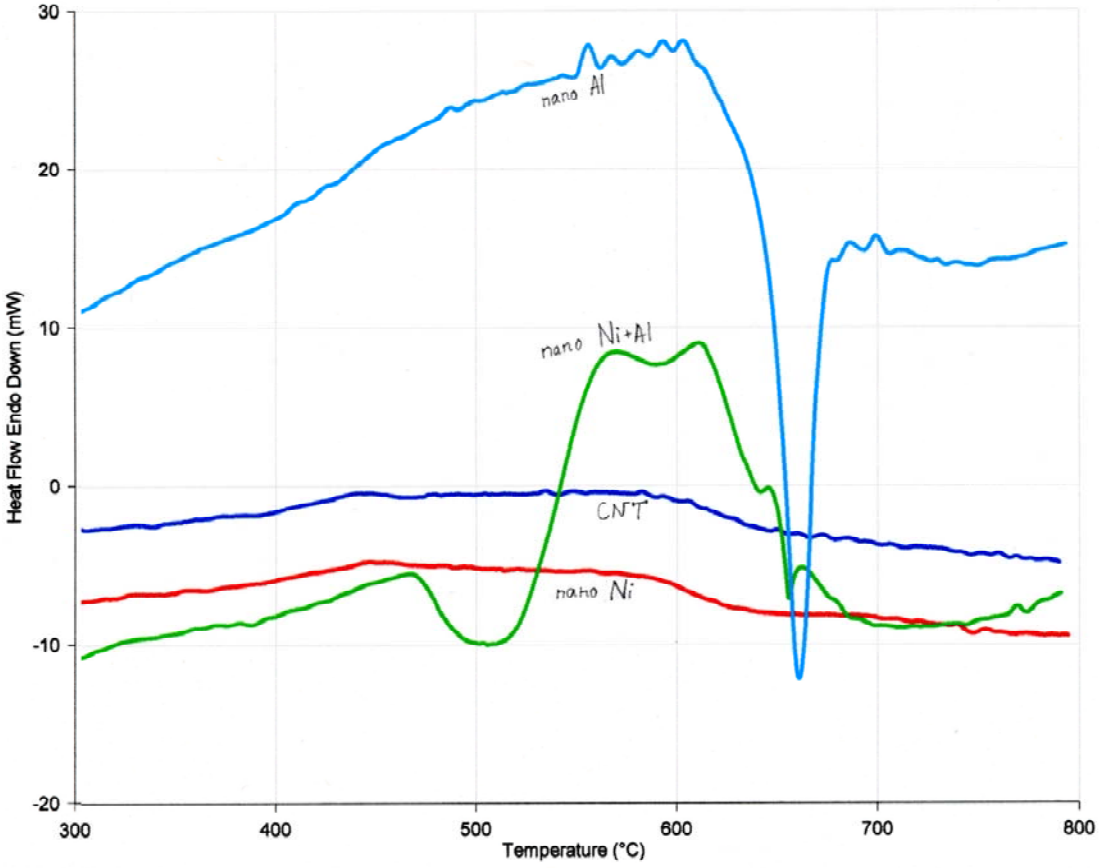

Figure 7.14: DTA of starting powders

VIII CONCLUSIONS AND RECOMMENDATIONS

This thesis research started with the goals of characterizing the constitutive relationships for finite deformation and shock induced chemical reactions of reactive structural materials, by the use of ab initio techniques or density functional theories based techniques, to avoid extensive number of tests for different mixtures, different ratios of mixtures and different shock conditions. These materials are also known by the names such as structural energetic materials or multifunctional materials that had the capabilities of both strength and energetic characteristics. First, it was noted that both these fields were very new research areas. In the area of determining the constitutive relations, there is a significant amount of literature that is related to the determination of the equations of state of crystalline solids by the use of ab initio techniques that used density functional theory as the foundation. Reported studies also existed in characterizing some alloys. However the structural material of interest in this thesis was the reactive structural material which is considered as a mixture. Similarly, there was a significant amount of literature on the reactions of a solid and a gas by the use of density functional theory. However, the chemical reactions of two solids or condensed matter by ab initio techniques were relatively a new research area.

Thus simple problems of determining the equations of state and thermally-induced chemical reactions of the mixture of Ni and Al were selected. Even these simple problems required identification of primitive cells or layers. Then it was necessary to identify quantitative separation of components of the mixture. Then, it was necessary to

determine the convergence criteria for the density functional theory based calculations. Primarily, this involved selections of cutoff energies and K points for each selected mixture ratio. Reasonable results were obtained for the equation of state and one chemical reaction for the formation of Ni_3Al, as suggested in the phase diagram.

Now, the future requires formulation of general procedures for shock induced or assisted chemical reactions of different reactive material mixtures. A first extension of this work is to reproduce different parts of the phase diagram for Ni and Al. In parallel, it is also necessary to establish procedures for determining the equations of state of different combination of mixtures of reactive materials that may have more than two components of the mixture and binders and different synthesis procedures.

Some other suggestions are to establish the optimum sizes of super cells and bridging the results to continuum scale computations. Then, it is necessary to extend the ab initio computations to study shock induced or assisted chemical reactions.

APPENDIX A

A BRIEF INTRODUCTION TO THE DENSITY FUNCTIONAL THEORY & THE APPLICATIONS OF THE THEORY

The details discussed in this Appendix are based on the lecture notes by Professor Hanagud and Dr. Xia Lu.

A.1 INTRODUCTION

In continuum mechanics-based linear elasticity theory, it is possible to derive the constitutive relationship or stress-strain relationships if knowledge of the strain energy is available. However, the constitutive relationships do have elastic constants. Experiments or tests are necessary to determine these constants. There are techniques to determine such elastic constants, without conducting tests or experiments. This is possible if we formulate the problem at a level beyond the continuum. In this level, the material is as a system of ions (nuclei) and electrons. Then, the quantum mechanics –based formulations are necessary in the formulation. Benefits of such a formulation have applications far beyond linear elasticity. Applications are sought in diverse fields, such as, chemical reactions, dielectric functions of materials, finite deformations of materials, alloys, mixtures and. study of different phases of materials including warm dense matter phase. In this appendix, the explanations relate simply to constitutive relationships and simple chemical reactions.

A.2 SCHRÖDINGER'S EQUATIONS AND THE ENERGY

For a multi-body system of ion and electrons, the Hamiltonian in the framework of quantum mechanics is as follows:

$$\hat{H} = -\frac{1}{2}\sum_{i=1}^{N}\nabla_i^2 - \frac{1}{2}\sum_{A=1}^{M}\frac{1}{M_A}\nabla_A^2 - \sum_{i=1}^{N}\sum_{A=1}^{M}\frac{Z_A}{r_{iA}} + \sum_{i=1}^{N}\sum_{j>i}^{N}\frac{1}{r_{ij}} + \sum_{A=1}^{M}\sum_{B>A}^{M}\frac{Z_A Z_B}{R_{AB}} \tag{A.1}$$

or

$$H = [T_N + T_e + V_{ee}(\vec{r}) + V_{NN}(\vec{R}) + V_{Ne}(\vec{r},\vec{R})] \tag{A.2}$$

The notations in this equation are as follows:

$$\nabla_i^2 = \frac{\partial^2}{\partial x_i^2} + \frac{\partial^2}{\partial y_i^2} + \frac{\partial^2}{\partial z_i^2};\ \nabla_A^2 = \frac{\partial^2}{\partial x_A^2} + \frac{\partial^2}{\partial y_A^2} + \frac{\partial^2}{\partial z_A^2} \tag{A.3}$$

- N nuclei:
  Coordinates $\vec{R} \equiv \vec{R}_1,\ldots,\vec{R}_N$
  Momenta $\vec{P} \equiv \vec{P}_1,\ldots,\vec{P}_N$
  Charges $Z_1,\ldots,Z_N$
  Masses $M_1,\ldots,M_N$
- Ne electrons:
  Coordinates $\vec{r} \equiv \vec{r}_1,\ldots,\vec{r}_{Ne}$
  Momenta $\vec{p} \equiv \vec{p}_1,\ldots,\vec{p}_{Ne}$
  Masses m
- Wave functions
  Electron $\Psi(x,\vec{R})$
  Nuclear $\chi(\vec{R})$
  Total $\hat{\Phi}(x,\vec{R})$

  where $x \equiv (\vec{r},s)$

T_N and T_e are the kinetic energies for the ions and electrons, respectively. V_{ee} and V_{NN} are the electrostatic potentials of electrons and ions respectively. V_{Ne} is the electrostatic interactions between the ions and electrons. The Schrödinger equation for a coupled electron-ion system is given by

$$[T_N + T_e + V_{ee}(\vec{r}) + V_{NN}(\vec{R}) + V_{Ne}(\vec{r},\vec{R})]\hat{\Phi}(x,\vec{R}) = E\hat{\Phi}(x,\vec{R}) \tag{A.4}$$

In this equation E is the energy of the system. $\hat{\Phi}(\mathrm{x},\vec{\mathrm{R}})$ is the wave function of the system. Since the electrons move much faster in comparison to the ions, we can approximate the system by a Born-Oppenheimer approximation (BO). The BO approximations states that the electrons move instantaneously as if the ions are fixed in space. Then the wave function of the system can be decoupled into the product of the electron wave function and the ion wave function.

$$\hat{\Phi}(\mathrm{x},\vec{\mathrm{R}}) = \Psi(\mathrm{x},\vec{\mathrm{R}})\chi(\vec{\mathrm{R}}) \tag{A.5}$$

As seen, the electron wave function depends on the ion position. Substituting the equation (A.5) into the equation (A.2), the Schrödinger equations for the coupled system can be reduced to a system of decoupled ion system and electron system.

$$\begin{cases} [\mathrm{T_e} + \mathrm{V_{ee}}(\vec{\mathrm{r}}) + \mathrm{V_{Ne}}(\vec{\mathrm{r}},\vec{\mathrm{R}})]\Psi_{\mathrm{n}}(\mathrm{x},\vec{\mathrm{R}}) = \mathrm{e_n}(\vec{\mathrm{R}})\Psi_{\mathrm{n}}(\mathrm{x},\vec{\mathrm{R}}) \\ [\mathrm{T_N} + \mathrm{V_{NN}}(\vec{\mathrm{R}}) + \mathrm{e}(\vec{\mathrm{R}})]\chi(\vec{\mathrm{R}}) = \varepsilon\chi(\vec{\mathrm{R}}) \end{cases} \tag{A.6}$$

Therefore, the total energy of the system consists of two parts: the contribution by the ions and the contribution by the electrons.

$$\mathrm{E}(\vec{\mathrm{R}}) = \mathrm{e}_0(\vec{\mathrm{R}}) + \varepsilon(\vec{\mathrm{R}}) \tag{A.7}$$

Techniques to find exact solutions of the equations in (A.6), which is a strong nonlinear system, is very difficult on the basis of currently available techniques. Two well known

techniques are the Hartree-Fock method and the density functional theory. In the first technique, the approximate representation of the wave function for the electron systems is in the form of a determinant known as the Slater determinant to characterize the interchangeable properties of electrons. Then the electron system of the equation (A.6) reduces to a one wave equation.

The second technique, which forms the foundation for this thesis depends on the Hohenberg and Kohn Theorem (1965), which states as follows.

[1] The ground-state energy of a many body system is a unique functional of the electron density

$$E_0 = E[n(\vec{r})] \tag{A.7}$$

The functional has its minimum at the equilibrium density $n_0(\vec{r})$

$$E_0 = E[n_0(\vec{r})] = \min_{n \to n_0}\{E[n(\vec{r})]\} \tag{A.8}$$

The electron density is defined as the probability of finding any of the N electrons within a differential volume element.

$$n(\vec{r}) = N_e \int ... \int \left|\Psi(x)\right|^2 ds_1 d\vec{r}_2 ... d\vec{r}_{Ne} \tag{A.9}$$

The energy of the electron system is defined as a functional

$$E[n] = T_e[n] + E_{ee}[n] + \int V_{Ne}(\vec{r}) n(\vec{r}) d^3r \tag{A.10}$$

Then, the solution of the equations becomes a variation problem, which is to find the density $n_0(\vec{r})$ to minimize the energy functional in the equation (A.6). This variation problem is presented in the equation (A.8).

Although the formulation of this variation problem, which is known as the density functional theory, is very elegant, the formulation of the problem is not complete because forms for the kinetic energy $T_e[n]$, the electron-electron repulsion energy $E_{ee}[n]$ and the nuclei-electron interaction potential $\int V_{Ne}(\vec{r})n(\vec{r})d^3r$ (as functions of the electron density) are unknown for a general many electron systems.

Thus, one approach to the solution is to start from a known reference system. Based on the selected reference system, it is possible to approximate the general system by adding corrections to the reference system. One of these techniques is known as the Kohn-Sham theory, which selects a system of non-interacting gas of electrons as the reference system (non-interacting means electrons do not interact via Coulomb repulsion). This reference system is chosen to have the same electron density as the density of the many electron system. That is,

$$n^{ks}(\vec{r}) = n_0(\vec{r}) \tag{A.11}$$

For the non-interacting gas system,

$$n^{ks}(\vec{r}) = \sum_i |\phi_i(\vec{r})|^2 \tag{A.12}$$

In this equation, $\phi_i(\vec{r})$ is the one electron-wave function, called Kohn-Sham orbitals. The energy for the non-interacting gas system is given by

$$E^{ks}[n^{ks}] = T_e^{ks}[n^{ks}] + E_{ee}^{ks}[n^{ks}(\vec{r})] + \int n^{ks}(\vec{r})V_{Ne}[n^{ks}(\vec{r})]d^3r \tag{A.13}$$

The forms for the functionals in the equation (A.13) are as follows

$$T_e^{ks}[n^{ks}] = \sum_i \int \phi_i^*(\vec{r})\left(-\frac{\hbar^2}{2m}\nabla^2\right)\phi_i(\vec{r})d^3r, \quad E_{ee}^{ks}[n^{ks}] = \frac{1}{2}\int \frac{n^{ks}(\vec{r})n^{ks}(\vec{r}')}{|\vec{r}-\vec{r}'|}d^3rd^3r' \tag{A.14}$$

For the interacting electron system, the electron density is $n_0(\vec{r})$. The energy for the interacting electron system is

$$E[n_0] = T_e[n_0] + E_{ee}[n_0] + \int V_{Ne}(\vec{r}) n_0(\vec{r}) d^3r \tag{A.15}$$

As stated, the forms for the functionals in the equation (A.15) are unknown. Then, an exchange-correlation functional is introduced to accommodate the difference between these two systems. This exchange-correlation functional describes the interactions between the electrons, which are not included in the non-interacting electron system.

$$E^{xc}[n_0] = E[n_0] - E^{ks}[n^{ks}] = E[n^{ks}] - E^{ks}[n^{ks}] \tag{A.16}$$

Therefore, the energy of the interacting system can be rewritten as follows.

$$E_0 = E[n_0] = E^{xc}[n^{ks}] + E^{ks}[n^{ks}] \tag{A.17}$$

The variation problem, which is to find an electron density of the interacting system n_0 to minimize its energy, is reduced to another variation problem, which is to find an electron density of the non-interacting system n^{ks} to minimize the energy of the corrected non-interacting system. Take the variation with respect to the Kohn-Sham orbitals, we obtain

$$\left(-\frac{\hbar^2}{2m}\nabla^2 + e^2 \int \frac{n^{ks}(\vec{r}')}{|\vec{r} - \vec{r}'|} d^3r + V_{Ne}(\vec{r}) + \mu^{xc}[n^{ks}] \right) \phi_i(\vec{r}) = \varepsilon_i \phi_i(\vec{r}) \tag{A.18}$$

In this equation $\mu^{xc}[n^{ks}]$ is known as the exchange-correlation potential.

$$\mu^{xc}[n^{ks}] = \frac{\partial E^{xc}[n^{ks}]}{\partial n^{ks}} \tag{A.19}$$

The energy of the interacting electron system as described in the equation (A.18) is given by

$$E_0 = \sum_i \varepsilon_i - \frac{1}{2} \int\int \frac{n^{ks}(\vec{r}) n^{ks}(\vec{r}')}{|\vec{r} - \vec{r}'|} d^3r d^3r' + \int n^{ks}(\vec{r}) \left\{ \varepsilon^{xc}[n^{ks}(\vec{r})] - \mu^{xc}[n^{ks}(\vec{r})] \right\} d^3r \tag{A.20}$$

In this equation, ε_i are the eigen values of the problem in the equation (A.18). $\varepsilon^{xc}[n^{ks}]$ is the exchange-correlation energy of a homogenous electron gas system, which is known as the Fermi-Thomas exchange-correlation energy. It is to be noted that the exchange-correlation energy is not known for a general system.

To solve for the equation (A.18), which challenges the current computational capabilities, it is necessary to consider additional approximations. These approximations s form three groups of categories. The first group is about the selection for the exchange-correlation functional. The second group is to choose the basis functions to represent the Kohn-Sham orbitals. The third group is to reduce the degrees of freedom of the interacting system by introducing the frozen core concept.

A.3 APPROXIMATION OF EXCHANGE-CORRELATION FUNCTIONALS

For the exchange-correlation functional, several current techniques are proposed in the literature. More new techniques are still being developed. The simplest technique is called the local density approximation (LDA). In this technique, the Fermi-Thomas exchange-correlation functional $\varepsilon^{xc}[n^{ks}]$ is used to replace $\mu^{xc}[n^{ks}]$ in the equation (A.18). For a spin-polarized system,

$$n^{ks}(\vec{r}) = n^{ks}(\vec{r},\uparrow) + n^{ks}(\vec{r},\downarrow). \tag{A.21}$$

The LDA is extended to the local spin density approximation (LDSA) to include the spin effects. The exchange part is given by

$$\varepsilon^{x}(\vec{r}) = -\frac{3e^2}{4\pi}(3\pi^2)^{1/3}\left(\frac{n^{ks}(\vec{r},\uparrow)^{4/3} + n^{ks}(\vec{r},\downarrow)^{4/3}}{n^{ks}(\vec{r})}\right) \tag{A.22}$$

The correlation functional $\varepsilon^c(\vec{r})$ is fitted to the ground-state energy of a homogenous electron gas calculated using quantum Monte Carlo simulations.

There is a consideration about the effects of the gradient of electron density to the exchange-correlation energy. Therefore

$$E^{xc}[n(\vec{r},\uparrow),n(\vec{r},\downarrow)] = \int f[n(\vec{r},\uparrow),n(\vec{r},\downarrow),\nabla n(\vec{r},\uparrow),\nabla n(\vec{r},\downarrow)]d^3r \qquad (A.23)$$

Current strategy is to adjust the function f such that it satisfies all known properties of the exchange-correlation hole and energy of different variants: *Perdew-Wang (PW), Becke-Perdew (BP), Lee-Yang-Parr(LYP), Perdew-Burke-Ernzernhof (PBE)* have proposed such functions.

A.4 FROZEN-CORE APPROXIMATION

Most physical properties of solids are dependent on the *valence* electrons to a much greater degree than that of the tightly bound *core* electrons. Therefore, the core electrons can be approximated to be *frozen* in their core configurations. This approximation considerably simplifies the task of solving the Kohn Sham equations, by eliminating all the degrees of freedom related to the core electrons. Then, the nuclear potential is replaced by a *weaker pseudopotential*, which takes into account the effects of the nucleus and the core electrons. Pseudopotentials act on a set of *pseudo "wave functions"* rather than the true valence "wave functions".

$$\left(-\frac{\hbar^2}{2m}\nabla^2+e^2\int\frac{n^{ks}(\vec{r}')}{|\vec{r}-\vec{r}'|}d^3r+V_{Ne}(\vec{r})+\mu^{xc}[n]\right)\phi_i(\vec{r})=\varepsilon_i\phi_i(\vec{r}) \qquad i=1,\ldots,N$$

Frozen core

$$\left(-\frac{\hbar^2}{2m}\nabla^2+e^2\int\frac{n^{ks}(\vec{r}')}{|\vec{r}-\vec{r}'|}d^3r+V_{pseudo}(\vec{r})+\mu^{xc}[n]\right)\tilde{\phi}_i(\vec{r})=\varepsilon_i\tilde{\phi}_i(\vec{r}) \qquad i=1,\ldots,N_{valence}$$

(A.24)

In this equation, $\tilde{\phi}_i(\vec{r})$ *is the Pseudo valence wavefunctions*. We can see that the number of DOFs reduces from the number of all the electrons to the number of only valence electrons. As shown in Fig. A.1, the space is divided into an interstitial region and a core region. The core region consists of spheres of a core radius r_c surrounding the nuclei. The rest of the space is the interstitial region. Pseudopotentials are constructed such that they match the true potential in the interstitial region. Similarly, each pseudo wave function (dotted lines in Fig. A.1, following the Vienna Ab Initio Simulation program (VASP) must match the corresponding true wave function (solid lines in Fig. A.1) in the interstitial region. The pseudopotentials are constructed in such a way that there are no radial nodes in the pseudo wave function $\tilde{\phi}_l$ in the core region (i.e. the strong oscillations of the valence orbitals ϕ_l are smoothed out). Usually, to replace the true wave function by a node-less pseudo wave function requires that

$$\int_0^{r_c}\phi_l(r)\phi_l^*(r)4\pi r^2dr=\int_0^{r_c}\tilde{\phi}_l(r)\tilde{\phi}_l^*(r)4\pi r^2dr \qquad (A.25)$$

$$\phi_l(r_c)^{(n)}=\tilde{\phi}_l(r_c)^{(n)},\quad n=0,1,2 \qquad (A.26)$$

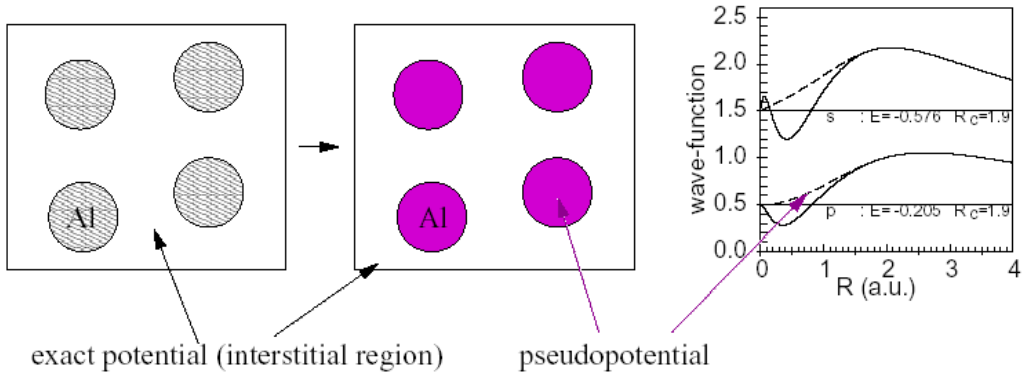

Figure A.1: Pseudo potential and pseudo wave function**.**

The condition in the equation (A.25) is to preserve the charge of pseudo wave function inside the core region to be equal to the true charge. This condition is also called the norm conservation. The condition in the equation (A.26) requires that up to the second order derivative, the pseudo wave functions have the same derivatives as the true wave functions.

In some cases for a hybrid p and d states, the norm conservation condition is relaxed. Augmentation charges inside the cutoff sphere can be added to correct the charge. This technique is called the ultrasoft pseudopotentials. It gives more freedom to form pseudopotentials for the p and d states. This leads to a much softer potentials in the core region, then significantly smoother pseudo wave functions, and reduce the size of the basis set required.

A.5 BASIS FUNCTIONS

It is possible to use a series expansion to represent some functions. Similarly, we can choose various sets of basis functions to represent the Kohn-Sham orbitals. The following lists the current commonly used basis sets.

- *Slater type or Gaussian type orbitals*

- *Plane waves* (PW): Plane waves are not localized. Large numbers of plane waves are needed to reproduce atomic cores → pseudopotential
- *Linearized augmented plane waves* (LAPW): Add atomic-like states to the plane-wave basis --- Expand the valence part of molecular orbitals in plane waves, the core part in compact atomic basis function
- *Projector augmented waves* (PAW): The wave function is a superposition of different terms: a plane wave part, the so-called pseudowavefunction, and expansions into atomic and pseudo atomic orbitals at each atom.

A.6 SOLUTION PROCEDURE

Up to this point, we have discussed various techniques to simplify the problem of an interacting electron system in the equation (A.18). To solve the equation (A.24), a self-consistency scheme is normally used. The procedure is as follows.

[1] Start with a density (for the 1st iteration, superposition of atomic densities is typically used).

[2] Establish grid for charge density and exchanger correlation potential

[3] Compute Kohn-Sham (KS) matrix (equivalent to the F matrix in Hartree-Fock method) elements and overlap integrals matrix.

[4] Solve the equations for expansion coefficients to obtain KS orbitals.

[5] Calculate new density.

[6] If density or energy changed substantially, go to step 1.

[7] If Self Consistent Field (SCF) cycle converged and geometry optimization is not requested, go to step 10.

[8] Calculate derivatives of energy vs. atom coordinates, and update atom coordinates. This may require denser integration grids and recomputing of Coulomb and exchange-correlation potential.

[9] If gradients are still large, or positions of nuclei moved appreciably, go to step 1.

[10] Calculate properties and print results.

After solving the equation (A.24), we can obtain the energy of the interacting electron system as given in the equation (A.20). Substituting the electron energy into the equation (A.5b), we can solve the equation (A.5b) to obtain the energy of the ion system. Therefore, the total energy for a coupled ion-electron system can be obtained from the equation (A.6). As known, given nuclei positions $\vec{R}$, we can obtain the total energy of the system $E(\vec{R})$.

APPENDIX B

Crystalline Structures

Crystal Groups and Classes: A perfect crystal is a periodic structure of unit cells. The primitive unit cell contains a minimum number of atoms. Crystallography groups are composed of 32 classes of symmetry derived from observations of the external crystal form. From these 32 classes, 230 space groups are distinguishable using x-ray analysis.

In the following, we give several examples of common space groups for metals. A face-centered cubic crystal is at the space group 225, possessing a symmetry of Fm $\bar{3}$m. A primitive unit cell of a face-centered cubic contains four atoms at the corners (Fig. B.2). A body centered cubic is at the space group 229, possessing a symmetry of Im $\bar{3}$m. A primitive unit cell of a body-centered cubic contains only one atom at the center (Fig. B.3).

The crystal lattice can be described by three lattice vectors. Or by (a, b, c) and (α, β, γ).

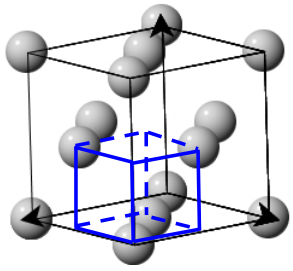

Figure B.1: Face-centered cubic

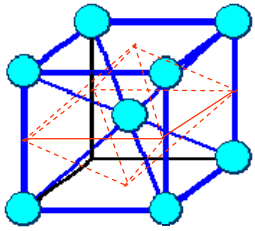

Figure B.2: Body-centered cubic

Classification of Crystals:

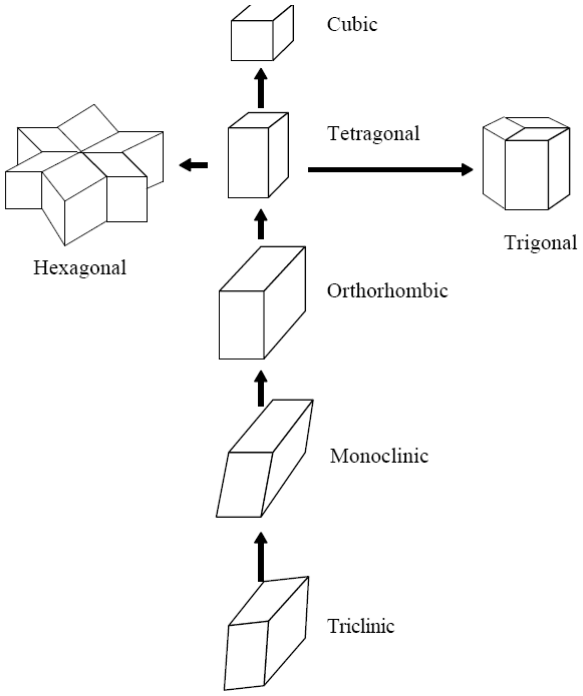

Figure B.3: Classification of Crystals

Sections of a Cubic Crystal:

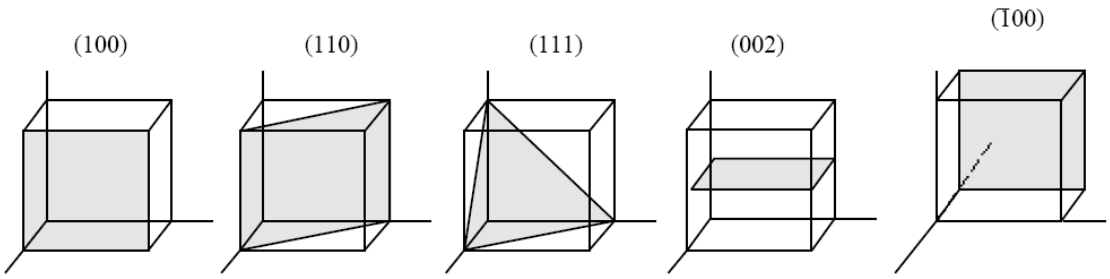

Figure B.4: Sections of Cubic Crystals

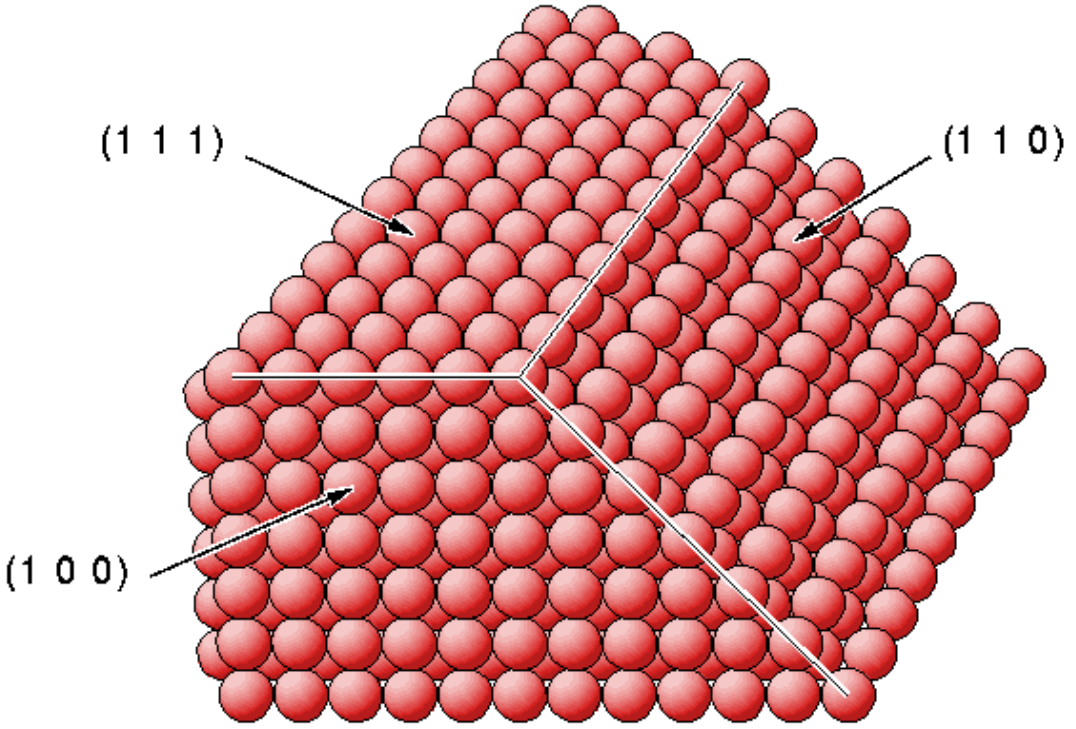

Figure B.5: FCC Different planes showing Sections

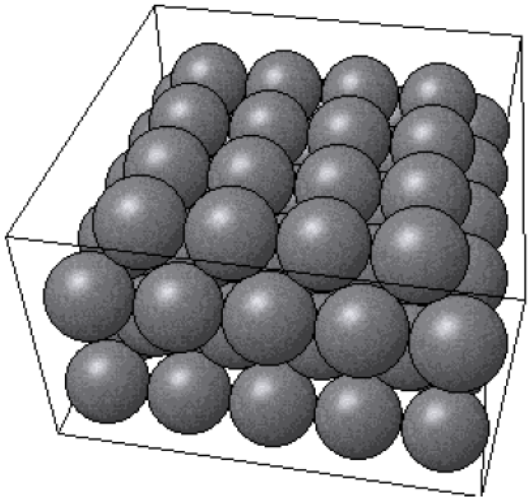

FCC(100)

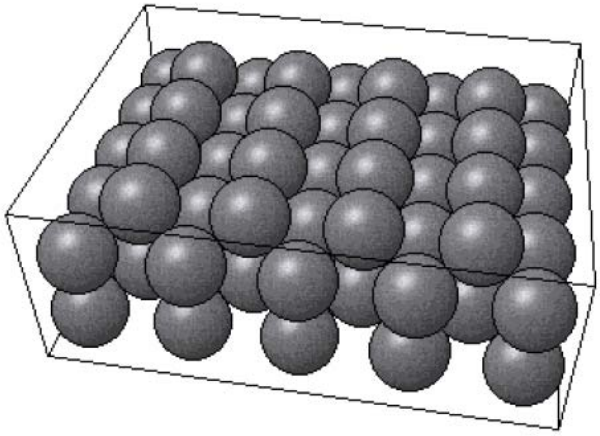

FCC(110)

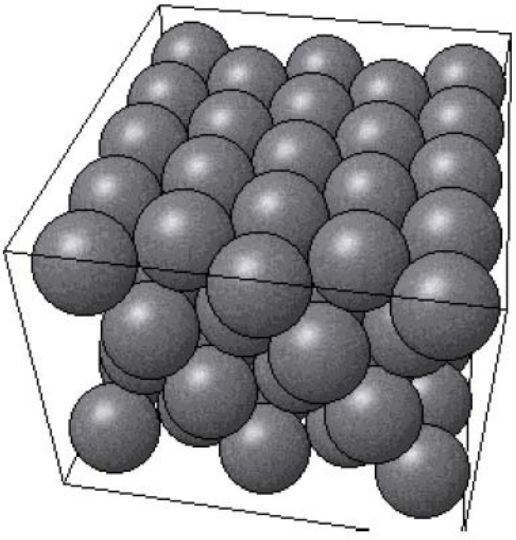

FCC(111)

Figure B.6: FCC 100, 110 & 111 Sections

FCC Adsorption Sites:

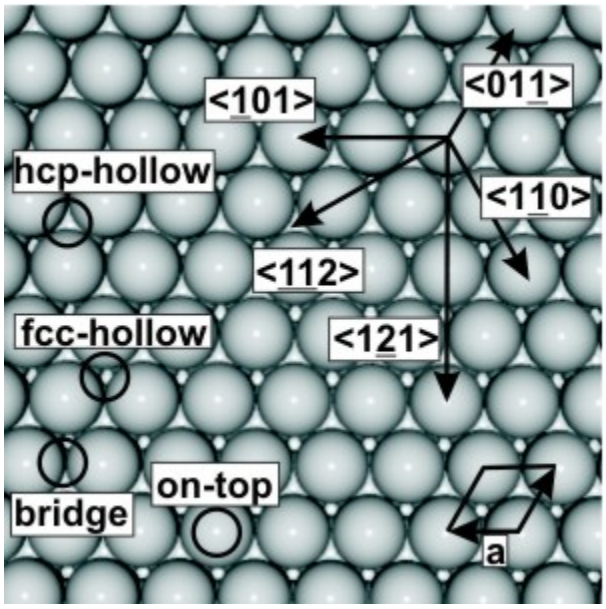

Figure B.7: Adsorption sites

APPENDIX C

INPUT TO AB INITIO PROGRAMS

This Appendix contains inputs for some of the performed VASP calculations for the W+CO, Ni+Al and Ti+H2 systems.

W+CO SYSTEM

POTCARs:
PAW_PBE W 08Apr2002
PAW_PBE C 08Apr2002

Inputs bulk W
==========
SYSTEM = bcc w
 ENCUT = 800 => ENCUT varied to 400, 500, ..., 1600
 ISTART = 0;
 ISMEAR = 0; SIGMA = 0.1
 IBRION = 2; ISIF = 7; NSW = 10
 NBANDS = 20
 EDIFF = 1E-07; EDIFFG = 1E-06

K-Points
 0
Monkhorst Pack
 5 5 5 => k-points grid varied to 1x1x1, 2x2x2, ..., 15x15x15
 0 0 0

W bcc bulk:
  3.16
  1.0000000000000000 0.0000000000000000 0.0000000000000000
  0.0000000000000000 1.0000000000000000 0.0000000000000000
  0.0000000000000000 0.0000000000000000 1.0000000000000000
    2
Direct
  0.0000000000000000 0.0000000000000000 0.0000000000000000

0.5000000000000000 0.5000000000000000 0.5000000000000000

Inputs CO
==========
SYSTEM = CO in SC aW=3.172168546 strain=1.00
 ENCUT = 700
 ISTART = 0;
 ISMEAR = 0; SIGMA = 0.1
 IBRION = 2; ISIF = 2; NSW = 150
 NGX = 78; NGY = 68; NGZ = 134;
 NBANDS = 180; LREAL = .FALSE.
 EDIFF = 1E-06; EDIFFG = 1E-06

K-Points
 0
Monkhorst Pack
 5 5 1
 0 0 0

POSCAR:
W+CO (1.00) (aW = 3.1721685460561386, CO=1.14273048632876) :
   1.00000000000000
     8.9722475599318674   0.0000000000000000   0.0000000000000000
     0.0000000000000000   7.7701943159439386   0.0000000000000000
     0.0000000000000000   0.0000000000000000   15.4943570919411258
  1   1
Selective dynamics
Direct
  0.2500000000000000 0.5001845214439564 0.5208407210535770   T   T   T
  0.2500000000000000 0.5001845214439564 0.5945921183879730   T   T   T

CONTCAR:
W+CO (1.00) (aW = 3.1721685460561386, CO
   1.00000000000000
     8.9722475599318674   0.0000000000000000   0.0000000000000000
     0.0000000000000000   7.7701943159439386   0.0000000000000000
     0.0000000000000000   0.0000000000000000   15.4943570919411258
   1   1
Selective dynamics
Direct
  0.2500000000000000 0.5001845214439555 0.5208376659982591   T   T   T
  0.2500000000000000 0.5001845214439555 0.5945951734432867   T   T   T

Inputs W 0.975
==========
SYSTEM = W(111) SC aW=3.172168546 strain<1.00
ENCUT = 700
ISTART = 0;
ISMEAR = 0; SIGMA = 0.1
IBRION = 2; ISIF = 2; NSW = 150
NGX = 78; NGY = 68; NGZ = 134;
NBANDS = 180; LREAL = .True.
EDIFF = 1E-06; EDIFFG = 1E-06

K-Points
0
Monkhorst Pack
5 5 1
0 0 0

POSCAR:
W (0.975) :
1.00000000000000
8.7479413709335692 0.0000000000000000 0.0000000000000000
0.0000000000000000 7.5759394580453394 0.0000000000000000
0.0000000000000000 0.0000000000000000 15.3569981646425973
28
Selective dynamics
Direct
0.0000000000000000 0.0000000000000000 0.0499999999999972 F F F
0.5000000000000000 0.0000000000000000 0.0499999999999972 F F F
0.7500000000000000 0.5000000000000000 0.0499999999999972 F F F
0.2500000000000000 0.5000000000000000 0.0499999999999972 F F F
0.0000000000000000 0.3333333333333357 0.1081385123491145 F F F
0.5000000000000000 0.3333333333333357 0.1081385123491145 F F F
0.7500000000000000 0.8333333333333357 0.1081385123491145 F F F
0.2500000000000000 0.8333333333333357 0.1081385123491145 F F F
0.0000000000000000 0.6666666666666643 0.1662770246982319 F F F
0.5000000000000000 0.6666666666666643 0.1662770246982319 F F F
0.7500000000000000 0.1666666666666643 0.1662770246982319 F F F
0.2500000000000000 0.1666666666666643 0.1662770246982319 F F F
0.0000000000000000 0.0000624417956115 0.2250208309296103 T T T
0.5000000000000000 0.0000624417956115 0.2250208309296103 T T T
0.7500000000000000 0.5000624417956115 0.2250208309296103 T T T
0.2500000000000000 0.5000624417956115 0.2250208309296103 T T T
0.0000000000000000 0.3334986176223252 0.2925497072851362 T T T
0.5000000000000000 0.3334986176223252 0.2925497072851362 T T T

0.7500000000000000 0.8334986176223252 0.2925497072851362 T T T
0.2500000000000000 0.8334986176223252 0.2925497072851362 T T T
0.0000000000000000 0.6667733473317088 0.3434981547967778 T T T
0.5000000000000000 0.6667733473317088 0.3434981547967778 T T T
0.7500000000000000 0.1667733473317088 0.3434981547967778 T T T
0.2500000000000000 0.1667733473317088 0.3434981547967778 T T T
0.0000000000000000 0.9998862423301899 0.3944083405683612 T T T
0.5000000000000000 0.9998862423301899 0.3944083405683612 T T T
0.7500000000000000 0.4998862423301898 0.3944083405683612 T T T
0.2500000000000000 0.4998862423301898 0.3944083405683612 T T T

CONTCAR:
W (0.975) :
1.00000000000000
8.7479413709335692 0.0000000000000000 0.0000000000000000
0.0000000000000000 7.5759394580453394 0.0000000000000000
0.0000000000000000 0.0000000000000000 15.3569981646425973
28
Selective dynamics
Direct
0.0000000000000000 0.0000000000000000 0.0499999999999972 F F F
0.5000000000000000 0.0000000000000000 0.0499999999999972 F F F
0.7500000000000000 0.5000000000000000 0.0499999999999972 F F F
0.2500000000000000 0.5000000000000000 0.0499999999999972 F F F
0.0000000000000000 0.3333333333333357 0.1081385123491145 F F F
0.5000000000000000 0.3333333333333357 0.1081385123491145 F F F
0.7500000000000000 0.8333333333333357 0.1081385123491145 F F F
0.2500000000000000 0.8333333333333357 0.1081385123491145 F F F
0.0000000000000000 0.6666666666666643 0.1662770246982319 F F F
0.5000000000000000 0.6666666666666643 0.1662770246982319 F F F
0.7500000000000000 0.1666666666666643 0.1662770246982319 F F F
0.2500000000000000 0.1666666666666643 0.1662770246982319 F F F
0.0000000000000000 0.0000589716803529 0.2249472881239787 T T T
0.5000000000000000 0.0000589716803529 0.2249472881239787 T T T
0.7500000000000000 0.5000589716803530 0.2249472881239787 T T T
0.2500000000000000 0.5000589716803530 0.2249472881239787 T T T
0.0000000000000000 0.3334698032396028 0.2924308973578180 T T T
0.5000000000000000 0.3334698032396028 0.2924308973578180 T T T
0.7500000000000000 0.8334698032396028 0.2924308973578180 T T T
0.2500000000000000 0.8334698032396028 0.2924308973578180 T T T
0.0000000000000000 0.6667778058931347 0.3433851358753003 T T T
0.5000000000000000 0.6667778058931347 0.3433851358753003 T T T
0.7500000000000000 0.1667778058931348 0.3433851358753003 T T T
0.2500000000000000 0.1667778058931348 0.3433851358753003 T T T
0.0000000000000000 0.9998920200848969 0.3942400836722988 T T T

```
 0.5000000000000000  0.9998920200848969  0.3942400836722988   T   T   T
 0.7500000000000000  0.4998920200848969  0.3942400836722988   T   T   T
 0.2500000000000000  0.4998920200848969  0.3942400836722988   T   T   T


Inputs W 1.0
==================
 SYSTEM = W(111) SC aW=3.172168546 strain=1.00
 ENCUT = 700
 ISTART = 0;
 ISMEAR = 0; SIGMA = 0.1
 IBRION = 2; ISIF = 2; NSW = 150
 NGX = 78; NGY = 68; NGZ = 134;
 NBANDS = 180; LREAL = .True.
 EDIFF = 1E-06; EDIFFG = 1E-06


K-Points
 0
Monkhorst Pack
 5  5  1
 0  0  0


POSCAR:
W (1.00) (aW = 3.1721685460561386) :
   1.00000000000000
     8.9722475599318674    0.0000000000000000    0.0000000000000000
     0.0000000000000000    7.7701943159439386    0.0000000000000000
     0.0000000000000000    0.0000000000000000   15.4943570919411258
  28
Selective dynamics
Direct
  0.0000000000000000  0.0000000000000000  0.0499999999999972   F   F   F
  0.5000000000000000  0.0000000000000000  0.0499999999999972   F   F   F
  0.7500000000000000  0.5000000000000000  0.0499999999999972   F   F   F
  0.2500000000000000  0.5000000000000000  0.0499999999999972   F   F   F
  0.0000000000000000  0.3333333333333357  0.1091006246052260   F   F   F
  0.5000000000000000  0.3333333333333357  0.1091006246052260   F   F   F
  0.7500000000000000  0.8333333333333357  0.1091006246052260   F   F   F
  0.2500000000000000  0.8333333333333357  0.1091006246052260   F   F   F
  0.0000000000000000  0.6666666666666643  0.1682012492104619   F   F   F
  0.5000000000000000  0.6666666666666643  0.1682012492104619   F   F   F
  0.7500000000000000  0.1666666666666643  0.1682012492104619   F   F   F
  0.2500000000000000  0.1666666666666643  0.1682012492104619   F   F   F
  0.9996594730550240 -0.0000220804453254  0.2202245794404178   T   T   T
```

0.5003405269449760 -0.0000220804453254 0.2202245794404178 T T T
0.7500000000000000 0.5000416700803326 0.2202415234341149 T T T
0.2500000000000000 0.5001153175201469 0.2123600518487248 T T T
0.0001993513889346 0.3335929541062235 0.2878958676029512 T T T
0.4998006486110654 0.3335929541062235 0.2878958676029512 T T T
0.7500000000000000 0.8323021835400322 0.2889272414063013 T T T
0.2500000000000000 0.8342487847177863 0.2882760996350535 T T T
0.0016996144733222 0.6656678735646093 0.3376901233468914 T T T
0.4983003855266779 0.6656678735646093 0.3376901233468914 T T T
0.7500000000000000 0.1674093323211862 0.3360948280282421 T T T
0.2500000000000000 0.1681375761954534 0.3371915242943748 T T T
0.9995182624341934 0.0006717146108736 0.3833753653657150 T T T
0.5004817375658066 0.0006717146108736 0.3833753653657150 T T T
0.7500000000000000 0.4988612780369560 0.3835053095480336 T T T
0.2500000000000000 0.5001845214439564 0.3867473750432512 T T T

CONTCAR:
W (1.00) (aW = 3.1721685460561386) :
1.00000000000000
8.9722475599318674 0.0000000000000000 0.0000000000000000
0.0000000000000000 7.7701943159439386 0.0000000000000000
0.0000000000000000 0.0000000000000000 15.4943570919411258
28
Selective dynamics
Direct
0.0000000000000000 0.0000000000000000 0.0499999999999972 F F F
0.5000000000000000 0.0000000000000000 0.0499999999999972 F F F
0.7500000000000000 0.5000000000000000 0.0499999999999972 F F F
0.2500000000000000 0.5000000000000000 0.0499999999999972 F F F
0.0000000000000000 0.3333333333333357 0.1091006246052260 F F F
0.5000000000000000 0.3333333333333357 0.1091006246052260 F F F
0.7500000000000000 0.8333333333333357 0.1091006246052260 F F F
0.2500000000000000 0.8333333333333357 0.1091006246052260 F F F
0.0000000000000000 0.6666666666666643 0.1682012492104619 F F F
0.5000000000000000 0.6666666666666643 0.1682012492104619 F F F
0.7500000000000000 0.1666666666666643 0.1682012492104619 F F F
0.2500000000000000 0.1666666666666643 0.1682012492104619 F F F
0.0000034191264794 0.0000565266099660 0.2200172276540948 T T T
0.4999965808735205 0.0000565266099660 0.2200172276540948 T T T
0.7500000000000000 0.5000435910288485 0.2200212420045605 T T T
0.2500000000000000 0.5000578594376476 0.2200194723065924 T T T
-0.0000035897763793 0.3333796134260548 0.2882023624320542 T T T
0.5000035897763793 0.3333796134260548 0.2882023624320542 T T T
0.7500000000000000 0.8333762052766730 0.2881902487321006 T T T
0.2500000000000000 0.8333770633025469 0.2882073664015677 T T T

-0.0000102304579757 0.6666900891125299 0.3365484177737052 T T T
0.5000102304579757 0.6666900891125299 0.3365484177737052 T T T
0.7500000000000000 0.1666834273591386 0.3365449513201329 T T T
0.2500000000000000 0.1667055942360136 0.3365479441255977 T T T
0.0000131337219483 0.0000787303053706 0.3833160856042020 T T T
0.4999868662780518 0.0000787303053706 0.3833160856042020 T T T
0.7500000000000000 0.5000537633879270 0.3833173538685716 T T T
0.2500000000000000 0.5000951689098270 0.3833194402502982 T T T

Inputs W 1.03
==========
SYSTEM = W(111) SC aW=3.172168546 strain>1.00
ENCUT = 700
ISTART = 0;
ISMEAR = 0; SIGMA = 0.1
IBRION = 2; ISIF = 2; NSW = 150
NGX = 78; NGY = 68; NGZ = 134;
NBANDS = 180; LREAL = .True.
EDIFF = 1E-06; EDIFFG = 1E-06

K-Points
0
Monkhorst Pack
5 5 1
0 0 0

POSCAR:
W (1.03) (aW = 3.1721685460561386) :
1.03000000000000
8.9722475599318674 0.0000000000000000 0.0000000000000000
0.0000000000000000 7.7701943159439386 0.0000000000000000
0.0000000000000000 0.0000000000000000 15.4943570919411258
28
Selective dynamics
Direct
0.0000000000000000 0.0000000000000000 0.0499999999999972 F F F
0.5000000000000000 0.0000000000000000 0.0499999999999972 F F F
0.7500000000000000 0.5000000000000000 0.0499999999999972 F F F
0.2500000000000000 0.5000000000000000 0.0499999999999972 F F F
0.0000000000000000 0.3333333333333357 0.1091006246052260 F F F
0.5000000000000000 0.3333333333333357 0.1091006246052260 F F F
0.7500000000000000 0.8333333333333357 0.1091006246052260 F F F
0.2500000000000000 0.8333333333333357 0.1091006246052260 F F F

0.0000000000000000 0.6666666666666643 0.1682012492104619 F F F
0.5000000000000000 0.6666666666666643 0.1682012492104619 F F F
0.7500000000000000 0.1666666666666643 0.1682012492104619 F F F
0.2500000000000000 0.1666666666666643 0.1682012492104619 F F F
0.0000000000000000 0.0000432437007099 0.2200613496300725 T T T
0.5000000000000000 0.0000432437007099 0.2200613496300725 T T T
0.7500000000000000 0.5000432437007100 0.2200613496300725 T T T
0.2500000000000000 0.5000432437007100 0.2200613496300725 T T T
0.0000000000000000 0.3333688061837887 0.2882890792861474 T T T
0.5000000000000000 0.3333688061837887 0.2882890792861474 T T T
0.7500000000000000 0.8333688061837887 0.2882890792861474 T T T
0.2500000000000000 0.8333688061837887 0.2882890792861474 T T T
0.0000000000000000 0.6666718424150652 0.3366308635448612 T T T
0.5000000000000000 0.6666718424150652 0.3366308635448612 T T T
0.7500000000000000 0.1666718424150651 0.3366308635448612 T T T
0.2500000000000000 0.1666718424150651 0.3366308635448612 T T T
0.0000000000000000 0.0000515800868524 0.3834057489750923 T T T
0.5000000000000000 0.0000515800868524 0.3834057489750923 T T T
0.7500000000000000 0.5000515800868524 0.3834057489750923 T T T
0.2500000000000000 0.5000515800868524 0.3834057489750923 T T T

CONTCAR:
W (1.03) (aW = 3.1721685460561386) :
1.03000000000000
8.9722475599318674 0.0000000000000000 0.0000000000000000
0.0000000000000000 7.7701943159439386 0.0000000000000000
0.0000000000000000 0.0000000000000000 15.4943570919411258
28
Selective dynamics
Direct
0.0000000000000000 0.0000000000000000 0.0499999999999972 F F F
0.5000000000000000 0.0000000000000000 0.0499999999999972 F F F
0.7500000000000000 0.5000000000000000 0.0499999999999972 F F F
0.2500000000000000 0.5000000000000000 0.0499999999999972 F F F
0.0000000000000000 0.3333333333333357 0.1091006246052260 F F F
0.5000000000000000 0.3333333333333357 0.1091006246052260 F F F
0.7500000000000000 0.8333333333333357 0.1091006246052260 F F F
0.2500000000000000 0.8333333333333357 0.1091006246052260 F F F
0.0000000000000000 0.6666666666666643 0.1682012492104619 F F F
0.5000000000000000 0.6666666666666643 0.1682012492104619 F F F
0.7500000000000000 0.1666666666666643 0.1682012492104619 F F F
0.2500000000000000 0.1666666666666643 0.1682012492104619 F F F
0.0000000000000000 0.0000273723097391 0.2121011797332833 T T T
0.5000000000000000 0.0000273723097391 0.2121011797332833 T T T
0.7500000000000000 0.5000273723097393 0.2121011797332833 T T T

0.2500000000000000 0.5000273723097393 0.2121011797332833 T T T
0.0000000000000000 0.3333116513157100 0.2801152898017266 T T T
0.5000000000000000 0.3333116513157100 0.2801152898017266 T T T
0.7500000000000000 0.8333116513157099 0.2801152898017266 T T T
0.2500000000000000 0.8333116513157099 0.2801152898017266 T T T
0.0000000000000000 0.6666138982031063 0.3249848913786861 T T T
0.5000000000000000 0.6666138982031063 0.3249848913786861 T T T
0.7500000000000000 0.1666138982031062 0.3249848913786861 T T T
0.2500000000000000 0.1666138982031062 0.3249848913786861 T T T
0.0000000000000000 0.0000906475949615 0.3679326718477737 T T T
0.5000000000000000 0.0000906475949615 0.3679326718477737 T T T
0.7500000000000000 0.5000906475949615 0.3679326718477737 T T T
0.2500000000000000 0.5000906475949615 0.3679326718477737 T T T

Inputs WCO 0.975
==========
SYSTEM = W+CO(111) SC aW=3.172168546 strain<1.00
ENCUT = 700
ISTART = 0;
ISMEAR = 0; SIGMA = 0.1
IBRION = 2; ISIF = 2; NSW = 150
NGX = 78; NGY = 68; NGZ = 134;
NBANDS = 180; LREAL = .True.
EDIFF = 1E-06; EDIFFG = 1E-06

K-Points
0
Monkhorst Pack
5 5 1
0 0 0

POSCAR:
W+CO (0.975) :
1.00000000000000
8.7479413709335692 0.0000000000000000 0.0000000000000000
0.0000000000000000 7.5759394580453394 0.0000000000000000
0.0000000000000000 0.0000000000000000 15.3569981646425973
28 1 1
Selective dynamics
Direct
0.0000000000000000 0.0000000000000000 0.0499999999999972 F F F
0.5000000000000000 0.0000000000000000 0.0499999999999972 F F F
0.7500000000000000 0.5000000000000000 0.0499999999999972 F F F

0.2500000000000000 0.5000000000000000 0.0499999999999972 F F F
0.0000000000000000 0.3333333333333357 0.1081385123491145 F F F
0.5000000000000000 0.3333333333333357 0.1081385123491145 F F F
0.7500000000000000 0.8333333333333357 0.1081385123491145 F F F
0.2500000000000000 0.8333333333333357 0.1081385123491145 F F F
0.0000000000000000 0.6666666666666643 0.1662770246982319 F F F
0.5000000000000000 0.6666666666666643 0.1662770246982319 F F F
0.7500000000000000 0.1666666666666643 0.1662770246982319 F F F
0.2500000000000000 0.1666666666666643 0.1662770246982319 F F F
0.0000000000000000 0.0000624417956115 0.2250208309296103 T T T
0.5000000000000000 0.0000624417956115 0.2250208309296103 T T T
0.7500000000000000 0.5000624417956115 0.2250208309296103 T T T
0.2500000000000000 0.5000624417956115 0.2250208309296103 T T T
0.0000000000000000 0.3334986176223252 0.2925497072851362 T T T
0.5000000000000000 0.3334986176223252 0.2925497072851362 T T T
0.7500000000000000 0.8334986176223252 0.2925497072851362 T T T
0.2500000000000000 0.8334986176223252 0.2925497072851362 T T T
0.0000000000000000 0.6667733473317088 0.3434981547967778 T T T
0.5000000000000000 0.6667733473317088 0.3434981547967778 T T T
0.7500000000000000 0.1667733473317088 0.3434981547967778 T T T
0.2500000000000000 0.1667733473317088 0.3434981547967778 T T T
0.0000000000000000 0.9998862423301899 0.3944083405683612 T T T
0.5000000000000000 0.9998862423301899 0.3944083405683612 T T T
0.7500000000000000 0.4998862423301898 0.3944083405683612 T T T
0.2500000000000000 0.4998862423301898 0.3944083405683612 T T T
0.2500000000000000 0.4998862423301898 0.5265956325271374 T T T
0.2500000000000000 0.4998862423301898 0.6010063947490073 T T T

CONTCAR:
W+CO (0.975) :
1.00000000000000
8.7479413709335692 0.0000000000000000 0.0000000000000000
0.0000000000000000 7.5759394580453394 0.0000000000000000
0.0000000000000000 0.0000000000000000 15.3569981646425973
28 1 1
Selective dynamics
Direct
0.0000000000000000 0.0000000000000000 0.0499999999999972 F F F
0.5000000000000000 0.0000000000000000 0.0499999999999972 F F F
0.7500000000000000 0.5000000000000000 0.0499999999999972 F F F
0.2500000000000000 0.5000000000000000 0.0499999999999972 F F F
0.0000000000000000 0.3333333333333357 0.1081385123491145 F F F
0.5000000000000000 0.3333333333333357 0.1081385123491145 F F F
0.7500000000000000 0.8333333333333357 0.1081385123491145 F F F
0.2500000000000000 0.8333333333333357 0.1081385123491145 F F F

```
 0.0000000000000000  0.6666666666666643  0.1662770246982319   F   F   F
 0.5000000000000000  0.6666666666666643  0.1662770246982319   F   F   F
 0.7500000000000000  0.1666666666666643  0.1662770246982319   F   F   F
 0.2500000000000000  0.1666666666666643  0.1662770246982319   F   F   F
-0.0001239085433197 -0.0002174703810077  0.2252924530725592   T   T   T
 0.5001239085433197 -0.0002174703810077  0.2252924530725592   T   T   T
 0.7500000000000000  0.5001755975900307  0.2252859095552023   T   T   T
 0.2500000000000000  0.5002134886358325  0.2188305643470533   T   T   T
 0.0009179503187002  0.3342670168932363  0.2921717276455398   T   T   T
 0.4990820496813003  0.3342670168932363  0.2921717276455398   T   T   T
 0.7500000000000000  0.8321388998537558  0.2929806872394403   T   T   T
 0.2500000000000000  0.8332516688416102  0.2922844706659495   T   T   T
 0.0022900079273608  0.6652275584048928  0.3447216129722330   T   T   T
 0.4977099920726392  0.6652275584048928  0.3447216129722330   T   T   T
 0.7500000000000000  0.1670970633910115  0.3426212994176910   T   T   T
 0.2500000000000000  0.1694065668109955  0.3441585436815596   T   T   T
-0.0000907980111572  0.0005608346635612  0.3943425972865000   T   T   T
 0.5000907980111571  0.0005608346635612  0.3943425972865000   T   T   T
 0.7500000000000000  0.4982691394690592  0.3946044665614231   T   T   T
 0.2500000000000000  0.5006167310328338  0.4006572470553769   T   T   T
 0.2500000000000000  0.5000384452199542  0.5355793335387713   T   T   T
 0.2500000000000000  0.5003350843376974  0.6115270662455325   T   T   T


Inputs WCO 1.0
==================
 SYSTEM = W+CO(111) SC aW=3.172168546 strain=1.00
 ENCUT = 700
 ISTART = 0;
 ISMEAR = 0; SIGMA = 0.1
 IBRION = 2; ISIF = 2; NSW = 150
 NGX = 78; NGY = 68; NGZ = 134;
 NBANDS = 180; LREAL = .True.
 EDIFF = 1E-06; EDIFFG = 1E-06


K-Points
 0
Monkhorst Pack
 5  5  1
 0  0  0


POSCAR:
W+CO (1.00) (aW = 3.1721685460561386) :
   1.00000000000000
```

```
   8.9722475599318674    0.0000000000000000    0.0000000000000000
   0.0000000000000000    7.7701943159439386    0.0000000000000000
   0.0000000000000000    0.0000000000000000   15.4943570919411258
  28   1   1
Selective dynamics
Direct
  0.0000000000000000  0.0000000000000000  0.0499999999999972   F   F   F
  0.5000000000000000  0.0000000000000000  0.0499999999999972   F   F   F
  0.7500000000000000  0.5000000000000000  0.0499999999999972   F   F   F
  0.2500000000000000  0.5000000000000000  0.0499999999999972   F   F   F
  0.0000000000000000  0.3333333333333357  0.1091006246052260   F   F   F
  0.5000000000000000  0.3333333333333357  0.1091006246052260   F   F   F
  0.7500000000000000  0.8333333333333357  0.1091006246052260   F   F   F
  0.2500000000000000  0.8333333333333357  0.1091006246052260   F   F   F
  0.0000000000000000  0.6666666666666643  0.1682012492104619   F   F   F
  0.5000000000000000  0.6666666666666643  0.1682012492104619   F   F   F
  0.7500000000000000  0.1666666666666643  0.1682012492104619   F   F   F
  0.2500000000000000  0.1666666666666643  0.1682012492104619   F   F   F
  0.9996594730550240 -0.0000220804453254  0.2202245794404178   T   T   T
  0.5003405269449760 -0.0000220804453254  0.2202245794404178   T   T   T
  0.7500000000000000  0.5000416700803326  0.2202415234341149   T   T   T
  0.2500000000000000  0.5001153175201469  0.2123600518487248   T   T   T
  0.0001993513889346  0.3335929541062235  0.2878958676029512   T   T   T
  0.4998006486110654  0.3335929541062235  0.2878958676029512   T   T   T
  0.7500000000000000  0.8323021835400322  0.2889272414063013   T   T   T
  0.2500000000000000  0.8342487847177863  0.2882760996350535   T   T   T
  0.0016996144733222  0.6656678735646093  0.3376901233468914   T   T   T
  0.4983003855266779  0.6656678735646093  0.3376901233468914   T   T   T
  0.7500000000000000  0.1674093323211862  0.3360948280282421   T   T   T
  0.2500000000000000  0.1681375761954534  0.3371915242943748   T   T   T
  0.9995182624341934  0.0006717146108736  0.3833753653657150   T   T   T
  0.5004817375658066  0.0006717146108736  0.3833753653657150   T   T   T
  0.7500000000000000  0.4988612780369560  0.3835053095480336   T   T   T
  0.2500000000000000  0.5001845214439564  0.3867473750432512   T   T   T
  0.2500000000000000  0.5037021302758671  0.5208407210535770   T   T   T
  0.2500000000000000  0.5038443351765516  0.5961812237166526   T   T   T


CONTCAR:
W+CO (1.00) (aW = 3.1721685460561386) :
   1.00000000000000
   8.9722475599318674    0.0000000000000000    0.0000000000000000
   0.0000000000000000    7.7701943159439386    0.0000000000000000
   0.0000000000000000    0.0000000000000000   15.4943570919411258
  28   1   1
Selective dynamics
```

Direct

0.0000000000000000	0.0000000000000000	0.0499999999999972	F	F	F
0.5000000000000000	0.0000000000000000	0.0499999999999972	F	F	F
0.7500000000000000	0.5000000000000000	0.0499999999999972	F	F	F
0.2500000000000000	0.5000000000000000	0.0499999999999972	F	F	F
0.0000000000000000	0.3333333333333357	0.1091006246052260	F	F	F
0.5000000000000000	0.3333333333333357	0.1091006246052260	F	F	F
0.7500000000000000	0.8333333333333357	0.1091006246052260	F	F	F
0.2500000000000000	0.8333333333333357	0.1091006246052260	F	F	F
0.0000000000000000	0.6666666666666643	0.1682012492104619	F	F	F
0.5000000000000000	0.6666666666666643	0.1682012492104619	F	F	F
0.7500000000000000	0.1666666666666643	0.1682012492104619	F	F	F
0.2500000000000000	0.1666666666666643	0.1682012492104619	F	F	F
0.9997119502558418	0.9999500553087449	0.2201814806234401	T	T	T
0.5002880497441582	0.9999500553087449	0.2201814806234401	T	T	T
0.7500000000000000	0.5000885413435976	0.2201930346937128	T	T	T
0.2500000000000000	0.5001321741260577	0.2124089695557279	T	T	T
0.0002070118359710	0.3335958620420905	0.2877927922333136	T	T	T
0.4997929881640291	0.3335958620420905	0.2877927922333136	T	T	T
0.7500000000000000	0.8322556927325427	0.2888222615979348	T	T	T
0.2500000000000000	0.8342456245672030	0.2881881364030155	T	T	T
0.0017187370720904	0.6656544525830697	0.3376493103569281	T	T	T
0.4982812629279094	0.6656544525830697	0.3376493103569281	T	T	T
0.7500000000000000	0.1673960674034512	0.3359873877597832	T	T	T
0.2500000000000000	0.1682288811042054	0.3371516685368213	T	T	T
0.9995733221206345	0.0006787622998209	0.3832670768958304	T	T	T
0.5004266778793655	0.0006787622998209	0.3832670768958304	T	T	T
0.7500000000000000	0.4988270073786022	0.3834076256196274	T	T	T
0.2500000000000000	0.5002852882376704	0.3867105529995143	T	T	T
0.2500000000000000	0.5036632173559398	0.5208104816240728	T	T	T
0.2500000000000000	0.5042166792013352	0.5960887377240920	T	T	T

Inputs WCO 1.3

==========

SYSTEM = W+CO(111) SC aW=3.172168546 strain>1.00
ENCUT = 700
ISTART = 0;
ISMEAR = 0; SIGMA = 0.1
IBRION = 2; ISIF = 2; NSW = 150
NGX = 78; NGY = 68; NGZ = 134;
NBANDS = 180; LREAL = .True.
EDIFF = 1E-06; EDIFFG = 1E-06

K-Points
 0
Monkhorst Pack
 5 5 1
 0 0 0

POSCAR:
W+CO (1.03) (aW = 3.1721685460561386) :
   1.03000000000000
     8.9722475599318674   0.0000000000000000   0.0000000000000000
     0.0000000000000000   7.7701943159439386   0.0000000000000000
     0.0000000000000000   0.0000000000000000   15.4943570919411258
  28 1 1
Selective dynamics
Direct
  0.0000000000000000 0.0000000000000000 0.0499999999999972   F   F   F
  0.5000000000000000 0.0000000000000000 0.0499999999999972   F   F   F
  0.7500000000000000 0.5000000000000000 0.0499999999999972   F   F   F
  0.2500000000000000 0.5000000000000000 0.0499999999999972   F   F   F
  0.0000000000000000 0.3333333333333357 0.1091006246052260   F   F   F
  0.5000000000000000 0.3333333333333357 0.1091006246052260   F   F   F
  0.7500000000000000 0.8333333333333357 0.1091006246052260   F   F   F
  0.2500000000000000 0.8333333333333357 0.1091006246052260   F   F   F
  0.0000000000000000 0.6666666666666643 0.1682012492104619   F   F   F
  0.5000000000000000 0.6666666666666643 0.1682012492104619   F   F   F
  0.7500000000000000 0.1666666666666643 0.1682012492104619   F   F   F
  0.2500000000000000 0.1666666666666643 0.1682012492104619   F   F   F
  0.0000000000000000 0.0000432437007099 0.2200613496300725   T   T   T
  0.5000000000000000 0.0000432437007099 0.2200613496300725   T   T   T
  0.7500000000000000 0.5000432437007100 0.2200613496300725   T   T   T
  0.2500000000000000 0.5000432437007100 0.2200613496300725   T   T   T
  0.0000000000000000 0.3333688061837887 0.2882890792861474   T   T   T
  0.5000000000000000 0.3333688061837887 0.2882890792861474   T   T   T
  0.7500000000000000 0.8333688061837887 0.2882890792861474   T   T   T
  0.2500000000000000 0.8333688061837887 0.2882890792861474   T   T   T
  0.0000000000000000 0.6666718424150652 0.3366308635448612   T   T   T
  0.5000000000000000 0.6666718424150652 0.3366308635448612   T   T   T
  0.7500000000000000 0.1666718424150651 0.3366308635448612   T   T   T
  0.2500000000000000 0.1666718424150651 0.3366308635448612   T   T   T
  0.0000000000000000 0.0000515800868524 0.3834057489750923   T   T   T
  0.5000000000000000 0.0000515800868524 0.3834057489750923   T   T   T
  0.7500000000000000 0.5000515800868524 0.3834057489750923   T   T   T
  0.2500000000000000 0.5000515800868524 0.3834057489750923   T   T   T
  0.2500000000000000 0.5000515800868524 0.5106052045390050   T   T   T
  0.2500000000000000 0.5000515800868524 0.5822077098007300   T   T   T

CONTCAR:
W+CO (1.03) (aW = 3.1721685460561386) :
1.03000000000000
8.9722475599318674 0.0000000000000000 0.0000000000000000
0.0000000000000000 7.7701943159439386 0.0000000000000000
0.0000000000000000 0.0000000000000000 15.4943570919411258
28 1 1
Selective dynamics
Direct
0.0000000000000000 0.0000000000000000 0.0499999999999972 F F F
0.5000000000000000 0.0000000000000000 0.0499999999999972 F F F
0.7500000000000000 0.5000000000000000 0.0499999999999972 F F F
0.2500000000000000 0.5000000000000000 0.0499999999999972 F F F
0.0000000000000000 0.3333333333333357 0.1091006246052260 F F F
0.5000000000000000 0.3333333333333357 0.1091006246052260 F F F
0.7500000000000000 0.8333333333333357 0.1091006246052260 F F F
0.2500000000000000 0.8333333333333357 0.1091006246052260 F F F
0.0000000000000000 0.6666666666666643 0.1682012492104619 F F F
0.5000000000000000 0.6666666666666643 0.1682012492104619 F F F
0.7500000000000000 0.1666666666666643 0.1682012492104619 F F F
0.2500000000000000 0.1666666666666643 0.1682012492104619 F F F
-0.0003102060971887 0.0000718185885011 0.2121852984274025 T T T
0.5003102060971885 0.0000718185885011 0.2121852984274025 T T T
0.7500000000000000 0.5000342307443172 0.2121125159721313 T T T
0.2500000000000000 0.5001154534659327 0.2039270900152407 T T T
-0.0005012374908645 0.3331334974150655 0.2797633290271864 T T T
0.5005012374908647 0.3331334974150655 0.2797633290271864 T T T
0.7500000000000000 0.8326458050913000 0.2805947219198134 T T T
0.2500000000000000 0.8348755150852171 0.2804139915064733 T T T
0.0012613916418994 0.6659081714743541 0.3257913436414201 T T T
0.4987386083581007 0.6659081714743541 0.3257913436414201 T T T
0.7500000000000000 0.1676210920122692 0.3246676006587404 T T T
0.2500000000000000 0.1678617520714180 0.3254730104625290 T T T
-0.0005924782911716 0.0007158659599700 0.3678249618854756 T T T
0.5005924782911712 0.0007158659599700 0.3678249618854756 T T T
0.7500000000000000 0.4988937951475690 0.3678484815973297 T T T
0.2500000000000000 0.5009317289170108 0.3696990901570659 T T T
0.2500000000000000 0.5000255577187540 0.4996419930414042 T T T
0.2500000000000000 0.4999127840860622 0.5728027052464061 T T T

****

Ni+Al SYSTEM

1) Script file, which creates and submits inputs for Ni+Al mixture on the Venus cluster.

```
*****************************************************
#!/bin/bash
# This file requires files POTCAR, pbs-script and vasp.
# a = lattice fraction
# v = volume fraction
# e = ENCUT
# k = KPOINTS grid
# gapM = gap b/n Ni and Al
# gapUp = gap ontop of cell

gapM=3
gapUp=4
NAMEDIR="NiAl_2.5b"
#0.50       0.55       0.60       0.65       0.70       0.75       0.80       0.85
#0.90       0.92       0.94       0.96       0.98
#0.99       0.992      0.994      0.996      0.998      1.002      1.004      1.006      1.008      1.01
#1.02       1.04       1.06       1.08       1.10
#1.15       1.20       1.25       1.30       1.35       1.40       1.45       1.50
#for a in 0.7937 0.8193 0.8434 0.8662 0.8879 0.9086 0.9283 0.9473 ; do
#for a in 0.9655 0.9726 0.9796 0.9865 0.9933 ; do
for a in 0.996655 0.997326 0.997996 0.998665 0.999333 1.000666 1.001332 1.001996 1.002660 1.003322; do
#for a in 1.00 ; do
#for a in 1.0066 1.0132 1.0196 1.0260 1.0323 ; do
#for a in 1.0477 1.0627 1.0772 1.0914 1.1052 1.1187 1.1319 1.1447 ; do
  for e in 600 ; do
    for k in 5; do


 dNi=$(echo "scale=15; 2.02823149566316" | bc -l)
 dAl=$(echo "scale=15; 2.33653653941042" | bc -l)
 A3=$(echo "scale=15; ($dNi*2+$dAl*2)+($gapM+$gapUp)/$a" | bc -l)
 z1=$(echo "scale=15; 0.7/($A3*$a)" | bc -l)
 z2=$(echo "scale=15; $z1+$dNi/($A3)" | bc -l)
 z3=$(echo "scale=15; $z2+$dNi/($A3)" | bc -l)
 z4=$(echo "scale=15; $z3+$gapM/($A3*$a)" | bc -l)
 z5=$(echo "scale=15; $z4+$dAl/($A3)" | bc -l)
 z6=$(echo "scale=15; $z5+$dAl/($A3)" | bc -l)


v=$(echo "scale=2; $a^3" | bc)
mkdir $NAMEDIR"_"$v

cat >INCAR <<!
 general:
   SYSTEM =  Ni-Al (111) interface
   ENCUT  = $e;
   ISMEAR =    0  ; SIGMA = 0.2;

 ISTART = 0;
 IBRION = 2; ISIF = 2; NSW = 1;
 LORBIT = .TRUE;
 EDIFF = 1E-6; EDIFFG = 1E-5;
 NBANDS = 170;
 NGX = 58; NGY = 58; NGZ = 126;
 LREAL= Auto
!

cat >KPOINTS <<!
K-Points
 0
```

```
Monkhorst Pack
 $k  $k  1
 0  0  0
!

cat >POSCAR <<!
mixture 3Ni 3Al (aNi = 3.513, aAl=4.047, cell=2.5*bAl, gapM=$gapM, gapUp=$gapUp) :
  $a
            7.154152858654890  0.000000000000000  0.000000000000000
            -3.577076429327450 6.195678118152200  0.000000000000000
            0.000000000000000  0.000000000000000  $A3
  12   12
Direct
            0.000000000000000  0.000000000000000  $z1        Ni A
            0.347220163083766  0.000000000000000  $z1        Ni A
            0.347220163083766  0.347220163083766  $z1        Ni A
            0.000000000000000  0.347220163083766  $z1        Ni A
            0.115740054361255  0.231480108722510  $z2        Ni B
            0.462960217445021  0.231480108722510  $z2        Ni B
            0.462960217445021  0.578700271806277  $z2        Ni B
            0.115740054361256  0.578700271806277  $z2        Ni B
            0.231480108722510  0.115740054361255  $z3        Ni C
            0.578700271806276  0.115740054361255  $z3        Ni C
            0.578700271806276  0.462960217445021  $z3        Ni C
            0.231480108722510  0.462960217445021  $z3        Ni C
            0.000000000000000  0.000000000000000  $z4        Al A
            0.400000000000000  0.000000000000000  $z4        Al A
            0.400000000000000  0.400000000000000  $z4        Al A
            0.000000000000000  0.400000000000000  $z4        Al A
            0.133333333333333  0.266666666666666  $z5        Al B
            0.533333333333333  0.266666666666666  $z5        Al B
            0.533333333333333  0.666666666666666  $z5        Al B
            0.133333333333333  0.666666666666666  $z5        Al B
            0.266666666666667  0.133333333333333  $z6        Al C
            0.666666666666667  0.133333333333333  $z6        Al C
            0.666666666666667  0.533333333333334  $z6        Al C
            0.266666666666667  0.533333333333334  $z6        Al C
!

cp INCAR $NAMEDIR"_"$v/.
cp KPOINTS $NAMEDIR"_"$v/.
cp POSCAR  $NAMEDIR"_"$v/.
cp POTCAR  $NAMEDIR"_"$v/.
cp pbs-script $NAMEDIR"_"$v/.
cd $NAMEDIR"_"$v
qsub pbs-script
cd ../

done
done
done

rm INCAR
rm POSCAR
rm KPOINTS
**********************************************************
```

End of script file.

2) Example of a "pbs-script" file, used to submit jobs on the Venus cluster:

```
**********************************************************
#!/bin/sh
#PBS -l walltime=720:00:00
#PBS -N NiAl1.88
#PBS -l nodes=1:ppn=4
#PBS -j oe
```

```
# the following give the path for the exe file and the name of the output
 exef=./vasp
 outf=out.3

# ----- the remaining part need not change -----

 cd $PBS_O_WORKDIR
 jobid=`echo $PBS_JOBID |cut -f1 -d"."`
 $cp $PBS_NODEFILE $PBS_O_WORKDIR/$PBS_JOBNAME.hostss
 $cp $PBS_NODEFILE $PBS_O_WORKDIR/$PBS_JOBNAME.hosts$jobid
 nprocs=`cat $PBS_NODEFILE | wc -l`
export  P4_SOCKBUFSIZE=0x40000
export P4_GLOBMEMSIZE=16777296

 echo "Job started on `hostname` at `date`" > $outf
  cat $PBS_NODEFILE                                          >> $outf
 cat $PBS_NODEFILE|sort -u|gawk '{print $1":4"}'>mpd.hosts
n_node=`cat mpd.hosts|wc -l`
echo $n_node>>$outf
mpdboot -n $n_node
 sleep 1
if [ $? -eq "0" ]; then
              echo "mpiexec -machinefile $PBS_NODEFILE -n $nprocs $exef >> $outf" >>$outf
              mpiexec  -machinefile $PBS_NODEFILE -n $nprocs   $exef >>$outf
              echo "Job Ended at `date`"                                  >>$outf
              mpdallexit
              exit 0
else
              echo "error mpdboot">>$outf
              exit 1
fi
```

****

End of "pbs-script" file.

****

Ti+H2 SYSTEM

==========

POTCAR files:

PAW_GGA Ti_pv 07Sep2000

PAW_GGA H 07Jul1998

POSCAR and .xyz FILES FOR 3 Ti SUPERCELL SIZES

==========

POSCAR (Ti1x1)

```
Ti_1x1(aTi=2.93647940097882, c/a=1.57517351266119):
  1.0
  2.9364794009788200  0.0000000000000000  0.0000000000000000
  1.4682397004894100  2.5430657589373691  0.0000000000000000
  0.0000000000000000  0.0000000000000000  34.690984296727800
  7
Selective Dynamics
Direct
0.66667  0.66667  0.00000      F          F          F
0.33333  0.33333  0.06667      F          F          F
0.66667  0.66667  0.13333      F          F          F
0.33333  0.33333  0.20000      F          F          F
0.66667  0.66667  0.26667      T          T          T
0.33333  0.33333  0.33333      T          T          T
0.66667  0.66667  0.40000      T          T          T
```

POSCAR.xyz (Ti1x1)

```
7
GEOMETRY FILE / converted from VASP
Ti         2.93649    1.69539    0.00000
Ti         1.46823    0.84768    2.31285
Ti         2.93649    1.69539    4.62535
Ti         1.46823    0.84768    6.93820
Ti         2.93649    1.69539    9.25104
Ti         1.46823    0.84768    11.56355
Ti         2.93649    1.69539    13.87639
```

POSCAR (Ti2x2)

```
Ti_0001_2x2(aTi=2.93647940097882, c/a=1.57517351266119):
  1.0
          5.872958801957640   0.000000000000000  0.000000000000000
          2.936479400978820   5.086131517874740  0.000000000000000
          0.000000000000000   0.000000000000000  34.690984296727800
   28
Selective Dynamics
Direct
0.333333333333333  0.333333333333333  0.000000000000000  F  F  F  a
0.833333333333333  0.333333333333333  0.000000000000000  F  F  F  a
0.833333333333333  0.833333333333333  0.000000000000000  F  F  F  a
0.333333333333333  0.833333333333333  0.000000000000000  F  F  F  a
0.166666666666667  0.166666666666667  0.066666666666667  F  F  F  b
0.666666666666667  0.166666666666667  0.066666666666667  F  F  F  b
0.666666666666667  0.666666666666667  0.066666666666667  F  F  F  b
0.166666666666667  0.666666666666667  0.066666666666667  F  F  F  b
0.333333333333333  0.333333333333333  0.133333333333333  F  F  F  c
0.833333333333333  0.333333333333333  0.133333333333333  F  F  F  c
0.833333333333333  0.833333333333333  0.133333333333333  F  F  F  c
```

0.333333333333333	0.833333333333333	0.133333333333333	F	F	F	c
0.166666666666667	0.166666666666667	0.200000000000000	F	F	F	d
0.666666666666667	0.166666666666667	0.200000000000000	F	F	F	d
0.666666666666667	0.666666666666667	0.200000000000000	F	F	F	d
0.166666666666667	0.666666666666667	0.200000000000000	F	F	F	d
0.333333333333333	0.333333333333333	0.266666666666667	T	T	T	e
0.833333333333333	0.333333333333333	0.266666666666667	T	T	T	e
0.833333333333333	0.833333333333333	0.266666666666667	T	T	T	e
0.333333333333333	0.833333333333333	0.266666666666667	T	T	T	e
0.166666666666667	0.166666666666667	0.333333333333333	T	T	T	f
0.666666666666667	0.166666666666667	0.333333333333333	T	T	T	f
0.666666666666667	0.666666666666667	0.333333333333333	T	T	T	f
0.166666666666667	0.666666666666667	0.333333333333333	T	T	T	f
0.333333333333333	0.333333333333333	0.400000000000000	T	T	T	g
0.833333333333333	0.333333333333333	0.400000000000000	T	T	T	g
0.833333333333333	0.833333333333333	0.400000000000000	T	T	T	g
0.333333333333333	0.833333333333333	0.400000000000000	T	T	T	g

POSCAR.xyz (Ti2x2)

28
Geometry of 7-layer Ti slab

Ti	2.936479400978820	1.695377172624910	0.000000000000000
Ti	5.872958801957640	1.695377172624910	0.000000000000000
Ti	7.341198502447050	4.238442931562280	0.000000000000000
Ti	4.404719101468230	4.238442931562280	0.000000000000000
Ti	1.468239700489410	0.847688586312457	2.312732286448520
Ti	4.404719101468230	0.847688586312457	2.312732286448520
Ti	5.872958801957640	3.390754345249830	2.312732286448520
Ti	2.936479400978820	3.390754345249830	2.312732286448520
Ti	2.936479400978820	1.695377172624910	4.625464572897040
Ti	5.872958801957640	1.695377172624910	4.625464572897040
Ti	7.341198502447050	4.238442931562280	4.625464572897040
Ti	4.404719101468230	4.238442931562280	4.625464572897040
Ti	1.468239700489410	0.847688586312457	6.938196859345560
Ti	4.404719101468230	0.847688586312457	6.938196859345560
Ti	5.872958801957640	3.390754345249830	6.938196859345560
Ti	2.936479400978820	3.390754345249830	6.938196859345560
Ti	2.936479400978820	1.695377172624910	9.250929145794070
Ti	5.872958801957640	1.695377172624910	9.250929145794070
Ti	7.341198502447050	4.238442931562280	9.250929145794070
Ti	4.404719101468230	4.238442931562280	9.250929145794070
Ti	1.468239700489410	0.847688586312457	11.563661432242600
Ti	4.404719101468230	0.847688586312457	11.563661432242600
Ti	5.872958801957640	3.390754345249830	11.563661432242600
Ti	2.936479400978820	3.390754345249830	11.563661432242600
Ti	2.936479400978820	1.695377172624910	13.876393718691100
Ti	5.872958801957640	1.695377172624910	13.876393718691100
Ti	7.341198502447050	4.238442931562280	13.876393718691100
Ti	4.404719101468230	4.238442931562280	13.87639371869110

POSCAR (Ti4x4)

Ti_0001_4x4(aTi=2.93647940097882, c/a=1.57517351266119):
1.0

11.74591760391530	0.00000000000000	0.000000000000000
5.872958801957640	10.17226303574950	0.000000000000000
0.000000000000000	0.000000000000000	34.690984296727800

112
Selective Dynamics
Direct

0.166666666666667	0.166666666666667	0.000000000000000	F	F	F	a
0.416666666666667	0.166666666666667	0.000000000000000	F	F	F	a
0.666666666666667	0.166666666666667	0.000000000000000	F	F	F	a
0.916666666666667	0.166666666666667	0.000000000000000	F	F	F	a
0.166666666666667	0.416666666666667	0.000000000000000	F	F	F	a
0.416666666666667	0.416666666666667	0.000000000000000	F	F	F	a

0.666666666666667	0.416666666666667	0.000000000000000	F	F	F	a
0.916666666666667	0.416666666666667	0.000000000000000	F	F	F	a
0.166666666666667	0.666666666666667	0.000000000000000	F	F	F	a
0.416666666666667	0.666666666666667	0.000000000000000	F	F	F	a
0.666666666666667	0.666666666666667	0.000000000000000	F	F	F	a
0.916666666666667	0.666666666666667	0.000000000000000	F	F	F	a
0.166666666666667	0.916666666666667	0.000000000000000	F	F	F	a
0.416666666666667	0.916666666666667	0.000000000000000	F	F	F	a
0.666666666666667	0.916666666666667	0.000000000000000	F	F	F	a
0.916666666666667	0.916666666666667	0.000000000000000	F	F	F	a
0.083333333333333	0.083333333333333	0.066666666666667	F	F	F	b
0.333333333333333	0.083333333333333	0.066666666666667	F	F	F	b
0.583333333333333	0.083333333333333	0.066666666666667	F	F	F	b
0.833333333333333	0.083333333333333	0.066666666666667	F	F	F	b
0.083333333333333	0.333333333333333	0.066666666666667	F	F	F	b
0.333333333333333	0.333333333333333	0.066666666666667	F	F	F	b
0.583333333333333	0.333333333333333	0.066666666666667	F	F	F	b
0.833333333333333	0.333333333333333	0.066666666666667	F	F	F	b
0.083333333333333	0.583333333333333	0.066666666666667	F	F	F	b
0.333333333333333	0.583333333333333	0.066666666666667	F	F	F	b
0.583333333333333	0.583333333333333	0.066666666666667	F	F	F	b
0.833333333333333	0.583333333333333	0.066666666666667	F	F	F	b
0.083333333333333	0.833333333333333	0.066666666666667	F	F	F	b
0.333333333333333	0.833333333333333	0.066666666666667	F	F	F	b
0.583333333333333	0.833333333333333	0.066666666666667	F	F	F	b
0.833333333333333	0.833333333333333	0.066666666666667	F	F	F	b
0.166666666666667	0.166666666666667	0.133333333333333	F	F	F	c
0.416666666666667	0.166666666666667	0.133333333333333	F	F	F	c
0.666666666666667	0.166666666666667	0.133333333333333	F	F	F	c
0.916666666666667	0.166666666666667	0.133333333333333	F	F	F	c
0.166666666666667	0.416666666666667	0.133333333333333	F	F	F	c
0.416666666666667	0.416666666666667	0.133333333333333	F	F	F	c
0.666666666666667	0.416666666666667	0.133333333333333	F	F	F	c
0.916666666666667	0.416666666666667	0.133333333333333	F	F	F	c
0.166666666666667	0.666666666666667	0.133333333333333	F	F	F	c
0.416666666666667	0.666666666666667	0.133333333333333	F	F	F	c
0.666666666666667	0.666666666666667	0.133333333333333	F	F	F	c
0.916666666666667	0.666666666666667	0.133333333333333	F	F	F	c
0.166666666666667	0.916666666666667	0.133333333333333	F	F	F	c
0.416666666666667	0.916666666666667	0.133333333333333	F	F	F	c
0.666666666666667	0.916666666666667	0.133333333333333	F	F	F	c
0.916666666666667	0.916666666666667	0.133333333333333	F	F	F	c
0.083333333333333	0.083333333333333	0.200000000000000	F	F	F	d
0.333333333333333	0.083333333333333	0.200000000000000	F	F	F	d
0.583333333333333	0.083333333333333	0.200000000000000	F	F	F	d
0.833333333333333	0.083333333333333	0.200000000000000	F	F	F	d
0.083333333333333	0.333333333333333	0.200000000000000	F	F	F	d
0.333333333333333	0.333333333333333	0.200000000000000	F	F	F	d
0.583333333333333	0.333333333333333	0.200000000000000	F	F	F	d
0.833333333333333	0.333333333333333	0.200000000000000	F	F	F	d
0.083333333333333	0.583333333333333	0.200000000000000	F	F	F	d
0.333333333333333	0.583333333333333	0.200000000000000	F	F	F	d
0.583333333333333	0.583333333333333	0.200000000000000	F	F	F	d
0.833333333333333	0.583333333333333	0.200000000000000	F	F	F	d
0.083333333333333	0.833333333333333	0.200000000000000	F	F	F	d
0.333333333333333	0.833333333333333	0.200000000000000	F	F	F	d
0.583333333333333	0.833333333333333	0.200000000000000	F	F	F	d
0.833333333333333	0.833333333333333	0.200000000000000	F	F	F	d
0.166666666666667	0.166666666666667	0.266666666666667	T	T	T	e
0.416666666666667	0.166666666666667	0.266666666666667	T	T	T	e
0.666666666666667	0.166666666666667	0.266666666666667	T	T	T	e
0.916666666666667	0.166666666666667	0.266666666666667	T	T	T	e
0.166666666666667	0.416666666666667	0.266666666666667	T	T	T	e
0.416666666666667	0.416666666666667	0.266666666666667	T	T	T	e
0.666666666666667	0.416666666666667	0.266666666666667	T	T	T	e
0.916666666666667	0.416666666666667	0.266666666666667	T	T	T	e
0.166666666666667	0.666666666666667	0.266666666666667	T	T	T	e
0.416666666666667	0.666666666666667	0.266666666666667	T	T	T	e
0.666666666666667	0.666666666666667	0.266666666666667	T	T	T	e
0.916666666666667	0.666666666666667	0.266666666666667	T	T	T	e

0.166666666666667	0.916666666666667	0.266666666666667	T	T	T	e
0.416666666666667	0.916666666666667	0.266666666666667	T	T	T	e
0.666666666666667	0.916666666666667	0.266666666666667	T	T	T	e
0.916666666666667	0.916666666666667	0.266666666666667	T	T	T	e
0.083333333333333	0.083333333333333	0.333333333333333	T	T	T	f
0.333333333333333	0.083333333333333	0.333333333333333	T	T	T	f
0.583333333333333	0.083333333333333	0.333333333333333	T	T	T	f
0.833333333333333	0.083333333333333	0.333333333333333	T	T	T	f
0.083333333333333	0.333333333333333	0.333333333333333	T	T	T	f
0.333333333333333	0.333333333333333	0.333333333333333	T	T	T	f
0.583333333333333	0.333333333333333	0.333333333333333	T	T	T	f
0.833333333333333	0.333333333333333	0.333333333333333	T	T	T	f
0.083333333333333	0.583333333333333	0.333333333333333	T	T	T	f
0.333333333333333	0.583333333333333	0.333333333333333	T	T	T	f
0.583333333333333	0.583333333333333	0.333333333333333	T	T	T	f
0.833333333333333	0.583333333333333	0.333333333333333	T	T	T	f
0.083333333333333	0.833333333333333	0.333333333333333	T	T	T	f
0.333333333333333	0.833333333333333	0.333333333333333	T	T	T	f
0.583333333333333	0.833333333333333	0.333333333333333	T	T	T	f
0.833333333333333	0.833333333333333	0.333333333333333	T	T	T	f
0.166666666666667	0.166666666666667	0.400000000000000	T	T	T	g
0.416666666666667	0.166666666666667	0.400000000000000	T	T	T	g
0.666666666666667	0.166666666666667	0.400000000000000	T	T	T	g
0.916666666666667	0.166666666666667	0.400000000000000	T	T	T	g
0.166666666666667	0.416666666666667	0.400000000000000	T	T	T	g
0.416666666666667	0.416666666666667	0.400000000000000	T	T	T	g
0.666666666666667	0.416666666666667	0.400000000000000	T	T	T	g
0.916666666666667	0.416666666666667	0.400000000000000	T	T	T	g
0.166666666666667	0.666666666666667	0.400000000000000	T	T	T	g
0.416666666666667	0.666666666666667	0.400000000000000	T	T	T	g
0.666666666666667	0.666666666666667	0.400000000000000	T	T	T	g
0.916666666666667	0.666666666666667	0.400000000000000	T	T	T	g
0.166666666666667	0.916666666666667	0.400000000000000	T	T	T	g
0.416666666666667	0.916666666666667	0.400000000000000	T	T	T	g
0.666666666666667	0.916666666666667	0.400000000000000	T	T	T	g
0.916666666666667	0.916666666666667	0.400000000000000	T	T	T	g

POSCAR.xyz (Ti4x4)

112

Geometry of 7-layer Ti slab

Ti	2.93647940097882	1.69537717262491	0.00000000000000
Ti	5.87295880195764	1.69537717262491	0.00000000000000
Ti	8.80943820293646	1.69537717262491	0.00000000000000
Ti	11.74591760391530	1.69537717262491	0.00000000000000
Ti	4.40471910146823	4.23844293156228	0.00000000000000
Ti	7.34119850244705	4.23844293156228	0.00000000000000
Ti	10.27767790342590	4.23844293156228	0.00000000000000
Ti	13.21415730440470	4.23844293156228	0.00000000000000
Ti	5.87295880195764	6.78150869049965	0.00000000000000
Ti	8.80943820293646	6.78150869049965	0.00000000000000
Ti	11.74591760391530	6.78150869049965	0.00000000000000
Ti	14.68239700489410	6.78150869049965	0.00000000000000
Ti	7.34119850244705	9.32457444943702	0.00000000000000
Ti	10.27767790342590	9.32457444943702	0.00000000000000
Ti	13.21415730440470	9.32457444943702	0.00000000000000
Ti	16.15063670538350	9.32457444943702	0.00000000000000
Ti	1.46823970048941	0.84768858631246	2.31273228644852
Ti	4.40471910146823	0.84768858631246	2.31273228644852
Ti	7.34119850244705	0.84768858631246	2.31273228644852
Ti	10.27767790342590	0.84768858631246	2.31273228644852
Ti	2.93647940097882	3.39075434524983	2.31273228644852
Ti	5.87295880195764	3.39075434524983	2.31273228644852
Ti	8.80943820293646	3.39075434524983	2.31273228644852
Ti	11.74591760391530	3.39075434524983	2.31273228644852
Ti	4.40471910146823	5.93382010418720	2.31273228644852
Ti	7.34119850244705	5.93382010418720	2.31273228644852
Ti	10.27767790342590	5.93382010418720	2.31273228644852
Ti	13.21415730440470	5.93382010418720	2.31273228644852
Ti	5.87295880195764	8.47688586312457	2.31273228644852
Ti	8.80943820293646	8.47688586312457	2.31273228644852
Ti	11.74591760391530	8.47688586312457	2.31273228644852
Ti	14.68239700489410	8.47688586312457	2.31273228644852
Ti	2.93647940097882	1.69537717262491	4.62546457289704
Ti	5.87295880195764	1.69537717262491	4.62546457289704
Ti	8.80943820293646	1.69537717262491	4.62546457289704
Ti	11.74591760391530	1.69537717262491	4.62546457289704
Ti	4.40471910146823	4.23844293156228	4.62546457289704
Ti	7.34119850244705	4.23844293156228	4.62546457289704
Ti	10.27767790342590	4.23844293156228	4.62546457289704
Ti	13.21415730440470	4.23844293156228	4.62546457289704
Ti	5.87295880195764	6.78150869049965	4.62546457289704
Ti	8.80943820293646	6.78150869049965	4.62546457289704
Ti	11.74591760391530	6.78150869049965	4.62546457289704
Ti	14.68239700489410	6.78150869049965	4.62546457289704
Ti	7.34119850244705	9.32457444943702	4.62546457289704
Ti	10.27767790342590	9.32457444943702	4.62546457289704
Ti	13.21415730440470	9.32457444943702	4.62546457289704
Ti	16.15063670538350	9.32457444943702	4.62546457289704
Ti	1.46823970048941	0.84768858631246	6.93819685934556
Ti	4.40471910146823	0.84768858631246	6.93819685934556
Ti	7.34119850244705	0.84768858631246	6.93819685934556
Ti	10.27767790342590	0.84768858631246	6.93819685934556
Ti	2.93647940097882	3.39075434524983	6.93819685934556
Ti	5.87295880195764	3.39075434524983	6.93819685934556
Ti	8.80943820293646	3.39075434524983	6.93819685934556
Ti	11.74591760391530	3.39075434524983	6.93819685934556
Ti	4.40471910146823	5.93382010418720	6.93819685934556
Ti	7.34119850244705	5.93382010418720	6.93819685934556
Ti	10.27767790342590	5.93382010418720	6.93819685934556
Ti	13.21415730440470	5.93382010418720	6.93819685934556
Ti	5.87295880195764	8.47688586312457	6.93819685934556
Ti	8.80943820293646	8.47688586312457	6.93819685934556
Ti	11.74591760391530	8.47688586312457	6.93819685934556
Ti	14.68239700489410	8.47688586312457	6.93819685934556
Ti	2.93647940097882	1.69537717262491	9.25092914579407
Ti	5.87295880195764	1.69537717262491	9.25092914579407

Ti	8.80943820293646	1.69537717262491	9.25092914579407
Ti	11.74591760391530	1.69537717262491	9.25092914579407
Ti	4.40471910146823	4.23844293156228	9.25092914579407
Ti	7.34119850244705	4.23844293156228	9.25092914579407
Ti	10.27767790342590	4.23844293156228	9.25092914579407
Ti	13.21415730440470	4.23844293156228	9.25092914579407
Ti	5.87295880195764	6.78150869049965	9.25092914579407
Ti	8.80943820293646	6.78150869049965	9.25092914579407
Ti	11.74591760391530	6.78150869049965	9.25092914579407
Ti	14.68239700489410	6.78150869049965	9.25092914579407
Ti	7.34119850244705	9.32457444943702	9.25092914579407
Ti	10.27767790342590	9.32457444943702	9.25092914579407
Ti	13.21415730440470	9.32457444943702	9.25092914579407
Ti	16.15063670538350	9.32457444943702	9.25092914579407
Ti	1.46823970048941	0.84768858631246	11.56366143224260
Ti	4.40471910146823	0.84768858631246	11.56366143224260
Ti	7.34119850244705	0.84768858631246	11.56366143224260
Ti	10.27767790342590	0.84768858631246	11.56366143224260
Ti	2.93647940097882	3.39075434524983	11.56366143224260
Ti	5.87295880195764	3.39075434524983	11.56366143224260
Ti	8.80943820293646	3.39075434524983	11.56366143224260
Ti	11.74591760391530	3.39075434524983	11.56366143224260
Ti	4.40471910146823	5.93382010418720	11.56366143224260
Ti	7.34119850244705	5.93382010418720	11.56366143224260
Ti	10.27767790342590	5.93382010418720	11.56366143224260
Ti	13.21415730440470	5.93382010418720	11.56366143224260
Ti	5.87295880195764	8.47688586312457	11.56366143224260
Ti	8.80943820293646	8.47688586312457	11.56366143224260
Ti	11.74591760391530	8.47688586312457	11.56366143224260
Ti	14.68239700489410	8.47688586312457	11.56366143224260
Ti	2.93647940097882	1.69537717262491	13.87639371869110
Ti	5.87295880195764	1.69537717262491	13.87639371869110
Ti	8.80943820293646	1.69537717262491	13.87639371869110
Ti	11.74591760391530	1.69537717262491	13.87639371869110
Ti	4.40471910146823	4.23844293156228	13.87639371869110
Ti	7.34119850244705	4.23844293156228	13.87639371869110
Ti	10.27767790342590	4.23844293156228	13.87639371869110
Ti	13.21415730440470	4.23844293156228	13.87639371869110
Ti	5.87295880195764	6.78150869049965	13.87639371869110
Ti	8.80943820293646	6.78150869049965	13.87639371869110
Ti	11.74591760391530	6.78150869049965	13.87639371869110
Ti	14.68239700489410	6.78150869049965	13.87639371869110
Ti	7.34119850244705	9.32457444943702	13.87639371869110
Ti	10.27767790342590	9.32457444943702	13.87639371869110
Ti	13.21415730440470	9.32457444943702	13.87639371869110
Ti	16.15063670538350	9.32457444943702	13.87639371869110

INCAR, KPOINTS and POSCAR files for Ti+H2 SYSTEM:
- convergence studies, and geometry optimization
==========

H2 , Convergence Studies
==========

ENCUT varied as 400, 600, 800, 1000
KPOINTS grid = kxkx1 where k varied as 5, 9, 11, 15, 19

```
     ISTART = 0
      general:
     IBRION = 2
     SYSTEM =  H2 1atom each layer
        ENCUT  = 600
        ISMEAR =    0 ; SIGMA = 0.05
        EDIFF = 1E-6; EDIFFG = 1E-5
        ALGO = Fast
        PREC = med
        SPIN = 2
     ISIF = 3
     NGX = 26; NGY = 26; NGZ = 278;
     LWAVE = .FALSE.
     LCHARG = .FALSE.
     LVTOT = .FALSE.


K-Points
 0
Monkhorst Pack
 11 11  1
 0  0  0


2H(H-H=0.74):
   1.00000000000000
     2.9364794009788202    0.0000000000000000    0.0000000000000000
     1.4682397004894101    2.5430657589373702    0.0000000000000000
     0.0000000000000000    0.0000000000000000   34.6909842967277982
   2
Selective dynamics
Direct
  0.6666700000000034  0.6666700000000034  0.4288259333158848   T   T   T
  0.6666700000000034  0.6666700000000034  0.4501571239696460   T   T   T
```

Ti , Convergence Studies
==========

ENCUT varied as 400, 600, 800, 870, 1000, 1200
KPOINTS grid = kxkx1 where k varied as 5, 9, 11, 15, 19

```
     SYSTEM = Ti HCP
     NWRITE = 1
     LCHARG = .FALSE.
     LVTOT = .FALSE.
     ALGO = Fast
     ISTART = 0;
     ISMEAR = 1; SIGMA = 0.1
     IBRION = 2;ISIF = 2; NSW = 200
     PREC = med
```

```
      ENCUT = 600;
      NGX = 26; NGY = 26; NGZ = 278;
      NBANDS = 50;
      EDIFF = 1E-6; EDIFFG = 1E-5
      ISPIN = 1
      POTIM = 0.35
      NFREE = 5


K-Points
 0
Monkhorst Pack
11  11  1
0   0   0
```

POSCAR file:

```
Ti_1x1(aTi=2.93647940097882, c/a=1.57517351266119):
   1.0
   2.9364794009788200  0.0000000000000000  0.0000000000000000
   1.4682397004894100  2.5430657589373691  0.0000000000000000
   0.0000000000000000  0.0000000000000000  34.690984296727800
   7
Selective Dynamics
Direct
0.66667   0.66667   0.00000 F F       F
0.33333   0.33333   0.06667 F F       F
0.66667   0.66667   0.13333 F F       F
0.33333   0.33333   0.20000 F F       F
0.66667   0.66667   0.26667 T T       T
0.33333   0.33333   0.33333 T T       T
0.66667   0.66667   0.40000 T T       T
```

CONTCAR file, case encut=600, kpoints grid=11x11x1:

```
Ti_1x1(aTi=2.93647940097882, c/a=1.57517
   1.00000000000000
     2.9364794009788202    0.0000000000000000    0.0000000000000000
     1.4682397004894101    2.5430657589373693    0.0000000000000000
     0.0000000000000000    0.0000000000000000   34.6909842967277982
   7
Selective dynamics
Direct
  0.6666700000000034  0.6666700000000034  0.0000000000000000   F   F   F
  0.3333299999999966  0.3333299999999966  0.0666700000000020   F   F   F
  0.6666700000000034  0.6666700000000034  0.1333300000000008   F   F   F
  0.3333299999999966  0.3333299999999966  0.2000000000000028   F   F   F
  0.6666680057820695  0.6666680057820695  0.2664092636074630   T   T   T
  0.3333267713133465  0.3333267713133465  0.3351626305206291   T   T   T
  0.6666696874465295  0.6666696874465295  0.3971982275108611   T   T   T

**********************************************************************
```

Ti+H2, Strain studies.
==========

The volume strain (v/v_0) values for Ti are taken as s= 0.98, 0.96, 0.94, 0.92, 0.90, 0.85, 1.02, 1.04, 1.06, 1.08, 1.10, 1.15

POSCAR files with Ti-H distance = 0.8:
==========

```
Ti1x1+H2(aTi=2.93647940097882, c/a=1.57517 d=0.8)
   1.00000000000000
     2.9364794009788202    0.0000000000000000    0.0000000000000000
     1.4682397004894101    2.5430657589373693    0.0000000000000000
     0.0000000000000000    0.0000000000000000   34.6909842967277982
   7   2
Selective dynamics
Direct
  0.6666700000000034  0.6666700000000034  0.0000000000000000   F   F   F
  0.3333299999999966  0.3333299999999966  0.0666700000000020   F   F   F
  0.6666700000000034  0.6666700000000034  0.1333300000000008   F   F   F
  0.3333299999999966  0.3333299999999966  0.2000000000000028   F   F   F
  0.6666680057820695  0.6666680057820695  0.2664092636074630   T   T   T
  0.3333267713133465  0.3333267713133465  0.3351626305206291   T   T   T
  0.6666696874465295  0.6666696874465295  0.3971982275108611   T   T   T
  0.6666696874465295  0.6666696874465295  0.4202589741635717   T   T   T
  0.6666696874465295  0.6666696874465295  0.4415901648173289   T   T   T

TiH2_1x1_s=0.85
Ti_1x1(aTi=2.93647940097882, c/a=1.57517 d=0.8)
  0.947268237000000
     2.9364794009788202    0.0000000000000000    0.0000000000000000
     1.4682397004894101    2.5430657589373693    0.0000000000000000
     0.0000000000000000    0.0000000000000000   34.6909842967277982
   7  2
Selective dynamics
Direct
  0.6666700000000034  0.6666700000000034  0.0000000000000000   F   F   F
  0.3333299999999966  0.3333299999999966  0.0666700000000020   F   F   F
  0.6666700000000034  0.6666700000000034  0.1333300000000008   F   F   F
  0.3333299999999966  0.3333299999999966  0.2000000000000028   F   F   F
  0.6666657005243791  0.6666657005243791  0.2758853599314555   T   T   T
  0.3333361080970617  0.3333361080970617  0.3507873061509868   T   T   T
  0.6666675943794463  0.6666675943794463  0.4196447358117072   T   T   T
  0.6666675943794463  0.6666675943794463  0.4439892094802680   T   T   T
  0.6666675943794463  0.6666675943794463  0.4665078476236870   T   T   T
-------------------------------------------------------------------------------------
---------------
TiH2_1x1_s=0.90
Ti_1x1(aTi=2.93647940097882, c/a=1.57517 d=0.8)
  0.965489384000000
     2.9364794009788202    0.0000000000000000    0.0000000000000000
     1.4682397004894101    2.5430657589373693    0.0000000000000000
     0.0000000000000000    0.0000000000000000   34.6909842967277982
   7  2
Selective dynamics
Direct
  0.6666700000000034  0.6666700000000034  0.0000000000000000   F   F   F
  0.3333299999999966  0.3333299999999966  0.0666700000000020   F   F   F
  0.6666700000000034  0.6666700000000034  0.1333300000000008   F   F   F
  0.3333299999999966  0.3333299999999966  0.2000000000000028   F   F   F
  0.6666645732813725  0.6666645732813725  0.2727500333074210   T   T   T
  0.3333357165737406  0.3333357165737406  0.3452228957819972   T   T   T
  0.6666679398011944  0.6666679398011944  0.4114386687535819   T   T   T
  0.6666679398011944  0.6666679398011944  0.4353237026388540   T   T   T
  0.6666679398011944  0.6666679398011944  0.4574173589827310   T   T   T
-------------------------------------------------------------------------------------
---------------
```

```
TiH2_1x1_s=0.92
Ti_1x1(aTi=2.93647940097882, c/a=1.57517 d=0.8)
  0.972588826000000
     2.9364794009788202    0.0000000000000000    0.0000000000000000
     1.4682397004894101    2.5430657589373693    0.0000000000000000
     0.0000000000000000    0.0000000000000000   34.6909842967277982
   7  2
Selective dynamics
Direct
  0.6666700000000034  0.6666700000000034  0.0000000000000000   F   F   F
  0.3333299999999966  0.3333299999999966  0.0666700000000020   F   F   F
  0.6666700000000034  0.6666700000000034  0.1333300000000008   F   F   F
  0.3333299999999966  0.3333299999999966  0.2000000000000028   F   F   F
  0.6666651979547034  0.6666651979547034  0.2712979492734162   T   T   T
  0.3333340529338495  0.3333340529338495  0.3429893219479793   T   T   T
  0.6666694358732532  0.6666694358732532  0.4082605739329304   T   T   T
  0.6666694358732532  0.6666694358732532  0.4319712582799360   T   T   T
  0.6666694358732532  0.6666694358732532  0.4539036413009160   T   T   T
--------------------------------------------------------------------------------
---------------
TiH2_1x1_s=0.94
Ti_1x1(aTi=2.93647940097882, c/a=1.57517 d=0.8)
  0.979586108000000
     2.9364794009788202    0.0000000000000000    0.0000000000000000
     1.4682397004894101    2.5430657589373693    0.0000000000000000
     0.0000000000000000    0.0000000000000000   34.6909842967277982
   7  2
Selective dynamics
Direct
  0.6666700000000034  0.6666700000000034  0.0000000000000000   F   F   F
  0.3333299999999966  0.3333299999999966  0.0666700000000020   F   F   F
  0.6666700000000034  0.6666700000000034  0.1333300000000008   F   F   F
  0.3333299999999966  0.3333299999999966  0.2000000000000028   F   F   F
  0.6666667328962528  0.6666667328962528  0.2699128336887846   T   T   T
  0.3333290495566978  0.3333290495566978  0.3407760200433096   T   T   T
  0.6666659627939230  0.6666659627939230  0.4051472411527222   T   T   T
  0.6666659627939230  0.6666659627939230  0.4286885576989450   T   T   T
  0.6666659627939230  0.6666659627939230  0.4504642755042010   T   T   T
--------------------------------------------------------------------------------
---------------
TiH2_1x1_s=0.96
Ti_1x1(aTi=2.93647940097882, c/a=1.57517 d=0.8)
  0.986484829000000
     2.9364794009788202    0.0000000000000000    0.0000000000000000
     1.4682397004894101    2.5430657589373693    0.0000000000000000
     0.0000000000000000    0.0000000000000000   34.6909842967277982
   7  2
Selective dynamics
Direct
  0.6666700000000034  0.6666700000000034  0.0000000000000000   F   F   F
  0.3333299999999966  0.3333299999999966  0.0666700000000020   F   F   F
  0.6666700000000034  0.6666700000000034  0.1333300000000008   F   F   F
  0.3333299999999966  0.3333299999999966  0.2000000000000028   F   F   F
  0.6666676907424787  0.6666676907424787  0.2685964946892667   T   T   T
  0.3333323160919415  0.3333323160919415  0.3386232839519127   T   T   T
  0.6666668734845493  0.6666668734845493  0.4021148254234460   T   T   T
  0.6666668734845493  0.6666668734845493  0.4254915119925510   T   T   T
  0.6666668734845493  0.6666668734845493  0.4471149470689740   T   T   T
--------------------------------------------------------------------------------
---------------
TiH2_1x1_s=0.98
Ti_1x1(aTi=2.93647940097882, c/a=1.57517 d=0.8)
  0.993288388000000
     2.9364794009788202    0.0000000000000000    0.0000000000000000
     1.4682397004894101    2.5430657589373693    0.0000000000000000
     0.0000000000000000    0.0000000000000000   34.6909842967277982
   7   2
Selective dynamics
Direct
  0.6666700000000034  0.6666700000000034  0.0000000000000000   F   F   F
  0.3333299999999966  0.3333299999999966  0.0666700000000020   F   F   F
```

```
  0.6666700000000034  0.6666700000000034  0.1333300000000008   F   F   F
  0.3333299999999966  0.3333299999999966  0.2000000000000028   F   F   F
  0.6666593743700732  0.6666593743700732  0.2674680760641105   T   T   T
  0.3333292993612098  0.3333292993612098  0.3368794424634171   T   T   T
  0.6666682068219867  0.6666682068219867  0.3996246470745018   T   T   T
  0.6666682068219867  0.6666682068219867  0.4228412143185260   T   T   T
  0.6666682068219867  0.6666682068219867  0.4443165390192490   T   T   T
-------------------------------------------------------------------------------------------
--------------
TiH2_1x1_s=1.00
Ti_1x1(aTi=2.93647940097882, c/a=1.57517 d=0.8)
   1.00000000000000
     2.9364794009788202    0.0000000000000000    0.0000000000000000
     1.4682397004894101    2.5430657589373693    0.0000000000000000
     0.0000000000000000    0.0000000000000000   34.6909842967277982
   7   2
Selective dynamics
Direct
  0.6666700000000034  0.6666700000000034  0.0000000000000000   F   F   F
  0.3333299999999966  0.3333299999999966  0.0666700000000020   F   F   F
  0.6666700000000034  0.6666700000000034  0.1333300000000008   F   F   F
  0.3333299999999966  0.3333299999999966  0.2000000000000028   F   F   F
  0.6666680057820695  0.6666680057820695  0.2664092636074630   T   T   T
  0.3333267713133465  0.3333267713133465  0.3351626305206291   T   T   T
  0.6666696874465295  0.6666696874465295  0.3971982275108611   T   T   T
  0.6666696874465295  0.6666696874465295  0.4202589741635720   T   T   T
  0.6666696874465295  0.6666696874465295  0.4415901648173290   T   T   T
-------------------------------------------------------------------------------------------
--------------
TiH2_1x1_s=1.02
Ti_1x1(aTi=2.93647940097882, c/a=1.57517 d=0.8)
   1.00662271000000
     2.9364794009788202    0.0000000000000000    0.0000000000000000
     1.4682397004894101    2.5430657589373693    0.0000000000000000
     0.0000000000000000    0.0000000000000000   34.6909842967277982
   7  2
Selective dynamics
Direct
  0.6666700000000034  0.6666700000000034  0.0000000000000000   F   F   F
  0.3333299999999966  0.3333299999999966  0.0666700000000020   F   F   F
  0.6666700000000034  0.6666700000000034  0.1333300000000008   F   F   F
  0.3333299999999966  0.3333299999999966  0.2000000000000028   F   F   F
  0.6666658397684593  0.6666658397684593  0.2653542195517527   T   T   T
  0.3333304471288701  0.3333304471288701  0.3333195484790497   T   T   T
  0.6666683817687401  0.6666683817687401  0.3945723874314048   T   T   T
  0.6666683817687401  0.6666683817687401  0.4174814142431590   T   T   T
  0.6666683817687401  0.6666683817687401  0.4386722640440310   T   T   T
-------------------------------------------------------------------------------------------
--------------
TiH2_1x1_s=1.04
Ti_1x1(aTi=2.93647940097882, c/a=1.57517 d=0.8)
   1.01315940400000
     2.9364794009788202    0.0000000000000000    0.0000000000000000
     1.4682397004894101    2.5430657589373693    0.0000000000000000
     0.0000000000000000    0.0000000000000000   34.6909842967277982
   7  2
Selective dynamics
Direct
  0.6666700000000034  0.6666700000000034  0.0000000000000000   F   F   F
  0.3333299999999966  0.3333299999999966  0.0666700000000020   F   F   F
  0.6666700000000034  0.6666700000000034  0.1333300000000008   F   F   F
  0.3333299999999966  0.3333299999999966  0.2000000000000028   F   F   F
  0.6666603974676566  0.6666603974676566  0.2644067004343467   T   T   T
  0.3333306852296550  0.3333306852296550  0.3317460248403920   T   T   T
  0.6666669342076418  0.6666669342076418  0.3923331238781996   T   T   T
  0.6666669342076418  0.6666669342076418  0.4150943464081050   T   T   T
  0.6666669342076418  0.6666669342076418  0.4361484772482680   T   T   T
-------------------------------------------------------------------------------------------
--------------
TiH2_1x1_s=1.06
Ti_1x1(aTi=2.93647940097882, c/a=1.57517 d=0.8)
```

```
   1.01961282200000
     2.9364794009788202    0.0000000000000000    0.0000000000000000
     1.4682397004894101    2.5430657589373693    0.0000000000000000
     0.0000000000000000    0.0000000000000000   34.6909842967277982
   7  2
Selective dynamics
Direct
  0.6666700000000034  0.6666700000000034  0.0000000000000000   F   F   F
  0.3333299999999966  0.3333299999999966  0.0666700000000020   F   F   F
  0.6666700000000034  0.6666700000000034  0.1333300000000008   F   F   F
  0.3333299999999966  0.3333299999999966  0.2000000000000028   F   F   F
  0.6666646969188846  0.6666646969188846  0.2635933256849510   T   T   T
  0.3333362954476109  0.3333362954476109  0.3302777821276398   T   T   T
  0.6666719745706232  0.6666719745706232  0.3902509596732003   T   T   T
  0.6666719745706232  0.6666719745706232  0.4128681199865400   T   T   T
  0.6666719745706232  0.6666719745706232  0.4337889932763790   T   T   T
--------------------------------------------------------------------------------
---------------
TiH2_1x1_s=1.08
Ti_1x1(aTi=2.93647940097882, c/a=1.57517 d=0.8)
   1.02598556800000
     2.9364794009788202    0.0000000000000000    0.0000000000000000
     1.4682397004894101    2.5430657589373693    0.0000000000000000
     0.0000000000000000    0.0000000000000000   34.6909842967277982
   7  2
Selective dynamics
Direct
  0.6666700000000034  0.6666700000000034  0.0000000000000000   F   F   F
  0.3333299999999966  0.3333299999999966  0.0666700000000020   F   F   F
  0.6666700000000034  0.6666700000000034  0.1333300000000008   F   F   F
  0.3333299999999966  0.3333299999999966  0.2000000000000028   F   F   F
  0.6666643615057534  0.6666643615057534  0.2627467521264934   T   T   T
  0.3333355931954435  0.3333355931954435  0.3287144399286472   T   T   T
  0.6666726039106782  0.6666726039106782  0.3879846239538693   T   T   T
  0.6666726039106782  0.6666726039106782  0.4104613013769870   T   T   T
  0.6666726039106782  0.6666726039106782  0.4312522279933720   T   T   T
--------------------------------------------------------------------------------
---------------
TiH2_1x1_s=1.10
Ti_1x1(aTi=2.93647940097882, c/a=1.57517 d=0.8)
   1.03228011500000
     2.9364794009788202    0.0000000000000000    0.0000000000000000
     1.4682397004894101    2.5430657589373693    0.0000000000000000
     0.0000000000000000    0.0000000000000000   34.6909842967277982
   7  2
Selective dynamics
Direct
  0.6666700000000034  0.6666700000000034  0.0000000000000000   F   F   F
  0.3333299999999966  0.3333299999999966  0.0666700000000020   F   F   F
  0.6666700000000034  0.6666700000000034  0.1333300000000008   F   F   F
  0.3333299999999966  0.3333299999999966  0.2000000000000028   F   F   F
  0.6666663012487253  0.6666663012487253  0.2619188852421740   T   T   T
  0.3333378979401706  0.3333378979401706  0.3271372793017045   T   T   T
  0.6666704829401272  0.6666704829401272  0.3857856066494638   T   T   T
  0.6666704829401272  0.6666704829401272  0.4081252277635550   T   T   T
  0.6666704829401272  0.6666704829401272  0.4287893772940900   T   T   T
--------------------------------------------------------------------------------
---------------
TiH2_1x1_s=1.15
Ti_1x1(aTi=2.93647940097882, c/a=1.57517 d=0.8)
   1.04768955300000
     2.9364794009788202    0.0000000000000000    0.0000000000000000
     1.4682397004894101    2.5430657589373693    0.0000000000000000
     0.0000000000000000    0.0000000000000000   34.6909842967277982
   7  2
Selective dynamics
Direct
  0.6666700000000034  0.6666700000000034  0.0000000000000000   F   F   F
  0.3333299999999966  0.3333299999999966  0.0666700000000020   F   F   F
  0.6666700000000034  0.6666700000000034  0.1333300000000008   F   F   F
  0.3333299999999966  0.3333299999999966  0.2000000000000028   F   F   F
```

```
  0.6666640534804138  0.6666640534804138  0.2601673008814309   T   T   T
  0.3333328088969314  0.3333328088969314  0.3237219699127208   T   T   T
  0.6666676857737623  0.6666676857737623  0.3808670347006249   T   T   T
  0.6666676857737623  0.6666676857737623  0.4028780842397540   T   T   T
  0.6666676857737623  0.6666676857737623  0.4232383050634480   T   T   T

**************************************************************************
```

POSCAR files with Ti-H distance = 1.2:

==========

```
TiH2_1x1_s=0.85
Ti_1x1(aTi=2.93647940097882, c/a=1.57517 d=1.2)
  0.947268237000000
     2.9364794009788202    0.0000000000000000    0.0000000000000000
     1.4682397004894101    2.5430657589373693    0.0000000000000000
     0.0000000000000000    0.0000000000000000   34.6909842967277982
   7  2
Selective dynamics
Direct
  0.6666700000000034  0.6666700000000034  0.0000000000000000   F   F   F
  0.3333299999999966  0.3333299999999966  0.0666700000000020   F   F   F
  0.6666700000000034  0.6666700000000034  0.1333300000000008   F   F   F
  0.3333299999999966  0.3333299999999966  0.2000000000000028   F   F   F
  0.6666657005243791  0.6666657005243791  0.2758853599314555   T   T   T
  0.3333361080970617  0.3333361080970617  0.3507873061509868   T   T   T
  0.6666675943794463  0.6666675943794463  0.4196447358117072   T   T   T
  0.6666675943794463  0.6666675943794463  0.4561614463145480   T   T   T
  0.6666675943794463  0.6666675943794463  0.4786800844579670   T   T   T
--------------------------------------------------------------------------------------------
---------------
TiH2_1x1_s=0.90
Ti_1x1(aTi=2.93647940097882, c/a=1.57517 d=1.2)
  0.965489384000000
     2.9364794009788202    0.0000000000000000    0.0000000000000000
     1.4682397004894101    2.5430657589373693    0.0000000000000000
     0.0000000000000000    0.0000000000000000   34.6909842967277982
   7  2
Selective dynamics
Direct
  0.6666700000000034  0.6666700000000034  0.0000000000000000   F   F   F
  0.3333299999999966  0.3333299999999966  0.0666700000000020   F   F   F
  0.6666700000000034  0.6666700000000034  0.1333300000000008   F   F   F
  0.3333299999999966  0.3333299999999966  0.2000000000000028   F   F   F
  0.6666645732813725  0.6666645732813725  0.2727500333074210   T   T   T
  0.3333357165737406  0.3333357165737406  0.3452228957819972   T   T   T
  0.6666679398011944  0.6666679398011944  0.4114386687535819   T   T   T
  0.6666679398011944  0.6666679398011944  0.4472662195814900   T   T   T
  0.6666679398011944  0.6666679398011944  0.4693598759253670   T   T   T
--------------------------------------------------------------------------------------------
---------------
TiH2_1x1_s=0.92
Ti_1x1(aTi=2.93647940097882, c/a=1.57517 d=1.2)
  0.972588826000000
     2.9364794009788202    0.0000000000000000    0.0000000000000000
     1.4682397004894101    2.5430657589373693    0.0000000000000000
     0.0000000000000000    0.0000000000000000   34.6909842967277982
   7  2
Selective dynamics
Direct
  0.6666700000000034  0.6666700000000034  0.0000000000000000   F   F   F
  0.3333299999999966  0.3333299999999966  0.0666700000000020   F   F   F
  0.6666700000000034  0.6666700000000034  0.1333300000000008   F   F   F
  0.3333299999999966  0.3333299999999966  0.2000000000000028   F   F   F
  0.6666651979547034  0.6666651979547034  0.2712979492734162   T   T   T
  0.3333340529338495  0.3333340529338495  0.3429893219479793   T   T   T
  0.6666694358732532  0.6666694358732532  0.4082605739329304   T   T   T
  0.6666694358732532  0.6666694358732532  0.4438266004534390   T   T   T
  0.6666694358732532  0.6666694358732532  0.4657589834744180   T   T   T
```

```
--------------------------------------------------------------------------------------------
--------------
TiH2_1x1_s=0.94
Ti_1x1(aTi=2.93647940097882, c/a=1.57517 d=1.2)
  0.979586108000000
     2.9364794009788202    0.0000000000000000    0.0000000000000000
     1.4682397004894101    2.5430657589373693    0.0000000000000000
     0.0000000000000000    0.0000000000000000   34.6909842967277982
   7  2
Selective dynamics
Direct
  0.6666700000000034  0.6666700000000034  0.0000000000000000   F   F   F
  0.3333299999999966  0.3333299999999966  0.0666700000000020   F   F   F
  0.6666700000000034  0.6666700000000034  0.1333300000000008   F   F   F
  0.3333299999999966  0.3333299999999966  0.2000000000000028   F   F   F
  0.6666667328962528  0.6666667328962528  0.2699128336887846   T   T   T
  0.3333290495566978  0.3333290495566978  0.3407760200433096   T   T   T
  0.6666659627939230  0.6666659627939230  0.4051472411527222   T   T   T
  0.6666659627939230  0.6666659627939230  0.4404592159720570   T   T   T
  0.6666659627939230  0.6666659627939230  0.4622349337773130   T   T   T
--------------------------------------------------------------------------------------------
--------------
TiH2_1x1_s=0.96
Ti_1x1(aTi=2.93647940097882, c/a=1.57517 d=1.2)
  0.986484829000000
     2.9364794009788202    0.0000000000000000    0.0000000000000000
     1.4682397004894101    2.5430657589373693    0.0000000000000000
     0.0000000000000000    0.0000000000000000   34.6909842967277982
   7  2
Selective dynamics
Direct
  0.6666700000000034  0.6666700000000034  0.0000000000000000   F   F   F
  0.3333299999999966  0.3333299999999966  0.0666700000000020   F   F   F
  0.6666700000000034  0.6666700000000034  0.1333300000000008   F   F   F
  0.3333299999999966  0.3333299999999966  0.2000000000000028   F   F   F
  0.6666676907424787  0.6666676907424787  0.2685964946892667   T   T   T
  0.3333323160919415  0.3333323160919415  0.3386232839519127   T   T   T
  0.6666668734845493  0.6666668734845493  0.4021148254234460   T   T   T
  0.6666668734845493  0.6666668734845493  0.4371798552771040   T   T   T
  0.6666668734845493  0.6666668734845493  0.4588032903535270   T   T   T
--------------------------------------------------------------------------------------------
--------------
TiH2_1x1_s=0.98
Ti_1x1(aTi=2.93647940097882, c/a=1.57517 d=1.2)
  0.993288388000000
     2.9364794009788202    0.0000000000000000    0.0000000000000000
     1.4682397004894101    2.5430657589373693    0.0000000000000000
     0.0000000000000000    0.0000000000000000   34.6909842967277982
   7   2
Selective dynamics
Direct
  0.6666700000000034  0.6666700000000034  0.0000000000000000   F   F   F
  0.3333299999999966  0.3333299999999966  0.0666700000000020   F   F   F
  0.6666700000000034  0.6666700000000034  0.1333300000000008   F   F   F
  0.3333299999999966  0.3333299999999966  0.2000000000000028   F   F   F
  0.6666593743700732  0.6666593743700732  0.2674680760641105   T   T   T
  0.3333292993612098  0.3333292993612098  0.3368794424634171   T   T   T
  0.6666682068219867  0.6666682068219867  0.3996246470745018   T   T   T
  0.6666682068219867  0.6666682068219867  0.4344494979405380   T   T   T
  0.6666682068219867  0.6666682068219867  0.4559248226412610   T   T   T
--------------------------------------------------------------------------------------------
--------------
TiH2_1x1_s=1.00
Ti_1x1(aTi=2.93647940097882, c/a=1.57517 d=1.2)
   1.00000000000000
     2.9364794009788202    0.0000000000000000    0.0000000000000000
     1.4682397004894101    2.5430657589373693    0.0000000000000000
     0.0000000000000000    0.0000000000000000   34.6909842967277982
   7   2
Selective dynamics
Direct
```

```
  0.6666700000000034  0.6666700000000034  0.0000000000000000   F   F   F
  0.3333299999999966  0.3333299999999966  0.0666700000000020   F   F   F
  0.6666700000000034  0.6666700000000034  0.1333300000000008   F   F   F
  0.3333299999999966  0.3333299999999966  0.2000000000000028   F   F   F
  0.6666680057820695  0.6666680057820695  0.2664092636074630   T   T   T
  0.3333267713133465  0.3333267713133465  0.3351626305206291   T   T   T
  0.6666696874465295  0.6666696874465295  0.3971982275108611   T   T   T
  0.6666696874465295  0.6666696874465295  0.4317893474899270   T   T   T
  0.6666696874465295  0.6666696874465295  0.4531205381436840   T   T   T
-------------------------------------------------------------------------------------------
---------------
TiH2_1x1_s=1.02
Ti_1x1(aTi=2.93647940097882, c/a=1.57517 d=1.2)
   1.00662271000000
     2.9364794009788202    0.0000000000000000    0.0000000000000000
     1.4682397004894101    2.5430657589373693    0.0000000000000000
     0.0000000000000000    0.0000000000000000   34.6909842967277982
   7  2
Selective dynamics
Direct
  0.6666700000000034  0.6666700000000034  0.0000000000000000   F   F   F
  0.3333299999999966  0.3333299999999966  0.0666700000000020   F   F   F
  0.6666700000000034  0.6666700000000034  0.1333300000000008   F   F   F
  0.3333299999999966  0.3333299999999966  0.2000000000000028   F   F   F
  0.6666658397684593  0.6666658397684593  0.2653542195517527   T   T   T
  0.3333304471288701  0.3333304471288701  0.3333195484790497   T   T   T
  0.6666683817687401  0.6666683817687401  0.3945723874314048   T   T   T
  0.6666683817687401  0.6666683817687401  0.4289359276490360   T   T   T
  0.6666683817687401  0.6666683817687401  0.4501267774499080   T   T   T
-------------------------------------------------------------------------------------------
---------------
TiH2_1x1_s=1.04
Ti_1x1(aTi=2.93647940097882, c/a=1.57517 d=1.2)
   1.01315940400000
     2.9364794009788202    0.0000000000000000    0.0000000000000000
     1.4682397004894101    2.5430657589373693    0.0000000000000000
     0.0000000000000000    0.0000000000000000   34.6909842967277982
   7  2
Selective dynamics
Direct
  0.6666700000000034  0.6666700000000034  0.0000000000000000   F   F   F
  0.3333299999999966  0.3333299999999966  0.0666700000000020   F   F   F
  0.6666700000000034  0.6666700000000034  0.1333300000000008   F   F   F
  0.3333299999999966  0.3333299999999966  0.2000000000000028   F   F   F
  0.6666603974676566  0.6666603974676566  0.2644067004343467   T   T   T
  0.3333306852296550  0.3333306852296550  0.3317460248403920   T   T   T
  0.6666669342076418  0.6666669342076418  0.3923331238781996   T   T   T
  0.6666669342076418  0.6666669342076418  0.4264749576730580   T   T   T
  0.6666669342076418  0.6666669342076418  0.4475290885132210   T   T   T
-------------------------------------------------------------------------------------------
---------------
TiH2_1x1_s=1.06
Ti_1x1(aTi=2.93647940097882, c/a=1.57517 d=1.2)
   1.01961282200000
     2.9364794009788202    0.0000000000000000    0.0000000000000000
     1.4682397004894101    2.5430657589373693    0.0000000000000000
     0.0000000000000000    0.0000000000000000   34.6909842967277982
   7  2
Selective dynamics
Direct
  0.6666700000000034  0.6666700000000034  0.0000000000000000   F   F   F
  0.3333299999999966  0.3333299999999966  0.0666700000000020   F   F   F
  0.6666700000000034  0.6666700000000034  0.1333300000000008   F   F   F
  0.3333299999999966  0.3333299999999966  0.2000000000000028   F   F   F
  0.6666646969188846  0.6666646969188846  0.2635933256849510   T   T   T
  0.3333362954476109  0.3333362954476109  0.3302777821276398   T   T   T
  0.6666719745706232  0.6666719745706232  0.3902509596732003   T   T   T
  0.6666719745706232  0.6666719745706232  0.4241767001432100   T   T   T
  0.6666719745706232  0.6666719745706232  0.4450975734330490   T   T   T
-------------------------------------------------------------------------------------------
---------------
```

```
TiH2_1x1_s=1.08
Ti_1x1(aTi=2.93647940097882, c/a=1.57517 d=1.2)
   1.02598556800000
     2.9364794009788202    0.0000000000000000    0.0000000000000000
     1.4682397004894101    2.5430657589373693    0.0000000000000000
     0.0000000000000000    0.0000000000000000   34.6909842967277982
   7  2
Selective dynamics
Direct
  0.6666700000000034  0.6666700000000034  0.0000000000000000   F   F   F
  0.3333299999999966  0.3333299999999966  0.0666700000000020   F   F   F
  0.6666700000000034  0.6666700000000034  0.1333300000000008   F   F   F
  0.3333299999999966  0.3333299999999966  0.2000000000000028   F   F   F
  0.6666643615057534  0.6666643615057534  0.2627467521264934   T   T   T
  0.3333355931954435  0.3333355931954435  0.3287144399286472   T   T   T
  0.6666726039106782  0.6666726039106782  0.3879846239538693   T   T   T
  0.6666726039106782  0.6666726039106782  0.4450975734330490   T   T   T
  0.6666726039106782  0.6666726039106782  0.4424905667049310   T   T   T
-------------------------------------------------------------------------------------------
---------------
TiH2_1x1_s=1.10
Ti_1x1(aTi=2.93647940097882, c/a=1.57517 d=1.2)
   1.03228011500000
     2.9364794009788202    0.0000000000000000    0.0000000000000000
     1.4682397004894101    2.5430657589373693    0.0000000000000000
     0.0000000000000000    0.0000000000000000   34.6909842967277982
   7  2
Selective dynamics
Direct
  0.6666700000000034  0.6666700000000034  0.0000000000000000   F   F   F
  0.3333299999999966  0.3333299999999966  0.0666700000000020   F   F   F
  0.6666700000000034  0.6666700000000034  0.1333300000000008   F   F   F
  0.3333299999999966  0.3333299999999966  0.2000000000000028   F   F   F
  0.6666663012487253  0.6666663012487253  0.2619188852421740   T   T   T
  0.3333378979401706  0.3333378979401706  0.3271372793017045   T   T   T
  0.6666704829401272  0.6666704829401272  0.3857856066494638   T   T   T
  0.6666704829401272  0.6666704829401272  0.4192950383206010   T   T   T
  0.6666704829401272  0.6666704829401272  0.4399591878511350   T   T   T
-------------------------------------------------------------------------------------------
---------------
TiH2_1x1_s=1.15
Ti_1x1(aTi=2.93647940097882, c/a=1.57517 d=1.2)
   1.04768955300000
     2.9364794009788202    0.0000000000000000    0.0000000000000000
     1.4682397004894101    2.5430657589373693    0.0000000000000000
     0.0000000000000000    0.0000000000000000   34.6909842967277982
   7  2
Selective dynamics
Direct
  0.6666700000000034  0.6666700000000034  0.0000000000000000   F   F   F
  0.3333299999999966  0.3333299999999966  0.0666700000000020   F   F   F
  0.6666700000000034  0.6666700000000034  0.1333300000000008   F   F   F
  0.3333299999999966  0.3333299999999966  0.2000000000000028   F   F   F
  0.6666640534804138  0.6666640534804138  0.2601673008814309   T   T   T
  0.3333328088969314  0.3333328088969314  0.3237219699127208   T   T   T
  0.6666676857737623  0.6666676857737623  0.3808670347006249   T   T   T
  0.6666676857737623  0.6666676857737623  0.4138836090093180   T   T   T
  0.6666676857737623  0.6666676857737623  0.4342438298330120   T   T   T
-------------------------------------------------------------------------------------------
---------------
```

APPENDIX D

INPUT TO PHONON

This Appendix contains an example input to the PHONON program, used to compute the thermal contribution to the energy for calculations of the equation of state.

Introduction

Using PHONON

PHONON. Phonon is a software for calculating phonon dispersion curves, and phonon density spectra of crystals, crystals with defects, surfaces, adsorbed atoms on surfaces, etc. from either a set of force constants, or from a set of Hellmann-Feynman forces calculated within an *ab initio* program.

VASP is used as the *ab initio* program here. Phonon builds a crystal structure, using one of the 230 crystallographic space groups, finds the force constant from the Hellmann-Feynman forces, builds the dynamical matrix, diagonalizes it, and calculates the phonon dispersion relations, and their intensities. Phonon finds the polarization vectors, and the irreducible representations (Gamma point) of phonon modes, and calculates the total and partial phonon density of states. It plots the internal energy, free energy, entropy, heat capacity and tensor of mean square displacements (Debey-Waller factor). Phonon finds the dynamical structure factor for the coherent inelastic neutron scattering and the incoherent doubly differential scattering cross section for a single crystal and polycrystal. For polar cystals the LO/TO mode splitting can be included.

PHONON is used together with VASP to generate Energy-Temperature curves for a given volume (or density) of the studied supercell. The collection of various E-T curves generates a surface, which is the Energy-Temperature-Volume surface used for studies of the Equation of State. The knowledge of Energy-Temperature can also be used to find the binding energy of a system at a temperature different than 0 K.

Part I: Outline

The following instructions give an example for using PHONON. The molecular system chosen for the example is expanded FCC aluminum with lattice = 1.10*a_{Al} , where a_{Al} = 4.05 Å. The supercell here is identical to the unit cell.

Used executables: vasp-par (VASP executable), GenPos, GenHFfile, myrun
Used softwares: WinSCP (file transfer), PuTTY or SecureCRT (terminal)

The PHONON – VASP procedure follows 4 main stages (a,b,c,d). The detailed steps (1,2,…,18) are described in Part II.

Stages:

- **a) VASP → unit cell optimization**
- **b) PHONON → supercell creation**
- **c) VASP → supercell optimization**
- **d) PHONON → HF forces, E_{free} calculation, plots**

a) VASP (step 1)

inputs	outputs
INCAR → job details POSCAR → structure POTCAR → PP KPOINTS	CONTCAR → optimized structure (other files)

b) PHONON (steps 2-6)
Creates file Al_110.d44

c) VASP (steps 7-12)
copy file Al_110.d44 to VASP directory, rename to DISCAR

run the binaries:
>>GenPos → HFPOSCAR, pos_Aa, pos_Ab (and "run')
>>./myrun → out_Aa, out_Ab
>>GenHFfile → HFFILE (contains the HF forces)

GenPos uses DISCAR(from b) and CONTCAR (from a).
./myrun uses pos_Aa and pos_Ab and runs VASP. ('myrun' replaces 'run').
GenHFfile uses DISCAR, HFPOSCAR, out_Aa and out_Ab.

PHONON disturbs 1 atom and generates HF forces. The pos_aA and pos_Ab are the generated position files with disturbed positions (they are the input POSCAR files). The out_aA and out_Ab are the results of the VASP optimization with these disturbed positions (they are the output OUTCAR files).

d) PHONON (steps 13-18)
copy file HFFILE to the Phonon directory; rename to Al_110
Do steps 13-18. Create all data and figure files (*.d18, d19, d26, d27, d28, d29).

Part II: Steps

Stage a)	1. Open VASP, run ./vasp with the initial unit cell input.
Stage b)	2. Open PHONON, File →New Project, type in the name of your project. 3. Create→Symmetry & Unit Cell→Intern.Tables Crystal., type in the name of the crystal model, lattice constant and angle. 4. Create→Particles→Particle positions, type in the mass of the crystal atom. 5. Create→Interaction Range→Supercell, type in the parameters needed. 6. Create→Hellmann Feynman F.→Supercell, type in Number of Atoms in Supercell and coordinate parameters.
Stage c)	7. The *.d44 file should have already been generated till this step. Using WinSCP to transfer this file to the computer on which VASP is running. 8. Open PUTTY to get connected with the computer on which VASP is running. 9. Type "cp *.d44 DISCAR" and extract information from the relative OUTCAR file to replace CONTCAR file. 10. Type ./GenPos to generate files 'run' and 'pos_Aa' etc. 11. Change the path of VASP in the 'run' file to the correct path and type ./run to generate out_Aa etc. If 'run' gives errors, use ./myrun ('myrun' is provided there by us). 12. Type ./GenHFfile to generate HFFILE. Use WinSCP to transfer the HFFILE to the computer on which PHONON is running.
Stage d)	13. Create→Hellmann Feynman F.→Import H-F file, type in the name of the H-F file and choose the force unit. 14. Create→Hellmann Feynman F.→Browse H-F file to check if the H-F file imported is correct. If so, Create→Hellmann Feynman F.→Do Report. 15. Create→Dispersion Curves→Set Points, and Wave Vectors, type in the appropriate parameters. 16. Create→Dispersion Curves→Do Report, and Plot to get the dispersion curve. 17. Create→Density of States→Set Points, Do Report, and Plot DOS to get the curve. 18. Create→Thermodynamic F.→Plot Internal Energy to get the curve.

The PHONON figure files can be read with a postscript program. (e.g. GhostView).

Part III: Details of Steps

Step 1.

```
rusi@abinitio1:~/VASP/Al_110> lamboot -v

LAM 7.1.1/MPI 2 C++ - Indiana University

n-1<23046> ssi:boot:base:linear: booting n0 (localhost)
n-1<23046> ssi:boot:base:linear: finished
```

```
rusi@abinitio1:~/VASP/Al_110> vasp-par
 running on    1 nodes
 distr:  one band on    1 nodes,    1 groups
 vasp.4.6.28 25Jul05 complex
 POSCAR found :  1 types and    4 ions
 LDA part: xc-table for Ceperly-Alder, standard interpolation
 POSCAR, INCAR and KPOINTS ok, starting setup
 WARNING: wrap around errors must be expected
 FFT: planning ...           1
 reading WAVECAR
 WARNING: random wavefunctions but no delay for mixing, default for NELMDL
 entering main loop
       N       E                     dE             d eps       ncg     rms          rms(c)
DAV:   1    -0.584391271731E+00   -0.58439E+00   -0.23761E+03   160   0.237E+02
DAV:   2    -0.135956422575E+02   -0.13011E+02   -0.12518E+02   188   0.489E+01
DAV:   3    -0.139405294861E+02   -0.34489E+00   -0.34258E+00   196   0.626E+00
DAV:   4    -0.139418790812E+02   -0.13496E-02   -0.13495E-02   180   0.524E-01
DAV:   5    -0.139418864439E+02   -0.73627E-05   -0.73623E-05   204   0.351E-02    0.150E+00
DAV:   6    -0.139064481988E+02    0.35438E-01   -0.74797E-03   180   0.302E-01    0.932E-01
DAV:   7    -0.138818094278E+02    0.24639E-01   -0.21677E-02   168   0.499E-01    0.515E-02
DAV:   8    -0.138818325597E+02   -0.23132E-04   -0.28403E-04   192   0.714E-02    0.110E-02
DAV:   9    -0.138818380778E+02   -0.55181E-05   -0.47205E-06   184   0.751E-03    0.198E-03
DAV:  10    -0.138818363026E+02    0.17752E-05   -0.77435E-08   176   0.111E-03    0.481E-04
DAV:  11    -0.138818361073E+02    0.19528E-06   -0.74530E-09   116   0.318E-04    0.347E-05
DAV:  12    -0.138818361367E+02   -0.29378E-07   -0.70634E-10   128   0.115E-04
   1 F= -.13881836E+02 E0= -.13871849E+02  d E =-.199735E-01
 writing wavefunctions
rusi@abinitio1:~/VASP/Al_110>
```

Step 2.

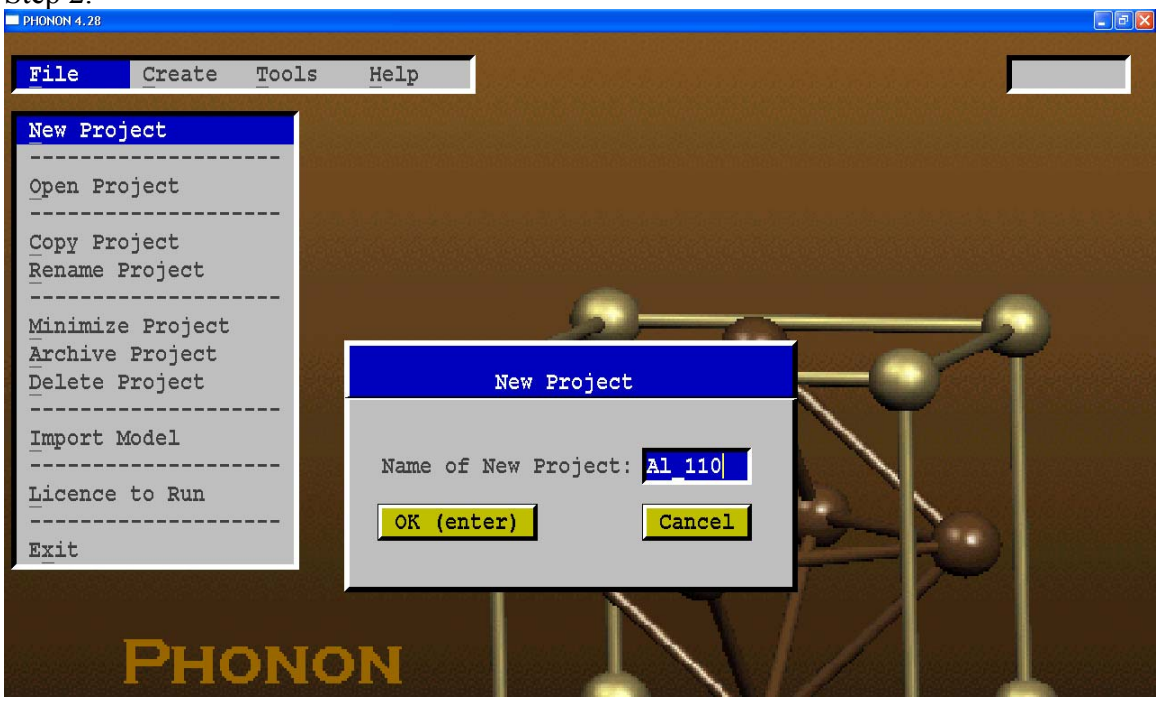

Step 3.

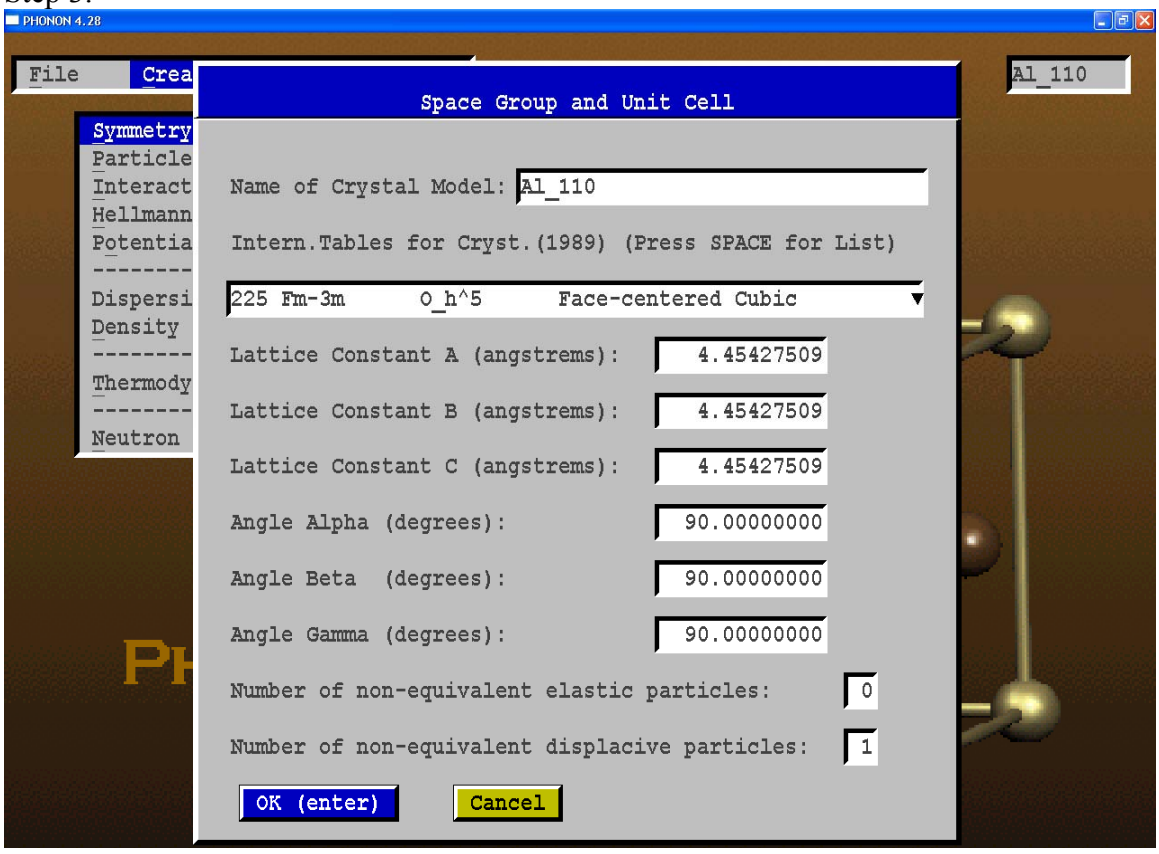
PHONON 4.28
File
Crea
Al_110
Symmetry
Particle
Interact
Hellmann
Potentia
Dispersi
Density
Thermody
Neutron
Space Group and Unit Cell
Name of Crystal Model: Al_110
Intern.Tables for Cryst.(1989) (Press SPACE for List)
225 Fm-3m O_h^5 Face-centered Cubic
Lattice Constant A (angstrems): 4.45427509
Lattice Constant B (angstrems): 4.45427509
Lattice Constant C (angstrems): 4.45427509
Angle Alpha (degrees): 90.00000000
Angle Beta (degrees): 90.00000000
Angle Gamma (degrees): 90.00000000
Number of non-equivalent elastic particles: 0
Number of non-equivalent displacive particles: 1
OK (enter)
Cancel

Step 4.

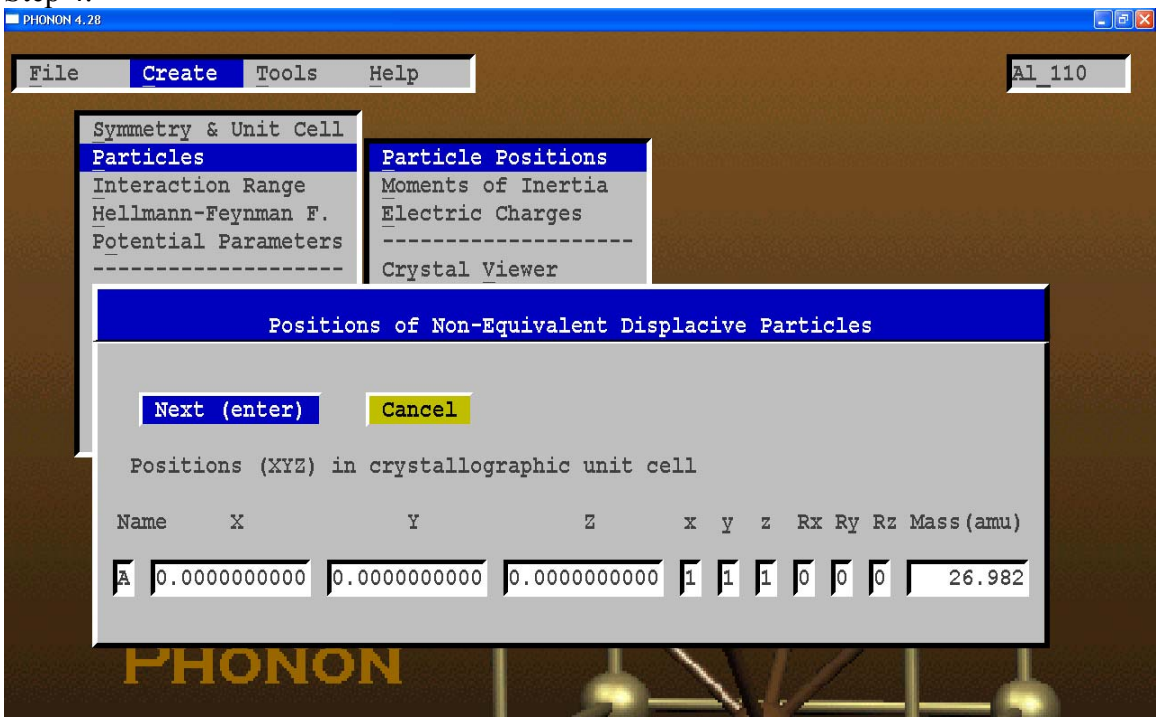
PHONON 4.28
File
Create
Tools
Help
Al_110
Symmetry & Unit Cell
Particles
Interaction Range
Hellmann-Feynman F.
Potential Parameters
Particle Positions
Moments of Inertia
Electric Charges
Crystal Viewer
Positions of Non-Equivalent Displacive Particles
Next (enter)
Cancel
Positions (XYZ) in crystallographic unit cell
Name X Y Z x y z Rx Ry Rz Mass(amu)
A 0.0000000000 0.0000000000 0.0000000000 1 1 1 0 0 0 26.982
PHONON

Step 5.

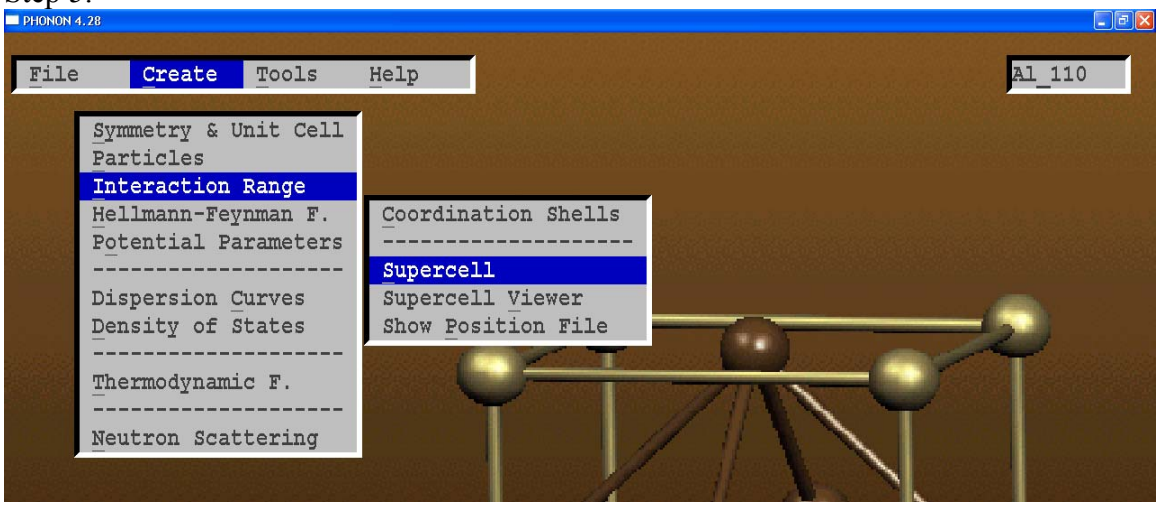
PHONON 4.28
File
Create
Tools
Help
Al_110
Symmetry & Unit Cell
Particles
Interaction Range
Hellmann-Feynman F.
Potential Parameters
Dispersion Curves
Density of States
Thermodynamic F.
Neutron Scattering
Coordination Shells
Supercell
Supercell Viewer
Show Position File

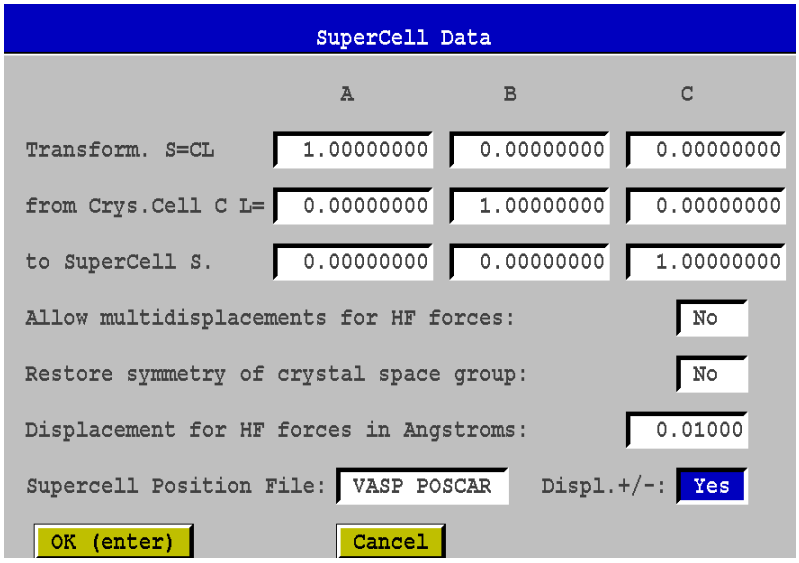
SuperCell Data
A
B
C
Transform. S=CL
1.00000000
0.00000000
0.00000000
from Crys.Cell C L=
0.00000000
1.00000000
0.00000000
to SuperCell S.
0.00000000
0.00000000
1.00000000
Allow multidisplacements for HF forces:
No
Restore symmetry of crystal space group:
No
Displacement for HF forces in Angstroms:
0.01000
Supercell Position File:
VASP POSCAR
Displ.+/-:
Yes
OK (enter)
Cancel

Step 6.

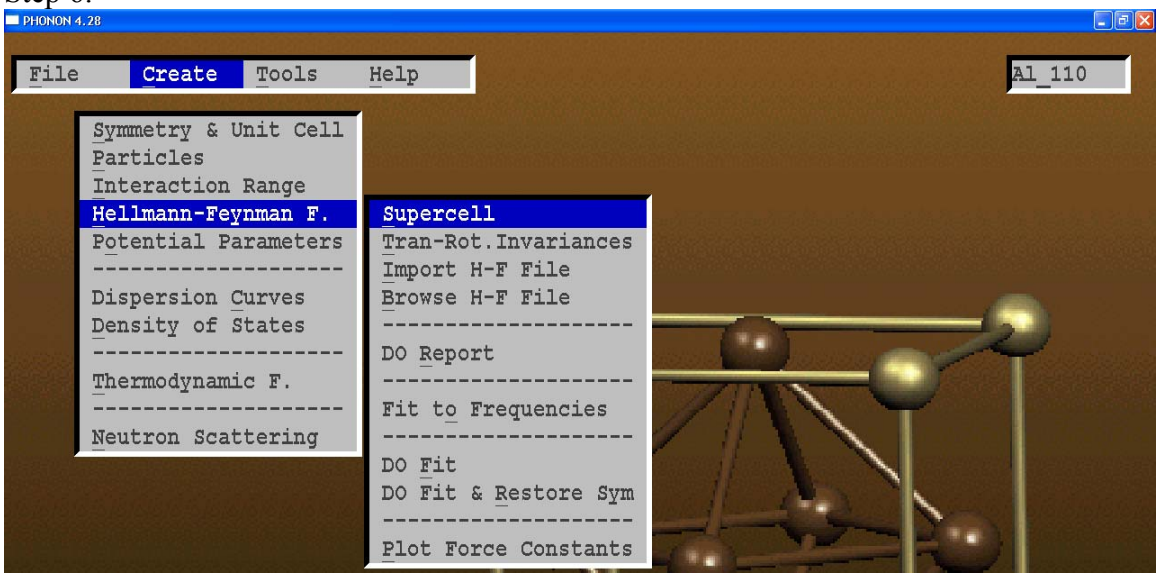

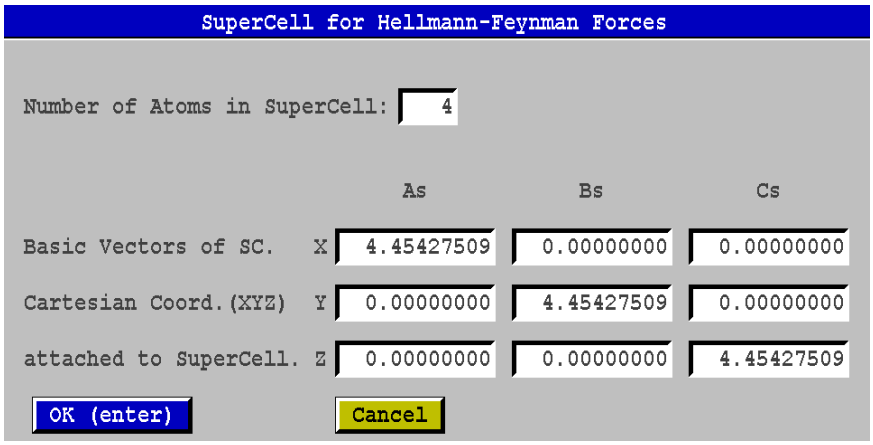

Files in the PHONON directory after completing step 6:

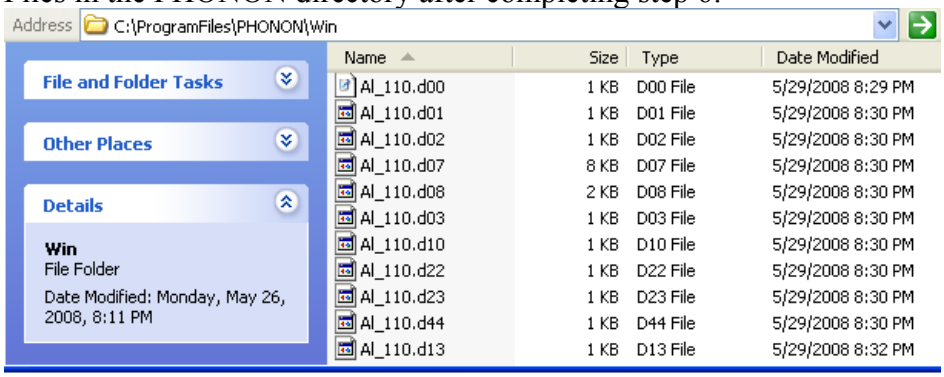

Steps 7-12.

>>GenPos

```
rusi@abinitio1:~/VASP/Al_110> GenPos
  Program <genpos>, ver.4.24
  generates all POSCARs of VASP
  needed to find Hellmann-Feynman forces.
  Necessery displacements must be given in DISCAR
  which is <project>.d44 of Phonon
  Names of new POSCAR files with atoms displaced
  are generated automatically.
  This program reads CONTCAR (not POSCAR).
  You need CONTCAR and DISCAR in current directory.
  Program <genpos> copies CONTCAR to HFPOSCAR.
  It also generates <run> script.
  Use: <chmod a+x run> before running this script.
 Press any key to continue
PAUSE prompt>
rusi@abinitio1:~/VASP/Al_110>
```

>>./myrun

```
rusi@abinitio1:~/VASP/Al_110> ./myrun
Pos_Aa
 running on    1 nodes
 distr:  one band on    1 nodes,    1 groups
 vasp.4.6.28 25Jul05 complex
 POSCAR found :  1 types and    4 ions
 LDA part: xc-table for Ceperly-Alder, standard interpolation
 POSCAR, INCAR and KPOINTS ok, starting setup
 WARNING: wrap around errors must be expected
 FFT: planning ...           1
 reading WAVECAR
 WARNING: random wavefunctions but no delay for mixing, default for NELMDL
 entering main loop
       N       E                     dE             d eps       ncg     rms          rms(c)
DAV:   1     -0.179812943690E+01   -0.17981E+01   -0.23099E+03   240   0.233E+02
DAV:   2     -0.136421062024E+02   -0.11844E+02   -0.11401E+02   296   0.462E+01
DAV:   3     -0.139405815792E+02   -0.29848E+00   -0.29644E+00   296   0.576E+00
DAV:   4     -0.139418778136E+02   -0.12962E-02   -0.12961E-02   288   0.517E-01
DAV:   5     -0.139418857212E+02   -0.79076E-05   -0.79081E-05   284   0.366E-02    0.150E+00
DAV:   6     -0.139064199533E+02    0.35466E-01   -0.75278E-03   272   0.302E-01    0.932E-01
DAV:   7     -0.138817813531E+02    0.24639E-01   -0.21701E-02   244   0.499E-01    0.515E-02
DAV:   8     -0.138817996111E+02   -0.18258E-04   -0.29237E-04   288   0.716E-02    0.141E-02
DAV:   9     -0.138818070544E+02   -0.74433E-05   -0.81638E-06   272   0.104E-02    0.209E-03
DAV:  10     -0.138818069142E+02    0.14016E-06   -0.39658E-07   308   0.226E-03    0.988E-04
DAV:  11     -0.138818061869E+02    0.72737E-06   -0.35533E-08   164   0.752E-04    0.186E-04
DAV:  12     -0.138818060456E+02    0.14127E-06   -0.20707E-09   168   0.205E-04    0.284E-05
DAV:  13     -0.138818060516E+02   -0.59736E-08   -0.18063E-10   168   0.547E-05
   1 F= -.13881806E+02 E0= -.13871819E+02  d E =-.199735E-01
 writing wavefunctions
Pos_Ab
 running on    1 nodes
 distr:  one band on    1 nodes,    1 groups
 vasp.4.6.28 25Jul05 complex
 POSCAR found :  1 types and    4 ions
 LDA part: xc-table for Ceperly-Alder, standard interpolation
 POSCAR, INCAR and KPOINTS ok, starting setup
 WARNING: wrap around errors must be expected
 FFT: planning ...           1
 reading WAVECAR
 WARNING: random wavefunctions but no delay for mixing, default for NELMDL
 entering main loop
       N       E                     dE             d eps       ncg     rms          rms(c)
DAV:   1     -0.179928445393E+01   -0.17993E+01   -0.23101E+03   240   0.233E+02
DAV:   2     -0.136416598788E+02   -0.11842E+02   -0.11399E+02   296   0.462E+01
DAV:   3     -0.139405814097E+02   -0.29892E+00   -0.29685E+00   296   0.576E+00
DAV:   4     -0.139418778574E+02   -0.12964E-02   -0.12963E-02   288   0.517E-01
DAV:   5     -0.139418857224E+02   -0.78650E-05   -0.78644E-05   284   0.365E-02    0.150E+00
DAV:   6     -0.139064199497E+02    0.35466E-01   -0.75269E-03   272   0.302E-01    0.932E-01
DAV:   7     -0.138817813673E+02    0.24639E-01   -0.21700E-02   244   0.499E-01    0.515E-02
DAV:   8     -0.138817996623E+02   -0.18295E-04   -0.29266E-04   288   0.716E-02    0.140E-02
DAV:   9     -0.138818070305E+02   -0.73682E-05   -0.81812E-06   268   0.104E-02    0.210E-03
DAV:  10     -0.138818069134E+02    0.11714E-06   -0.40008E-07   304   0.227E-03    0.988E-04
DAV:  11     -0.138818061899E+02    0.72350E-06   -0.35932E-08   160   0.756E-04    0.188E-04
DAV:  12     -0.138818060460E+02    0.14385E-06   -0.20784E-09   168   0.206E-04    0.284E-05
DAV:  13     -0.138818060518E+02   -0.58007E-08   -0.18271E-10   164   0.551E-05
   1 F= -.13881806E+02 E0= -.13871819E+02  d E =-.199735E-01
 writing wavefunctions
rusi@abinitio1:~/VASP/Al_110>
```

>>GenHFfile

```
rusi@abinitio1:~/VASP/Al_110>
rusi@abinitio1:~/VASP/Al_110>
rusi@abinitio1:~/VASP/Al_110> GenHFfile
  Program <genHFfile>, ver.4.24
  generates from out_Aa, out_Ab, etc.
  the HFFILE for PHONON.
  In current directory must be DISCAR and HFPOSCAR.
  The output HFFILE contains Hellmann-Feynman forces.
 Press any key to continue
PAUSE prompt>
rusi@abinitio1:~/VASP/Al_110>
```

Step 13.

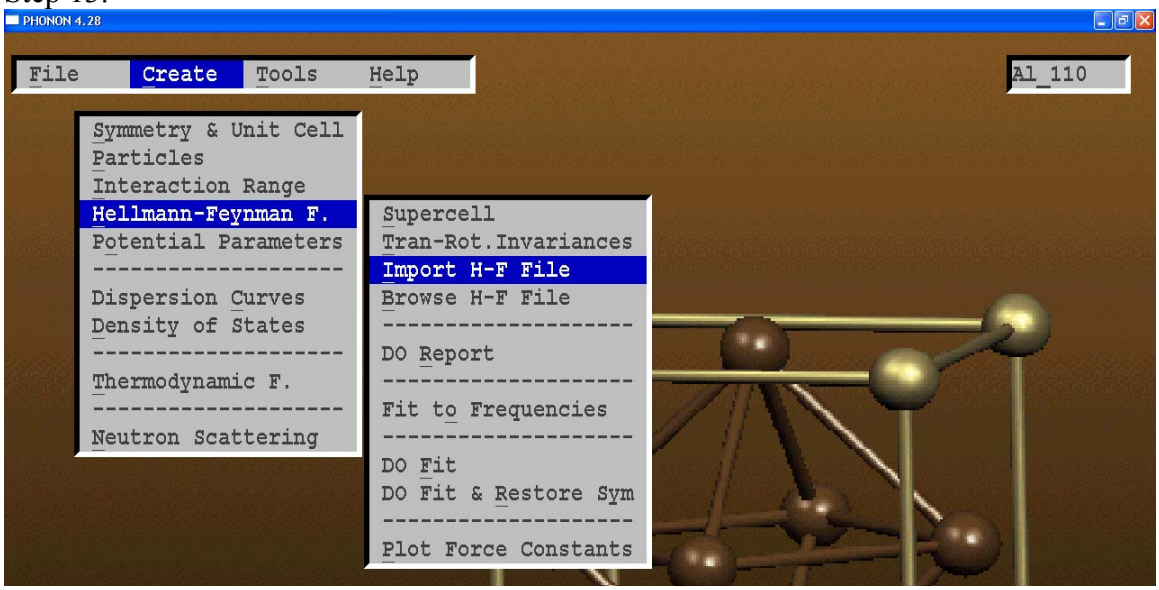
PHONON 4.28
File
Create
Tools
Help
Al_110
Symmetry & Unit Cell
Particles
Interaction Range
Hellmann-Feynman F.
Potential Parameters
Dispersion Curves
Density of States
Thermodynamic F.
Neutron Scattering
Supercell
Tran-Rot.Invariances
Import H-F File
Browse H-F File
DO Report
Fit to Frequencies
DO Fit
DO Fit & Restore Sym
Plot Force Constants

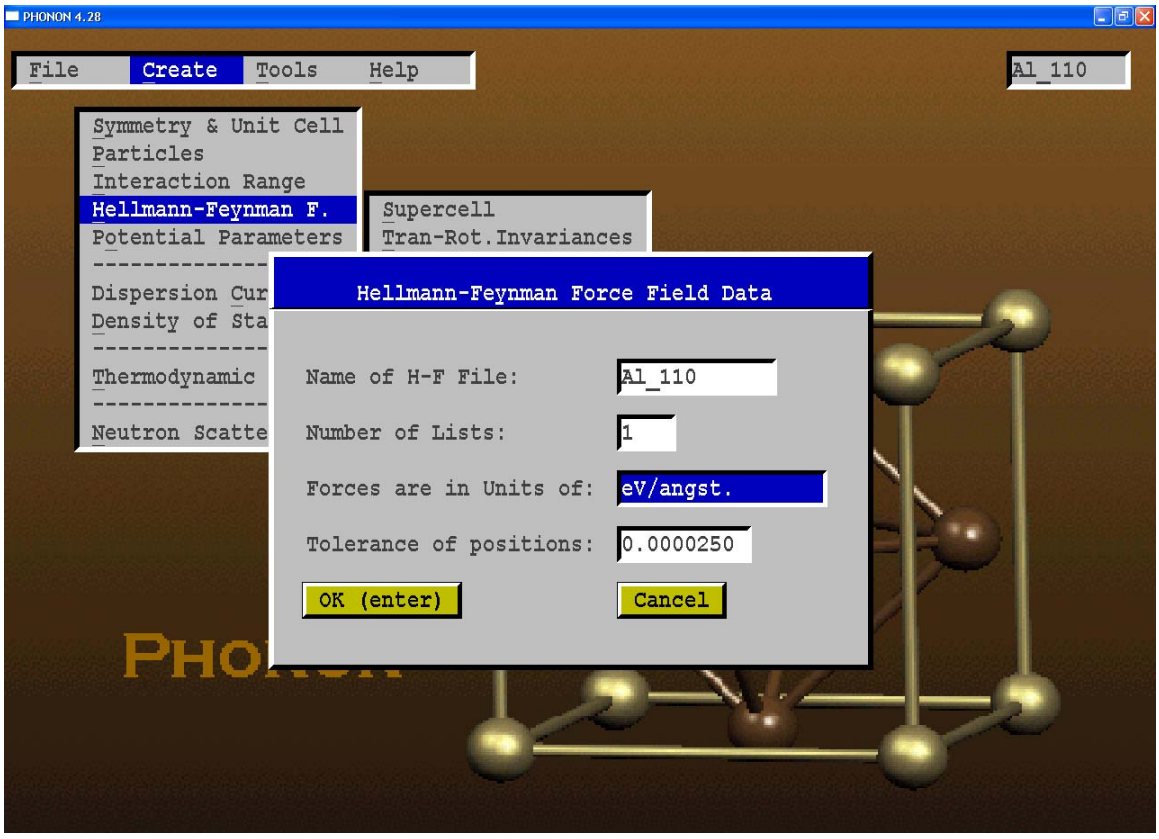
PHONON 4.28
File
Create
Tools
Help
Al_110
Symmetry & Unit Cell
Particles
Interaction Range
Hellmann-Feynman F.
Potential Parameters
Supercell
Tran-Rot.Invariances
Hellmann-Feynman Force Field Data
Name of H-F File:
Al_110
Number of Lists:
1
Forces are in Units of:
eV/angst.
Tolerance of positions:
0.0000250
OK (enter)
Cancel

Step 14.

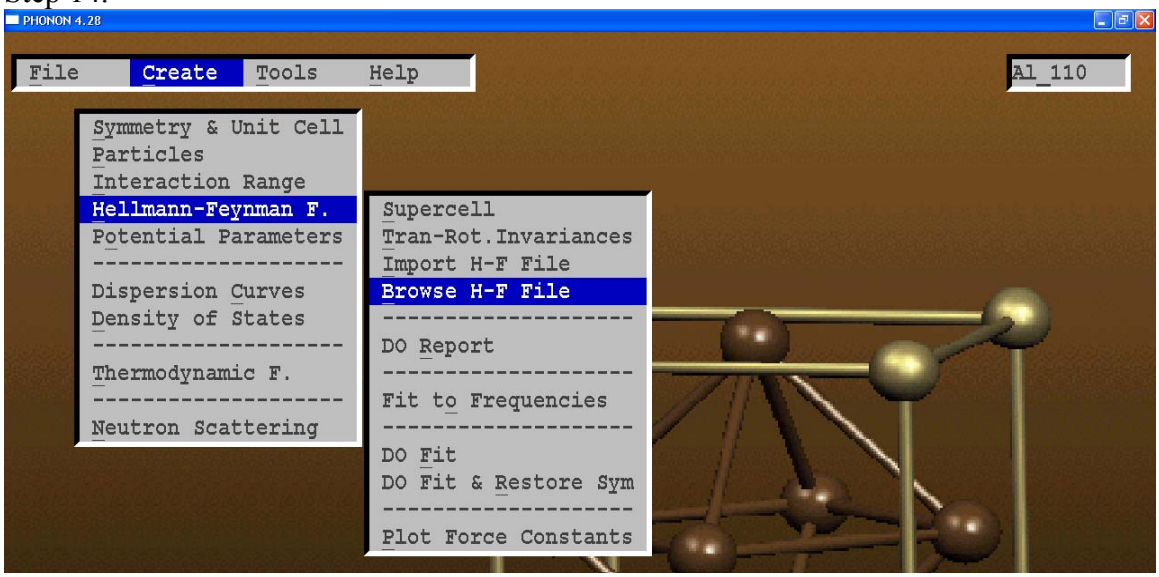
PHONON 4.28
File
Create
Tools
Help
Al_110
Symmetry & Unit Cell
Particles
Interaction Range
Hellmann-Feynman F.
Potential Parameters
Dispersion Curves
Density of States
Thermodynamic F.
Neutron Scattering
Supercell
Tran-Rot.Invariances
Import H-F File
Browse H-F File
DO Report
Fit to Frequencies
DO Fit
DO Fit & Restore Sym
Plot Force Constants

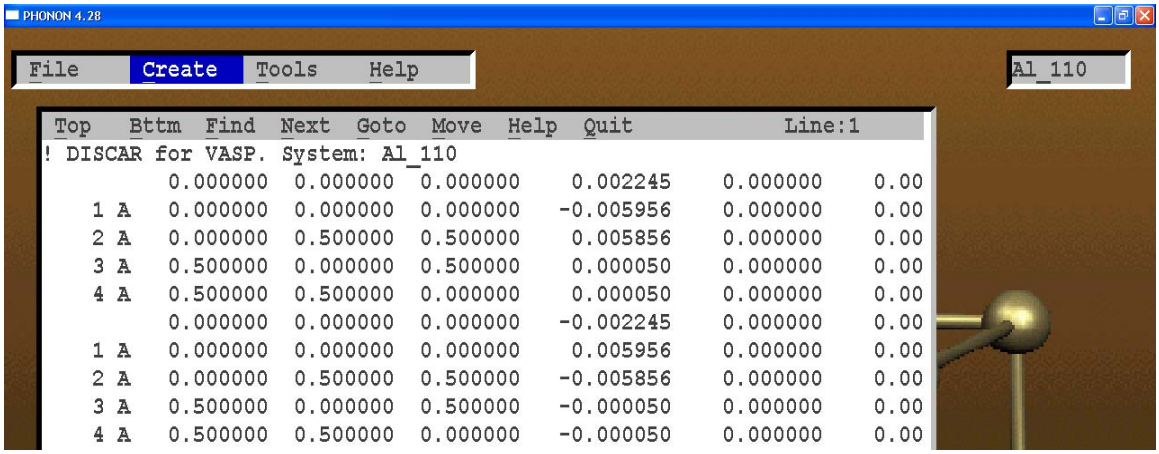
PHONON 4.28
File
Create
Tools
Help
Al_110
Top Bttm Find Next Goto Move Help Quit Line:1
! DISCAR for VASP. System: Al_110
0.000000 0.000000 0.000000 0.002245 0.000000 0.00
1 A 0.000000 0.000000 0.000000 -0.005956 0.000000 0.00
2 A 0.000000 0.500000 0.500000 0.005856 0.000000 0.00
3 A 0.500000 0.000000 0.500000 0.000050 0.000000 0.00
4 A 0.500000 0.500000 0.000000 0.000050 0.000000 0.00
0.000000 0.000000 0.000000 -0.002245 0.000000 0.00
1 A 0.000000 0.000000 0.000000 0.005956 0.000000 0.00
2 A 0.000000 0.500000 0.500000 -0.005856 0.000000 0.00
3 A 0.500000 0.000000 0.500000 -0.000050 0.000000 0.00
4 A 0.500000 0.500000 0.000000 -0.000050 0.000000 0.00

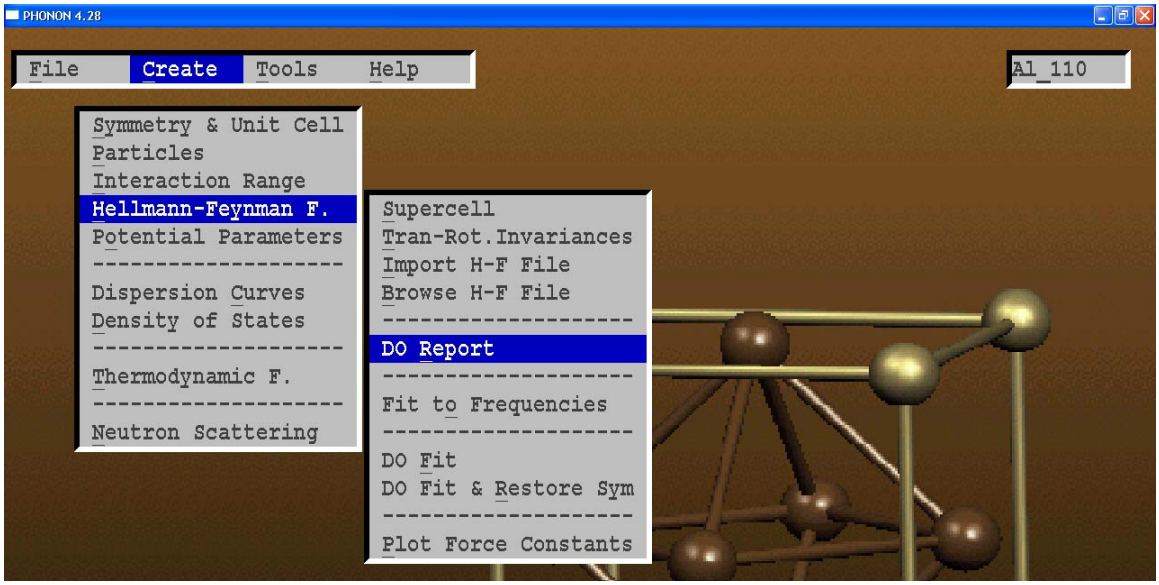
PHONON 4.28
File
Create
Tools
Help
Al_110
Symmetry & Unit Cell
Particles
Interaction Range
Hellmann-Feynman F.
Potential Parameters
Dispersion Curves
Density of States
Thermodynamic F.
Neutron Scattering
Supercell
Tran-Rot.Invariances
Import H-F File
Browse H-F File
DO Report
Fit to Frequencies
DO Fit
DO Fit & Restore Sym
Plot Force Constants

Step 15. Dispersion Curves. SET POINTS.

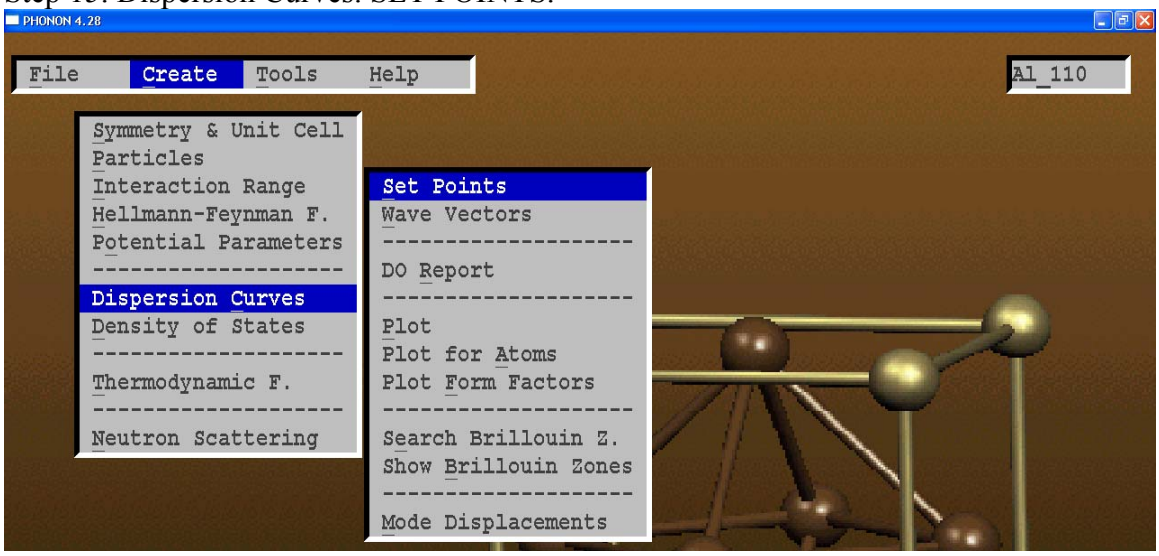

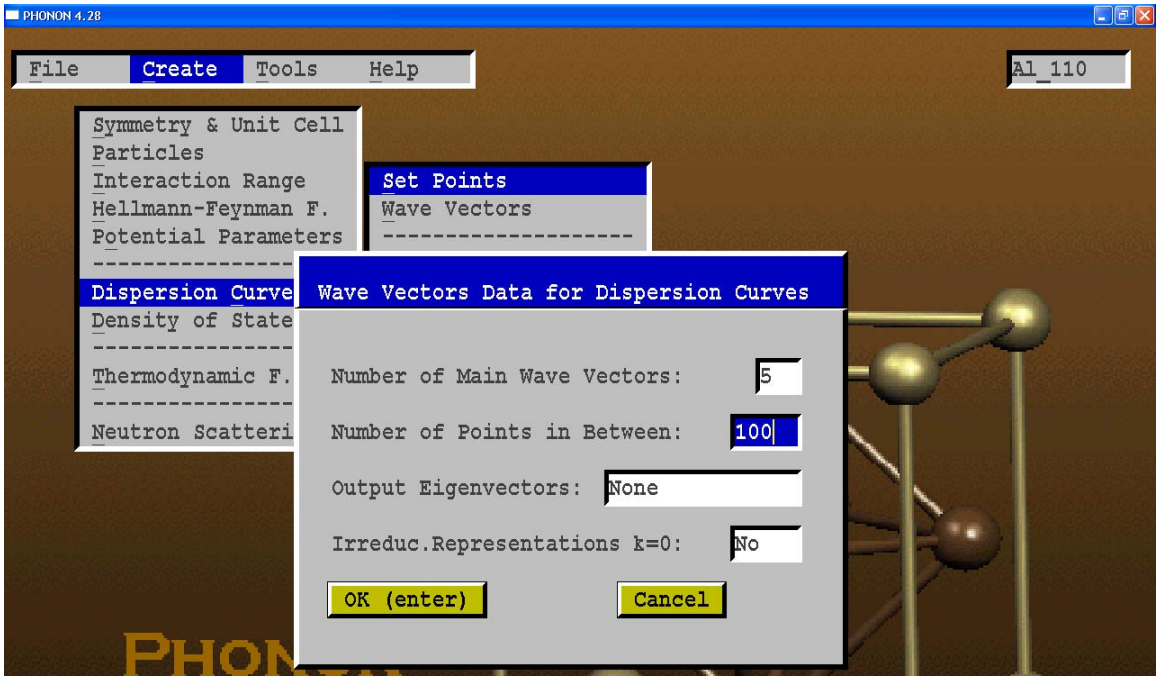

Step 15. Dispersion Curves. WAVE VECTORS.

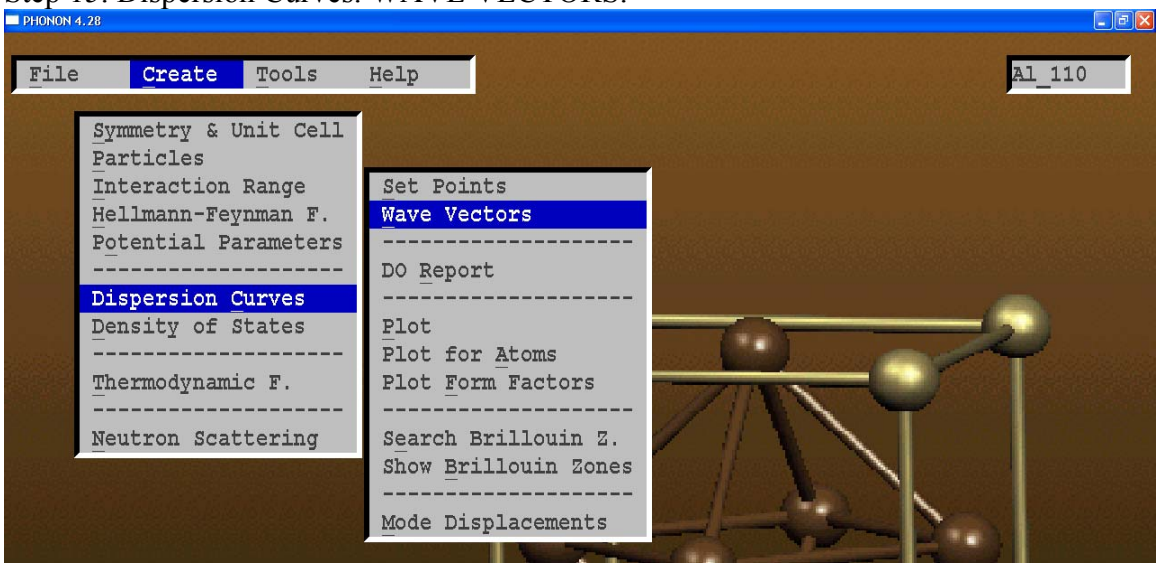

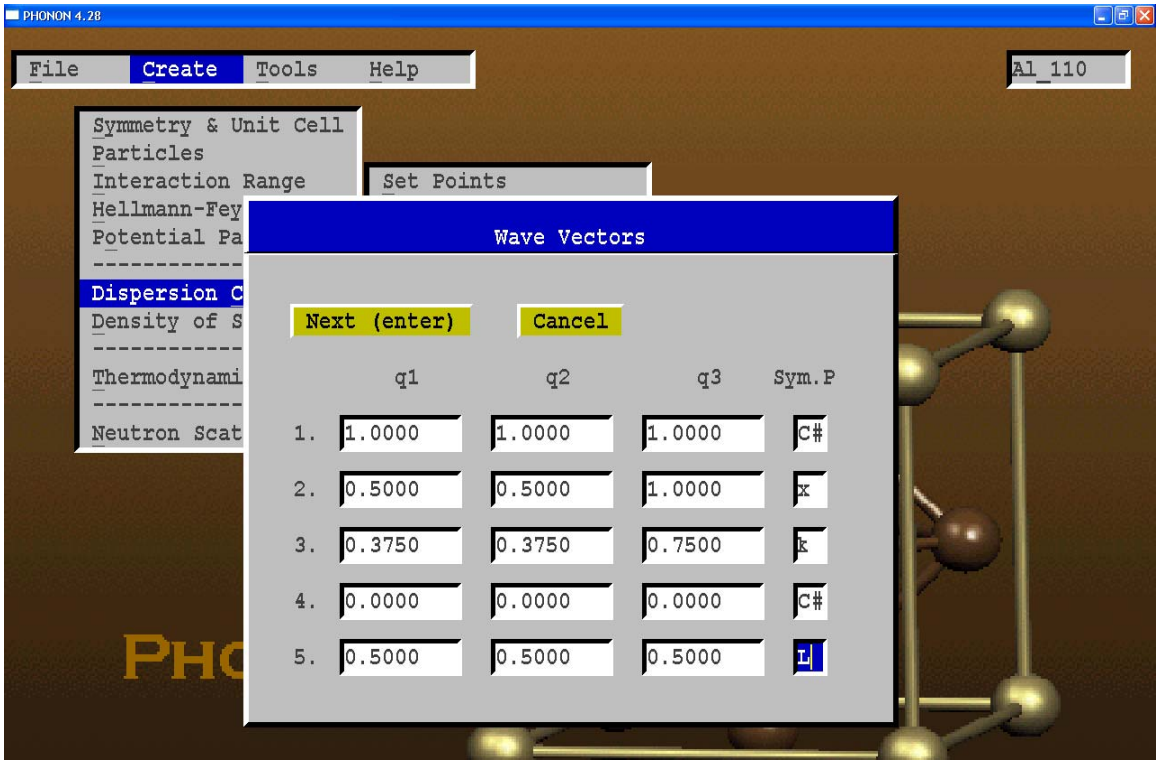

Step 16. Dispersion Curves. DO REPORT and PLOT.

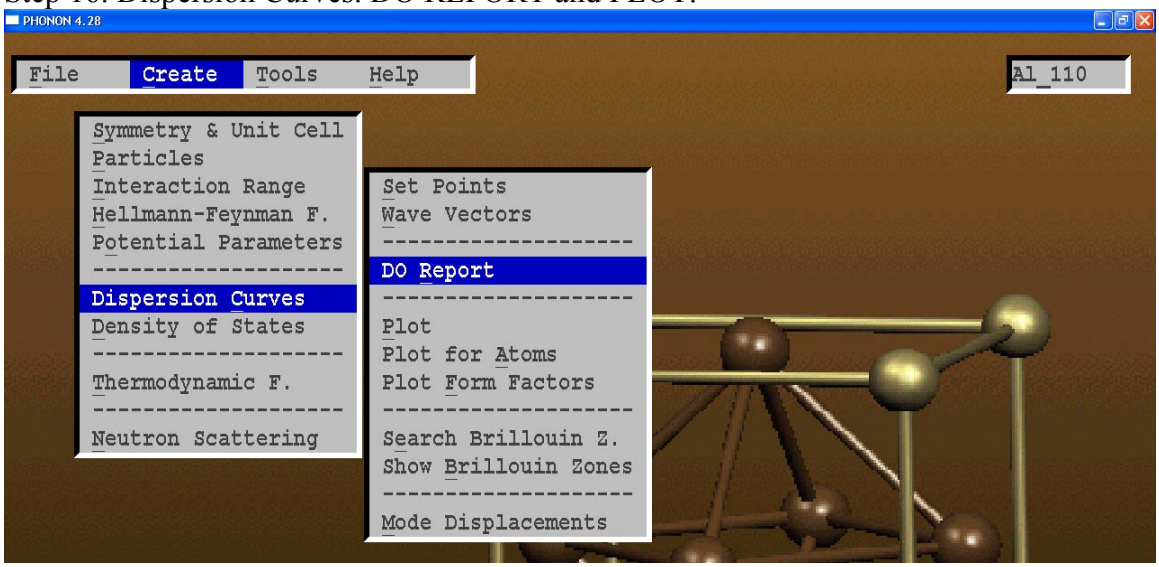

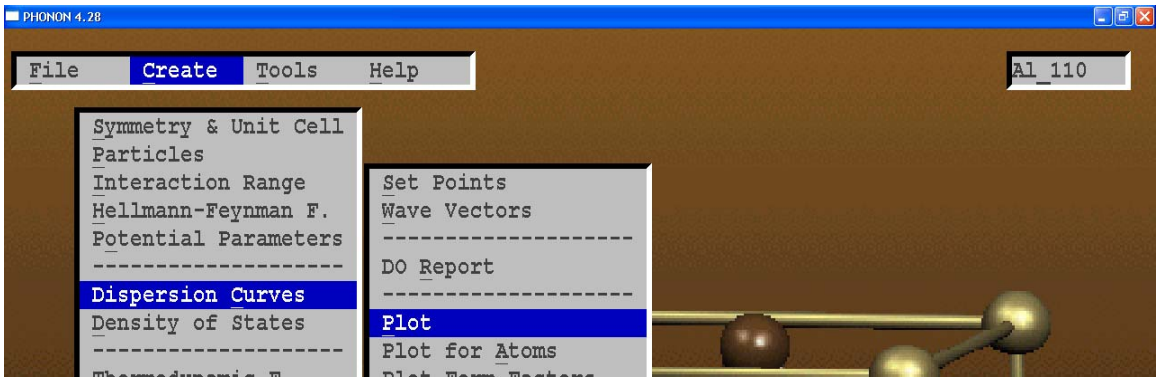

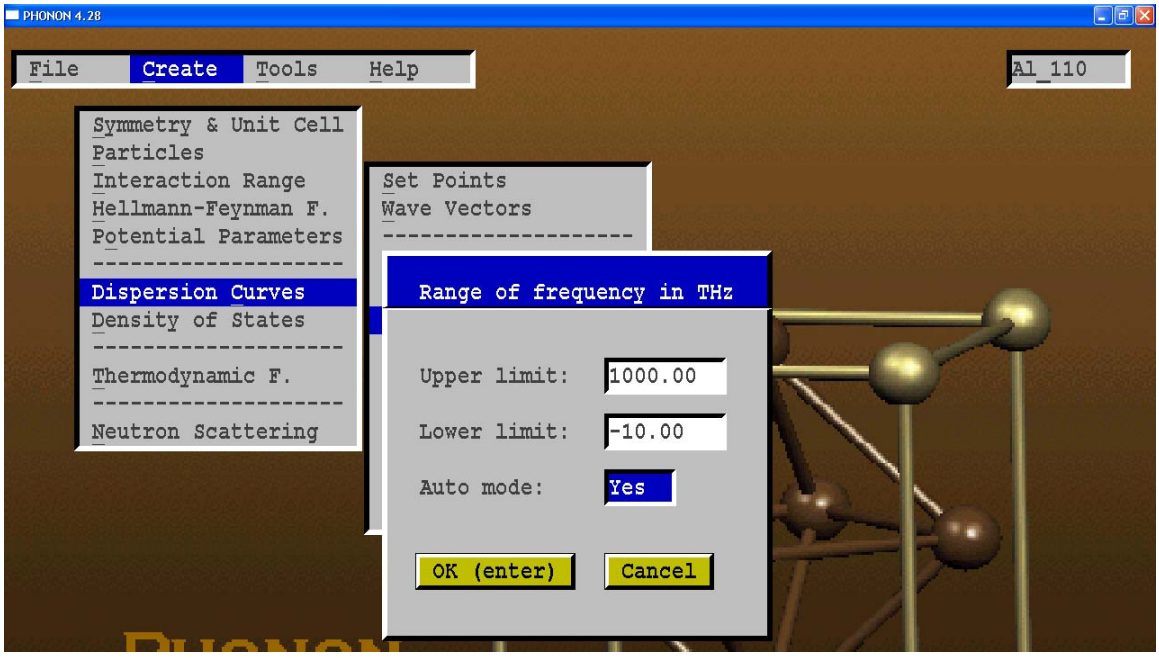

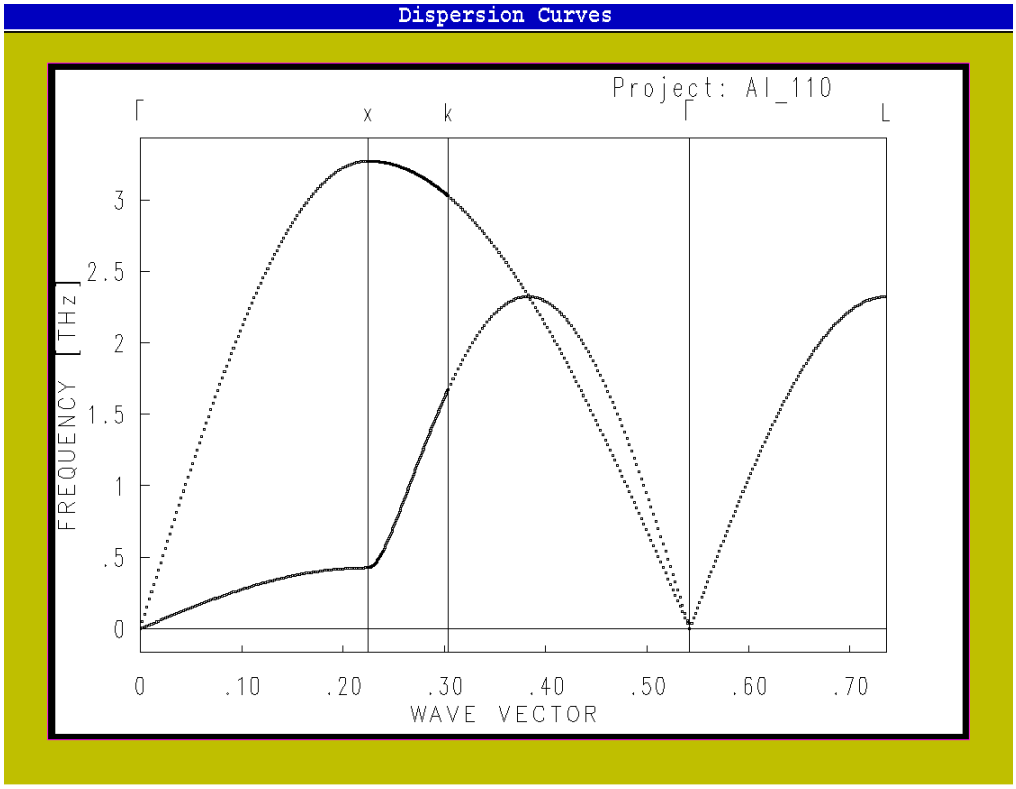
Dispersion Curves
Project: Al_110
Γ
X
k
Γ
L
FREQUENCY [THz]
3
2.5
2
1.5
1
.5
0
0
.10
.20
.30
.40
.50
.60
.70
WAVE VECTOR

Step17. Density of States. SET POINTS and DO REPORT.

(accept the defaults)

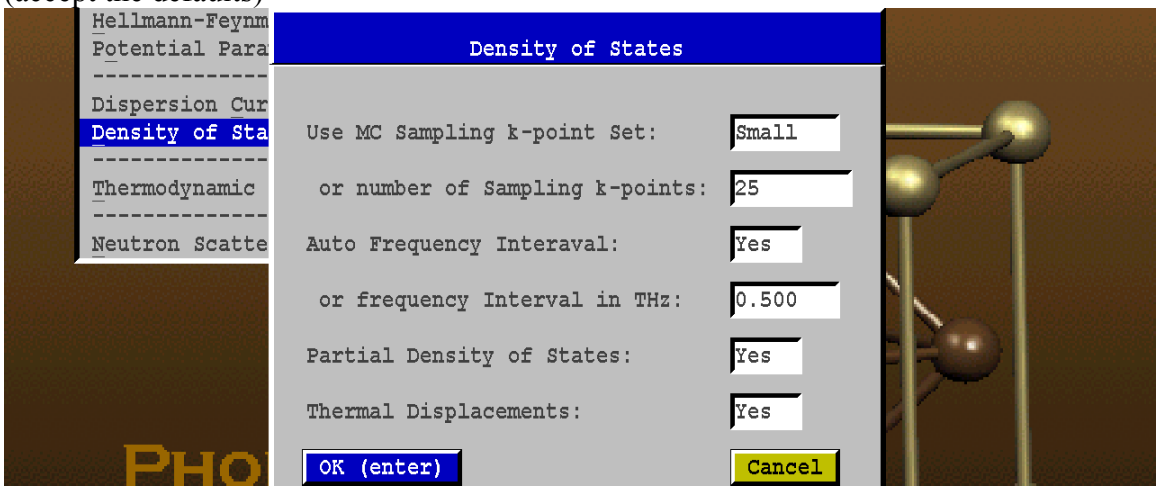

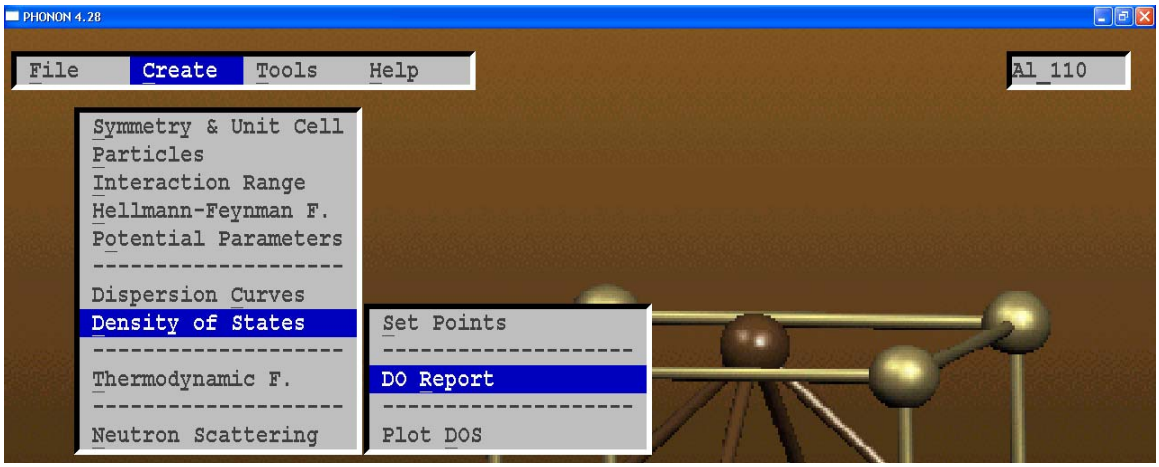

Step17. Density of States. PLOT.

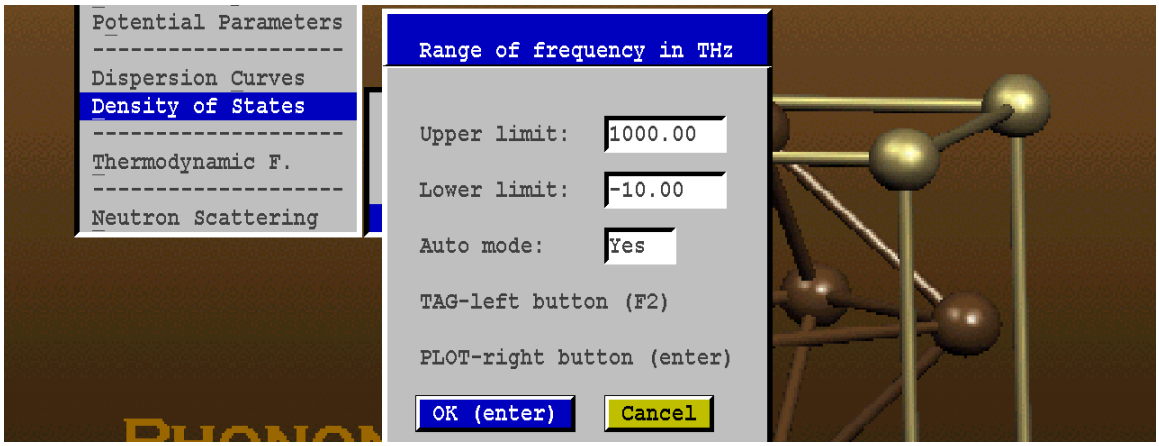

(L-click/ R-click over 'Total')

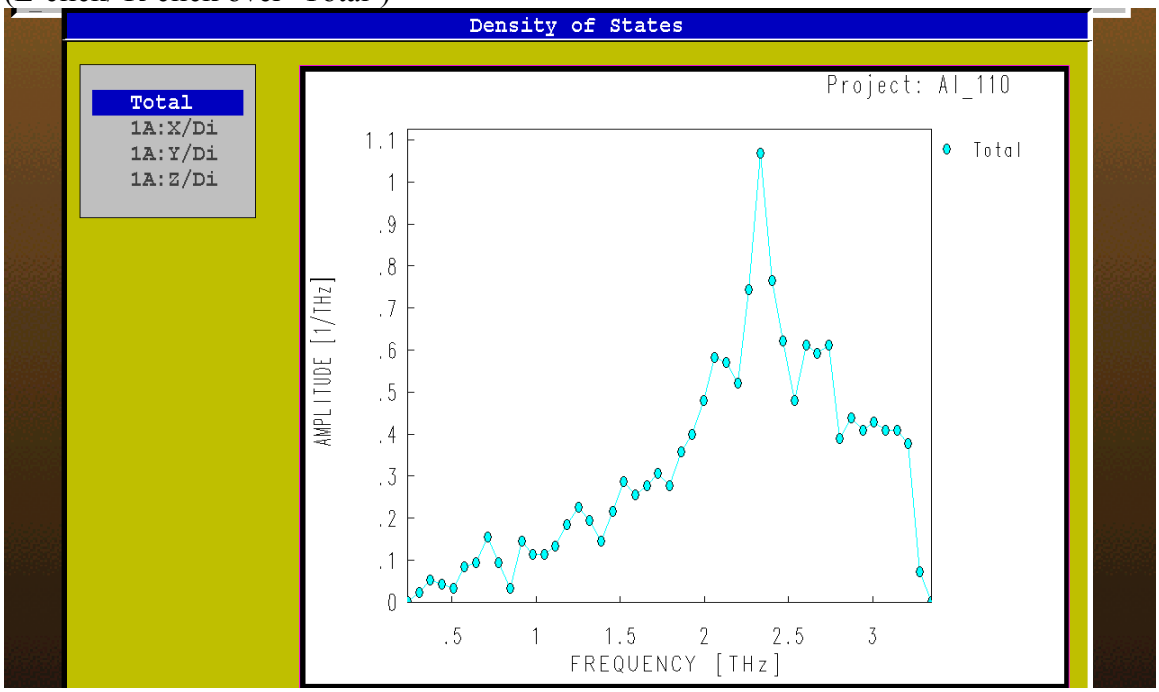

Step18. Internal Energy.

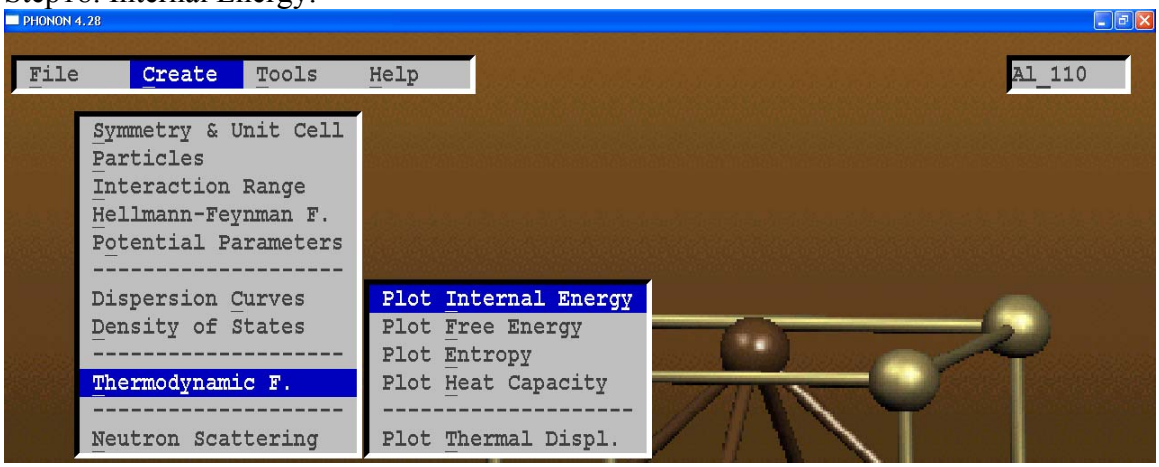

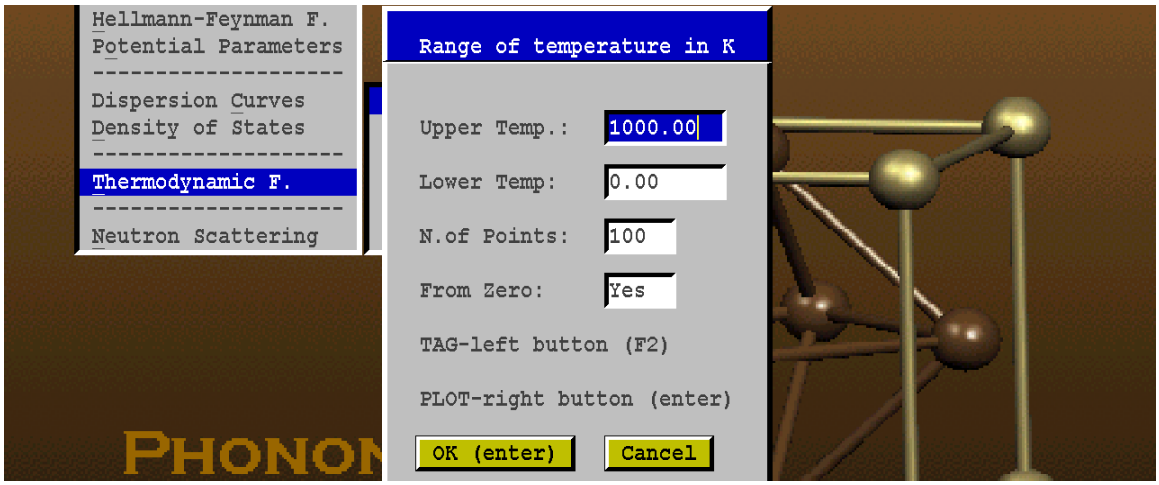

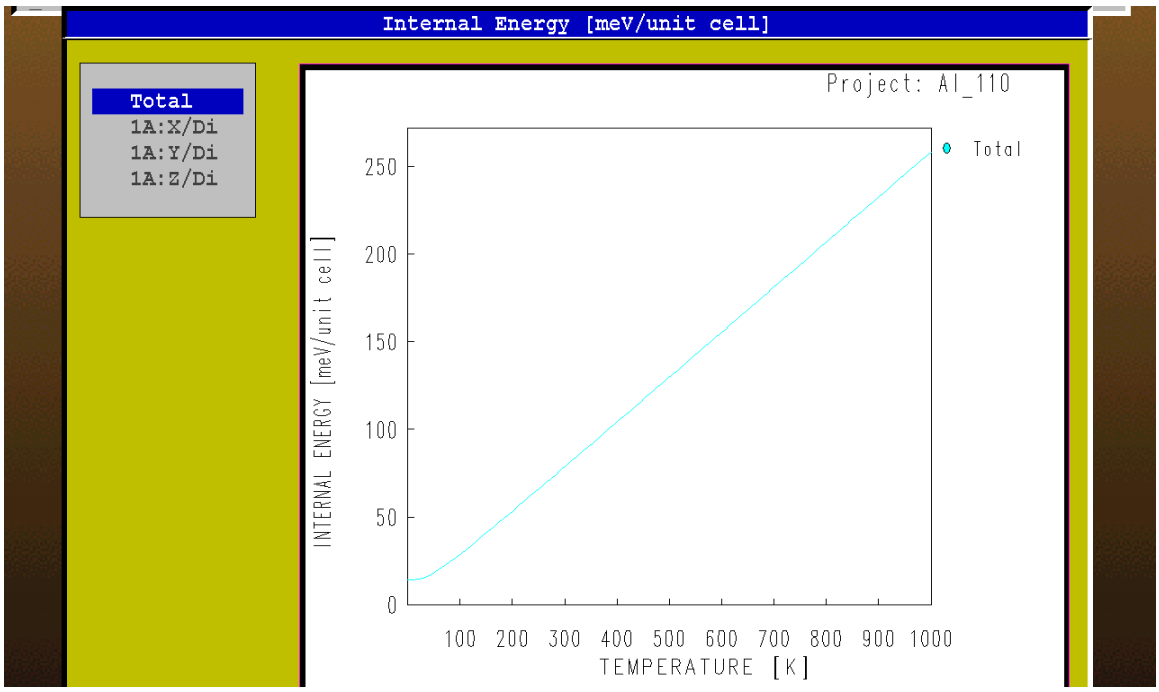

Step18. Free Energy

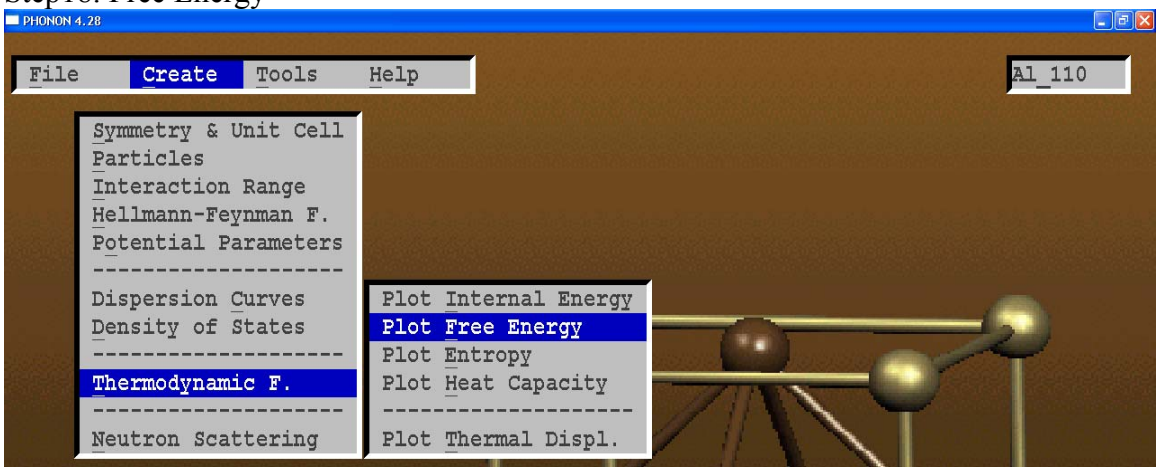

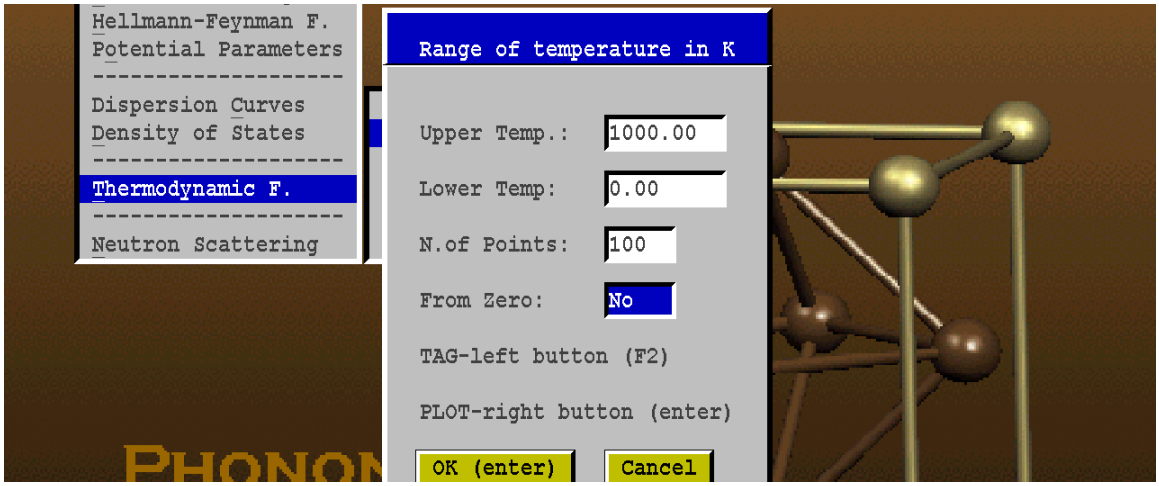

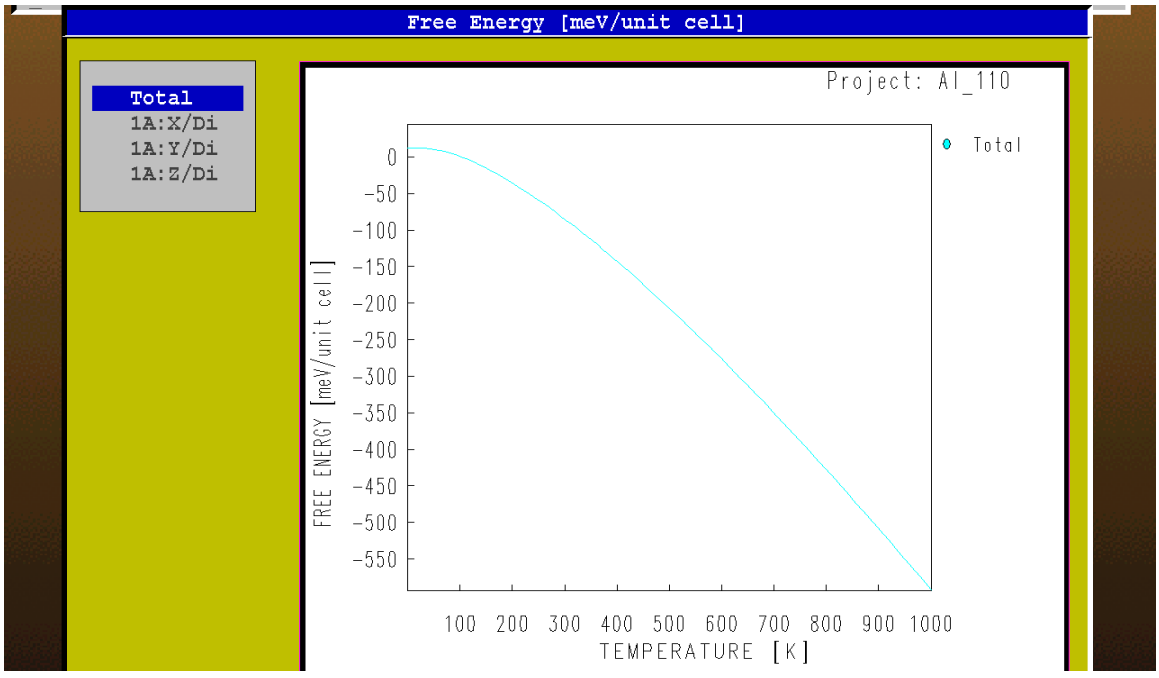

Part IV: Details explained

1. abinitio1.ae.gatech.edu: /home/rusi/VASP/Al_110

Input files:
- INCAR → job details
- KPOINTS → kpoints
- POSCAR → structure
- POTCAR → PP file

INCAR

```
SYSTEM =fcc al
 ISTART = 1;
 ISMEAR = 0; SIGMA = 0.1
 IBRION = 2; ISIF = 3; NSW = 0
 NBANDS = 20
 EDIFF = 1E-07; EDIFFG = 0.1E-05
```

KPOINTS

```
K-Points
 0
Monkhorst Pack
 3 3 3
 0  0  0
```

POSCAR

```
Al:
   4.45427508900000
   1.0000000000000000  0.0000000000000000  0.0000000000000000
   0.0000000000000000  1.0000000000000000  0.0000000000000000
   0.0000000000000000  0.0000000000000000  1.0000000000000000
     4
Direct
   0.0000000000000000  0.0000000000000000  0.0000000000000000
   0.0000000000000000  0.5000000000000000  0.5000000000000000
   0.5000000000000000  0.0000000000000000  0.5000000000000000
   0.5000000000000000  0.5000000000000000  0.0000000000000000
```

POTCAR

```
PAW_GGA Al 05Jan2001
3.00000000000000000
parameters from PSCTR are:
   VRHFIN =Al: s2p1
   LEXCH  = 91
   EATOM  =    53.6910 eV,    3.9462 Ry

   TITEL  = PAW_GGA Al 05Jan2001
   LULTRA =        F    use ultrasoft PP ?
   IUNSCR =        1    unscreen: 0-lin 1-nonlin 2-no
   RPACOR =    1.500    partial core radius
   ...
```

Execute:

```
>> vasp-par
```

Output files:

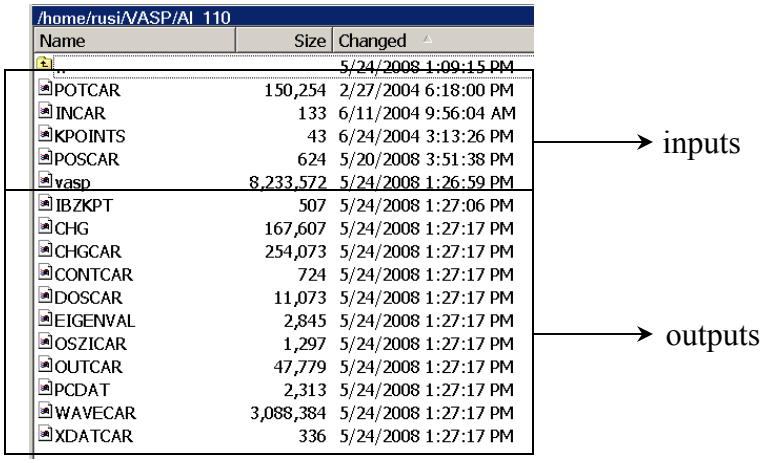

CONTCAR

```
Al:
   4.45427508900000
     1.0000000000000000    0.0000000000000000    0.0000000000000000
     0.0000000000000000    1.0000000000000000    0.0000000000000000
     0.0000000000000000    0.0000000000000000    1.0000000000000000
   4
Direct
  0.9977549999999979  0.0000000000000000  0.0000000000000000
  0.0000000000000000  0.5000000000000000  0.5000000000000000
  0.5000000000000000  0.0000000000000000  0.5000000000000000
  0.5000000000000000  0.5000000000000000  0.0000000000000000

  0.00000000E+00  0.00000000E+00  0.00000000E+00
  0.00000000E+00  0.00000000E+00  0.00000000E+00
  0.00000000E+00  0.00000000E+00  0.00000000E+00
  0.00000000E+00  0.00000000E+00  0.00000000E+00
```

COMPARE
```
4.45427508900000 (from POSCAR)
4.45427508900000 (from CONTCAR)
```

2. PHONON – execute steps 2 to 6
3. VASP

Copy CONTCAR *.d44→DISCAR

DISCAR

```
DISCAR for VASP. System: Al_110
     1  Number of displacements
A    1     0.002245   0.000000   0.000000
     4     1  Number of atoms in SC
A    1
```

```
[root@f15lab1 Al_110]# ls
CONTCAR  DISCAR  GenHFfile  GenPos
```

```
[root@f15lab1 Al_110]# ./GenPos
Incorrectly built binary which accesses errno, h_errno or _res directly. Needs t
o be fixed.
  Program <genpos>, ver.4.22
  generates all POSCARs of VASP
  needed to find Hellmann-Feynman forces.
  Necessery displacements must be given in DISCAR
  which is <project>.d44 of Phonon
  Names of new POSCAR files with atoms displaced
  are generated automatically.
  This program reads CONTCAR (not POSCAR).
  You need CONTCAR and DISCAR in current directory.
  Program <genpos> copies CONTCAR to HFPOSCAR.
  It also generates <run> script.
  Use: <chmod a+x run> before running this script.
FORTRAN PAUSE  Press any key to continue
Type GO to resume execution, any other input will terminate the job
go
Execution resumes after PAUSE
[root@f15lab1 Al_110]# cd ..
```

Outputs:

HFPOSCAR (copied CONTCAR)

```
Al:
   4.45427508900000
   1.0000000000000000  0.0000000000000000  0.0000000000000000
   0.0000000000000000  1.0000000000000000  0.0000000000000000
   0.0000000000000000  0.0000000000000000  1.0000000000000000
     4
Direct
   0.9977549999999979  0.0000000000000000  0.0000000000000000
   0.0000000000000000  0.5000000000000000  0.5000000000000000
   0.5000000000000000  0.0000000000000000  0.5000000000000000
   0.5000000000000000  0.5000000000000000  0.0000000000000000
```

Pos_Aa (generated position file with disturbed positions)

```
Al:
   4.45427508900000
   1.0000000000000000  0.0000000000000000  0.0000000000000000
   0.0000000000000000  1.0000000000000000  0.0000000000000000
   0.0000000000000000  0.0000000000000000  1.0000000000000000
     4
Direct
   0.9999999999999980  0.0000000000000000  0.0000000000000000
   0.0000000000000000  0.5000000000000000  0.5000000000000000
   0.5000000000000000  0.0000000000000000  0.5000000000000000
   0.5000000000000000  0.5000000000000000  0.0000000000000000
```

run

```
#!/bin/bash

  VASP=vasp

  rm WAVECAR
  rm CHGCAR
  rm CHG
  cp pos_Aa POSCAR
  $VASP >>out.vasp 2>>err.vasp &
  wait
  cp OUTCAR out_Aa
```

after ./GenPos

/home/rusi/VASP/Al_110

Name	Size	Changed
..		5/25/2008 12:32:11 PM
vasp	8,233,572	6/10/2004 2:14:36 PM
GenHFfile	381,043	6/24/2004 2:21:46 PM
GenPos	381,780	6/24/2004 2:21:46 PM
CONTCAR	724	5/24/2008 1:27:18 PM
DISCAR	160	5/25/2008 11:57:36 AM
run	153	5/25/2008 12:29:21 PM
HFPOSCAR	624	5/25/2008 12:29:21 PM
pos_Aa	624	5/25/2008 12:29:21 PM

edit “run” file (in pico or vi) and then change to executable (type chmod a+x run):

```
#!/bin/bash

  VASP= ./vasp

  rm WAVECAR
  rm CHGCAR
  rm CHG
  cp pos_Aa POSCAR
  $VASP >>out.vasp 2>>err.vasp &
  wait
  cp OUTCAR out_Aa
```

/home/rusi/VASP/Al_110

Name	Size	Changed	Rights
..		5/25/2008 1:43:57 PM	rwxr-xr-x
POTCAR	150,254	2/27/2004 6:18:00 PM	rw-r--r--
INCAR	133	6/11/2004 9:56:04 AM	rw-r--r--
KPOINTS	43	6/24/2004 3:13:26 PM	rw-r--r--
POSCAR	624	5/20/2008 3:51:38 PM	rw-r--r--
IBZKPT	507	5/24/2008 1:27:06 PM	rw-r--r--
CHGCAR	254,073	5/24/2008 1:27:18 PM	rw-r--r--
CHG	167,607	5/24/2008 1:27:18 PM	rw-r--r--
CONTCAR	724	5/24/2008 1:27:18 PM	rw-r--r--
DOSCAR	11,073	5/24/2008 1:27:18 PM	rw-r--r--
EIGENVAL	2,845	5/24/2008 1:27:18 PM	rw-r--r--
OSZICAR	1,297	5/24/2008 1:27:18 PM	rw-r--r--
OUTCAR	47,779	5/24/2008 1:27:18 PM	rw-r--r--
PCDAT	2,313	5/24/2008 1:27:18 PM	rw-r--r--
XDATCAR	336	5/24/2008 1:27:18 PM	rw-r--r--
WAVECAR	3,088,384	5/24/2008 1:27:18 PM	rw-r--r--

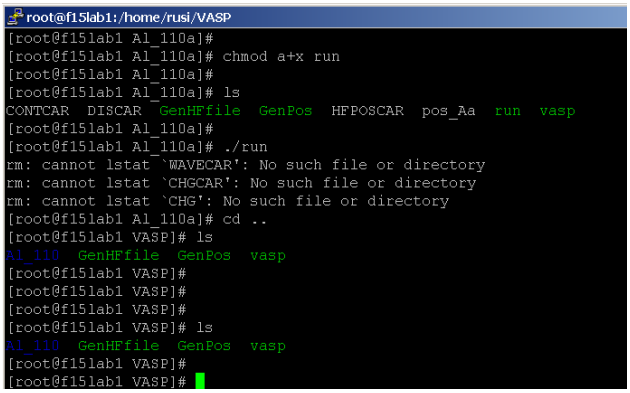

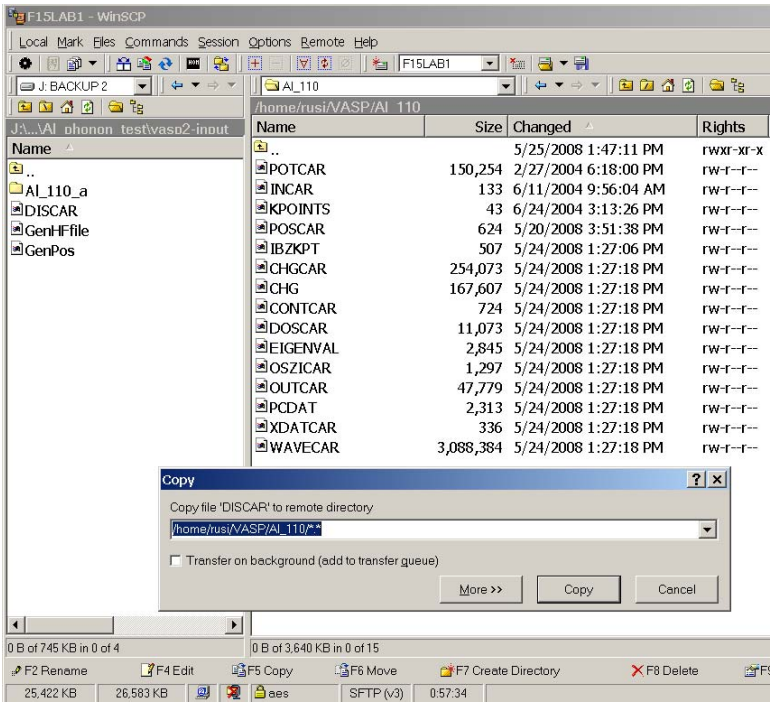
F15LAB1 - WinSCP
Local Mark Files Commands Session Options Remote Help
F15LAB1
J: BACKUP 2
Al_110
/home/rusi/VASP/Al_110
J:\...\Al_phonon_test\vasp2-input
Name
Size
Changed
Rights
..
Al_110_a
DISCAR
GenHFfile
GenPos
5/25/2008 1:47:11 PM rwxr-xr-x
POTCAR 150,254 2/27/2004 6:18:00 PM rw-r--r--
INCAR 133 6/11/2004 9:56:04 AM rw-r--r--
KPOINTS 43 6/24/2004 3:13:26 PM rw-r--r--
POSCAR 624 5/20/2008 3:51:38 PM rw-r--r--
IBZKPT 507 5/24/2008 1:27:06 PM rw-r--r--
CHGCAR 254,073 5/24/2008 1:27:18 PM rw-r--r--
CHG 167,607 5/24/2008 1:27:18 PM rw-r--r--
CONTCAR 724 5/24/2008 1:27:18 PM rw-r--r--
DOSCAR 11,073 5/24/2008 1:27:18 PM rw-r--r--
EIGENVAL 2,845 5/24/2008 1:27:18 PM rw-r--r--
OSZICAR 1,297 5/24/2008 1:27:18 PM rw-r--r--
OUTCAR 47,779 5/24/2008 1:27:18 PM rw-r--r--
PCDAT 2,313 5/24/2008 1:27:18 PM rw-r--r--
XDATCAR 336 5/24/2008 1:27:18 PM rw-r--r--
WAVECAR 3,088,384 5/24/2008 1:27:18 PM rw-r--r--
Copy
Copy file 'DISCAR' to remote directory
/home/rusi/VASP/Al_110/*.*
Transfer on background (add to transfer queue)
More >>
Copy
Cancel
0 B of 745 KB in 0 of 4
0 B of 3,640 KB in 0 of 15
F2 Rename
F4 Edit
F5 Copy
F6 Move
F7 Create Directory
F8 Delete
25,422 KB
26,583 KB
aes
SFTP (v3)
0:57:34

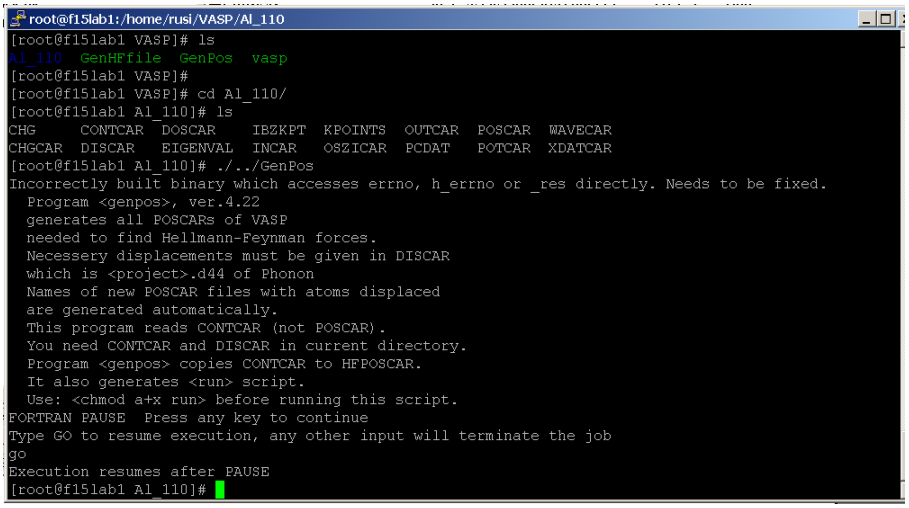
root@f15lab1:/home/rusi/VASP/Al_110
[root@f15lab1 VASP]# ls
Al_110 GenHFfile GenPos vasp
[root@f15lab1 VASP]#
[root@f15lab1 VASP]# cd Al_110/
[root@f15lab1 Al_110]# ls
CHG CONTCAR DOSCAR IBZKPT KPOINTS OUTCAR POSCAR WAVECAR
CHGCAR DISCAR EIGENVAL INCAR OSZICAR PCDAT POTCAR XDATCAR
[root@f15lab1 Al_110]# ./../GenPos
Incorrectly built binary which accesses errno, h_errno or _res directly. Needs to be fixed.
Program <genpos>, ver.4.22
generates all POSCARs of VASP
needed to find Hellmann-Feynman forces.
Necessery displacements must be given in DISCAR
which is <project>.d44 of Phonon
Names of new POSCAR files with atoms displaced
are generated automatically.
This program reads CONTCAR (not POSCAR).
You need CONTCAR and DISCAR in current directory.
Program <genpos> copies CONTCAR to HFPOSCAR.
It also generates <run> script.
Use: <chmod a+x run> before running this script.
FORTRAN PAUSE Press any key to continue
Type GO to resume execution, any other input will terminate the job
go
Execution resumes after PAUSE
[root@f15lab1 Al_110]#

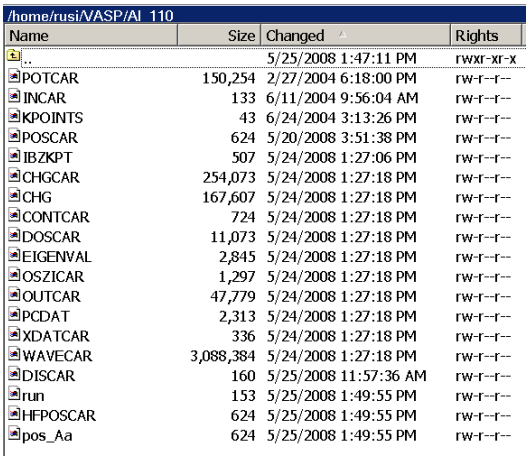
/home/rusi/VASP/Al_110
Name
Size
Changed
Rights
..
5/25/2008 1:47:11 PM rwxr-xr-x
POTCAR 150,254 2/27/2004 6:18:00 PM rw-r--r--
INCAR 133 6/11/2004 9:56:04 AM rw-r--r--
KPOINTS 43 6/24/2004 3:13:26 PM rw-r--r--
POSCAR 624 5/20/2008 3:51:38 PM rw-r--r--
IBZKPT 507 5/24/2008 1:27:06 PM rw-r--r--
CHGCAR 254,073 5/24/2008 1:27:18 PM rw-r--r--
CHG 167,607 5/24/2008 1:27:18 PM rw-r--r--
CONTCAR 724 5/24/2008 1:27:18 PM rw-r--r--
DOSCAR 11,073 5/24/2008 1:27:18 PM rw-r--r--
EIGENVAL 2,845 5/24/2008 1:27:18 PM rw-r--r--
OSZICAR 1,297 5/24/2008 1:27:18 PM rw-r--r--
OUTCAR 47,779 5/24/2008 1:27:18 PM rw-r--r--
PCDAT 2,313 5/24/2008 1:27:18 PM rw-r--r--
XDATCAR 336 5/24/2008 1:27:18 PM rw-r--r--
WAVECAR 3,088,384 5/24/2008 1:27:18 PM rw-r--r--
DISCAR 160 5/25/2008 11:57:36 AM rw-r--r--
run 153 5/25/2008 1:49:55 PM rw-r--r--
HFPOSCAR 624 5/25/2008 1:49:55 PM rw-r--r--
pos_Aa 624 5/25/2008 1:49:55 PM rw-r--r--

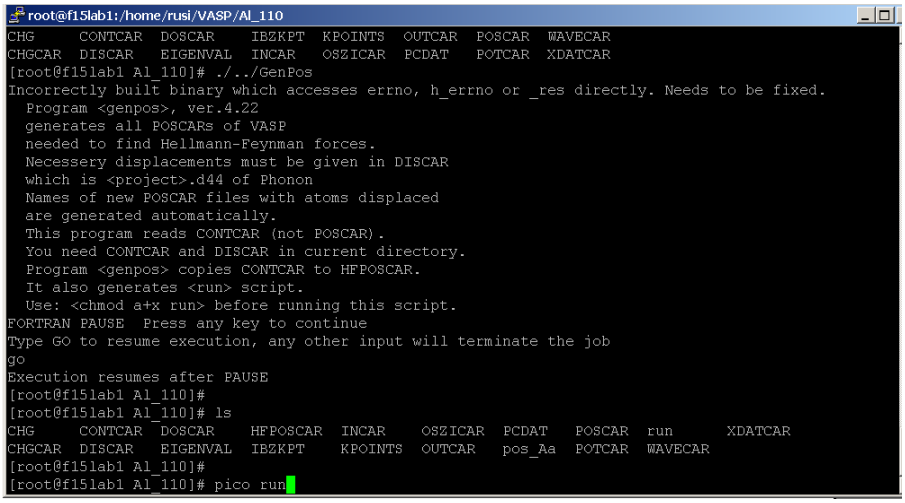
root@f15lab1:/home/rusi/VASP/Al_110
CHG CONTCAR DOSCAR IBZKPT KPOINTS OUTCAR POSCAR WAVECAR
CHGCAR DISCAR EIGENVAL INCAR OSZICAR PCDAT POTCAR XDATCAR
[root@f15lab1 Al_110]# ./../GenPos
Incorrectly built binary which accesses errno, h_errno or _res directly. Needs to be fixed.
Program <genpos>, ver.4.22
generates all POSCARs of VASP
needed to find Hellmann-Feynman forces.
Necessery displacements must be given in DISCAR
which is <project>.d44 of Phonon
Names of new POSCAR files with atoms displaced
are generated automatically.
This program reads CONTCAR (not POSCAR).
You need CONTCAR and DISCAR in current directory.
Program <genpos> copies CONTCAR to HFPOSCAR.
It also generates <run> script.
Use: <chmod a+x run> before running this script.
FORTRAN PAUSE Press any key to continue
Type GO to resume execution, any other input will terminate the job
go
Execution resumes after PAUSE
[root@f15lab1 Al_110]#
[root@f15lab1 Al_110]# ls
CHG CONTCAR DOSCAR HFPOSCAR INCAR OSZICAR PCDAT POSCAR run XDATCAR
CHGCAR DISCAR EIGENVAL IBZKPT KPOINTS OUTCAR pos_Aa POTCAR WAVECAR
[root@f15lab1 Al_110]#
[root@f15lab1 Al_110]# pico run

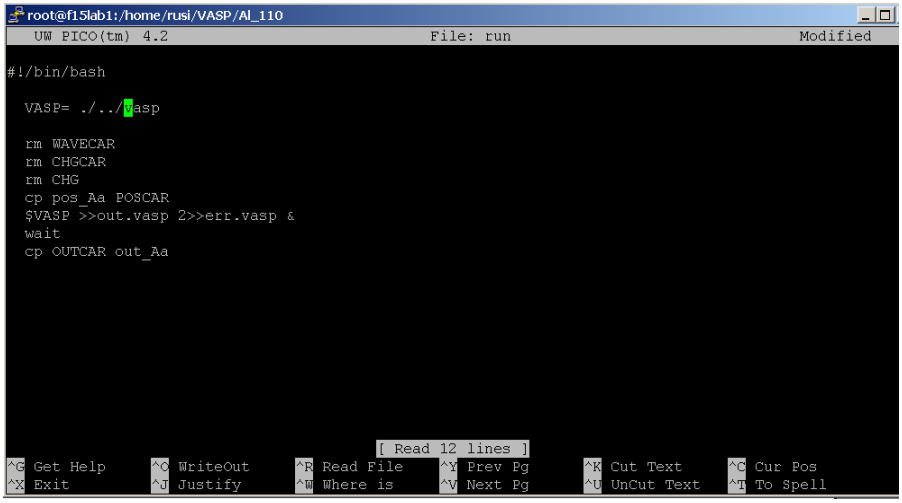
root@f15lab1:/home/rusi/VASP/Al_110
UW PICO(tm) 4.2 File: run Modified
#!/bin/bash
VASP= ./../vasp
rm WAVECAR
rm CHGCAR
rm CHG
cp pos_Aa POSCAR
$VASP >>out.vasp 2>>err.vasp &
wait
cp OUTCAR out_Aa
[Read 12 lines]
^G Get Help ^O WriteOut ^R Read File ^Y Prev Pg ^K Cut Text ^C Cur Pos
^X Exit ^J Justify ^W Where is ^V Next Pg ^U UnCut Text ^T To Spell

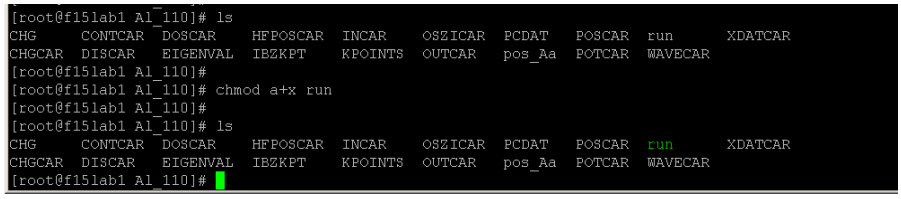
[root@f15lab1 Al_110]# ls
CHG CONTCAR DOSCAR HFPOSCAR INCAR OSZICAR PCDAT POSCAR run XDATCAR
CHGCAR DISCAR EIGENVAL IBZKPT KPOINTS OUTCAR pos_Aa POTCAR WAVECAR
[root@f15lab1 Al_110]#
[root@f15lab1 Al_110]# chmod a+x run
[root@f15lab1 Al_110]#
[root@f15lab1 Al_110]# ls
CHG CONTCAR DOSCAR HFPOSCAR INCAR OSZICAR PCDAT POSCAR run XDATCAR
CHGCAR DISCAR EIGENVAL IBZKPT KPOINTS OUTCAR pos_Aa POTCAR WAVECAR
[root@f15lab1 Al_110]#

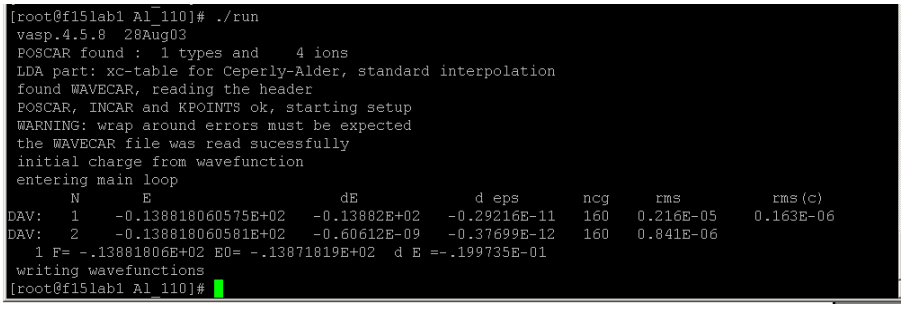
[root@f15lab1 Al_110]# ./run
vasp.4.5.8 28Aug03
POSCAR found : 1 types and 4 ions
LDA part: xc-table for Ceperly-Alder, standard interpolation
found WAVECAR, reading the header
POSCAR, INCAR and KPOINTS ok, starting setup
WARNING: wrap around errors must be expected
the WAVECAR file was read sucessfully
initial charge from wavefunction
entering main loop
N E dE d eps ncg rms rms(c)
DAV: 1 -0.138818060575E+02 -0.13882E+02 -0.29216E-11 160 0.216E-05 0.163E-06
DAV: 2 -0.138818060581E+02 -0.60612E-09 -0.37699E-12 160 0.841E-06
1 F= -.13881806E+02 E0= -.13871819E+02 d E =-.199735E-01
writing wavefunctions
[root@f15lab1 Al_110]#

Before ./run

/home/rusi/VASP/Al_110

Name	Size	Changed
..		5/25/2008 1:47:11 PM
POTCAR	150,254	2/27/2004 6:18:00 PM
INCAR	133	6/11/2004 9:56:04 AM
KPOINTS	43	6/24/2004 3:13:26 PM
POSCAR	624	5/20/2008 3:51:38 PM
IBZKPT	507	5/24/2008 1:27:06 PM
CHGCAR	254,073	5/24/2008 1:27:18 PM
CHG	167,607	5/24/2008 1:27:18 PM
CONTCAR	724	5/24/2008 1:27:18 PM
DOSCAR	11,073	5/24/2008 1:27:18 PM
EIGENVAL	2,845	5/24/2008 1:27:18 PM
OSZICAR	1,297	5/24/2008 1:27:18 PM
OUTCAR	47,779	5/24/2008 1:27:18 PM
PCDAT	2,313	5/24/2008 1:27:18 PM
XDATCAR	336	5/24/2008 1:27:18 PM
WAVECAR	3,088,384	5/24/2008 1:27:18 PM
DISCAR	160	5/25/2008 11:57:36 AM
run	153	5/25/2008 1:49:55 PM
HFPOSCAR	624	5/25/2008 1:49:55 PM
pos_Aa	624	5/25/2008 1:49:55 PM

After ./run

/home/rusi/VASP/Al_110

Name	Size	Changed
..		5/26/2008 3:09:19 AM
POTCAR	150,254	2/27/2004 6:18:00 PM
INCAR	133	6/11/2004 9:56:04 AM
KPOINTS	43	6/24/2004 3:13:26 PM
DISCAR	160	5/25/2008 11:57:36 AM
HFPOSCAR	624	5/25/2008 1:49:55 PM
pos_Aa	624	5/25/2008 1:49:55 PM
run	159	5/25/2008 1:51:22 PM
IBZKPT	507	5/25/2008 1:51:55 PM
out.vasp	0	5/25/2008 1:51:57 PM
err.vasp	0	5/25/2008 1:51:57 PM
CONTCAR	724	5/25/2008 1:51:57 PM
DOSCAR	11,073	5/25/2008 1:51:57 PM
EIGENVAL	2,845	5/25/2008 1:51:57 PM
OSZICAR	326	5/25/2008 1:51:57 PM
OUTCAR	31,002	5/25/2008 1:51:57 PM
PCDAT	2,313	5/25/2008 1:51:57 PM
POSCAR	624	5/25/2008 1:51:57 PM
XDATCAR	336	5/25/2008 1:51:57 PM
out_Aa	31,002	5/25/2008 1:51:57 PM

out_Aa

```
vasp.4.5.8  28Aug03
 executed on             LinuxIFC date 2008.05.25  13:51:55
 serial version


 -----------------------------------------------------------------


 INCAR:
 POTCAR:   PAW_GGA Al 05Jan2001
 POTCAR:   PAW_GGA Al 05Jan2001
   VRHFIN =Al: s2p1
   LEXCH  = 91
   EATOM  =    53.6910 eV,    3.9462 Ry

   TITEL  = PAW_GGA Al 05Jan2001
   LULTRA =        F    use ultrasoft PP ?
   IUNSCR =        1    unscreen: 0-lin 1-nonlin 2-no
...
```

```
[root@f15lab1 VASP]# cd Al_110
[root@f15lab1 Al_110]# ls
CONTCAR  EIGENVAL  IBZKPT   OSZICAR  out.vasp  POSCAR  XDATCAR
DISCAR   err.vasp  INCAR    out_Aa   PCDAT     POTCAR
DOSCAR   HFPOSCAR  KPOINTS  OUTCAR   pos_Aa    run
[root@f15lab1 Al_110]#
[root@f15lab1 Al_110]# ./../GenHFfile
```

```
[root@f15lab1 Al_110]#
[root@f15lab1 Al_110]# ./../GenHFfile
Incorrectly built binary which accesses errno, h_errno or _res directly. Needs t
o be fixed.
  Program <genHFfile>, ver.4.22
  generates from out_Aa, out_Ab, etc.
  the HFFILE for PHONON.
  In current directory must be DISCAR and HFPOSCAR.
  The output HFFILE contains Hellmann-Feynman forces.
FORTRAN PAUSE  Press any key to continue
Type GO to resume execution, any other input will terminate the job
go
Execution resumes after PAUSE
[root@f15lab1 Al_110]#
```

/home/rusi/VASP/Al_110

Name	Size	Changed
..		5/26/2008 3:09:19 AM
POTCAR	150,254	2/27/2004 6:18:00 PM
INCAR	133	6/11/2004 9:56:04 AM
KPOINTS	43	6/24/2004 3:13:26 PM
DISCAR	160	5/25/2008 11:57:36 AM
HFPOSCAR	624	5/25/2008 1:49:55 PM
pos_Aa	624	5/25/2008 1:49:55 PM
run	159	5/25/2008 1:51:22 PM
IBZKPT	507	5/25/2008 1:51:55 PM
out.vasp	0	5/25/2008 1:51:57 PM
err.vasp	0	5/25/2008 1:51:57 PM
CONTCAR	724	5/25/2008 1:51:57 PM
DOSCAR	11,073	5/25/2008 1:51:57 PM
EIGENVAL	2,845	5/25/2008 1:51:57 PM
OSZICAR	326	5/25/2008 1:51:57 PM
OUTCAR	31,002	5/25/2008 1:51:57 PM
PCDAT	2,313	5/25/2008 1:51:57 PM
POSCAR	624	5/25/2008 1:51:57 PM
XDATCAR	336	5/25/2008 1:51:57 PM
out_Aa	31,002	5/25/2008 1:51:57 PM
HFFILE	423	5/26/2008 4:12:01 AM

HFFILE

```
! DISCAR for VASP. System: Al_110

          0.99775  0.00000  0.00000    0.002245    0.000000    0.000000
    1 A   0.99775  0.00000  0.00000    0.005957    0.000000    0.000000
    2 A   0.00000  0.50000  0.50000   -0.005856    0.000000    0.000000
    3 A   0.50000  0.00000  0.50000   -0.000050    0.000000    0.000000
    4 A   0.50000  0.50000  0.00000   -0.000050    0.000000    0.000000
```

4. PHONON

Copied, removed spaces and renamed HFFILE to Al_110

Al_110

```
! DISCAR for VASP. System: Al_110
          0.99775  0.00000  0.00000    0.002245    0.000000    0.000000
    1 A   0.99775  0.00000  0.00000    0.005957    0.000000    0.000000
    2 A   0.00000  0.50000  0.50000   -0.005856    0.000000    0.000000
    3 A   0.50000  0.00000  0.50000   -0.000050    0.000000    0.000000
    4 A   0.50000  0.50000  0.00000   -0.000050    0.000000    0.000000
```

Inputs for PHONON

Al_110	407	File	5/26/2008 4:32:29 AM
Al_110.d00	459	D00 File	5/24/2008 2:23:34 PM
Al_110.d01	700	D01 File	5/25/2008 11:57:35 AM
Al_110.d02	119	D02 File	5/24/2008 2:35:33 PM
Al_110.d03	242	D03 File	5/25/2008 11:57:35 AM
Al_110.d07	7,896	D07 File	5/25/2008 11:57:35 AM
Al_110.d08	1,260	D08 File	5/25/2008 11:57:35 AM
Al_110.d10	397	D10 File	5/25/2008 11:57:35 AM
Al_110.d13	552	D13 File	5/25/2008 12:04:49 PM
Al_110.d22	312	D22 File	5/25/2008 11:57:35 AM
Al_110.d23	542	D23 File	5/25/2008 11:57:35 AM
Al_110.d44	160	D44 File	5/25/2008 11:57:35 AM

REFERENCES

1.1 Y. Horie, R.A. Graham and I.K. Simonsen, Materials Letters, 3, 354-359, 1985

1.2 I. Song and N.N. Thadhani, metallurgical transactions, A, 23 A, 41, 1992

1.3 N.N. Thadhani et. al., J.Appl.Phys., 82, 1113, 1997

1.4 L. Thiers et. al., Combustion and Flame, 131, 198-209, 2002

1.5 S.S. Bastonov, Materials Science and Engineering, A,210, 57, 1996

1.6 L.S. Bennet et. al., Appl, Phys. Letters, 61, 5, 520, 1992

1.7 L.S. Bennet and Horie, Shock Waves, 4, 127, 1994

1.7 L.S. Bennet et. al., J.Appl.Phys, 76, 3394, 1994

1.8 S.S. Bastonov et. al., Sov. J. Chem. Phys, 10, 2635, 1993

1.9 M.B. Bosolough, J.Chem. Phys, 92, 1839, 1990

1.10 Y. Horie et. al., J.Appl.Phys, 63, 5718, 1988

1.11 Y. Yang et. al., Appl. Phys. Letters, 70, 3365, 1997

1.12 K.Yano et. al., J.Appl.Phys, 84, 1292, 1998

1.13 P.Zhu et. al., Materials Science and Engineering, A329, 57, 2002

1.14 J.E. Freek et. al., J. Phys. Chem, C, 112, 7436, 2008

1.15 J.C. Sang et. al., Bull. Korean. Chem. Soc, 25, 9, 1314, 2004

1.16 H.T. Chen et. al., J. Phys. Chem, 112, 3341, 2008

1.17 T.H. Lee and J.W. Rabalais, Surface Science, 75, 29, 1978

1.18 B.J. Hopkins, Surface Science, 52, 715, 1975

1.19 P. Maciejewski et. al., Surface Science, 330, 156, 1995

1.20 L. Chen, D.S. Sholl, J.K. Johnson, J. Phys. Chem, 110, 1344, 2006

1.21 D. Leckel, Energy Fuels, 23, 2342, 2009

1.22 A.Y. Khodakov et. al., Chem. Rev, 107, 1692, 2007

1.23 C.M. Balonek, Catalysis Letters, 138, 8, 2010

2.1 S.H. Fischer and M.C. Grubelich, Sand 98-1176C, Sandia Natl. Lab. 1998

2.2 S. Hanagud, Final Report, AFOSR/DOD MURI, 2008

2.3 D.C. Swift et. al., Phys. Rev B, 40, 7501, 1989

2.4 X. Xu and W. Zhang, Science Press, 235, 1986

2.5 J.C. Boettger and S.B. Trickey, Phys.Rev B, 53, 3007, 1996

2.6 J.C. Boettger and W.C. Wallace, Phys. Rev B, 55, 2840, 1997

2.7 O.H. Nielson and R.M. Martin, Phys. Rev. Lett, 50, 697, 1983

2.8 O.H. Nielson and R.M. Martin, Phys. Rev. B, 32, 3780, 1986

2.9 M. Tuckerman, J.of Phys.: Condensed Matter, 14,R1297, 2002

2.10 Y.L. Page and P. Saxe, Phys. Rev. B, 65, 104104, 2002

2.11 A. Zunger et. al., Phys.Rev. Lett, 65, 353, 1990

2.12 T. Jiang, PhD Thesis, Georgia Tech, 2006

2.13 Z. Wu, PhD Thesis, Georgia Tech, 2009

2.14 D. Reding, PhD Thesis, Georgia Tech, 2009

2.15 D. Reding and S. Hanagud, J.Appl.Phys. Phys., 2009

2.16 V. Narayanan, PhD Thesis, Georgia Tech, 2005

2.17 J. Ehrlich, J.Chem. Phys, 34, 39, 1961

2.18 M. Madey, J.Chem.Phys, 42, 1965

2.19 F.J.E. Scheijen et. al., J. Phys. Chem C, 2008

3.1 A. Schlapka et. al., Phys. Rev. Lett, 91,1, 016101, 2003

3.2 M. Gsell et. al., Science, 280,717, 1998

3.3 M. Mavrikakis et. al, Phys. Rev. Lett, 81, 2819, 1998

3.4 J. Greenly et. al., Angew. Chem. Int. ed. , 43, 4296, 2004

3.5 A. Ruban et. al., J.Mol.Catal, A, 115, 421, 1997

3.6 J. Wintterlin et. al., Angew. Chem, Int.ed, 42, 2850, 20034.1

4.1 Baroni, S. et. al., Rev. Mod. Phys., v. 73, 2001, pp. 516 – 557.

4.2 Cohen, R. E., and Gülseren, O., Phys. Rev. B 63, 2001, pp. 224101 – 224110.

4.3 Dal Corso, A., and de Gironcoli, S., Phys. Rev. B, v. 62, n. 1, 2001, pp. 62 273

4.4 Godwal, B. K. and Jeanloz, R., Phys. Rev. B 40, 1989, pp. 7501 – 7507.

4.5 Godwal, B.K, Sikka, S.K et. al., Phys. Rev. B, v. 20, n. 6, 1979, 2362.

4.6 Gunnarsson, O., et. al., Phys. Rev. B., v. 10, n. 4, 1974, pp. 10 1319 – 10 1327.

4.7 Katsnelson, M.I, et. al., Phil. Mag. B., v. 75, 1997, pp. 407 – 418.

4.8 Kresse, G., and Hafner, J, J. Phys.: Condens. Matter, v. 6, 1994, pp. 8245 – 8257.

4.9 Louie, S. G., et. al., Phys. Rev. B., v. 26, n. 4, 1982, pp. 26 1738 – 26 1742.

4.10 Moriarty, J.A. et. al., J. Phys. Condens. Matter., n. 14, 2002, pp. 2825 – 2857.

4.11 Moroni, E. G. et. al., Phys. Rev. B, v. 56, n. 24, 1997, pp. 15629 – 15646.

4.12 Nellis, W.J et. al., Phys. Rev. Lett., v. 60, n. 4, 1988, pp. 1414 – 1417.

4.13 http://www.sainc.com /onr/detsymp/PaperSubmit/FinalManuscript/pdf/Schmitt-133.pdf .

4.14 Sikka, S. K.et,al, Phys. Rev. B 38, 1988, pp. 10926 – 10928.

4.15 Svane, A., and Gunnarsson, Phys. Rev. Lett., v. 65, n. 9, 1990, pp. 1148 – 1151.

4.16 Swift, D. C et. al., Phys. Rev. B, v. 64, 2001, pp. 214107 1- 214107 – 14.

4.17 Vanderbilt, D., Phys. Rev. B., v. 41, n. 11, 1990, pp. 41 7892 – 41 9922.

4.18 Yoffa, E. J. et. al., DPhys. Rev. B, v. 19, n. 2, 1979, 1203.

6.1 Schroeder, T., "The Miracle of Space in the Tank", Max Planck Research, March 2009, pp.73, http://www.mpg.de/796596/W004_Materials-Technology_072-079.pdf (last checked August 2011)

6.2 vanden Berg, A.W.C.; Areán, C.O. , Chem. Commun. 2008, 668–681.

6.3 Rosi, N.L.; et. al., Science 2003, 300, 1127–1129.

6.4 Chen, B. et. al., Angew. Chem. Int. Ed. 2005, 44, 4745–4749

6.5 Mueller, T.; Ceder, G., J. Phys. Chem. B. 2005, 109, 17974–17983

6.6 Perdew, J.P.; Wang, Y., Phys. Rev. B.1992, 45, 13244–13249

6.7 Zhao, D. et. al., Energy Environ. Sci. 2008, 1, 222–235.

6.8. Klontazas, E. et. al., Nano Lett. 2008, 8, 1572–1576.

6.9 Ma, S., Pure Appl. Chem., Vol. 81, No. 12, 2235–2251, 2009.

VITA

ROUSSISLAVA STEFANOVA ZAHARIEVA

Roussislava Stefanova Zaharieva was born in Sofia, Bulgaria. She received her Bachelor of Science degree in Aeronautics from California Institute of Technology in June 2001. While at Caltech, she participated in Undergraduate Research in the Solid Mechanics Division of GALCIT. She received her Masters degree in Aerospace Engineering from Georgia Institute of Technology in December 2004. She continued her graduate studies for a doctoral degree at Georgia Tech, and conducted experimental work in the Structural Dynamics and Smart Structures Laboratory in the School of Aerospace as well as the High-strain-rate Laboratory in the School of Material Science. In addition, in 2006 and 2009, she was research engineer at Millennium Dynamics Corporation, where she worked on structural health monitoring. In 2010 she was a visiting scholar in Pennsylvania State University, Department of Mechanical and Nuclear Engineering, where she performed atomistic modeling of chemical reactions. Her later research at Georgia Tech focused on ab initio modeling and investigation of thermal and shock-induced chemical reactions in multifunctional energetic structural materials.